A metabolomics view into perturbations of the plasma lipidome following traumatic brain injury

Harrison John Szemray
Bachelor of Biomedical Science

A thesis submitted to the Murdoch University
to fulfil the requirements for the degree of
Accelerated Master of Research with training

School of Medical, Molecular and Forensic Sciences
Murdoch University
Perth, Western Australia
2021

Author's Declaration

I Harrison Szemray verify that in submitting this thesis:

- The thesis is my own account of the research conducted by me, except where other sources are fully acknowledged in the appropriate format.
- The extent to which the work of others has been acknowledged at the beginning of each relevant chapter and signed by myself and my Principal Supervisor.
- That any editing and proof-reading by professional editors comply with the standards approved by the Research Degrees and Scholarship Committee.
- That all necessary ethics and safety approvals were obtained, including their relevant approval or permit numbers, as appropriate.

Harrison John Szemray

Luke Gray Whiley (Primary supervisor)

Abstract

Traumatic Brain Injury (TBI) is a neurological disorder caused when a sudden external force is applied to the head, resulting in various pathophysiological changes dependent on the amount of force applied. There is an emerging interest in altering TBI diagnosis from a subjective to an objective measure. Multiple studies have demonstrated that various lipid classes and species show abnormal concentration levels from hours to months post-TBI, that can be used to differentiate between repetitive, mild, moderate, and severe TBI.

The purpose of this thesis was to explore varying TBI injuries using liquid chromatography mass spectrometry to further elucidate lipidomic perturbations following a singular and repeated TBI in vivo, and further provide a comprehensive lipidomic signature of clinical mild traumatic brain injury (mTBI) at ≤48 hours and 28 days post injury. Study one utilised a rodent model to examine lipidomic changes associated in a singular mild traumatic brain injury (1x mTBI) and two consecutive mild traumatic brain injuries (2x mTBI) (sham control group n = 6, 1x mTBI n = 7, 2x mTBI n = 7). Lipidomic profiles indicated significant separation between the three study groups (i.e., sham control, 1x mTBI, and 2x mTBI). From multivariate analysis, a predictive model was constructed using the sham control and 2x mTBI groups that projected the metabolic position of 1x mTBI centrally in the model, indicating a progression of biomarker severity as the TBI intervention occurrence increases. Compared to sham controls, 1x and 2x mTBI rats both showed decreased levels of PS 14:0/18:2 and HCER d18:0/26:0 and PI 20:0/18:2 and increases in FFA 18:3. However, when comparing sham to 2x mTBI, decreases in concentrations of LPE 20:1, LPE 22:6, LPE 22:5, PI 16:0/18:2 and PI 16:0/18:3 were observed. Collectively these findings indicate that mTBI induces unique changes to lipid species in an injury dose-specific pattern.

Study two (Chapter 4) we aimed to provide a comprehensive lipidomic signature of clinical mTBI patients at injury inception (i.e., time of diagnosis ≤48 hours) and follow-up (i.e., 35 days post mTBI injury) in 30 patients. Using liquid chromatography mass spectrometry 225 lipid species were deemed significantly different between the control and mTBI patients at the

inception and follow-up timepoints. Multivariate analysis of this cohort displayed minimal variation between age and sex balanced controls and mTBI patients at inception. However, mTBI patients had a consistent metabolic shift from patient inception to follow-up, demonstrating perturbed plasma lipidome. Perturbation could be classified in patients regardless of the mTBI causing injury (i.e., fall, assault, or motor vehicle accident). Data from these studies will inform the design of future investigations of lipid metabolism and mechanisms following mTBI and repeat mTBI (rmTBI), allowing identification of novel biomarkers and the optimum 'window of opportunity' for therapeutic intervention in mTBI.

Acknowledgements

Firstly, I would like to acknowledge and thank my research supervisors, Dr Luke Gray Whiley and Dr Nathan Lawler of Murdoch University. I feel privileged to have taken my research journey under their guidance and have valued their feedback, academic experience, kind words and good humour throughout the past year. Further, I would also like to acknowledge the team at the Australian National Phenomics Centre for their constant support and Murdoch University's School of Medical, Molecular and Forensic Sciences.

I would also like to acknowledge the Neuroscience team at Curtain University for their collaboration. Special thanks must go to Dr Chidozie Anyaegbu, Professor Melinda Fitzgerald and Dr Sarah Hellewell.

Lastly, I would like to thank my family and friends for their never-ending support throughout the process. Special thanks to Kai for the endless supply of laughs and never turning down a beer.

Table of Contents

List of Figures

List of Tables

List of Abbreviations

TBI	Traumatic brain injury
mTBI	Mild traumatic brain injury
rmTBI	Repeated mild traumatic brain injury
TAG	Triacylglycerides
DAG	Diacylglycerides
MAG	monoacylglycerols
FFA	free fatty acids
SM	sphingomyelins
CERs	Ceramides
DCER	Dihydroceramides
HCER	Hexosylceramides
LCER	Lactosylceramides
CE	Cholesterol esters
PC	Phosphocholines
PE	Phosphoethanolamines
PG	Phosphoglycerols
PI	Phosphoinositols
PS	Phosphoserines
LPC	Lysophosphocholines
LPE	Lysophosphoethanolamines
LPG	Lysophosphoglycerols
LPI	Lysophosphoinositols
PCA	Principal Component Analysis
OPLS-DA	Orthogonal partial to least squares discriminant analysis
QC	Quality control

SD	Standard deviation
UPLC	Ultra-performance liquid chromatograph

1 Introduction

1.1 Background

Traumatic Brain Injury (TBI) is a neurological disorder caused when a sudden external force is applied to the head and resulting in various pathophysiological changes dependent on the amount of force applied (1). In 2019, approximately sixty-nine million people (95% CI 64-74 million) were diagnosed with TBI due to motor vehicle accidents alone (2). Furthermore, if the plethora of alternative TBI causing events (e.g., falls, assaults, sports injuries, explosions, and penetrating head injuries) were accounted for, the estimated incidence of TBI would be much higher.

Metabolic phenotyping utilises biological samples such as urine, sweat, saliva, and blood to provide a detailed biochemical classification of pathophysiological states that translate to disease diagnosis or prognosis at an individual level (3). Metabolomic biomarkers are small molecule metabolites within a biological system that can be measured and used to predict or indicate disease (3). Currently, the majority of the literature available focuses on protein biomarkers of TBI, which have been demonstrated to lack the specificity and sensitivity to accurately assess TBI severity and predict patient prognosis (4, 5). A potential alternative source of TBI biomarkers is lipids. These molecules comprise the majority of structures within the brain and readily cross the blood-brain barrier, highlighting lipids as a potential biomarker as they are accessible in whole blood, plasma or serum (1). Furthermore, lipids are key molecules in a plethora of biochemical and physiological roles in the human body, including cellular signalling, immune responses, membrane lipid structure, and inflammatory pathways (6-8).

Multiple studies have demonstrated that various lipid classes and species show abnormal concentration levels from hours to months post-TBI. These can be used to differentiate between the types of TBI (i.e., mild, moderate, and severe). However, to our knowledge to date, no paper has applied a comprehensive lipid analysis to create a lipidomic signature of TBI in animal and human cohorts.

Phospholipids have been the primary target group for TBI biomarkers and have been reported to display long term decreases for years post-TBI. Emmerich et al. (2017) highlighted a possible recovery period at six months post-TBI as PL levels returned to statistically similar levels as controls. However, at 12 and 24-month follow-ups, all PL classes decreased, with SM being significantly low (9). These metabolic shifts in the lipidome are explored in more detail in the review of literature. The findings from the above studies highlight the potential for lipids as a valuable resource for TBI biomarkers. The recent improvement of blood plasma lipid analysis methods now allows for the identification of up to 1200 lipid species. Thus, highlighting the need to further explore the plasma lipidome for associations with TBI.

1.2 Thesis organisation

This thesis has been designed to present the data collected during the degree of Accelerated Master of Research with Training as a coherent piece of work incorporating a series of stand-alone manuscripts. This thesis consists of five chapters. Chapter one provides a general introduction to the thesis. Chapter two provides a review of the literature for lipidomics in Traumatic Brain Injury. Chapters three and four present the experimental studies. Lastly, Chapter five consists of a general discussion about the experimental studies and future directions. Each experimental chapter (i.e., chapters three and 4) are written and presented to conform with the respective journals for submission. Manuscripts have been slightly altered to aid in the readability of the thesis, such as a single referencing style was used throughout the thesis. Furthermore, tables and figures were labelled consistently throughout the thesis.

1.3 Purpose of the research

The available literature using lipid biomarkers as a method to create a lipidomic signature in animals and humans following TBI remains limited, highlighting the demand for further research to determine whether alterations in the blood plasma lipidome can accurately reflect TBI the pathology of TBI.

The proposed studies will use in vivo models to profile lipid biomarkers present in the blood plasma of TBI. Furthermore, the studies will identify biomarkers of interest that can act as possible biomarkers of TBI pathophysiology. The first study (chapter 3) aims to determine the lipidomic perturbations following a TBI insult using an in vivo rat model and further, demonstrate the effects of TBI severity (i.e., a single concussion (1x mTBI) or two consecutive concussions (2x mTBI)). The second study (chapter 4) aims to compare data from a comprehensive lipid analysis of age and sex balanced healthy controls, and human mTBI patients at ≤48 hours and 28 days post injury, by mapping perturbations in the mTBI patients' plasma lipidome. This study provides metabolites that we can now track and follow in future TBI research.

2 Review of the literature

2.1 Introduction

Traumatic brain injury (TBI) is a major health problem worldwide, affecting all ages. It can lead to significant cognitive, psychological, and physical health complications and portrays a considerable socioeconomic burden. Research into TBI has increased over the past decade, especially in biomarker identification, to meet the demand for more accurate and personalised treatment. A large proportion of the human brain is composed of a variety of lipid classes, including sphingolipids, fatty acids, sterols, phospholipids and glycerolipids. There is accumulating evidence in studies conducted on TBI patients and experimental models of TBI that the injury causes a complex response in a variety of lipid classes (9-18). These changes can be detected in the blood, providing novel insights into the pathophysiological response to TBI and provide a potential source of biomarkers. This literature review looks at the current knowledge of blood plasma lipids as prognostic biomarkers for TBI.

Traumatic brain injury (TBI) is a neurological disorder caused when a mechanical rotational force is applied to the head, resulting in various pathophysiological mechanisms. In 2019, sixty-nine million people worldwide (95% CI 64-74 million) were estimated to experience TBI annually from motor vehicle accidents (2). When considering other TBI causing factors (e.g., falls, assault, sports injuries), this total is likely to be much larger. For instance, McCory et al. has shown the general population is most likely to experience a TBI during day-to-day accidents (i.e., falls and motor vehicle accidents) or through participation in contact sports (i.e., Australian Football League, field hockey, rugby, gridiron, boxing, and wrestling) (19). In Australia, individuals hospitalised due to TBI were 7.5 times more likely to die when compared to other non-TBI patients, with the majority of the cohort populated by males, younger age groups and patients with more severe TBI (20). This is possibly due to the young/male demographic demonstrating more risk-taking behaviours and increased participation in contact sports. This level of activity places an individual at risk and more susceptible to concussion (19). Beyond the

health risks, TBI carries a considerable socioeconomic burden; patients have increased health care costs, risk of unemployment, and divorce rates (21).

Traumatic brain injuries disrupt normal cellular functions via shear, direct and rotational forces. TBI pathophysiology can be divided into two injury types: primary injury and secondary injury. Primary TBI injuries occur from the initial trauma to the brain and can result in epidural haematoma, subdural haematoma, subarachnoid haemorrhaging and intraventricular haemorrhage, causing damage to the vasculature, neural and glial tissues (22). Secondary injury is the leading cause of TBI caused deaths in hospitals (23) and occurs days to months following primary injury, causing damage to the brain at a cellular and molecular level. At this stage, breakdown of the blood-brain barrier and cell death occurs (24).

To date, TBI severity is classified by the Glasgow Coma Scale (GCS) in combination with computer tomography (CT) or magnetic resonance imaging (MRI) to confirm abnormal brain structure. The GCS assesses patient consciousness, as a score, based on eye movement, verbal communication and gross motor skills. TBI can be classified into three grades, mild (GCS 13-15) (also known as concussion), moderate (GCS 9-12) or severe (GCS 3-8) (25). The current method for diagnosis of TBI is limited for four significant reasons; i) No universally standard definition of TBI exists, ii) The current method does not provide any reflection of patient outcome, iii) No standardised guidelines exist for diagnosing or treating TBI exists, and iv) Current classification of TBI severity is based on subjective observation of the patient and patient self-reporting of the incident and symptoms, often leading to misdiagnosis (26). Additionally, other factors interfere with the use of GCS such as; i) Pre-existing factors (e.g. language barriers, intellectual disabilities and hearing loss, ii) Effects of treatment (e.g. intubation of patients), iii) Effects of other injuries (e.g. spinal cord injuries) (27). The most common and severe issue of not objectively quantifying TBI is misdiagnosis because it is deleterious to patient health and can lead to further brain damage, permanently impaired brain function, or even death (20, 28). The current approach to TBI diagnosis and treatment has major shortcomings as it does not consider the secondary pathophysiological mechanisms of TBI, which, if considered, could aid the patients' diagnosis and recovery through precision medicine.

2.2 The demand for biomarkers

Over the past decade, biomarkers have improved the scientific communities understanding of complex pathophysiological mechanisms. TBI is no longer recognised as a singular event, but a progressive and delayed process hallmarked by neurodegeneration resulting from multiple dependent and independent biological reactions at subcellular, cellular and tissue levels. A 2018 study of emergency department medical records and parental self-reporting displayed higher TBI identification rates from parental observation than medical records (29), highlighting the need to develop prognostic TBI biomarkers for various environments, such as sports, militaries, and hospitals

2.2.1 Mild TBI and sports-related concussions

Mild TBI, commonly referred to as concussion, frequently occurs in contact sports and is highly prevalent among professional, amateur, and recreational athletes (19). Furthermore, repeated concussions commonly occur due to the current on-site method used for concussion detection and return to play. The incidence of sports-related concussion, often accounted for as mild TBI, ranges from 0.58 per 1000 athletes (30-32). It is highly likely that these reports do not truly represent the incidence, as concussions/mild TBIs are often not diagnosed or treated and therefore remain undocumented in the scientific literature (33). In contact sports, if a biomarker that could accurately detect mild TBI/concussion was present rapidly in the blood post-injury, it could be used to more accurately assess an athlete's condition to return to play and mitigate the risk of repeated concussion leading to TBI.

2.2.2 Military

Mild TBI is a common occurrence in the military environment and can occur from multiple factors, including training and concussive blasts (11). Like sport related TBI, treatment decisions are controlled by an accurate recount of impact type and severity. Both TBI and post-traumatic stress disorder (PTSD) present with long-term neurological dysfunction and remain challenging to diagnose due to military personnel presenting with both diseases and overlapping clinical presentation, often leading to misdiagnosis of TBI. Emmerich et al. demonstrated that

PL species were elevated in soldiers' brain tissue who had TBI, PTSD and both neurological conditions (10). A major limitation of the study was that the time between TBI/PTSD injury and blood collection could not be provided. Continuous monitoring of blood biomarkers would allow for an informed decision about returning to active combat once biomarker levels return to normal levels.

2.2.3 Hospital

TBI biomarkers would provide invaluable diagnostic and prognostic insights in the clinical setting. The current use of the GCS in combination with CT or MRI to diagnose moderate to severe TBI is accurate in detecting more apparent TBI signs such as changes in brain structure and blood haemorrhages; however, there are less noticeable forms of brain injuries such as diffuse axonal injury which are often missed (18). Continuous monitoring of blood biomarkers with a high degree of specificity and sensitivity would allow for more efficient patient stratification, treatment, and disease prognosis.

2.3 Metabolic profiling

Metabolic phenotyping utilises biological material to provide an in-depth biochemical classification of physiological and pathological states related to disease diagnosis or prognosis at an individual level (3). Metabolomic biomarkers are small molecule metabolites in a biological system that can be measured and used to predict or indicate a disease state within a biological system. Most of the literature focuses on protein biomarkers of TBI, which have so far lacked specificity and sensitivity to quantify mTBI accurately (1). An alternative marker for monitoring TBI brain injury is lipids, as they are the most abundant molecule in the brain and readily cross the blood-brain barrier making this molecule a prime candidate for TBI biomarkers as they can be easily accessed in whole blood, serum, or plasma (1). Furthermore, lipid species are varied in biochemical composition and play many physiological roles throughout the human system, including signalling, inflammation, and immune responses. Due to their multitude of physiological roles, the human plasma lipid component is a rich source of metabolic information for discovering potential disease biomarkers. One such way of discovering metabolomic biomarkers is through the analytical technique of mass spectrometry.

2.3.1 Liquid-chromatography mass spectrometry as an analytical tool for metabolic profiling

Mass spectrometry is a useful tool in metabolomics, as it can detect metabolites in the nM to pM range (34). The mass-to-charge ratio (m/z) of molecules in a sample is measured using mass spectrometry (MS), making this technique highly sensitive and selective analytical tool (35, 36). MS is frequently used in conjunction with chromatographic techniques like liquid chromatography (LC). By evaluating the retention period, chromatographic separation can provide additional information on various physiochemical aspects of analytes. This separation prior to MS detection allows for better analyte resolution, especially in complex mixtures like biological fluids (37). The sensitivity and selectivity of LC-MS equipment combined make MS extremely useful for unravelling the complex metabolic pathways of neurological

conditions, such as Alzheimer's disease, Parkinson's disease, and brain cancer (38-40), as it allows for early diagnosis of disease and therapy monitoring via biomarkers (41) .

2.3.2 Data analysis

Due to the enormous volume and complexity of data generated by MS, data processing is one of the most critical steps in the metabolic phenotyping pipeline. The data from the instruments is first pre-processed to turn it into a format suitable for downstream processing. These approaches are particular to the analytical platform used to obtain the data (42), and include peak identification, peak alignment, and quantification, baseline correction, normalisation, and scaling. This is followed by statistical analysis, which examines metabolite variable change in order to uncover discriminatory traits that can distinguish between different observation groups (e.g. disease vs control) (42). Chemometric methods like univariate and multivariate statistics are the most widely employed approaches (43). Individual metabolite features are independently examined using univariate methods, which are chosen based on whether the data fulfils the normality assumptions (43, 44).

Multivariate procedures, in contrast to univariate methods, which analyse individual metabolites independently of one another, concurrently account for all metabolite properties in a sample and are effective for discovering patterns of correlations between these features. (42, 44). Principal component analysis (PCA) and orthogonal partial least square-discriminant analysis (OPLS-DA) are two commonly utilised techniques (45). PCA is an unsupervised technique used to show patterns of variability within a sample set and to evaluate repeatability by clustering quality control samples within and across batches. (45). OPLS-DA, on the other hand, is a supervised technique used as a descriptive and predictive modelling method for classifying sample group separation and highlighting discriminatory features (45, 46). Volcano plots are an alternative visualisation technique that demonstrates metabolites statistical significance of metabolites versus magnitude of change in observed groups (e.g. control vs disease), allowing for the identification of likely biomarkers (47).

2.4 Why lipids and what do they have to offer?

Lipids have been proven to be valuable biomarkers in major neurological conditions such as Alzheimer's Disease and Dementia (48, 49). Ideally, brain tissue is the best sample for TBI biomarker analysis. However, due to patient survival being the priority, this sample type is impractical for TBI biomarker analysis in the clinical setting. Compared to cerebrospinal fluid collection, the minimally invasive nature of phlebotomy makes blood an ideal candidate for TBI biomarker analysis. Additionally, lipids readily cross the blood-brain barrier and are hallmarks of neurodegeneration (50), further highlighting the value of blood lipids as prognostic biomarkers for TBI.

Various lipid classes can be readily found throughout the central nervous system; these include fatty acids, phospholipids, sphingolipids, glycerolipids and sterols. Fatty acids are vital components in the construction of more complex lipid species. They have varying chain lengths and can be polyunsaturated (e.g., arachidonic acid and docosahexaenoic acid), monosaturated (e.g., palmitoleic acid) or saturated (e.g., palmitic acid). Polyunsaturated fatty acids have signalling and structural roles in the brain, trigger lipid mediators, and activate various receptors (51). Phospholipids are major components of cell membranes and compose 45% of the brain (dry weight). This lipid class consists of a glycerol backbone with hydroxyl groups linked to fatty acids and a phosphodiester group. Major phospholipid (PL) species include phosphatidylcholine (PC), phosphatidylinositol (PI), sphingomyelin (SM), phosphatidylserine (PS) and phosphatidylethanolamine (PE). PL species maintain cellular structures such as membranes as they form the lipid bilayers and are crucial for creating lipid domains within membranes (52). Sphingolipids include phosphosphingolipids (e.g., sphingomyelins), ceramides, and glycosphingolipids. Sphingomyelins play a major role in both cellular signalling and the process of myelination (7). Glycerolipids are monosubstituted, disubstituted or trisubstituted glycerols, meaning that the glycerol backbone is conjoined to various fatty acyl residues. Disruption of this lipid class has been linked to alterations in synaptic plasticity and neurogenesis (53). Sterols are also a major component of lipid membranes. For example, cholesterols are a principal sterol in mammals and are highly enriched in the brain accounting for 20% of the total cholesterol

concentration in humans. Furthermore, this lipid class is essential for normal neuronal development and maintenance in the human species (54). The essential roles of lipids in humans' biological system further highlight the potential of lipids as valuable biomarkers for TBI.

2.4.1 Phospholipids

Phospholipids have been identified as key candidates for biomarkers of TBI. For instance, Sheth et al. (2015) collected plasma samples from rats and mice with TBI insult at 1 day and 7 days and analysed them for phospholipid content using high-performance liquid chromatography mass spectrometry (16). The findings demonstrated significantly increased sphingolipids in plasma between 6- and 24-hours post-injury, with the predominant lipid species being sphingomyelins (SM). The most significant increase was in SM 37:1 and SM 38:3. Sheth and colleagues (2015) proposed that the increase may be due to SM enriched exosomes passing through the blood brain barrier and their structure, resulting in a longer half-life in plasma (16).

Changes in phospholipids post-TBI have been reported in mice, with Emmerich et al. reporting the plasma phospholipid profiles of mice with mild TBI (9). Of the phospholipids analysed, several decreased. Mass spectrometry was used to create lipid profiles post-injury at 24 hours, 3, 6, 12, and 24 months, providing a comprehensive list of analytes present at each of the specified times. The concentration of specific analytes at different chronological points were compared to monitor the changes within an individual's lipidome post-TBI, reflecting the progression of TBI recovery. The results indicate that there were no significant changes in PL levels in plasma samples taken at the 24 hours post TBI injury. However, PL perturbations were observed at 3 months post TBI, with PC, LPC, PE, LPE, and PI decreased, but SM remained at a similar level to the controls. Of particular interest is the 6-month profile which demonstrated a 'possible recovery period' as PL returned to levels that were not statistically different from the control mice. At 12 months, PC, PE, and PI decreased in concentration relative to controls. All PL classes decreased at 24 months with SM concentrations significantly lower at the same timepoint (9). . The authors proposed that mild TBI may exacerbate the effect ageing has on the brain due to a decrease in phospholipids, providing a possible explanation to the theory that TBI contributes to diseases of the brain such as dementia (55). The findings of this study are important

because the study method controlled the effect ageing has on brain lipid composition, which was a rarely controlled variable in other studies. Regardless of these findings, more research is required to confirm if the possibility of a 'recovery period' by identifying a delayed pathological mechanism associated with TBI.

In a more recent study, Hogan et al. (2018) utilised controlled cortical impact to the lateral frontoparietal cortex of rats to induce TBI(13). Using an untargeted lipidomic approach, a battery of 26 serum lipids was identified that could discriminate lipid concentrations between rats with TBI vs control rats, demonstrating 85% accuracy at days 3 and 7 post-injury. The findings demonstrated, several phospholipids decreased (PE 20:4/16:0, 18:2/18:0, 18:0/22:4; PC 20:2/18:0, 16:0/16:0, 18:2/16:0, 18:2/22:1) which were not previously observed in previous lipidomic studies of TBI studies. Interestingly, SM d18:1/22:1 and lysoPC 20:2 in the TBI subjects were not significantly different between days 3 and 7, conflicting with an earlier study that reported an increase in SM concentration up to 24 hours post-injury (16). These results possibly indicate that SM is only present in blood up to 24 hours post-injury. In addition, the concentration of oxidised lysoPC 18:2 and PS 16:0/20:4 increased (13). Hogan et al. were unable to identify five biomarkers used in the 26-biomarker battery for TBI diagnosis, demonstrating a limitation in the study.

Fiandaca et al. developed a 6-lipid biomarker battery using blood plasma obtained from an athlete cohort consisting of 38 individuals diagnosed with mild TBI and 24 healthy controls. This study samples were taken at 2, 3 and 7 days and analysed using tandem mass spectrometry to measure the 6-plasma lipid biomarker panel. The measurement of the plasma lipid metabolites accurately differentiated mild TBI from controls up to six hours post-injury. Furthermore, the lipid metabolite battery was validated in two external cohorts where 31 civilians and 53 military personnel were used for external assessment. Three phospholipids were determined as valid biomarkers, phosphatidylethanolamine plasmalogen and lysophosphatidylcholine increased in concentration, diacyl-phosphatidylethanolamine decreased at ≤6 hours, as well as 2, 3, and 7 days post mild TBI injury (12). While this study's results show promise, further validation of the

biomarker panel in human and animal models is needed to prove the central nervous system specificity of the metabolites.

2.4.2 Fatty acyls

Fatty acyls play a major role in brain membrane function and fluidity(56). In 2016, Orešič et al. utilised a gas chromatography coupled with a time-of-flight mass spectrometer to analyse human blood serum obtained from hospitalised patients that had been diagnosed with TBI. Elevated concentrations of octanoic acid (OA) and decanoic acid (DA) are highly associated with moderate or severe TBI and poor patient outcomes (57). The study reported elevated concentrations of OA and DA for the first week post-injury. The extensive study population (n = 144) for biomarker discovery and validation of discovered biomarkers in an external independent cohort (n = 94) increased the validity of the study's results as it provides a smaller margin of error. Hogan et al. (2018) reported increased concentrations of stearic acid, arachidonic acid, docosapentaenoic acid and docosahexaenoic acid in rat serum TBI samples compared to controls at 3 and 7 days (13). This finding was further validated in an independent study by Fiandaca et al. on human plasma samples (see above 2.1.). However, the same study also reported a significant decrease in 2-hydroxypalmitic acid from the time of injury to seven days post-injury (12). The variation of lipid species identification across the three studies may be explained by Orešič et al.'s use of gas chromatography-mass spectrometry, while the other studies utilised liquid chromatography-mass spectrometry. At the time of publication, most of the literature favours liquid chromatography-mass spectrometry proposing it as the more effective method for lipid analysis because gas chromatography-mass spectrometry (GC-MS) requires derivatisation of samples, possibly introducing a source of variation in the sample.

2.4.3 Sterols

Sterol species are found in mammals commonly in the form of cholesterol and can be broken down into sub-fractions such as high-density lipoprotein cholesterol (HDL), low-density lipoprotein (LDL) and very low-density lipoprotein (VLDL). High density lipoproteins have been linked to patients recovering from TBI, particularly in those who lost consciousness. In a human study, Zong et al. (2020) demonstrated that patients with lower serum concentrations of HDL-C

had an increased risk of diffuse axonal injury (DAL) and a reduced probability of regaining consciousness 6 months post-DAL as a result of TBI (18). These results highlighted HDL-C as a valuable prognostic marker for TBI. Conclusions drawn from this retrospective study require further validation as the study design had limitations, such as lack of ethnic diversity and not accounting for the impact a patient's diet before TBI inducing injury may have had on HDL-C concentrations. Furthermore, cholesterol sulphate has been reported to decrease in serum post-TBI compared to non-TBI controls (13), supporting the finding of cholesterol-containing molecules as biomarkers for TBI.

Lipids have shown early potential as biomarkers in TBI diagnosis and prognosis prediction, but a further study from a range of samples is required before transfer to a clinical setting. Recent advancement in lipid analysis allows for a much more comprehensive analysis of blood plasma, a rich source of lipid analytes (1), providing an opportunity to identify novel biomarkers that can serve as prognostic markers for TBI. The readily accessible nature and minimally invasive process of collecting blood make it an optimal TBI biomarker source in a clinical setting. The majority of the literature focuses on single classes of lipid biomarkers for specific TBI pathologies and diagnostics, with most of the focus being placed on phospholipids as biomarkers for mTBI. In contrast, only Hogan et al. and Fiandaca et al. took a holistic approach to lipid biomarkers for predicting patient outcome and TBI prognosis (12, 13). To develop a prognostic TBI panel, the pathophysiology of TBI would have to be wholly understood, and the roles of all the biomarkers associated with various pathophysiological mechanisms play in the progression of the condition. Current studies conclude that various types of biomarkers, including lipid biomarkers, will become an invaluable tool in TBI clinical studies. However, the role of lipids as prognostic biomarkers in TBI is poorly understood, highlighting the demand for research in this area.

3 Plasma lipid profiles change with increasing numbers of mild traumatic brain injuries in rats

This chapter has been written in the style of a research article using the International Journal of Molecular Sciences guidelines for authors.

For this thesis chapter, I performed the lipidomics data acquisition, data analysis, interpretation, and writing, editing and reviewing the chapter.

Samples were provided by Curtin University.

Authorship order	Contribution (%)	Concept Development	Lipidomic Data Collection	Lipidomic Analyses	Drafting of chapter	Chapter review
Harrison Szemray	80%	X	X	X	X	X
Nathan Lawler	10%	X				X
Luke Whiley	10%	X				X

By signing this document, the Candidate and Principal Supervisor acknowledge that the above information is accurate and has been agreed to by all other authors.

Candidate **Principal Supervisor**

Abstract

Mild traumatic brain injury (mTBI) causes brain structural, cellular, and biochemical alterations, which may persist for days, weeks or years following single or repetitive injury. While pathology is difficult to detect *in vivo*, the extravasation of molecules into biofluids presents an attractive option to evaluate and monitor brain pathology. Many cellular constituents are transient or in concentrations below detectable limits; however, the abundance of brain lipids and their ability to cross the blood brain barrier suggests that lipidomic analysis of blood samples may provide superior insight into the neuropathological state. This study used liquid chromatography-mass spectrometry (LC-MS) to examine plasma lipids 11 days following sham, one (1x) or two (2x) mTBI in the rat. 18 lipid species were identified that accurately distinguished between sham control, 1x and 2x mTBI. Three distinct patterns were found: 1) lipids that *increased* significantly in concentration after mTBI (1x or 2x): Free fatty acid (FFA) 20:3, hexosylceramide (HCER) 22:0, phosphoethanolamine (PE) P-18:1/20:4 and cholesterol ester (CE) 14:0; 2) lipids that *decreased* significantly in concentration after mTBI (1x or 2x): phosphoserine (PS) 14:0/18:2, HCER d18:0/26 and phosphoinositol (PI) 20/18:2; 3) lipids that *increased* after 1x mTBI and *decreased* after 2x mTBI: Lysophosphoethanolamines (LPEs) 20:1, 22:5, 22:6, PIs 16:0/18:2, 16:0/18:3, 18:1/18:1, 18:1/18:2, lysophosphoglycerol (LPG) 18:2, FFA 18:3, and phosphocholine (PC) 20:0/22:4. These findings suggest that mTBI induces unique changes to lipid species in an injury dose-specific pattern. While further studies are needed to directly confirm whether these peripheral lipid changes are reflective of central pathophysiological changes, it noteworthy that the pattern of lipid change of increase with 1x mTBI and decrease after 2x rmTBI is consistent with our previous reports of differential brain pathology following 1x or 2x mTBI.

3.1 Introduction

Mild traumatic brain injury (mTBI) is increasingly recognised as a substantial public health problem, particularly in the sporting context where repeated mTBI (rmTBI) is prevalent. While most people recover in the weeks to months following mTBI, at least 20% of the 3.2 million people worldwide

that present to hospital each year experience persistent neuropsychological, cognitive, sleep or physical dysfunction (58), with those experiencing rmTBI at greater risk (59, 60). rmTBI is also associated with an increased risk of developing neurodegenerative diseases such as dementia and Parkinson's disease (61, 62). There are no effective treatments to address the pathobiological changes prompting ongoing mTBI symptoms, partly due to an incomplete understanding of the underlying mechanisms. Longitudinal mechanistic studies are challenging due to the small number of accessible indicators of damage that reflect pathology in the brain following single and repeated mTBI.

A rapid-onset pathophysiological feature of mTBI is terminal membrane depolarisation caused by the excessive release of neurotransmitters from damaged neurons and glia. This activates voltage-gated calcium and sodium channels, leading to the degradation of cell membranes and proteins by lipases and proteases (63). The associated increase in intracellular calcium and sodium levels also triggers excessive reactive oxygen species production, in turn causing oxidative damage to proteins, lipids, and other macromolecules (64). Such pathophysiological changes can cause degradation of the axonal cytoskeleton and extracellular matrix, resulting in the release of cellular components usually absent in the circulation (65).

There is growing evidence from experimental and clinical studies that TBI may induce unique alterations in brain lipid species which can be detected in the blood (9, 66). These studies support the concept that changes to lipids and their metabolites in the blood may reflect disruptions to the structural integrity of lipid-rich cell membranes in the brain. Depending on their structure and function, lipids can be classified into two categories: i) lipids that lack fatty acids (e.g. cholesterol and vitamins) and ii) fatty acid-containing lipids (66). The latter class includes storage lipids (e.g. mono-, di-, and tri-acylglycerols) and membrane lipids such as glycerophospholipids (e.g. phosphatidylcholine, PC; phosphatidylethanolamine, PE; phosphatidylserine, PS and phosphatidylinositol, PI) and sphingolipids (e.g. ceramide, sphingomyelin and glycosphingolipids). Phospholipid metabolites include lysophosphatidylcholine (LPC), lysophosphatidylethanolamine (LPE), lysophosphatidylglycerol (LPG) and lysophosphatidylinositol (LPI). Lipids account for 60% of the brain's dry weight, and ~75% of lipids in mammals are specific to neural tissues, highlighting the unique importance of lipids for brain function

(67). Indeed, lipids play several key roles in the central nervous system (CNS), including cell membrane formation, regulation of membrane-bound ion channels, neurotransmission, and immune signalling (68). Essential fatty acids (FAs) for generating cell membrane phospholipids are either synthesised in the brain or transported from the systemic circulation through the blood–brain barrier (BBB) (69, 70).

Plasma lipid levels are altered in both human and rodent mTBI studies, with a predominant focus on acute (≤ 3 days) and chronic (> 1 month) stages of injury. Clinical studies of populations vulnerable to rmTBI such as contact sports and military personnel have reported decreases in plasma markers both acutely and chronically, with a cohort of ice hockey players demonstrating decreases in plasma PC and LPC 55 hours post-injury (71). In soldiers who had experienced mTBI up to 10 years prior to lipid analysis, significant decreases in plasma levels of PC, LPC, PE, LPE, PI and SM were also detected and, interestingly, these changes were more pronounced in soldiers who had developed post-traumatic stress disorder (72). Similarly, in a closed-head mouse model of mTBI, the pattern of chronic decrease in plasma PC, LPC, PE, LPE and PI observed at 3, 12 and 24 months post-injury mimicked those detected in the soldiers with chronic mild TBI (9). In contrast to these peripheral decreases in plasma phospholipids, significant increases in PE, LPE, PC, LPC, and sphingomyelin have been reported in the mouse brain at acute (24 h) and chronic (3, 6, 9 and 12 months) time points post-rmTBI (73), suggesting that concomitant decreases and increases in plasma and brain lipids respectively may reflect lipid transport to the brain as a reparative response. However, the changes in plasma phospholipids at the sub-acute phase of rmTBI (day 4 – 14) have not been explored in a closed-head rodent model of rmTBI that incorporates the rotational movements that typically accompany human mTBI.

To address this knowledge gap, we used liquid chromatography-mass spectrometry (LC-MS) in conjunction with our well-characterised rat model of closed-head mTBI involving rotational acceleration (74-77) to profile the plasma lipidome of rats at day 11 following sham, one (1x) or two (2x) mTBI. Analyses were performed at day 11 because our previous studies showed that cellular indicators of damage, including microglial reactivity and oxidative stress, were most apparent at this subacute time (74, 76) compared to more acute (day 4; (77)) and chronic (3 months; (75)) timepoints. Female rats were

used to enable comparison of findings to previous work (78, 79), and to address the substantial under-representation of female animals in TBI literature.

3.2 Materials and methods

3.2.1 Animals and ethics

Adult female Piebald Viral Glaxo rats (160–200g) from the Animal Resource Centre (Murdoch, WA, Australia) were used for this study. Animals were housed in pairs under specific-pathogen-free conditions and a 12:12 hour light-dark cycle. Rats had free access to food and water. They were acclimatised to housing conditions for a minimum of one week prior to any procedures. All procedures involving rats were approved by The University of Western Australia Animal Ethics Committee (Approval Number RA/3/100/1699) in accordance with the Australian Code of Practice for the Care and Use of Animals for Scientific Purposes, issued by the National Health and Medical Research Council.

3.2.2 Closed-head weight-drop model of repeated mild traumatic brain injury

Twenty rats were randomly assigned to sham control (n = 6), 1x mTBI (n = 7) or 2x mTBI (n = 7) groups. Injuries were delivered at 24-hour intervals, using a closed-head, rotational acceleration weight-drop model of mTBI, which has been described in detail previously [20]. Briefly, rats were anaesthetised with 4% isoflurane in 4 L/min oxygen, and their heads were shaved before they were laid prone on a delicate task wiper (Kimwipes, Kimberly-Clark, Irving, TX, USA). The rat's head was aligned to ensure that the 250 g weight released from a 1 m height would impact midline 2–3 mm anterior to the front of the ears at the lambda suture line. Sham procedures were identical except for the weight drop to control for the effect of anaesthesia. Animals that received 1x mTBI received a sham procedure when mTBI was not administered, ensuring equal anaesthesia for all animals. All rats received analgesia (Carprofen, 4 mg/kg, s.c., Norbrook Laboratories, Tullamarine, VIC, Australia) immediately after sham or mTBI procedure before they were returned to their housing.

3.2.3 Plasma collection for lipidomics

At day 11 after the sham or mTBI (day 1), rats were deeply anesthetised using pentobarbital sodium (160 mg/kg i.p., Virbac; supplied by Provet, Malaga, WA, Australia). Peripheral blood (2 mL) was collected by cardiac puncture using a 23 G needle in a syringe, transferred to an EDTA vacutainer (BD Vacutainer; REF 367839; BD Biosciences) and mixed by gentle inversion of the tubes. Plasma was separated from whole blood by centrifugation at 1500 x g for 15 minutes at 4 ºC and stored at -80 ºC until use.

3.2.4 Sample preparation for Liquid Chromatography Mass Spectrometry (LC-MS)

Lipidomic analysis was completed using an established method previously described (80), resulting in the quantification of 856 lipid species from 10 µL of rat plasma. Sample extraction was completed using a Biomek i5 sample automation system (Beckman Coulter, Mount Waverley, VIC Australia). To each 10 µL plasma sample, 90 µL of extraction solvent (2-Propanol) containing stable-isotope-labelled internal standards (Lipidyzer™ Internal Standards Kit from Sciex, Framingham, MA, USA, and SPLASH LipidoMIX™, Lyso PI 17:1, Lyso PG 17:1, and Lyso PS 17:1, Avanti Polar Lipids, Alabaster, AL, USA) was added and then mixed for 20 minutes. Samples were then centrifuged (3500 x g for 10 minutes at 4 ºC). 70 µL aliquots of supernatant were then transferred into an Eppendorf 350 µL 96-well plate for LC-MS analysis. Samples were analysed within 24 hours of preparation. Sample volumes were extremely limited and therefore it was not possible to produce a pooled QC of study samples for analysis as per typical workflows in the field. Therefore a surrogate QC pool was prepared using a commercial pooled human plasma sample (BioIVT, NY, USA) and underwent replicate extraction (n = 5) using the method described. These replicate samples were periodically analysed throughout the analytical sequence to provide a standardised reference point..

3.2.5 Liquid Chromatography Mass Spectrometry (LC-MS)

The analytical system consisted of a Sciex ExionLC™ system coupled to an Exion Triple Quadrupole Linear Ion Trap (QTRAP) 6500+ MS Platform (SCIEX, Concord, ON, Canada). Lipid metabolites were chromatographically separated using a Waters Acquity BEH C_{18} reverse phase column (1.7 µm, 100 x 2.1 mm particle size; Waters Corp., Milford, MA, USA), maintained at 60°C. Full instrument settings are described in the appendix (7.1).

3.2.6 Data preprocessing

Peak picking and data normalisation were conducted using SkylineMS (81) (Version 21.1) and R Studio (82) (version 4.1) using in-house scripts. Chromatograms generated from this process can be viewed in the supplementary information (7.2). Lipid features were kept in the dataset if the relative standard deviation across the replicate QC samples was ≤ 30%. Logarithmic transformations were then applied to the raw data obtained from acquisition to normalise variance and to estimate the normal distribution required for univariate and multivariate analysis.

3.2.7 Statistical analyses

For multivariate statistics, the final data matrix was transferred to SIMCA 17.0.1 (Sartorius AG, Goettingen, Germany). Data were pareto-scaled prior to multivariate modelling. Principal components analysis (PCA) was performed to assess the measurement precision of the QC data, as well as to identify and remove outlier samples. Following PCA analysis, a supervised orthogonal projection to latent structure-discriminant analysis (OPLS-DA) was performed. Variable Importance for Projection Plot (VIP) were used to determine the importance of each lipid in the OPLS-DA model. Area under receiver operating characteristic curve (AUROC) were used to visualise and summarise the performance of the OPLS-DA model at distinguishing between the control, 1xmTBI and 2xmTBI groups. Following multivariate analysis, univariate tests were performed using a Kruskal-Wallis test, with Dunn's test applied post-hoc to determine intergroup differences (sham control, 1x mTBI and 2x mTBI). Statistical significance was deemed where $p \leq 0.05$. Box plots were produced using GraphPad Prism v8.0.0 (GraphPad Software, San Diego, California USA, www.graphpad.com).

3.3 Results

3.3.1 Multivariate analysis

Following data cleaning, the final dataset consisted of 856 reproducible lipids species from 19 different lipid classes. A PCA model was performed to assess the overall variation in the dataset (see appendix A.2). From the PCA, the replicate QC samples successfully clustered, demonstrating the reproducibility of the extraction and analysis. Three outlier samples (sham control group = 2, 1x mTBI =1) were identified within the PCA via Hotelling's T2 (95% CI) and removed from subsequent statistical analysis.

To identify the metabolic signature associated with TBI, supervised orthogonal projection to latent structure-discriminant analysis (OPLS-DA) was performed on the lipid data generated from sham control (n = 4), 1x mTBI (n = 6) and 2x mTBI (n = 7) groups (Figure 1). The sham control and 1x mTBI groups were classified with AUROC = 0.90 (R2 X = 0.637, R2 Y = 0.858, Q2 = 0.307); 1A (left), model and (right) corresponding loading). As demonstrated in Figure 1B, the 1x mTBI and 2x mTBI groups were classified with AUROC = 0.94 (R2 X = 0.558, R2 Y = 0.84, Q2 = 0.206). The model also discriminated the sham control and 2x mTBI groups with AUROC = 0.97 (R2 X = 0.603, R2 Y = 0.952, Q2 = 0.322) Figure 1C. To test the predictive capacity of this final model (Figure 1C), data acquired from the 1x mTBI group were projected onto the model (Figure 1D).

Given the results in the OPLS-DA models and to further stratify the three groups, a non-parametric Kruskal Wallis univariate analysis was performed using individual lipid species in the data set to clarify further which metabolites were driving the OPLS-DA models.

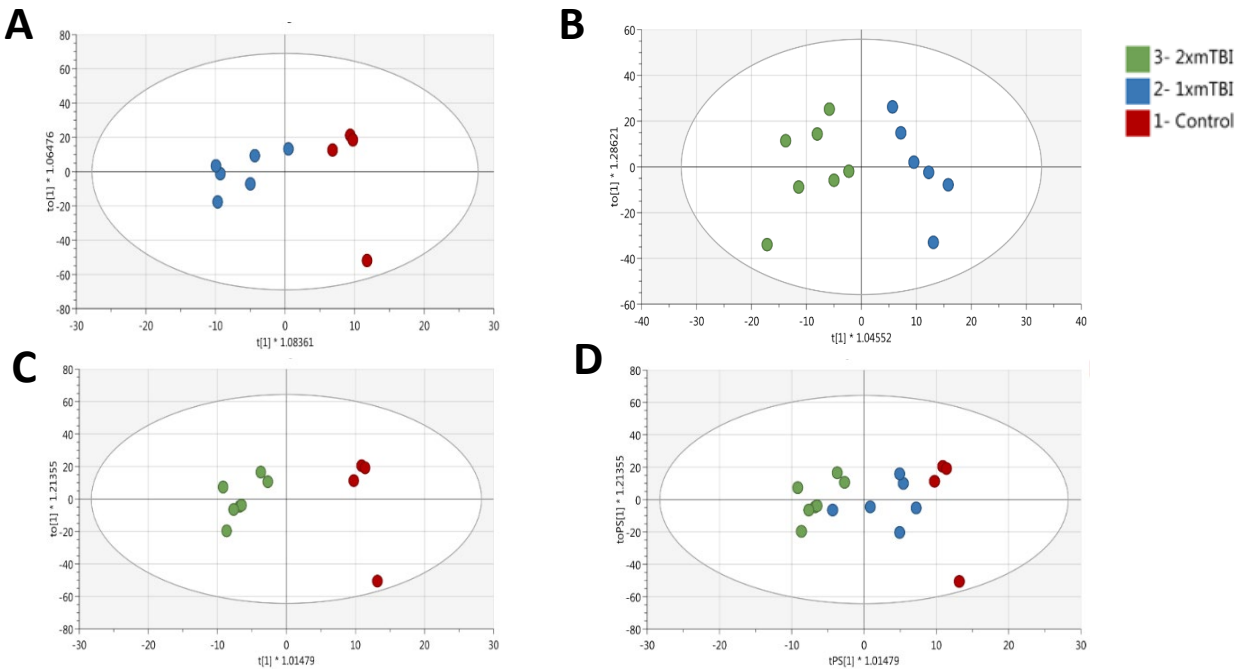

Figure 1. Orthogonal projection to latent structure-discriminant analysis (OPLS-DA) of plasma lipids following sham control, 1x or 2x mTBI.

A, OPLS-DA visualisations of sham control samples vs 1x mTBI samples. B, OPLS-DA Visualisations of 2x mTBI vs 1x mTBI. The model was scaled proportionally to R2x, R2x[1] = 0.143, R2Xo[1] = 0.415. C, OPLS-DA visualisations of sham control vs 2x mTBI. D, singular mTBI intervention (1x mTBI) was projected onto the final model for validation. The model was scaled proportionally to R2x, R2x[1] = 0.0886, R2Xo[1] = 0.548.

3.3.2 Individual plasma metabolites are altered in specific patterns in response to 1x or 2x mTBI

A non-parametric Kruskal Wallis Rank Sum Test was performed on all 856 individual lipid species identified in the data set, and a Post hoc Dunn's test was then completed to report inter-class differences (see appendix 7.4). 18 plasma lipids were found to be significantly different ($p \leq 0.05$) between the sham control, 1x mTBI and 2x mTBI groups, respectively. These lipids could be grouped into three distinct patterns based on response to injury at this subacute timepoint. Specifically, mTBI-related *increases* in concentration were found after mTBI for FFA 20:3 ($p = 0.04$), HCER 22:0 ($p = 0.04$), PE P-18:1/20:4 ($p = 0.02$), PE P-18:0/20:1 ($p = 0.05$), CE 14:0 ($p = 0.04$). Conversely, mTBI-related *decreases* were found for concentrations of lipids PS 14:0/18:2 ($p = 0.02$), HCER d18:0/26:0 ($p = 0.03$), and PI 20:0/18:2 ($p = 0.05$) when compared to the sham control (Figure 2).

The third pattern of lipids demonstrated opposing responses to single or repeated injury: When comparing 1x mTBI to sham control, *increased* concentrations of LPE 20:1 ($p = 0.01$), LPE 22:6 ($p = 0.01$), PI 16:0/18:2 ($p = 0.01$), LPE 22:5 ($p = 0.02$), PI 16:0/18:3 ($p = 0.03$), PI 18:1/18:1 ($p = 0.05$), LPG 18:2 ($p = 0.02$), PI 18:1/18:2 ($p = 0.04$), FFA 18:3 ($p = 0.05$), and PC 20:0/22:4 ($p = 0.05$) were observed. In contrast, the 2x mTBI group displayed significantly *decreased* concentrations of these same lipids when compared to both the sham control and 1x mTBI groups (Figure 2).

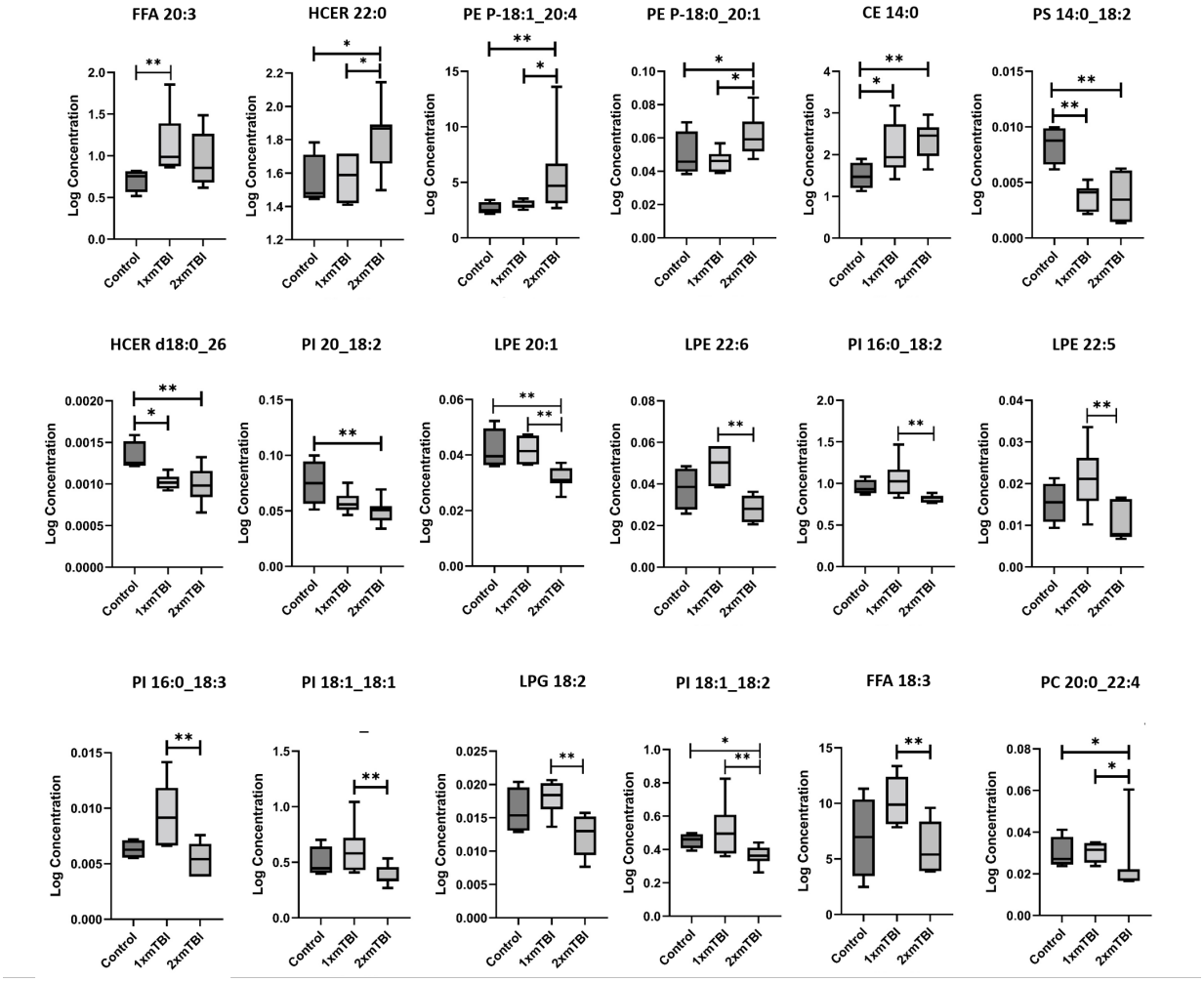

Figure 2. Three group box plot comparisons of significant plasma metabolites.

*Presented are metabolites that were deemed univariately significant in the Kruskal Wallis test ($p \leq 0.05$). Each lipid has three boxplots representing the minimum, first quartile, median, third quartile, and maximum for the sham control, 1xmTBI and 2xmTBI groups. Significant differences between groups are indicated above the boxplots by * ($p \leq 0.05$) or ** ($p \leq 0.01$).*

3.4 Discussion

Metabolic changes associated with mTBI are complex and can have central and peripheral physiological effects. LC-MS can provide unique insight into chemical perturbations which occur following TBI (11-13). Lipid species are broadly known to be disturbed following TBI; however, characterisation of individual lipid alterations after mTBI is an emerging line of enquiry (9, 83, 84). Here we applied a target lipid screen to measure 856 lipid species to investigate the effect of single vs. repetitive mTBI on the plasma lipidome in a rat mTBI model 11 days post injury, a time at which there are known oxidative and inflammatory mediators of secondary pathology (75, 77). The number rats (n = 20) used in this study places a limitation on the findings. This is particularly the case in the sham control group (n = 6), as 2/6 were removed as they were deemed outliers via Hotelling's T2 test (95% CI) during the principal component analysis (PCA). The two removed samples were both noted as haemolysed during sample acquisition. Although the samples were re-centrifuged to separate cellular contents and plasma prior to preparation, this may explain outlier identification. In future studies larger sample numbers would improve study validity. Furthermore, in the OPLS-DA modelling 1/4 of the controls is distinct from the other 3/4 which cluster tightly in the orthogonal plane suggesting noise that is orthogonal to the model separation.

The main finding of this study was the identification of 18 significantly altered lipids in rat plasma that could accurately distinguish between sham, 1x mTBI and 2x mTBI, indicating that the lipidome remains significantly altered in the subacute phase of mTBI, and that this pathology increases concomitant with repeated injury.

Multivariate OPLS-DA (sham control vs 1x mTBI; sham control vs 2x mTBI; 1x mTBI vs 2x mTBI) resulted in models with distinct separations between the classes. Furthermore, projection of the 1x mTBI intervention group onto the sham control vs 2x TBI model resulted in the 1x mTBI group predicted centrally between the sham control group and the 2x mTBI group, indicating that lipid alterations follow progressive trends with increasing mTBI insults. The

findings may provide further insight into the pathological consequences of increasing numbers of mTBI as seen in contact sports and military injuries.

Following multivariate modelling of the data, the univariate analysis indicated eighteen significant metabolites that distinguished between the sham, 1x mTBI and 2x mTBI groups. Further analysis of concentration ratios demonstrated three principal patterns across the identified biomarkers: i) increased lipid concentration with mTBI (1x or 2x); ii) decreased lipid concentration with mTBI (1x or 2x); iii) lipid concentrations that *increased* from sham control concentrations with 1x mTBI, however, *decreased* to a lower concentration than sham control or 1x mTBI in rats with 2x mTBI. Lipids conforming to the first identified pattern included PE(P-18:0/20:1), PE(P-18:1/20:4), FFA(20:3), HCER(22:0), and CE(14:0), which all increased in concentration with each additional mTBI. The two PE species, PE(P-18:0/20:1), and PE(P-18:1/20:4), have been linked to multiple neurodegenerative diseases including Parkinson's disease and Alzheimer's disease (85, 86), where they were found at increased concentrations in post-mortem brain. In addition, total PE concentrations significantly increased in the hippocampus at 24 hours after injury in a mouse model of repeated mTBI, and remain significantly elevated to 12 months post-injury (87). Given the roles for PE in myelin maintenance at the axonal node and vesicular formation (88, 89), the generalised mTBI-mediated increase in PE species 11 days post-injury may reflect heightened transport for reparative myelination at the node of Ranvier, for which we have previously described significant alteration after rmTBI in this model (76).

Free fatty acids such as FFA(20:3) are precursors to eicosanoids, which are important modulators of inflammation, cell signalling and vascular response (among others) throughout the central nervous system (90). These products of lipid peroxidation have been increasingly reported to accumulate after TBI in both tissue and biofluids, potentiating the pathological response (91, 92). As such, FFA concentrations have been suggested as a putative clinical biomarker of outcome (92). In the present study, our finding of increased plasma concentrations of FFA(20:3) with both 1x and 2x mTBI supports these clinical findings, potentially demonstrative of persisting lipid peroxidation and inflammation in this subacute post-injury period. Cholesterol esters increase

transiently in a rat CCI model, with CE(18:1) peaking at 3 days in the lesion and peri-lesional tissue (93). However, altered CE(14:0) has not previously been reported in a TBI model. Our results suggest the time course of CE alteration may be substantially different in closed head injury, with significant elevations in plasma still detected at 11 days post-injury in our closed-head rotational mTBI model. Indeed, the subacute elevations of lipids following this identified pattern warrant further investigation for capacity as injury biomarkers, given that they were readily detectable in plasma beyond the acute phase.

Regarding the second identified pattern of changes with decreased lipids, PE species have been previously reported to be down regulated in mouse brain lysosomes post TBI (73). Down regulation of PE's has been reported to decrease the viscosity of the lipid bilayer of cells (76). Additionally, it has been speculated that PE-P's may provide protection against oxidative stress (74), suggesting that down regulation of this lipid species post TBI may negatively impact normal CNS functions by reducing cellular defences against oxidative damage.

From the eighteen metabolites identified, PS(14:0/18:2), HCER(d18:0/26:0), and PI(20:0/18:2) displayed a biphasic response as the number of mTBIs increased. This third pattern of increases with 1x mTBI and decreases with 2x mTBI is paradoxical, although it mirrors our previous findings of microglial reactivity and oxidative damage in brain tissue in this model (75, 77), lending support to the biological plausibility of this finding. While these opposing responses to single and repeated injury are currently under investigation, they reveal that pathology may not follow a linear pattern with increasing injury but may instead involve distinct responses. Lipid species from the lysophosphoethanolamines (LPE) and phosphoinositols (PI) classes demonstrated an increased concentration in the 1x mTBI group when compared to the sham control group, however, the same metabolites decreased in the 2x mTBI group. Increases in LPE have been demonstrated in the hippocampus and cortex at 3, 6 and 12 months post-CCI in mice (87), suggesting that LPE alteration may be chronic after injury. LPEs have recently been shown to stimulate neurite outgrowth and reduce glutamate-mediated excitotoxicity in neuronal culture (94), indicating a beneficial role after injury. Likewise, PIs are key regulators of cytoskeletal

function and myelination, with tissue depletion linked to demyelination and axonal loss (95). The observed plasma decrease in LPE concentration after 2x mTBI may reflect a higher brain demand for reparative purposes.

The hypothesis for this study is the degree of lipidome perturbation in rat plasma will increase concomitantly with repeated injury in the subacute phase of mTBI. The sham control in the case of this study is the trauma caused by the closed-head weight-drop model. The control group described in the study is "non-brain trauma" as this group was only anesthetised twice throughout the study and did not experience brain trauma from the model. The 1 x mTBI group experienced one brain trauma and the 2 x mTBI group experienced two brain traumas. Therefore, given blood samples were drawn at the 11 days timepoint, which falls within the subacute time frame of mTBI, the use of sham control is adequate for the purposes of testing this hypothesis.

Our study also included small cohorts of rats in each group, and thus may have been underpowered, however, appropriate statistical methods were employed to account for the small cohort size and detect meaningful differences. Further work is needed to determine if these preliminary findings are replicable in a larger cohort, and to discover whether any key lipid changes were missed in this initial analysis. In future studies a non-head injury trauma model would be beneficial (e.g. burn/incision) as a pathophysiological comparison to the TBI model. Comparison of the lipid profiles between the two injury types may possibly provide insight into whether the key findings in these studies are directly linked to TBI injury. For example, lipids that cross the blood brain barrier after head injury will differ to lipids present in the burn model. If the changes are as a result of systemic inflammation, rather than TBI itself, then non-head trauma, trauma models will appear similar to head trauma, trauma models. Lastly, we cannot conclude to whether our findings in female rats are translatable to males. Studies show disparity in TBI research, with comparatively little known about female biological responses to injury (96). Since female sex hormones may be neuroprotective following TBI (78), future studies including both female and male rats are needed to identify sex-dependent changes in lipid profiles.

3.5 Conclusion

Lipids compose nearly 60% of the brain (97) and readily cross the blood-brain barrier (98), allowing for detection in whole blood, plasma or serum (1, 16). Furthermore, lipids are key molecules in a plethora of biochemical and physiological processes, including cellular signalling, immune responses, membrane lipid structure, and inflammatory pathways (7, 68, 99). Measuring the perturbations of the lipid species in clinically relevant mTBI models provides further insight into the underlying pathophysiology, and highlights lipid alteration as a potential therapeutic target to improve outcomes following mTBI. The findings from our lipidomic analysis build on reported TBI insights in the literature (13, 15-17, 93, 100). Furthermore, we provide novel insights into the lipidomic signature of mTBI. Given our finding of bi-directional lipid concentration changes in plasma with single and repeated injury, alteration of lipid species may be a new avenue for biomarker research in mTBI. Future work ought to establish the degree to which pathological brain changes are reflected by plasma lipids and characterise the temporal lipid profile after single and repetitive injury.

4 Profiling the perturbed plasma lipidome in human mTBI patients

This chapter has been written in the style of a research article using the Journal of Neurotrauma guidelines for authors.

For this thesis chapter, I performed the lipidomics data acquisition, data analysis, interpretation, and writing, editing, and reviewing the chapter.

Samples were provided by Curtin University.

Authorship order	Contribution (%)	Concept Development	Lipidomic Data Collection	Lipidomic Analyses	Drafting of chapter	Chapter review
Harrison Szemray	80%	X	X	X	X	X
Nathan Lawler	10%	X				X
Luke Whiley	10%	X				X

By signing this document, the Candidate and Principal Supervisor acknowledge that the above information is accurate and has been agreed to by all other authors.

Candidate **Principal Supervisor**

Link: Results from Chapter three indicate that in rats metabolic shifts occur in the plasma lipidome in the subacute phase at day 11 following mTBI which suggests a progression of biomarker severity as the TBI intervention increases. However, the relevance of these results to the clinical setting is unknown. Given the importance of clinical translation in the field of TBI the second study sought to explore perturbations in the blood plasma lipidome of human participants compared to age and sex balanced healthy controls by applying the same comprehensive lipid analysis used in the first study.

Abstract

There are currently no effective interventions for preventing secondary neurodegeneration that follows mTBI injury due to the underlying mechanisms of mTBI remaining poorly understood. Recently, mTBI research has shifted towards using small molecule or non-protein biomarkers in blood plasma or serum as it is minimally invasive biofluid. Recent advancements in plasma metabolomic analyses offer a unique insight into mTBI without relying on proteins. However, there is minimal literature that analyses the plasma lipidome in clinical mTBI. Therefore, it is evident that minimally invasive biomarkers are required to identify the metabolomic fingerprint of mTBI's pathological progression. The purpose of this study was to profile the plasma lipidome in clinical mTBI patients for future research of mTBI induced neurodegeneration. We identified 224 individual lipid species, and nine lipid classes were significantly perturbed in a cohort of thirty individuals diagnosed with mTBI at Royal Perth Hospital. The main findings of this study were: i) immediately post injury (Range = 1.25–45 h) mTBI patients indicate no statistical difference from control; ii) mTBI can be distinguished from control at patient follow-up (Range = 25–55 days). iii) Monoacylglycerols are the most prominent variable that drive the differences between the controls and mTBI patients at the inception and follow-up timepoints.

4.1 Introduction

Traumatic Brain Injury (TBI) is a neurological disorder caused when a sudden external force is applied to the head, resulting in pathophysiological changes with the severity primarily linked to the amount of force applied (1). Additionally, secondary factors such as previous injury and impact site may have some effect on TBI severity. In 2019, it was estimated that sixty-nine million people (95% CI 64-74 million) suffer from TBI and the associated sequela of conditions that occur post injury (2, 24). Furthermore, if the plethora of alternative TBI-causing events (e.g., falls, assaults, sports injuries, explosions, and penetrating head injuries) were accounted for, the estimated incidence of TBI would be much higher.

The effects of a TBI can disrupt normal cellular functions via i) a shear force acting in a direction that's unaligned but parallel to the head. ii) direct force applied to the head (i.e., physical assault). iii) rotational forces that cause rapid rotational acceleration of the head causing the brain to impact against the inside of the skull. These pathophysiology disturbances can be divided into two injury types: primary injury and secondary injury. Primary TBI injuries occur from the initial trauma to the brain and can result in epidural hematoma, subdural hematoma, subarachnoid haemorrhaging, and intraventricular haemorrhage, causing damage to the vasculature neural glial tissues (22). Secondary injury is the leading cause of TBI caused deaths in hospitals (23) and occurs days to months following primary injury, causing damage to the brain at a cellular and molecular level. At this stage, breakdown of the blood-brain barrier and cell death occurs (24).

Over the past decade there has been a surge in TBI biomarker research for use in clinical applications. Published methodologies have focused on proteins as biomarkers for mTBI, which have been found to be not specific or sensitive to mTBI (1, 101). Ideally, brain tissue is the best sample for mTBI biomarker analysis as it is the site of injury. However, due to patient survival being the priority, this sample type is impractical for mTBI biomarker analysis in the clinical setting. Compared to cerebrospinal fluid collection, the minimally invasive nature of phlebotomy makes blood an ideal candidate for mTBI biomarker analysis. A potential source of alternative mTBI biomarkers may be present in the lipidome. Although lipids are not currently used in

clinical analysis; however, lipids have been evaluated as potential biomarkers in major neurological conditions such as Alzheimer's Disease and Dementia (48, 49, 102-105). Furthermore, lipids readily cross the blood-brain barrier and are associated with neurodegeneration (50), further highlighting the potential of blood lipids as prognostic biomarkers for mTBI.

Plasma lipid perturbations have been previously reported in clinical mTBI studies but typically focus on the difference between types of TBI (i.e., mild TBI, moderate TBI, and severe TBI) or at acute (≤24 hours post TBI), subacute (1 day to 3 weeks post TBI) and chronic (>3 weeks post TBI) time points (106). Fiandaca and colleagues utilised tandem mass spectrometry to identify a six-metabolite panel (2-hydroxypalmitic acid, stearic acid, tauroursodeoxycholic acid, phosphatidylethanolamine plasmalogen, diacyl-phosphatidylethanolamine and lysophosphatidylcholine) where they observed difference between athletes who experienced an mTBI and non-mTBI athlete controls at ≤6 hours post mTBI (12). Using a similar approach Emmerich et al. (2017) observed a significant decrease in plasma concentration of PI, SM, LPC, LPE, PC, and PE lipid classes ten years post mTBI when compared to non-mTBI soldiers (11). Whilst previous studies on human cohorts have demonstrated that various lipid classes and species show abnormal concentration levels post mTBI at the acute and chronic phase. To the best of our knowledge, no clinical research has profiled the longitudinal changes in an mTBI cohort aged and sex balanced with healthy controls using a comprehensive lipidomics method

To address this gap in the literature, we utilised ultra-high performance liquid chromatography-mass spectrometry to characterise the plasma lipidome of mTBI patients admitted to Royal Perth Hospital (RPH) at patient inception (acute phase) to the emergency department and follow-up (chronic phase). We identified 225 lipid species that accurately distinguished between healthy controls and the mTBI at the inception and follow-up time points. Summed lipid class concentrations showed minimal variability between patient inception and control. However, analysis of plasma at patient follow-up demonstrated markedly increased concentrations of SM, DCER, PC, CER, HCER, and PE. Alternatively, the MAG lipid class decreased in concentration at follow-up.

4.2 Materials and methods

4.2.1 Participant recruitment and inclusion criteria

Recruitment for this study occurred between September 2015 and January 2018. The participant cohort and study protocols detailed in the present study were obtained from a larger study conducted at Royal Perth Hospital (RPH) Emergency Department (107) (n = 66). A total of 30 patients diagnosed with mTBI were selected for this study. Sample size estimates were not performed as this metabolomics study was regarded as an exploratory pilot study. In many instances the metabolites identified were substantial, indicating the sample size was adequate. Blood samples were collected at patient inception (I.e., day of mTBI insult or within 48 hrs). Patients who enrolled were then asked to return for a follow up blood sample and assessment within 40 days of mTBI diagnosis. Inclusion criteria for the study was set as: patients provided verbal confirmation that their closed head injury resulted from trauma or mechanical force and involved a change in brain function, were aged between 18 and 50 years old, had not received a brain CT scan, score >14 on the Glasgow Coma Scale and presented to the Emergency Department within 48 hrs of head injury. Patients were excluded from the study if they were unsuitable for MRI procedures, head injury was deemed to be caused by a seizure, were non-English speaking, had a previous medical history of cognitive impairment, were homeless or were substance dependent. A healthy control cohort (n = 36) were recruited using community members to serve as a baseline indicator for blood-based biomarker outcomes and where balanced for both age and sex to the mTBI cohort. Ethics approvals were obtained from the RPH Human Ethics Committee (RPH Ethics Approval Number REG15-062/ANZCTR:123615000543583) and Murdoch University Human Research Ethics Committee (Project Number: 2021/077).

4.2.2 Blood sample collection and study design

Blood sampling procedures followed previously established workflows of Gotz and colleagues (108). Briefly, patients who presented to ED of the hospital and met the study criteria were asked to provide written consent directly or from their next-of-kin for study involvement. Following consent, an on-duty research nursing staff member obtained a whole blood sample via

venepuncture and assessed the patient using the neuropsychologic testing battery. Following venepuncture, whole blood was centrifuged, and the plasma was aliquoted and stored at –80˚C until analysis.

4.2.3 Sample preparation for liquid chromatography mass spectrometry

On the day of analysis, plasma aliquots were thawed on ice, and 10 µl of plasma was transferred to a 96-well plate. Lipid extraction was completed using a Biomek i5 sample automation system (Beckman Coulter, Mount Waverley, VIC 3149, Australia) where 90 µL of extraction solvent (2-Propanol) containing Lipidyzer™ Internal Standards (Sciex, Framingham, MA, USA) and SPLASH LipidoMIX™ (Lyso PI 17:1, Lyso PG 17:1, and Lyso PS 17:1, Avanti Polar Lipids, Alabaster, AL, USA) was added to each sample well and then mixed for 20 minutes. Samples were then centrifuged at 20˚C (3500 x g for 10 minutes). An aliquot of 70 µL of each supernatant was then transferred into an Eppendorf 350 µL 96-well plate for liquid chromatography−mass spectrometry (LC-MS) analysis. Samples were placed in the autosampler for analysis, which was maintained at 10˚C, with all samples analysed within 24 hours of extraction. Quality control samples (QC) were prepared using a commercial pooled human plasma sample (BioIVT, NY, USA) and underwent replicate extraction (n=5) using the method described. These samples were periodically injected throughout the analytical sequence.

4.2.4 Liquid chromatography mass spectrometry

Samples were analyzed using Liquid Chromatography-Mass Spectrometry (LC-MS) for Lipidomics analysis. Separation was performed using a Exion liquid chromatography 1.0 system coupled to a Triple Quadrupole Linear Ion Trap 6500+ MS Platform (SCIEX, Concord, ON, Canada). Lipid metabolites were chromatographically separated using a Waters Acquity BEH C18 reverse-phase column (1.7 µm, 100 x 2.1 mm particle size; Waters Corp.), which was maintained at 60°C. Complete instrument settings are described in appendix (A.1)

4.2.5 Data analysis

Target LC-MS peaks were integrated using SkylineMS version 21.1 (109) . Chromatograms generated from this process can be viewed in the supplementary information

(7.5) Metabolites were normalised using SPLASH® Lipidomix® internal standards and lipidizer standards, providing each target lipid with a surrogate internal standard (1-5 per lipid class). A ratio was then created by dividing the peak area of the lipid by the peak area of the internal standard. Data were then checked and excluded if the relative standard deviation of the QCs >30% in the quality control samples. Logarithmic transformations were then applied to the raw data to normalise prior to univariate and multivariate analysis. Before any formal statistical models were tested, principal components analysis was performed on the complete data set with the scores plot labelled as either QC or Sample (See supplementary information 7.6). Here, the PCA was used to visually assess the measurement precision of data and identify and remove outliers resulting from poor sample collection or instrument error. After this assessment, the QC data were removed from any subsequent statistical analysis. Only reproducible peaks obtained from the process above were included for final statistical analysis.

4.2.6 Statistical analysis

Supervised multivariate statistical modelling was performed with 850 lipid species using orthogonal projections to latent structure discriminant analysis (OPLS-DA) using the R studio environment (version 1.4.1717) with the open-source package metabom8 (Version 1.00), available from Github (https://github.com/tkimhofer/metabom8 - date last accessed 16/10/2021). The Cliff's delta statistic was applied to the 850 measured lipids to assess the effect size of the group differences (i.e., control and follow-up) and the Benjammini-Hochberg procedure was applied to control the false discovery rate. Absolute Cliff's delta scores were interpreted as -1 to 1, indicating maximum difference, and zero, indicating no difference. Univariate analysis was conducted for each lipid metabolite and summed lipid classes (i.e., each lipid species concentration was summed for each individual lipid class). The null hypothesis was tested that there were no differences between the three sample groups means (i.e., control, inception, and follow-up) using a Kruskal-Wallis test. Where a significant main effect was observed, a Dunn's posthoc test was applied to determine intergroup differences. Statistical differences were determined as $p \leq 0.05$.

4.3 Results

On average, patients (females n = 11, males n = 19, average age = 29.03) were admitted to the ED 10.86 hours following injury (SD = 10.49, Range = 1.25–45 h) and attended follow-up 34.61 days later (SD = 7.19, Range = 25–55 days). Patients most common mTBI injuries were assaults, bicycle accidents, falls, sports injuries, being hit by falling objects and motor vehicle accidents.

Following the lipidomic analysis, the final data matrix consisted of 850 reproducible lipid species (RSD ≤ 30%), which was determined using the pooled QC samples. To visually assess the data reproducibility and identify any sample outliers, a principal component analysis model (PCA) was performed. From the PCA, we observed clustered QC samples and greater variance in the patient samples indicating good analytical reproducibility (see appendix A.4)

To elucidate the phenotypic lipid signature of mTBI, supervised OPLS-DA (Figure 1) was performed on the 850 lipids and generated using the healthy control cohort (n = 36) and the mTBI cohort (n = 30) follow up time point. The OPLS-DA classified the healthy control and mTBI follow up cohorts with AUROC = 0.83 (R^2 X = 0.58). Furthermore, to test the predictivity of the OPLS-DA model, the data acquired from the mTBI inception timepoint was projected into the OPLS-DA model to test if it is possible to predict plasma lipid disturbances at the 24-hour timepoint. Following projection of the inception timepoint, 43% were correctly classified with mTBI see Figure 1B. The eruptions plot Figure 1C shows the combined lipids and the Cliff's Delta effect size differences between the control and follow up groups. The plot emphasizes decreased levels of MAG (14:0, 22:4, 16:1, 18:1, 18:3), FFA (20:4, 20:3), DAG (20:0/20:0, 16:0/18:3), and LPC (20:4, 20:2) at follow up and increased levels of PC (18:1/22:6, 18:1/18:2) appear to drive the differences between the two groups.

Figure 3A

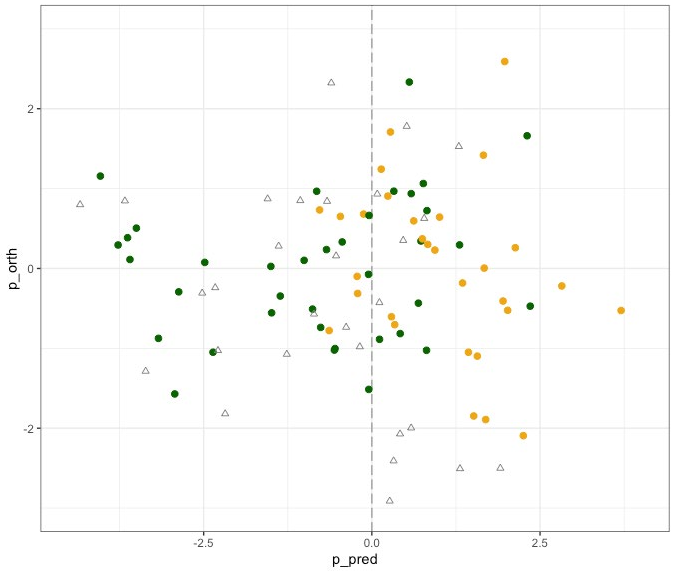

Figure 3B

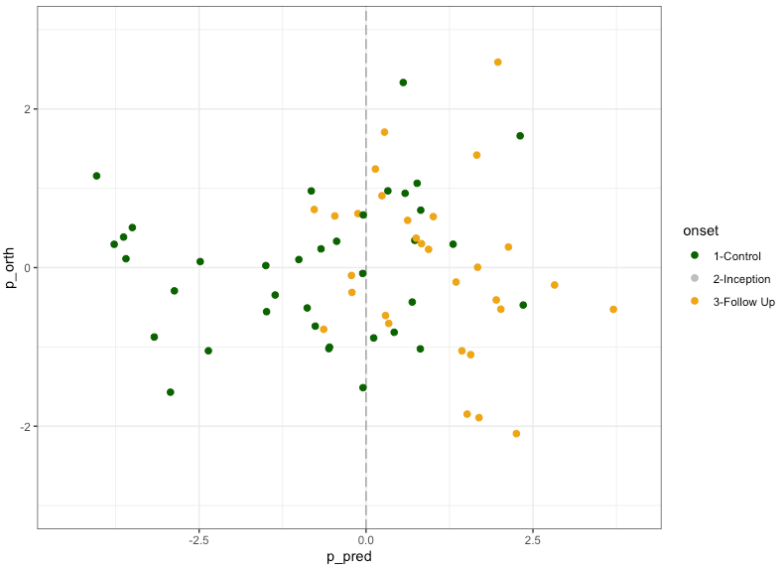

Figure 3C

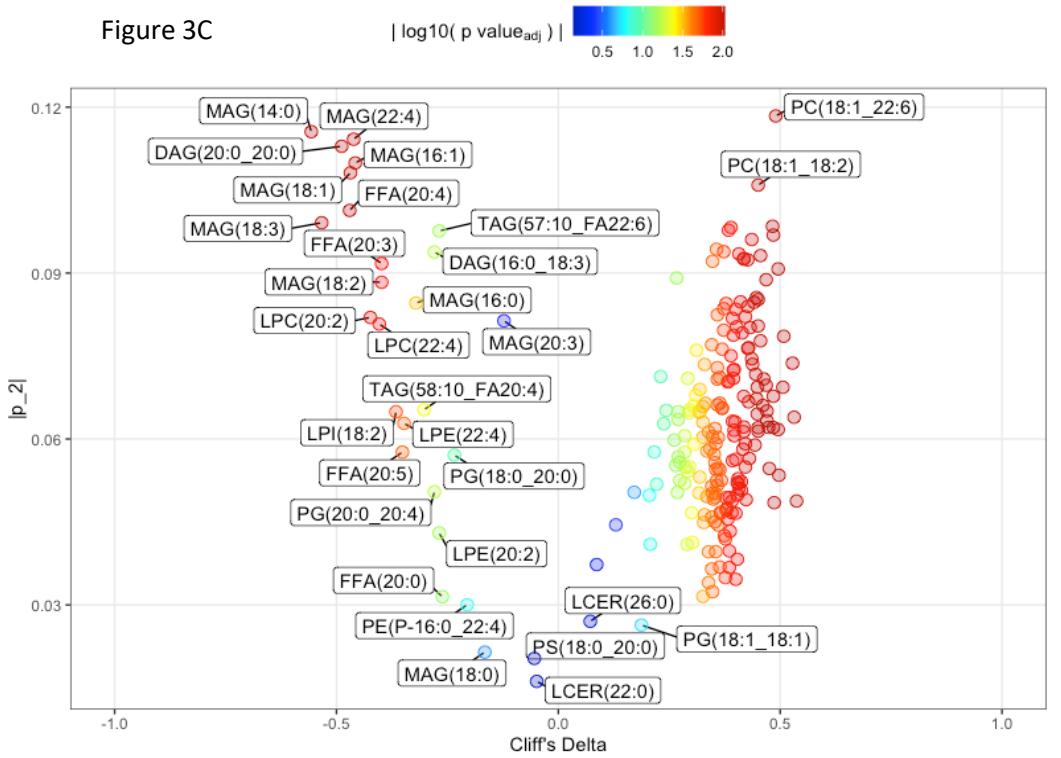

Figure 3. OPLS-DA model visualizations of healthy age and sex balanced controls and mTBI patients.

Figure 3A. Scores plot showing control (n = 36) and follow up (n = 30). Figure 3B. OPLS-DA model visualizations. Scores plot showing control (n = 36) and follow up (n = 30). Inception (n = 30) was projected for model validation. Figure 3C. Volcano plot of the 850 lipid species and the comparative effect size differences between the control, inception and follow up groups. The plot was formed from the Cliff's delta and log 10 p values of the data. Variables are color-coded for statistical significance.

Lipid Class	p value	Control-Inception	Control-Follow Up	Inception-Follow Up
Monoacylglycerols	3.13E-04	1.70E-01	1.10E-03	6.65E-05
Sphingomyelins	7.16E-04	3.01E-01	8.52E-04	2.49E-04
Diacylglycerides	1.72E-03	1.98E-01	3.28E-03	3.44E-04
Hexosylceramides	2.77E-03	4.22E-01	1.46E-03	1.27E-03
Ceramides	4.70E-03	2.69E-01	4.67E-03	1.11E-03
Phosphocholines	5.27E-03	3.49E-01	3.45E-03	1.64E-03
Phosphoethanolamines	2.03E-02	2.21E-01	1.98E-02	3.60E-03
Cholesterol esters	3.88E-02	3.35E-01	1.99E-02	9.08E-03
Lactosylceramides	4.04E-02	3.51E-02	2.20E-01	6.97E-03
Phosphoglycerols	7.84E-02	6.79E-02	1.99E-01	1.31E-02
Lysophosphoinositols	1.52E-01	4.52E-01	4.68E-02	4.35E-02
Phosphoinositols	1.53E-01	3.33E-01	2.99E-02	8.37E-02
Lysophosphocholines	2.24E-01	2.09E-01	4.18E-02	1.90E-01
Triacylglycerides	2.27E-01	2.02E-01	4.27E-02	1.99E-01
free fatty acids	2.41E-01	1.92E-01	4.64E-02	2.20E-01
Lysophosphoglycerols	3.28E-01	1.17E-01	3.91E-01	8.16E-02
Phosphoserines	6.37E-01	4.61E-01	1.87E-01	2.26E-01
Lysophosphoethanolami	6.75E-01	2.98E-01	1.91E-01	3.72E-01
Diacylglycerides	6.82E-01	2.81E-01	3.72E-01	1.94E-01

Table 1. Results from the Kruskal Wallis Rank Sum Test for summed lipid classes.
Analysis was performed on the 19 lipid classes identified in the data set. A Post hoc Dunn's test was then completed to report inter-class differences. Significance was deemed at less than or equal to 0.05. 9 lipid classes significantly distinguished between control, inception and follow up. Visualisation of these data as jitter plots can be found in the appendix (7.7)

Lipid Species	% relative standard deviation in the pooled quality control	*p* value	Control-Inception	Control-Follow Up	Inception-Follow Up
MAG(14:0)	2.38E+01	6.25E-06	3.40E-01	1.47E-05	6.31E-06
HCER(d18:0/26:0)	1.75E+01	2.14E-05	1.67E-01	1.46E-04	6.31E-06
HCER(14:0)	1.69E+01	8.53E-05	2.89E-01	1.66E-04	3.99E-05
DAG(20:0/20:0)	5.01E+01	8.85E-05	2.91E-01	1.69E-04	4.15E-05
CER(26:0)	1.55E+01	1.20E-04	1.14E-01	9.59E-04	2.06E-05
SM(14:0)	8.32E+00	1.57E-04	1.96E-01	5.17E-04	4.15E-05
MAG(18:3)	2.15E+01	1.98E-04	4.62E-01	9.41E-05	2.67E-04
MAG(22:4)	2.81E+01	3.89E-04	2.60E-01	6.67E-04	1.24E-04
PC(18:0/18:2)	9.75E+00	4.10E-04	4.00E-01	1.37E-04	6.41E-04
HCER(16:0)	8.82E+00	4.27E-04	2.78E-01	6.44E-04	1.45E-04
CER(14:0)	1.23E+01	4.50E-04	2.30E-01	9.16E-04	1.22E-04
PC(18:1/22:6)	1.48E+01	5.40E-04	4.91E-01	2.52E-04	5.03E-04
MAG(18:1)	1.70E+01	5.42E-04	3.15E-01	6.31E-04	2.10E-04
PC(20:0/20:4)	1.41E+01	7.63E-04	2.07E-01	1.63E-03	1.73E-04
HCER(18:1)	2.08E+01	7.84E-04	1.44E-01	2.81E-03	1.33E-04
LCER(14:0)	1.02E+01	7.91E-04	1.46E-01	2.78E-03	1.35E-04
DCER(20:1)	3.19E+01	8.60E-04	3.28E-01	2.04E-04	1.64E-03
HCER(20:1)	2.14E+01	8.69E-04	4.80E-01	4.27E-04	6.41E-04
CE(20:4)	2.03E+01	1.08E-03	2.54E-01	1.94E-04	3.00E-03
PC(16:0/18:2)	1.48E+01	1.14E-03	4.27E-01	6.76E-04	6.31E-04
HCER(d18:0/26:1)	2.74E+01	1.20E-03	1.40E-01	4.04E-03	1.92E-04
PC(18:0/20:1)	2.25E+01	1.28E-03	3.24E-01	1.21E-03	4.49E-04
SM(20:1)	7.14E+00	1.30E-03	4.72E-01	4.99E-04	1.09E-03
HCER(d18:0/20:0)	1.84E+01	1.37E-03	2.04E-01	2.06E-04	5.04E-03
FFA(20:4)	1.52E+01	1.38E-03	3.69E-01	3.61E-04	1.87E-03
CER(20:1)	1.62E+01	1.40E-03	3.06E-01	1.42E-03	4.49E-04
HCER(d18:0/22:0)	1.44E+01	1.60E-03	3.26E-01	1.44E-03	5.46E-04
MAG(16:1)	1.08E+01	1.63E-03	4.98E-01	6.74E-04	1.16E-03
PC(18:1/18:2)	1.12E+01	1.66E-03	4.34E-01	8.97E-04	8.79E-04
DCER(22:1)	1.15E+01	1.79E-03	3.81E-01	1.21E-03	7.51E-04
PC(18:1/20:4)	1.24E+01	1.82E-03	3.66E-01	1.31E-03	7.17E-04
DCER(26:1)	1.43E+01	1.95E-03	1.46E-01	5.48E-03	3.11E-04
HCER(22:0)	1.40E+01	2.22E-03	3.45E-01	1.71E-03	7.76E-04
PC(18:1/20:1)	1.91E+01	2.41E-03	3.03E-01	2.25E-03	7.05E-04
HCER(26:0)	1.67E+01	2.43E-03	3.57E-01	1.75E-03	8.79E-04
TAG(56:7/FA18:0)	1.40E+01	2.48E-03	1.18E-01	2.90E-04	1.59E-02
DCER(20:0)	1.38E+01	2.49E-03	1.81E-01	4.95E-03	4.49E-04
PC(16:0/20:1)	1.84E+01	2.49E-03	4.29E-01	1.30E-03	1.20E-03
PC(18:1/20:5)	2.03E+01	2.65E-03	2.80E-01	4.89E-04	4.91E-03
TAG(56:6/FA20:5)	1.25E+01	2.65E-03	1.45E-01	3.32E-04	1.27E-02

Table 2. Results from the Kruskal Wallis Rank Sum test for lipid species.
A Kruskal Wallis Rank Sum Test was performed on all 850 individual lipid species identified in the data set. A Post hoc Dunn's test was then completed to report inter-class differences. Significance was deemed at less than or equal to 0.05. 225 lipid species significantly distinguished between control, inception and follow up. The table includes the top 40 lipid species, the rest can be viewed in supplementary (7.9). Visualisation of these data can be found in the supplementary (7.8).

To elaborate on which lipid species within the nine lipid classes were driving the statistical differences and to identify any potential biomarkers outside of these classes, we applied the same methodology to all 850 lipid species from the final data set (Table 2). The Kruskal Wallis and Post hoc Dunn's test indicated that 225 individual lipid species were univariately significant between the control, patient inception, and follow-up groups. It is worthy of mention that not all these lipids were from the nine classes identified during summed class analysis (Table 1). A general trend in the data displays minimal statistical significance between the control and inception groups, whereas major statistical significance is indicated between control and follow-up, as well as inception and follow up.

4.4 Discussion

Lipids account for approximately 60% of the brain's dry weight and have been demonstrated to cross the blood-brain barrier, and can be readily accessible in whole blood, plasma, or serum, highlighting lipids as a potential biomarker in incidences of mTBI (1, 16, 110). In the present study, we applied a targeted lipid screen using liquid chromatography mass spectrometry to measure 850 lipids in human blood plasma. This study aimed to profile mTBI patients with two timepoints at inception and patient follow up compared to an age and sex balanced healthy control cohort. The main findings from the current study were: i) immediately post injury (Range = 1.25–45 h) mTBI patients increased concentrations of LCER and PE; ii) mTBI can be distinguished from control at the follow-up approximately 34.61 days later (Range = 25–55 days). iii) Monoacylglycerols are the most prominent variable that drive the differences between the controls and mTBI patients at the inception and follow-up timepoints.

Multivariate OPLS-DA modelling of the age and sex balanced healthy controls and the mTBI patients at the follow-up timepoint indicated that a metabolic shift is maintained between mTBI patients and controls (mean = 34.61 days) post mTBI injury (Figure 1A). Noticeably, 17% of the follow up data points are incorrectly classified in the model. After reviewing patient metadata, we suggest that the incorrect classifications are due to patients sustaining mTBI injuries

through various incidents including assaults, bicycle accidents, falls from varying heights, sport injuries, being hit by falling objects and motor vehicle accidents. The variation displayed by the follow-up timepoint possibly indicates an association of head trauma severity (i.e., force applied to the brain), and perturbations displayed in the plasma lipidome.

To further assess the validity of the OPLS-DA model we then projected data from the patient inception timepoint (≤48 hours post mTBI injury) onto the model (Figure 1B). Minimal metabolic separation was displayed between the control and the projected inception timepoint (Figure 1B) on the OPLS-DA. 43% of inception data points clustered with the follow-up samples, while the remainder clustered throughout the control group suggesting that lipid changes post mTBI may only be observed > 48 hours after initial mTBI injury. The posthoc Dunn test reported 25 out of 850 lipid species were statistically different between control and inception groups (Table 2). Further supporting the concept that lipidomic alterations caused by mTBI are not seen directly after injury and that it takes time for the pathological mechanisms of mTBI to occur. Fiandaca et al., reported a six-metabolite panel that could accurately classify acute mTBI at ≤6 hours and provides similar classification at 2, 3 and 7 days contradicts the findings in this study (12). Included in Fiandaca et al.'s 6 metabolite panel are PE (P-16:0/20:4) and FA (18:0) which we report as statistically insignificant in the RPH cohort. Interestingly, PE (16:0/22:6) was found to be statistically significant at the patient follow-up timepoint but not at the inception timepoint (≤48hours). Our results demonstrate a long-term perturbation far beyond the current no same day return to play guidelines used when an athlete has sustained a concussion (19).

In parallel to the OPLS-DA modelling, a volcano plot of the data revealed a significant decrease in the monoacylglycerol (MAG) lipids was driving the class difference between healthy controls and mTBI patients at the follow-up timepoint (Figure 1C). This finding was supported in univariate analysis of the data as 9 MAGs demonstrated statistical significance between the groups (table 2). At patient inception MAG plasma concentration levels were insignificantly elevated, at patient follow up plasma concentrations decrease past the minimum quartile reported in the inception group. To the best of our knowledge no-one else has reported these findings. Inhibition of monoacylglycerol lipase, the enzyme responsible for the breakdown of

monoacylglycerol, has been reported to promote neurological recovery in a mouse model of repetitive mTBI (111). Under normal metabolic conditions, 75% of TAGs are produced via the acetylation of MAG in the enterocytes of the intestines (112). Our findings indicate TAG significantly increase in concentration between the control and follow-up groups, suggesting a temporally accelerated metabolism of MAG following mTBI injury.

Following multivariate modelling, univariate statistical analysis further supported the concept of metabolic shift. Here, significant differences were observed in 225 lipid species between healthy control and the mTBI cohort at follow up (Table 2). Although it's likely not all these lipid species are directly associated with mTBI, some may provide insight into the various pathophysiological mechanisms of mTBI. Our results demonstrate a significantly increased concentration in eight sphingomyelin species (14:0, 18:0, 18:1, 20:1, 24:0, 24:1, 26:0 and 26:1) in the blood plasma at the patient follow-up timepoint. Sheth et al., reported significantly increased levels of SM in the blood plasma of rodents following mTBI, suggesting that SM may play an important role in mTBI pathophysiology (16). Experimental rodent models have indicated that inhibition of sphingomyelinase mitigates neuroinflammation, preserves mitochondria, and improves recovery of brain functionality (113, 114). Additionally, we report an increase in 11 CER species (14:0, 16:0, 18:0, 20:0, 20:1, 22:0, 22:1, 24:0, 24:1, 26:0 and 26:1). These findings support the results previously reported in an experimental model by Novgorodov and colleagues, who demonstrated that mTBI stimulates the biosynthesis of ceramide, which suggests that increased conversion of SM to CER occurs post mTBI injury after 48 hours (114). CE (14:0, 20:0, 20:4, 20:5, and 22:6) also demonstrated a significant increase, suggesting increased esterification of cholesterol following mTBI. We also report an increase in phospholipid lipid classes; PC (such as, 18:0/18:2, 18:1/22:6, 16:0/18:2 and 18:1/18:2) and PE (such as, P-18:1/22:6, P-18:1/20:5, P-18:0/22:4 and P-16:0/20:1) which supports the findings of Emmerich and colleagues' experimental model (9).

4.4.1 Limitations

While our study reveals important findings in lipid species associated with mTBI injuries, our study does have limitations. First our study only evaluated a small cohort which inherently

can reduce the statistical significance of our data; however, false discovery rates were applied, and our cohorts were aged, and sex balanced, minimising any spurious findings. Second, it was not possible to control the dietary intake of the participants over the course of the study. Research demonstrates that participants with higher body mass indexes or lipid rich diets have significantly altered lipid concentrations when compared to lower body mass index or reduced lipid diets (115, 116). As such, it is possible some metabolite changes are associated with diet and further follow-up studies are warranted to investigate the influence of diet and lipids. Third, the multi-ethnic cohort utilised in our study may have impacted results due to the large differences in plasma lipid concentrations in various ethnic groups (117). Fourth, we do not know the amount of force that caused the mTBI in participants (i.e., fall, sports related injury, or mild car crash). Future studies in human cohorts should try to control for injury events that have similar force characteristics (i.e., amount and type of force applied to the brain). Further TBI research in an environment controlled for injury type, diet and body mass index warrants further research, however, controlling these variables proves to be difficult in the TBI niche. A possible avenue that could possibly control these variables is TBI in the setting of professional sport, where diet, physical health and injuries are closely monitored.

4.5 Conclusion

The development of improved diagnostic apparatuses and clinical management for mTBI is hindered by the incomplete understanding of the dynamic interplay of multiple pathophysiological cascades that occurs as a secondary injury following primary injury. In this study, we established significant lipidomic profiles for mTBI at the sub-acute and acute phases. These data support current findings in both experimental and clinical models of mTBI. Additionally, we report for the first-time novel biomarkers that associate with mTBI; however, these require validation in a larger cohort. The identification of novel mTBI biomarkers allows future research to identify specific metabolic pathways that mTBI impacts. This study demonstrates a progressive metabolic shift in the lipidome following mTBI and provides further evidence for using blood-based lipid biomarkers in the diagnosis and management of mTBI. The lipid species identified in this study warrant further research as they may provide biological

information about the mechanisms of mTBI or the opportunity for therapeutic interventions leading to improved patient outcome. Metabolomic profiling of the plasma lipidome presents an alternative solution to mTBI diagnosis and management, that is not being met by current healthcare guidelines.

5 Thesis summary

5.1 General discussion

Mild traumatic brain injury, commonly referred to as concussion is the most prevalent form of traumatic brain injury (118, 119). There is a sequelae of mTBI physiological changes, including cognitive impairment effecting learning, memory, motor function, attention, and processing speed (120). Two types of injury occur following an mTBI: i) primary injury caused by application of force to the head; ii) secondary injury caused by neurodegeneration. Primary injury can be readily identified using MRI and CT scans, involves damage to the structural components of the brain(121). Secondary injury presents with a more complex diagnosis due to the plethora of pathological responses that occur post injury such as oedema (122), increased intercranial pressure (123), mitochondrial dysfunction (124), excitotoxicity (125), oxidative stress (126, 127), cerebral metabolic dysfunction (63, 128), inflammation (129). While most mTBI signs and symptoms are typically are resolved within 3 months; there is ongoing concern that symptoms can persist for years post-injury (130, 131).

There is growing evidence from experimental and clinical mTBI studies that different types of injury induce specific patterns of changes in various brain lipid species which can be detected in the blood plasma or serum (9-13, 15-17, 66). These studies support the concept that changes to lipids and their metabolites in the blood may reflect disruptions to the structural integrity of lipid-rich cell membranes in the brain, highlighting the potential value of lipids as biomarkers of the elusive pathophysiology of secondary injury following mTBI. In chapters 3 and 4 we applied mass-spectrometry based lipidomics to provide a comprehensive analysis of perturbations in plasma lipidome following mTBI injury to elucidate the complex metabolic changes associated with mTBI and identify potential biomarkers. In this chapter (general discussion) we present the principal findings which were; i) single mTBI events and repeated mTBI events can be classified in a rodent model at 11 days post injury; ii) mTBI in humans can be distinguished from healthy age and sex balanced controls at 28 days post injury, but not at less

than 48 hours.; iii) established a lipid panel of 4 metabolites that are unique to mTBI.; and iv) identified five lipid species that are unique to rmTBI.. Finally, this chapter considers the findings of the thesis by identifying possible research pathways for the future.

Chapter three utilised lipidomic pipelines to analyse the blood plasma lipidome signature in response to a single mTBI event (1x mTBI) and a double mTBI event (2x mTBI) collected at 11 days post-injury. Multivariate analysis demonstrated two distinct metabolic profiles (856 lipid species) between the sham control, 1x mTBI and 2x mTBI groups. Projection of the data points from the 1x mTBI cohort onto the multivariate OPLS-DA model indicated that 1x mTBI was metabolically positioned between the control and 2x mTBI cohorts, indicating a progression of biomarker severity as the frequency of mTBI intervention increases. Univariate analysis demonstrated 18 lipid species were significantly different between sham control, 1x and 2x mTBI cohorts. Compared to sham controls, 1x and 2x mTBI rats both showed decreased levels of PS 14:0/18:2 and HCER d18:0/26:0 and PI 20:0/18:2 and increased FFA 18:3 levels. However, only 2x mTBI decreased the concentrations of LPE 20:1, LPE 22:6, LPE 22:5, PI 16:0/18:2 and PI 16:0/18:3, compared to 1x mTBI that demonstrated no significant decrease. These findings suggest that mTBI induces unique changes to lipid species in an injury dose-specific pattern. While further studies are needed to directly confirm whether these peripheral lipid changes are reflective of lipid and other pathophysiological changes in the brain, it is noteworthy that the pattern of lipid change induced by 2x mTBI is in line with previous reports of differential microglia reactivity and oxidative damage in the brain following 2x mTBI. Data from this study will inform the design of future investigations of lipid metabolism and transport following mTBI.

Chapter four was conducted as follow up study to a larger clinical study of patients that were admitted to the Emergency Department (ED) at Royal Perth Hospital with mTBI (108). A total of 67 participant samples were utilised for lipidomic analysis where each patient was (age and sex balanced to a cohort of healthy controls n = 37, mTBI patients at ED inception n = 30, and patient follow up n = 30). The aim of this study was to profile the plasma lipidome in the clinical setting to provide a lipidomic signature of mTBI. The main findings from the chapter 4 were i) Plasma lipid concentrations at injury inception indicate no statistical difference from

control; ii) mTBI can be distinguished from control at the follow-up. iii) Monoacylglycerols are the most prominent variable that drive the differences between the control, inception and follow up groups. Liquid Chromatography Mass spectrometry analysis revealed minimal disruptions in the plasma lipidome at patient inception (i.e. within 48 hours), possibly reflecting the time it takes for the blood brain barrier to be disrupted allowing lipids from the CNS to reach the peripheral vascular system (132) or delayed metabolic dysregulation to occur. However, patient follow up (mean = 34.6 days), lipidomic analysis demonstrated a major perturbation in the plasma lipidome with 9 lipid classes and 225 lipid species significant altered. Our results demonstrate a long-term perturbation in lipids far beyond the current no same day return to play guidelines used when an athlete has sustained a concussion (19), or health and safety guidelines used in the workplace. If the lipids present in blood plasma truly reflect the pathologies of the brain following mTBI, these findings suggest that current guidelines may not adequately meet patient care needs.

In this thesis we identified 239 lipid species that display significant difference between controls and mTBI cohorts (lipids of significance identified in; chapter 3 n = 18; chapter 4 n =225). Whilst some of these may be biologically relevant to mTBI, many of these lipids may be influenced by external sources such as diet and activity (115). Interestingly, when inferring results from the studies (chapters 3 and 4) certain lipid species potentially confer specificity and sensitivity to mTBI. The statistical analysis of the data from chapters three and four, indicated four lipid species were significant for mTBI in the animal model and human participants ($p \leq 0.05$): i) HCER (d18:0/26:0) and (22:0); ii) FFA (20:3); iii) CE(14:0). First, HCER are precursors to gangliosides which are abundant in the brain, varying concentrations of these lipids may indicate altered sphingolipid metabolism after mTBI injury (133). Second, this thesis reports increased concentration levels of FFA (20:3) in mTBI. Increases in FFA have been associated with cellular injury events such as accumulation of oxidative species and uncoupling of oxidate phosphorylation (134).This lipid has also been found to be elevated in mild cognitive impairment and Alzheimer's disease as a compensatory mechanism for deficiency in linoleic acid (135). These findings suggests that FFA(20:3) plays a similar compensatory role in mTBI. Third, cholesteryl myristate (CE 14:0) is reported as a novel biomarker for mTBI. CE (14:0). Chen et al.

(2011), reported the anti-apoptotic effect of cholesterol myristate and its therapeutic significance in brain disease (136). We postulate that the increase in CE(14:0) is a natural reaction mechanism to mTBI induced apoptosis of neurons as this finding has previously been observed in glia (137).

We speculate five lipids to be significant biomarkers for rmTBI ($p \leq 0.01$): i) LPE (20:1) and (22:5); ii) PI (16:0/18:2), (18:1/18:1) and (18:1/18:2). First, Hisano et al. indicated LPEs reduce glutamate-mediated excitotoxicity and stimulate neurite outgrowth in neuronal cell culture (94). These findings would support the decrease in plasma concentrations of LPE (20:1) and (22:5) following rmTBI may be caused by an increased metabolic turnover of these lipids as a natural healing mechanism. Second, PI (16:0/18:2), (18:1/18:1) and (18:1/18:2) demonstrate a significant decrease following rmTBI. The PI lipid class are major regulators of myelination and cytoskeletal function, with depletion of PI in the tissue linked to demyelination and axonal loss (95). Therefore, it is possible the measure of LPE and PI within this thesis are linked to rmTBI and warrant further research in a human cohort.

The results from this thesis provide further support for the use of lipid-based biomarkers for mTBI. Results from chapter three will inform the design of future investigations of lipid metabolism and transport following rmTBI, allowing identification of novel biomarkers and the optimum 'window of opportunity' for therapeutic intervention. Findings from chapter four will form a foundation for future mTBI research in the clinical setting. Further interpretation of the data by scientist with specialisation in biochemistry would allow for the further elaboration of mTBI secondary neurodegeneration and possibly correlate specific perturbed lipid species with mTBI pathologies, paving the way for development of lipid biomarker for mTBI. A future avenue that warrants research is repeat sampling in a mTBI cohort allowing us to develop continuous monitoring via biomarkers to assess when a sportsman has returned to full health and can safely return to the sporting field.

5.2 Conclusion

To summarise, the lipidomic approach used throughout this thesis revealed that the plasma lipidome is significantly perturbed following mTBI and displays unique alterations following rmTBI. In chapter three, the rat model demonstrated 18 lipid species significantly distinguish between control, mTBI and rmTBI. In chapter four, analysis of mTBI in the clinical setting indicated that significant alterations of the blood plasma lipidome occur after 10.86 hours, continue to occur up to and possibly beyond 54 days post-mTBI injury. The lipid species identified in this thesis warrant further research as they may provide biological information about the mechanisms of mTBI and rmTBI, or the opportunity for therapeutic interventions leading to improved patient outcome.

6 References

1. Wang KK, Yang Z, Zhu T, Shi Y, Rubenstein R, Tyndall JA, et al. An update on diagnostic and prognostic biomarkers for traumatic brain injury. Expert Rev Mol Diagn. 2018;18(2):165-80.
2. Dewan MC, Rattani A, Gupta S, Baticulon RE, Hung YC, Punchak M, et al. Estimating the global incidence of traumatic brain injury. J Neurosurg. 2018;130(4):1-18.
3. Nicholson JK, Holmes E, Kinross JM, Darzi AW, Takats Z, Lindon JC. Metabolic phenotyping in clinical and surgical environments. Nature. 2012;491(7424):384-92.
4. Egea-Guerrero J, Revuelto-Rey J, Murillo-Cabezas F, Munoz-Sanchez M, Vilches-Arenas A, Sanchez-Linares P, et al. Accuracy of the S100 β protein as a marker of brain damage in traumatic brain injury. Brain injury. 2012;26(1):76-82.
5. Gan ZS, Stein SC, Swanson R, Guan S, Garcia L, Mehta D, et al. Blood Biomarkers for Traumatic Brain Injury: A Quantitative Assessment of Diagnostic and Prognostic Accuracy. Front Neurol. 2019;10(446):446.
6. Horn A, Jaiswal JK. Chapter Four - Structural and signaling role of lipids in plasma membrane repair. In: Andrade LO, editor. Current Topics in Membranes. 84: Academic Press; 2019. p. 67-98.
7. Hussain G, Wang J, Rasul A, Anwar H, Imran A, Qasim M, et al. Role of cholesterol and sphingolipids in brain development and neurological diseases. Lipids Health Dis. 2019;18(1):26.
8. Sunshine H, Iruela-Arispe ML. Membrane lipids and cell signaling. Curr Opin Lipidol. 2017;28(5):408-13.
9. Emmerich T, Abdullah L, Ojo J, Mouzon B, Nguyen T, Crynen G, et al. Mild TBI Results in a Long-Term Decrease in Circulating Phospholipids in a Mouse Model of Injury. Neuromolecular Med. 2017;19(1):122-35.
10. Plasma Lipidomic Profiling in a Military Population of Mild Traumatic Brain Injury and Post-Traumatic Stress Disorder with Apolipoprotein E ε4–Dependent Effect. Journal of Neurotrauma. 2016;33(14):1331-48.
11. Emmerich T, Zakirova Z, Klimas N, Sullivan K, Shetty AK, Evans JE, et al. Phospholipid profiling of plasma from GW veterans and rodent models to identify potential biomarkers of Gulf War Illness. PLoS One. 2017;12(4):e0176634.
12. Fiandaca MS, Mapstone M, Mahmoodi A, Gross T, Macciardi F, Cheema AK, et al. Plasma metabolomic biomarkers accurately classify acute mild traumatic brain injury from controls. PLoS One. 2018;13(4):e0195318.
13. Hogan SR, Phan JH, Alvarado-Velez M, Wang MD, Bellamkonda RV, Fernandez FM, et al. Discovery of Lipidome Alterations Following Traumatic Brain Injury via High-Resolution Metabolomics. J Proteome Res. 2018;17(6):2131-43.
14. Ji J, Kline AE, Amoscato A, Samhan-Arias AK, Sparvero LJ, Tyurin VA, et al. Lipidomics identifies cardiolipin oxidation as a mitochondrial target for redox therapy of brain injury. Nature Neuroscience. 2012;15(10):1407-13.
15. Li Y, Wu Q, Hu E, Wang Y, Lu H. Quantitative Mass Spectrometry Imaging of Metabolomes and Lipidomes for Tracking Changes and Therapeutic Response in Traumatic Brain Injury Surrounding Injured Area at Chronic Phase. ACS Chem Neurosci. 2021;12(8):1363-75.
16. Sheth SA, Iavarone AT, Liebeskind DS, Won SJ, Swanson RA. Targeted Lipid Profiling Discovers Plasma Biomarkers of Acute Brain Injury. PLoS One. 2015;10(6):e0129735.
17. Zheng F, Xia ZA, Zeng YF, Luo JK, Sun P, Cui HJ, et al. Plasma metabolomics profiles in rats with acute traumatic brain injury. PLoS One. 2017;12(8):e0182025.
18. Zhong YH, Zheng BE, He RH, Zhou Z, Zhang SQ, Wei Y, et al. Serum Levels of HDL Cholesterol are Associated with Diffuse Axonal Injury in Patients with Traumatic Brain Injury. Neurocrit Care. 2021;34(2):465-72.

19. McCrory P, Meeuwisse W, Dvorak J, Aubry M, Bailes J, Broglio S, et al. Consensus statement on concussion in sport-the 5(th) international conference on concussion in sport held in Berlin, October 2016. Br J Sports Med. 2017;51(11):838-47.
20. Lystad RP, Cameron CM, Mitchell RJ. Excess Mortality Among Adults Hospitalized With Traumatic Brain Injury in Australia: A Population-Based Matched Cohort Study. J Head Trauma Rehabil. 2019;34(3):E1-E9.
21. Norup A, Kruse M, Soendergaard PL, Rasmussen KW, Biering-Sorensen F. Socioeconomic Consequences of Traumatic Brain Injury: A Danish Nationwide Register-Based Study. J Neurotrauma. 2020;37(24):2694-702.
22. Brain injury medicine: Principles and practice. Zasler ND, Katz DI, Zafonte RD, editors. New York, NY, US: Demos Medical Publishing; 2007. xxviii, 1275-xxviii, p.
23. Rajasekaran G, Venkatesh R. Outcome in elderly individuals with moderate and severe head injury: a tertiary centre experience. International Journal of Research in Medical Sciences. 2018;6(11):7.
24. Capizzi A, Woo J, Verduzco-Gutierrez M. Traumatic Brain Injury: An Overview of Epidemiology, Pathophysiology, and Medical Management. Med Clin North Am. 2020;104(2):213-38.
25. Teasdale G, Jennett B. Assessment of coma and impaired consciousness. A practical scale. Lancet. 1974;2(7872):81-4.
26. Cook GA, Hawley JS. A review of mild traumatic brain injury diagnostics: current perspectives, limitations, and emerging technology. Mil Med. 2014;179(10):1083-9.
27. Jain S, Iverson LM. Glasgow Coma Scale. StatPearls. Treasure Island (FL): StatPearls Publishing

28. Bramlett HM, Dietrich WD. Long-Term Consequences of Traumatic Brain Injury: Current Status of Potential Mechanisms of Injury and Neurological Outcomes. J Neurotrauma. 2015;32(23):1834-48.
29. McKinlay A, Lin A, Than M. A comparison of emergency department medical records to parental self-reporting of traumatic brain injury symptoms. Concussion. 2018;3(1):CNC52.
30. Kerr ZY, Roos KG, Djoko A, Dalton SL, Broglio SP, Marshall SW, et al. Epidemiologic Measures for Quantifying the Incidence of Concussion in National Collegiate Athletic Association Sports. J Athl Train. 2017;52(3):167-74.
31. Kerr ZY, Zuckerman SL, Register-Mihalik JK, Wasserman EB, Valovich McLeod TC, Dompier TP, et al. Estimating Concussion Incidence Using Sports Injury Surveillance Systems: Complexities and Potential Pitfalls. Neurol Clin. 2017;35(3):409-34.
32. Zuckerman SL, Kerr ZY, Yengo-Kahn A, Wasserman E, Covassin T, Solomon GS. Epidemiology of Sports-Related Concussion in NCAA Athletes From 2009-2010 to 2013-2014: Incidence, Recurrence, and Mechanisms. Am J Sports Med. 2015;43(11):2654-62.
33. Meehan WP, 3rd, Mannix RC, O'Brien MJ, Collins MW. The prevalence of undiagnosed concussions in athletes. Clin J Sport Med. 2013;23(5):339-42.
34. Lindon JC, Holmes E, Nicholson JK. So what's the deal with metabonomics? Anal Chem. 2003;75(17):384a-91a.
35. Monteiro MS, Carvalho M, Bastos ML, Guedes de Pinho P. Metabolomics analysis for biomarker discovery: advances and challenges. Curr Med Chem. 2013;20(2):257-71.
36. Oldiges M, Lütz S, Pflug S, Schroer K, Stein N, Wiendahl C. Metabolomics: current state and evolving methodologies and tools. Appl Microbiol Biotechnol. 2007;76(3):495-511.
37. Dettmer K, Aronov PA, Hammock BD. Mass spectrometry-based metabolomics. Mass Spectrom Rev. 2007;26(1):51-78.
38. Whiley L, Legido-Quigley C. Current strategies in the discovery of small-molecule biomarkers for Alzheimer's disease. Bioanalysis. 2011;3(10):1121-42.
39. Adibhatla RM, Hatcher JF. Role of Lipids in Brain Injury and Diseases. Future lipidology: NIH Public Access; 2007. p. 403.
40. Schwartz SA, Weil RJ, Johnson MD, Toms SA, Caprioli RM. Protein profiling in brain tumors using mass spectrometry: feasibility of a new technique for the analysis of protein expression. Clin Cancer Res. 2004;10(3):981-7.

41. Reveglia P, Paolillo C, Ferretti G, De Carlo A, Angiolillo A, Nasso R, et al. Challenges in LC–MS-based metabolomics for Alzheimer's disease early detection: targeted approaches versus untargeted approaches. Metabolomics. 2021;17(9):78.
42. Alonso A, Marsal S, Julià A. Analytical Methods in Untargeted Metabolomics: State of the Art in 2015. Frontiers in Bioengineering and Biotechnology. 2015;3.
43. Madsen R, Lundstedt T, Trygg J. Chemometrics in metabolomics--a review in human disease diagnosis. Anal Chim Acta. 2010;659(1-2):23-33.
44. Broadhurst D, Kell D. Statistical strategies for avoiding false discoveries in metabolomics and related experiments. Metabolomics. 2006;2:171-96.
45. Worley B, Powers R. Multivariate Analysis in Metabolomics. Curr Metabolomics. 2013;1(1):92-107.
46. Fonville JM, Richards SE, Barton RH, Boulange CL, Ebbels TMD, Nicholson JK, et al. The evolution of partial least squares models and related chemometric approaches in metabonomics and metabolic phenotyping. Journal of Chemometrics. 2010;24(11-12):636-49.
47. Hur M, Campbell AA, Almeida-de-Macedo M, Li L, Ransom N, Jose A, et al.
48. Liu Y, Chan DKY, Thalamuthu A, Wen W, Jiang J, Paradise M, et al. Plasma lipidomic biomarker analysis reveals distinct lipid changes in vascular dementia. Comput Struct Biotechnol J. 2020;18:1613-24.
49. Proitsi P, Kim M, Whiley L, Simmons A, Sattlecker M, Velayudhan L, et al. Association of blood lipids with Alzheimer's disease: A comprehensive lipidomics analysis. Alzheimer's & Dementia. 2017;13(2):140-51.
50. Cruz-Haces M, Tang J, Acosta G, Fernandez J, Shi R. Pathological correlations between traumatic brain injury and chronic neurodegenerative diseases. Transl Neurodegener. 2017;6(1):20.
51. Dennis EA, Norris PC. Eicosanoid storm in infection and inflammation. Nat Rev Immunol. 2015;15(8):511-23.
52. Watson H. Biological membranes. Essays Biochem. 2015;59:43-69.
53. Ogasawara D, Deng H, Viader A, Baggelaar MP, Breman A, den Dulk H, et al. Rapid and profound rewiring of brain lipid signaling networks by acute diacylglycerol lipase inhibition. Proc Natl Acad Sci U S A. 2016;113(1):26-33.
54. Orth M, Bellosta S. Cholesterol: its regulation and role in central nervous system disorders. Cholesterol. 2012;2012:292598.
55. Vincent AS, Roebuck-Spencer TM, Cernich A. Cognitive changes and dementia risk after traumatic brain injury: implications for aging military personnel. Alzheimers Dement. 2014;10(3 Suppl):S174-87.
56. Haag M. Essential Fatty Acids and the Brain. The Canadian Journal of Psychiatry. 2003;48(3):195-203.
57. Oresic M, Posti JP, Kamstrup-Nielsen MH, Takala RSK, Lingsma HF, Mattila I, et al. Human Serum Metabolites Associate With Severity and Patient Outcomes in Traumatic Brain Injury. EBioMedicine. 2016;12:118-26.
58. Thomas E, Fitzgerald M, Cowen G. Post-concussion states: How do we improve our patients' outcomes? An Australian perspective. Journal of Concussion. 2020;4:2059700220960313.
59. Belanger HG, Spiegel E, Vanderploeg RD. Neuropsychological performance following a history of multiple self-reported concussions: a meta-analysis. J Int Neuropsychol Soc. 2010;16(2):262-7.
60. Martini DN, Broglio SP. Long-term effects of sport concussion on cognitive and motor performance: A review. Int J Psychophysiol. 2018;132(Pt A):25-30.
61. Decq P, Gault N, Blandeau M, Kerdraon T, Berkal M, ElHelou A, et al. Long-term consequences of recurrent sports concussion. Acta Neurochir (Wien). 2016;158(2):289-300.
62. Omalu B, Bailes J, Hamilton RL, Kamboh MI, Hammers J, Case M, et al. Emerging Histomorphologic Phenotypes of Chronic Traumatic Encephalopathy in American Athletes. Neurosurgery: Oxford Academic; 2011. p. 173-83.
63. Giza CC, Hovda DA. The new neurometabolic cascade of concussion. Neurosurgery. 2014;75 Suppl 4(0 4):S24-33.

64. Abdul-Muneer PM, Schuetz H, Wang F, Skotak M, Jones J, Gorantla S, et al. Induction of oxidative and nitrosative damage leads to cerebrovascular inflammation in an animal model of mild traumatic brain injury induced by primary blast. Free Radic Biol Med. 2013;60:282-91.
65. Garcia-Fresco GP, Sousa AD, Pillai AM, Moy SS, Crawley JN, Tessarollo L, et al. Disruption of axo-glial junctions causes cytoskeletal disorganization and degeneration of Purkinje neuron axons. Proc Natl Acad Sci U S A. 2006;103(13):5137-42.
66. Nessel I, Michael-Titus AT. Lipid profiling of brain tissue and blood after traumatic brain injury: A review of human and experimental studies. Semin Cell Dev Biol. 2021;112:145-56.
67. Bozek K, Wei Y, Yan Z, Liu X, Xiong J, Sugimoto M, et al. Organization and Evolution of Brain Lipidome Revealed by Large-Scale Analysis of Human, Chimpanzee, Macaque, and Mouse Tissues. Neuron: Cell Press; 2015. p. 695-702.
68. Membrane lipids and cell signaling, (2017).
69. Rapoport SI, Chang MCJ, Spector AA. Delivery and turnover of plasma-derived essential PUFAs in mammalian brain. Journal of Lipid Research: Elsevier; 2001. p. 678-85.
70. Smith QR, Nagura H. Fatty Acid Uptake and Incorporation in Brain Studies with the Perfusion Model. 2001.
71. Daley M, Dekaban G, Bartha R, Brown A, Stewart TC, Doherty T, et al. Metabolomics profiling of concussion in adolescent male hockey players: a novel diagnostic method. Metabolomics 2016 12:12: Springer; 2016. p. 1-9.
72. EmmerichTanja, AbdullahLaila, CrynenGogce, DretschMichael, EvansJames, Ait-GhezalaGhania, et al. Plasma Lipidomic Profiling in a Military Population of Mild Traumatic Brain Injury and Post-Traumatic Stress Disorder with Apolipoprotein E ε4–Dependent Effect. https://homeliebertpubcom/neu: Mary Ann Liebert, Inc. 140 Huguenot Street, 3rd Floor New Rochelle, NY 10801 USA 2016. p. 1331-48.
73. Ojo JO, Algamal M, Leary P, Abdullah L, Mouzon B, Evans JE, et al. Disruption in Brain Phospholipid Content in a Humanized Tau Transgenic Model Following Repetitive Mild Traumatic Brain Injury. Frontiers in Neuroscience: Frontiers Media SA; 2018.
74. Anyaegbu CC, Mao Y, McGonigle T, Raja S, Clarke T, Black AMB, et al. Simultaneous flow cytometric characterization of multiple cell types and metabolic states in the rat brain after repeated mild traumatic brain injury. J Neurosci Methods. 2021;359:109223.
75. Fehily B, Bartlett CA, Lydiard S, Archer M, Milbourn H, Majimbi M, et al. Differential responses to increasing numbers of mild traumatic brain injury in a rodent closed-head injury model. J Neurochem. 2019;149(5):660-78.
76. Mao Y, Black AMB, Milbourn HR, Krakonja S, Nesbit M, Bartlett CA, et al. The Effects of a Combination of Ion Channel Inhibitors in Female Rats Following Repeated Mild Traumatic Brain Injury. Int J Mol Sci. 2018;19(11).
77. Yates NJ, Lydiard S, Fehily B, Weir G, Chin A, Bartlett CA, et al. Repeated mild traumatic brain injury in female rats increases lipid peroxidation in neurons. Experimental Brain Research. 2017;235(7):2133-49.
78. Brotfain E, Gruenbaum SE, Boyko M, Kutz R, Zlotnik A, Klein M. Neuroprotection by Estrogen and Progesterone in Traumatic Brain Injury and Spinal Cord Injury. Curr Neuropharmacol. 2016;14(6):641-53.
79. Yates NJ, Lydiard S, Fehily B, Weir G, Chin A, Bartlett CA, et al. Repeated mild traumatic brain injury in female rats increases lipid peroxidation in neurons. Exp Brain Res. 2017;235(7):2133-49.
80. Gray N, Lawler NG, Zeng AX, Ryan M, Bong SH, Boughton BA, et al. Diagnostic Potential of the Plasma Lipidome in Infectious Disease: Application to Acute SARS-CoV-2 Infection. Metabolites. 2021;11(7):467.
81. Adams KJ, Pratt B, Bose N, Dubois LG, John-Williams LS, Perrott KM, et al. Skyline for Small Molecules: A Unifying Software Package for Quantitative Metabolomics. Journal of Proteome Research: American Chemical Society; 2020. p. 1447-58.
82. R: A language and environment for statistical computing, (2021).
83. Huguenard CJC, Cseresznye A, Evans JE, Oberlin S, Langlois H, Ferguson S, et al. Plasma Lipidomic Analyses in Cohorts With mTBI and/or PTSD Reveal Lipids Differentially Associated With Diagnosis and APOE ε4 Carrier Status. Frontiers in Physiology: Frontiers; 2020. p. 12.

84. Poblete RA, Arenas M, Sanossian N, Freeman WD, Louie SG. The role of bioactive lipids in attenuating the neuroinflammatory cascade in traumatic brain injury. Annals of Clinical and Translational Neurology: Wiley-Blackwell; 2020. p. 2524.
85. Fabelo N, Martín V, Santpere G, Marín R, Torrent L, Ferrer F, et al. Severe alterations in lipid composition of frontal cortex lipid rafts from Parkinson's disease and incidental Parkinson's disease. Mol Med: Mol Med; 2011. p. 1107-18.
86. Han X, Holtzman DM, McKeel DW, Jr. Plasmalogen deficiency in early Alzheimer's disease subjects and in animal models: molecular characterization using electrospray ionization mass spectrometry. J Neurochem. 2001;77(4):1168-80.
87. Ojo JO, Algamal M, Leary P, Abdullah L, Mouzon B, Evans JE, et al. Converging and Differential Brain Phospholipid Dysregulation in the Pathogenesis of Repetitive Mild Traumatic Brain Injury and Alzheimer's Disease. Frontiers in Neuroscience: Frontiers; 2019. p. 103.
88. Inaba T, Murate M, Tomishige N, Lee Y-F, Hullin-Matsuda F, Pollet B, et al. Formation of tubules and helical ribbons by ceramide phosphoethanolamine-containing membranes. Scientific Reports 2019 9:1: Nature Publishing Group; 2019. p. 1-13.
89. Patel D, Witt SN. Ethanolamine and Phosphatidylethanolamine: Partners in Health and Disease. Oxidative Medicine and Cellular Longevity: Hindawi Limited; 2017.
90. H H, JB C, N G. Arachidonic-acid-derived eicosanoids: roles in biology and immunopathology. Trends in molecular medicine: Trends Mol Med; 2008. p. 461-9.
91. Anthonymuthu TS, Kenny EM, Amoscato AA, Lewis J, Kochanek PM, Kagan VE, et al. Global assessment of oxidized free fatty acids in brain reveals an enzymatic predominance to oxidative signaling after trauma. Biochimica et Biophysica Acta (BBA) - Molecular Basis of Disease: Elsevier; 2017. p. 2601-13.
92. Williams KI, Higgs GA. Eicosanoids and inflammation. The Journal of Pathology: John Wiley & Sons, Ltd; 1988. p. 101-10.
93. Roux A, Muller L, Jackson SN, Post J, Baldwin K, Hoffer B, et al. Mass spectrometry imaging of rat brain lipid profile changes over time following traumatic brain injury. J Neurosci Methods. 2016;272:19-32.
94. Hisano K, Yoshida H, Kawase S, Mimura T, Haniu H, Tsukahara T, et al. Abundant oleoyl-lysophosphatidylethanolamine in brain stimulates neurite outgrowth and protects against glutamate toxicity in cultured cortical neurons. J Biochem. 2021;170(3):327-36.
95. Raghu P, Joseph A, Krishnan H, Singh P, Saha S. Phosphoinositides: Regulators of Nervous System Function in Health and Disease. Front Mol Neurosci. 2019;12(208):208.
96. Gupte R, Brooks W, Vukas R, Pierce J, Harris J. Sex Differences in Traumatic Brain Injury: What We Know and What We Should Know. J Neurotrauma. 2019;36(22):3063-91.
97. Chang CY, Ke DS, Chen JY. Essential fatty acids and human brain. Acta Neurol Taiwan. 2009;18(4):231-41.
98. Pifferi F, Laurent B, Plourde M. Lipid Transport and Metabolism at the Blood-Brain Interface: Implications in Health and Disease. Frontiers in Physiology: Frontiers; 2021. p. 407.
99. Horn A, Jaiswal JK. Structural and signaling role of lipids in plasma membrane repair. Current Topics in Membranes: Curr Top Membr; 2019. p. 67-98.
100. Mallah K, Quanico J, Raffo-Romero A, Cardon T, Aboulouard S, Devos D, et al. Matrix-Assisted Laser Desorption/Ionization-Mass Spectrometry Imaging of Lipids in Experimental Model of Traumatic Brain Injury Detecting Acylcarnitines as Injury Related Markers. Analytical Chemistry: Anal Chem; 2019. p. 11879-87.
101. Zetterberg H, Smith DH, Blennow K. Biomarkers of mild traumatic brain injury in cerebrospinal fluid and blood. Nat Rev Neurol. 2013;9(4):201-10.
102. Kim M, Nevado-Holgado A, Whiley L, Snowden SG, Soininen H, Kloszewska I, et al. Association between Plasma Ceramides and Phosphatidylcholines and Hippocampal Brain Volume in Late Onset Alzheimer's Disease. J Alzheimers Dis. 2017;60(3):809-17.
103. Proitsi P, Kim M, Whiley L, Pritchard M, Leung R, Soininen H, et al. Plasma lipidomics analysis finds long chain cholesteryl esters to be associated with Alzheimer's disease. Transl Psychiatry. 2015;5(1):e494.
104. Proitsi P, Kim M, Whiley L, Simmons A, Sattlecker M, Velayudhan L, et al. Association of blood lipids with Alzheimer's disease: A comprehensive lipidomics analysis. Alzheimers Dement. 2017;13(2):140-51.

105. Whiley L, Sen A, Heaton J, Proitsi P, Garcia-Gomez D, Leung R, et al. Evidence of altered phosphatidylcholine metabolism in Alzheimer's disease. Neurobiol Aging. 2014;35(2):271-8.
106. Toshkezi G, Kyle M, Longo SL, Chin LS, Zhao LR. Brain repair by hematopoietic growth factors in the subacute phase of traumatic brain injury. J Neurosurg. 2018;129(5):1286-94.
107. Gozt A, Licari M, Halstrom A, Milbourn H, Lydiard S, Black A, et al. Towards the Development of an Integrative, Evidence-Based Suite of Indicators for the Prediction of Outcome Following Mild Traumatic Brain Injury: Results from a Pilot Study. Brain Sciences. 2020;10(1):23.
108. Gozt A, Licari M, Halstrom A, Milbourn H, Lydiard S, Black A, et al. Towards the Development of an Integrative, Evidence-Based Suite of Indicators for the Prediction of Outcome Following Mild Traumatic Brain Injury: Results from a Pilot Study. Brain Sci. 2020;10(1).
109. MacLean B, Tomazela DM, Shulman N, Chambers M, Finney GL, Frewen B, et al. Skyline: an open source document editor for creating and analyzing targeted proteomics experiments. Bioinformatics. 2010;26(7):966-8.
110. Quehenberger O, Armando AM, Brown AH, Milne SB, Myers DS, Merrill AH, et al. Lipidomics reveals a remarkable diversity of lipids in human plasma. J Lipid Res. 2010;51(11):3299-305.
111. Zhang J, Teng Z, Song Y, Hu M, Chen C. Inhibition of monoacylglycerol lipase prevents chronic traumatic encephalopathy-like neuropathology in a mouse model of repetitive mild closed head injury. J Cereb Blood Flow Metab. 2015;35(3):443-53.
112. Pan X, Hussain MM. Gut triglyceride production. Biochim Biophys Acta. 2012;1821(5):727-35.
113. Kumar A, Henry RJ, Stoica BA, Loane DJ, Abulwerdi G, Bhat SA, et al. Neutral Sphingomyelinase Inhibition Alleviates LPS-Induced Microglia Activation and Neuroinflammation after Experimental Traumatic Brain Injury. J Pharmacol Exp Ther. 2019;368(3):338-52.
114. Novgorodov SA, Voltin JR, Wang W, Tomlinson S, Riley CL, Gudz TI. Acid sphingomyelinase deficiency protects mitochondria and improves function recovery after brain injury. J Lipid Res. 2019;60(3):609-23.
115. Kris-Etherton PM, Krummel D, Russell ME, Dreon D, Mackey S, Borchers J, et al. The effect of diet on plasma lipids, lipoproteins, and coronary heart disease. J Am Diet Assoc. 1988;88(11):1373-400.
116. Lamb MM, Ogden CL, Carroll MD, Lacher DA, Flegal KM. Association of body fat percentage with lipid concentrations in children and adolescents: United States, 1999-2004. Am J Clin Nutr. 2011;94(3):877-83.
117. Gazzola K, Snijder MB, Hovingh GK, Stroes ESG, Peters RJG, van den Born BH. Ethnic differences in plasma lipid levels in a large multiethnic cohort: The HELIUS study. J Clin Lipidol. 2018;12(5):1217-24.e1.
118. Cassidy JD, Carroll LJ, Peloso PM, Borg J, von Holst H, Holm L, et al. Incidence, risk factors and prevention of mild traumatic brain injury: results of the WHO Collaborating Centre Task Force on Mild Traumatic Brain Injury. J Rehabil Med. 2004(43 Suppl):28-60.
119. Shaw NA. The neurophysiology of concussion. Prog Neurobiol. 2002;67(4):281-344.
120. Rabinowitz AR, Levin HS. Cognitive sequelae of traumatic brain injury. Psychiatr Clin North Am. 2014;37(1):1-11.
121. Greve MW, Zink BJ. Pathophysiology of traumatic brain injury. Mt Sinai J Med. 2009;76(2):97-104.
122. Marmarou A, Fatouros PP, Barzo P, Portella G, Yoshihara M, Tsuji O, et al. Contribution of edema and cerebral blood volume to traumatic brain swelling in head-injured patients. J Neurosurg. 2000;93(2):183-93.
123. Stiefel MF, Tomita Y, Marmarou A. Secondary ischemia impairing the restoration of ion homeostasis following traumatic brain injury. J Neurosurg. 2005;103(4):707-14.
124. Robertson CL. Mitochondrial dysfunction contributes to cell death following traumatic brain injury in adult and immature animals. J Bioenerg Biomembr. 2004;36(4):363-8.

125. Robertson CL, Bell MJ, Kochanek PM, Adelson PD, Ruppel RA, Carcillo JA, et al. Increased adenosine in cerebrospinal fluid after severe traumatic brain injury in infants and children: association with severity of injury and excitotoxicity. Crit Care Med. 2001;29(12):2287-93.
126. Bayir H, Kagan VE, Borisenko GG, Tyurina YY, Janesko KL, Vagni VA, et al. Enhanced oxidative stress in iNOS-deficient mice after traumatic brain injury: support for a neuroprotective role of iNOS. J Cereb Blood Flow Metab. 2005;25(6):673-84.
127. Chong ZZ, Li F, Maiese K. Oxidative stress in the brain: novel cellular targets that govern survival during neurodegenerative disease. Prog Neurobiol. 2005;75(3):207-46.
128. Wu HM, Huang SC, Hattori N, Glenn TC, Vespa PM, Yu CL, et al. Selective metabolic reduction in gray matter acutely following human traumatic brain injury. J Neurotrauma. 2004;21(2):149-61.
129. Das M, Leonardo CC, Rangooni S, Pennypacker KR, Mohapatra S, Mohapatra SS. Lateral fluid percussion injury of the brain induces CCL20 inflammatory chemokine expression in rats. J Neuroinflammation. 2011;8:148.
130. Daneshvar DH, Riley DO, Nowinski CJ, McKee AC, Stern RA, Cantu RC. Long-term consequences: effects on normal development profile after concussion. Phys Med Rehabil Clin N Am. 2011;22(4):683-700, ix.
131. Hall RC, Hall RC, Chapman MJ. Definition, diagnosis, and forensic implications of postconcussional syndrome. Psychosomatics. 2005;46(3):195-202.
132. Wu Y, Wu H, Guo X, Pluimer B, Zhao Z. Blood-Brain Barrier Dysfunction in Mild Traumatic Brain Injury: Evidence From Preclinical Murine Models. Front Physiol. 2020;11(1030):1030.
133. Robert K Y, Tsai Y-T, Ariga T, Yanagisawa M. Structures, biosynthesis, and functions of gangliosides-an overview. Journal of oleo science. 2011;60(10):537-44.
134. Prins M, Greco T, Alexander D, Giza CC. The pathophysiology of traumatic brain injury at a glance. Dis Model Mech. 2013;6(6):1307-15.
135. Iuliano L, Pacelli A, Ciacciarelli M, Zerbinati C, Fagioli S, Piras F, et al. Plasma fatty acid lipidomics in amnestic mild cognitive impairment and Alzheimer's disease. J Alzheimers Dis. 2013;36(3):545-53.
136. Chen DF, Cao JH, Liu Y, Wu Y, Du SH, Li H, et al. BMP-Id pathway targeted by cholesterol myristate suppresses the apoptosis of PC12 cells. Brain Res. 2011;1367:33-42.
137. Raghupathi R, Graham DI, McIntosh TK. Apoptosis after traumatic brain injury. J Neurotrauma. 2000;17(10):927-38.
138. Broadhurst D, Goodacre R, Reinke SN, Kuligowski J, Wilson ID, Lewis MR, et al. Guidelines and considerations for the use of system suitability and quality control samples in mass spectrometry assays applied in untargeted clinical metabolomic studies. Metabolomics. 2018;14(6):72.

7 Supplementary materials for chapters 3 and 4

7.1 Liquid chromatography-mass spectrometry

Lipidomic analysis of the plasma samples was performed using a Waters ACQUITY ultra-performance liquid chromatography (UPLC; Waters Corp., Milford, MA, USA) system coupled to an Exion Triple Quad Linear Ion Trap 6500+ Lipidyzer Platform (SCIEX, Concord, ON, Canada) (QTRAP 6500+ LC-MS/MS system). The targeted method utilised had been previously developed in house at the Australian National Phenome Centre and has been shown to quantitate up to 1200 lipid target species depending on the sample. Chromatographic separation was achieved using a Waters Acquity BEH C18 Column (1.7 µm, 100 x 2.1 mm particle size; Waters Corp.), maintained at 60°C. The gradient consisted of 20/30/50, Isopropanol/Acetonitrile/H_2O + 10 mM Ammonium Acetate (A) and 90/9/1, Isopropanol/Acetonitrile/ H_2O + 10 mM Ammonium Acetate (B). The solvent was delivered at a flow rate of 0.4mL/min. The gradient consisted of 10% B at 0 minutes, 1 to 45% B in 2.7 minutes, 45 to 53% B in 0.1 minutes, 53 to 60% B in 5.2 minutes, 60 to 80% in 0.1 minutes, maintained at 80% B for 3.4 minutes, 80 to 100% B in 0.5 minutes, maintained at 100% B for 1 minute, and then equilibration at initial conditions for 1.99 minutes.

The QTRAP 6500+ LC-MS/MS system was operated in both negative and positive ion mode (ESI+/-) in a mass range of m/z 50-2000 according to the following parameters: curtain gas 20 p.s.i., collision gas medium, ion source temperature 300°C, ion source gas 2 at 60 arbitrary units, for a total duration of 15 minutes. Isolated lipid species windows were utilised where a detection window of 40-50 seconds and a target scan time of 0.15 seconds were applied. Negative-ion acquisition was conducted using the following parameters: IonSpray voltage of -4500 V, delustering potential (DP) of -80, entrance potential (EP) of -15, and collision cell exit potential (CXP) of -10. Positive-ion acquisition will also utilise

the following parameters: IonSpray voltage of 5500, DP of 60, EP of 10, and a CXP of 15. The instrument was calibrated prior to analysis (calibration error of fewer than 5 parts per million) using 0.5 mm sodium formate for both positive and negative ionisation.

7.2 Chromatograms of data from chapter 3 cohort

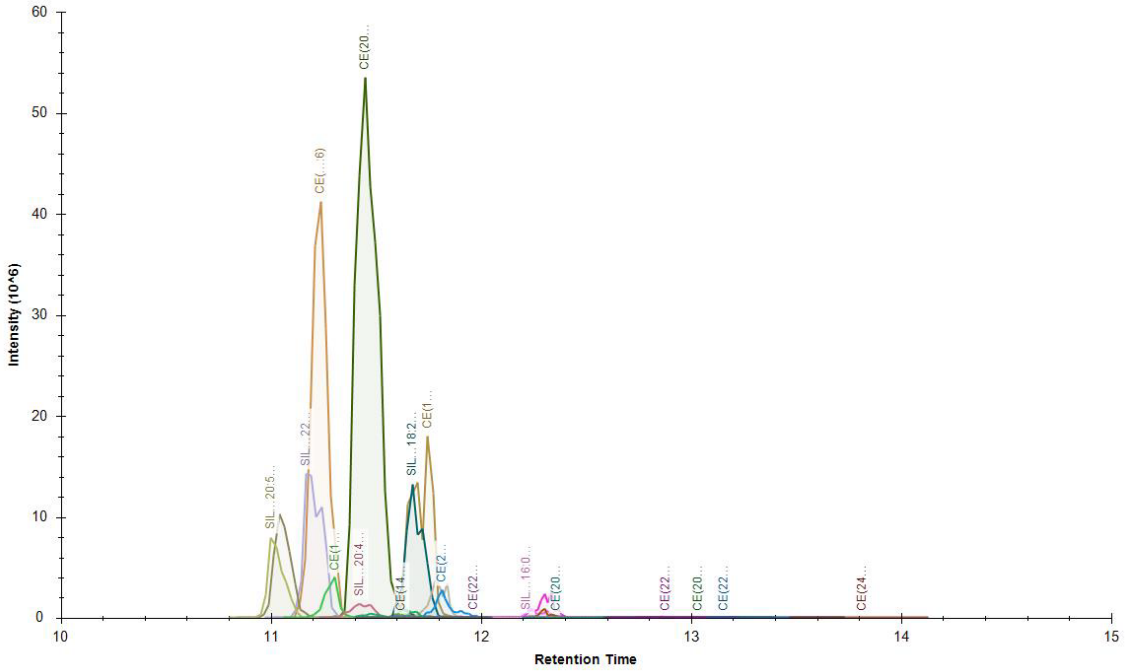
Intensity (10^6)
Retention Time
SIL...20:5...
SIL...22...
CE(...6)
CE(1...
CE(20...
SIL...20:4...
CE(14...
SIL...18:2...
CE(1...
CE(2...
CE(22...
SIL...16:0...
CE(20...
CE(22...
CE(20...
CE(22...
CE(24...

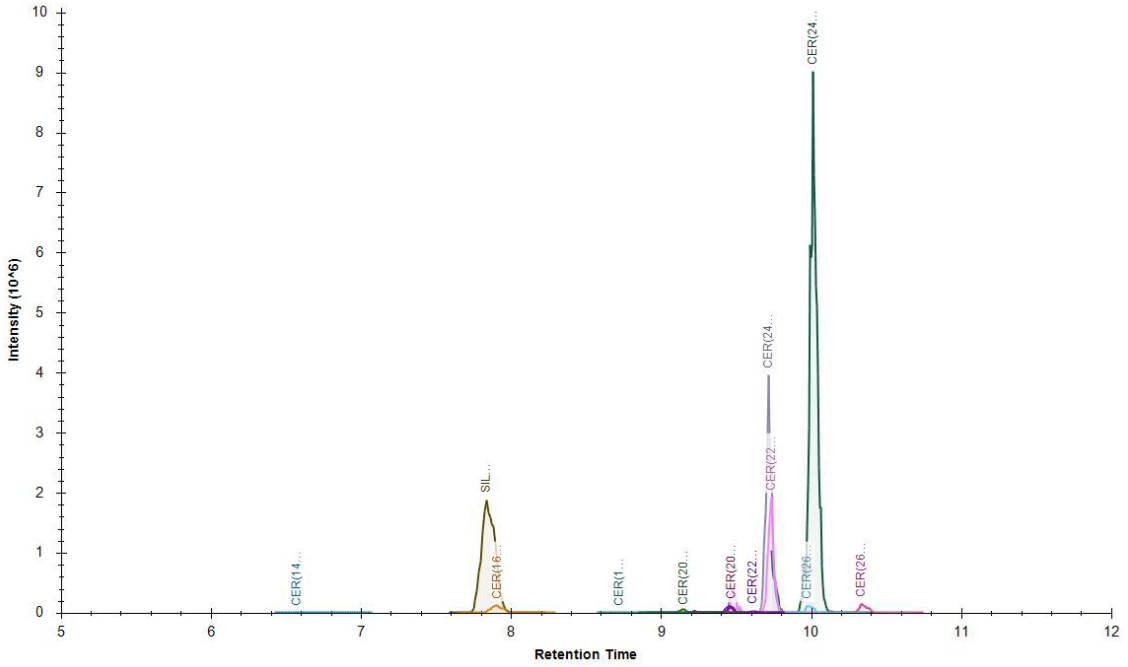
Intensity (10^6)
Retention Time
CER(14...
SIL...
CER(16...
CER(1...
CER(20...
CER(20...
CER(22...
CER(24...
CER(22...
CER(24...
CER(26...
CER(26...

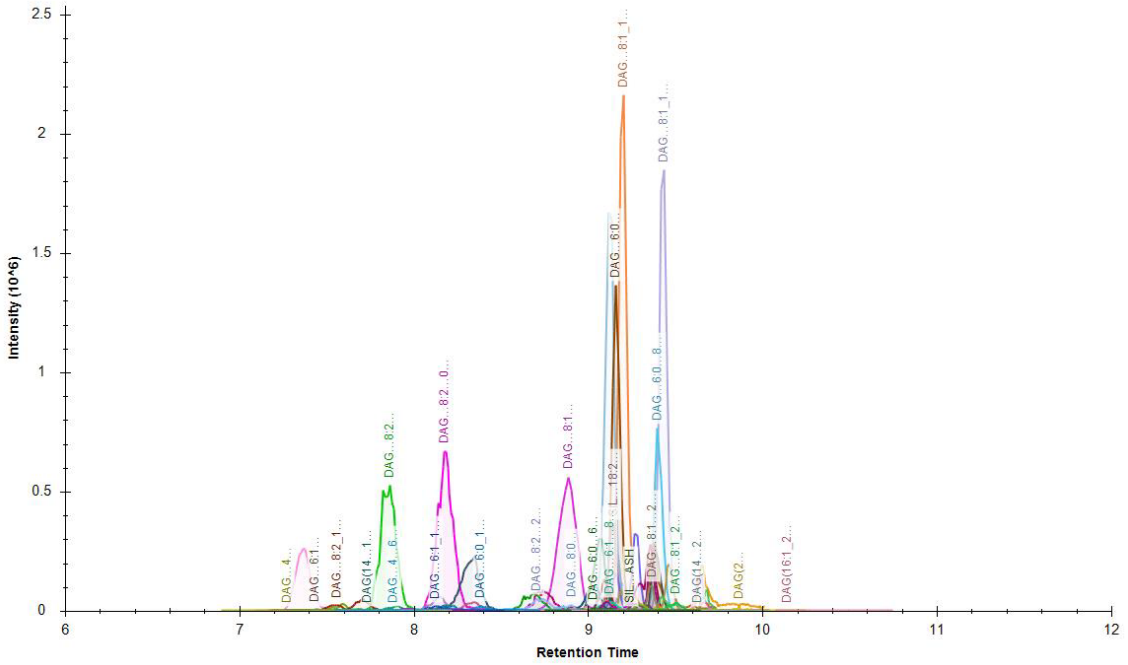
Intensity (10^6)
Retention Time
DAG...4...
DAG...6:1...
DAG...8:2_1...
DAG(14...1...
DAG...4...6...
DAG...8:2...
DAG...6:1_1...
DAG...8:2...0...
DAG...6:0_1...
DAG...8:2...2...
DAG...8:0...
DAG...8:1...
DAG...6:0...6...
DAG...6:1...8...
DAG...L...18:2...
SIL...ASH...
DAG...6:0...
DAG...8:1_1...
DAG...8:1...2...
DAG...8:1_2...
DAG...6:0...8...
DAG(14...2...
DAG(2...
DAG(16:1_2...

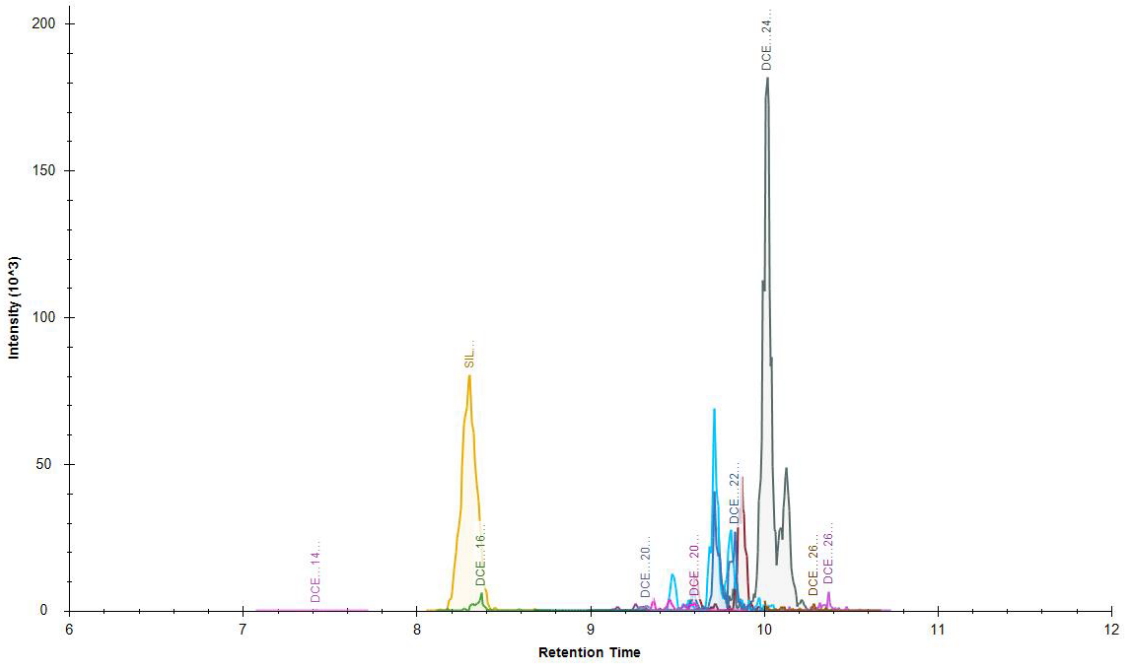
Intensity (10^3)
Retention Time
DCE...14...
SIL...
DCE...16...
DCE...20...
DCE...20...
DCE...22...
DCE...24...
DCE...26...
DCE...26...

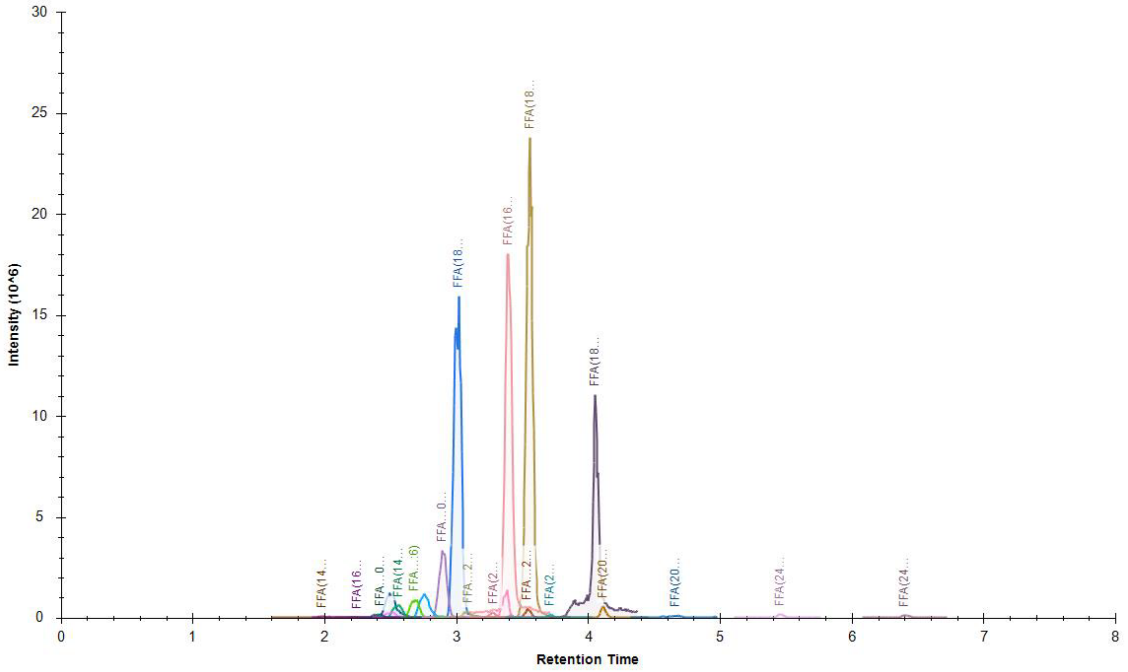
Intensity (10^6)
Retention Time
FFA(14...
FFA(16...
FFA...0...
FFA(14...
FFA...6)
FFA...0...
FFA(18...
FFA...2...
FFA(2...
FFA(16...
FFA(18...
FFA...2...
FFA(2...
FFA(18...
FFA(20...
FFA(20...
FFA(24...
FFA(24...

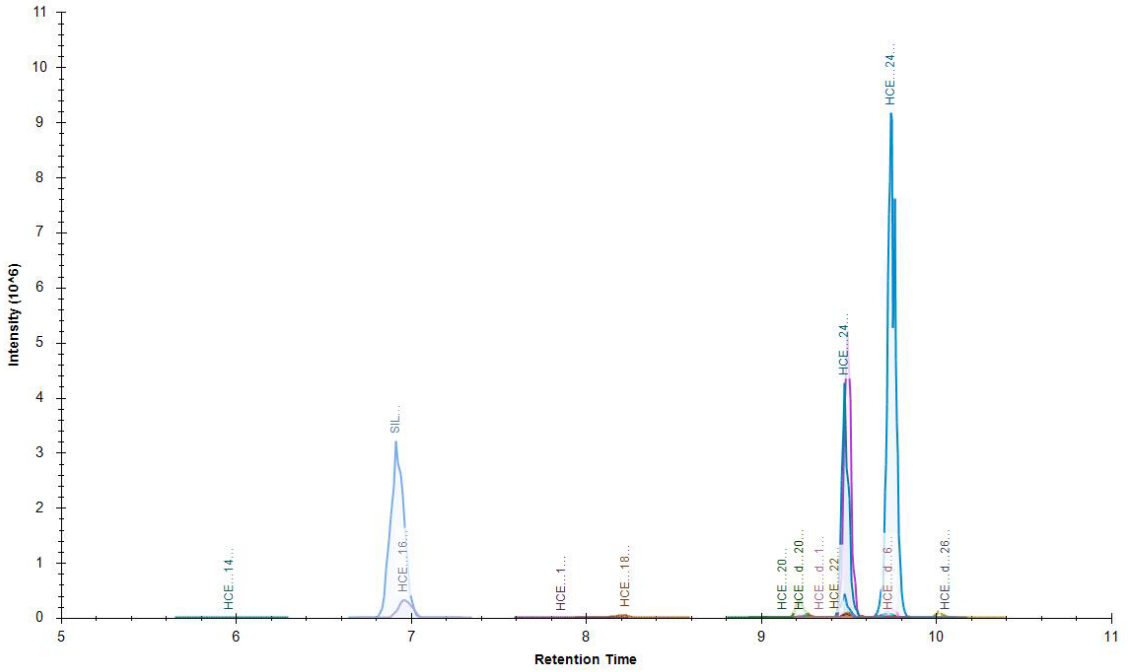
Intensity (10^6)
Retention Time
HCE...14...
SIL...
HCE...16...
HCE...1...
HCE...18...
HCE...20...
HCE...d...20...
HCE...d...1...
HCE...22...
HCE...24...
HCE...24...
HCE...d...6...
HCE...d...26...

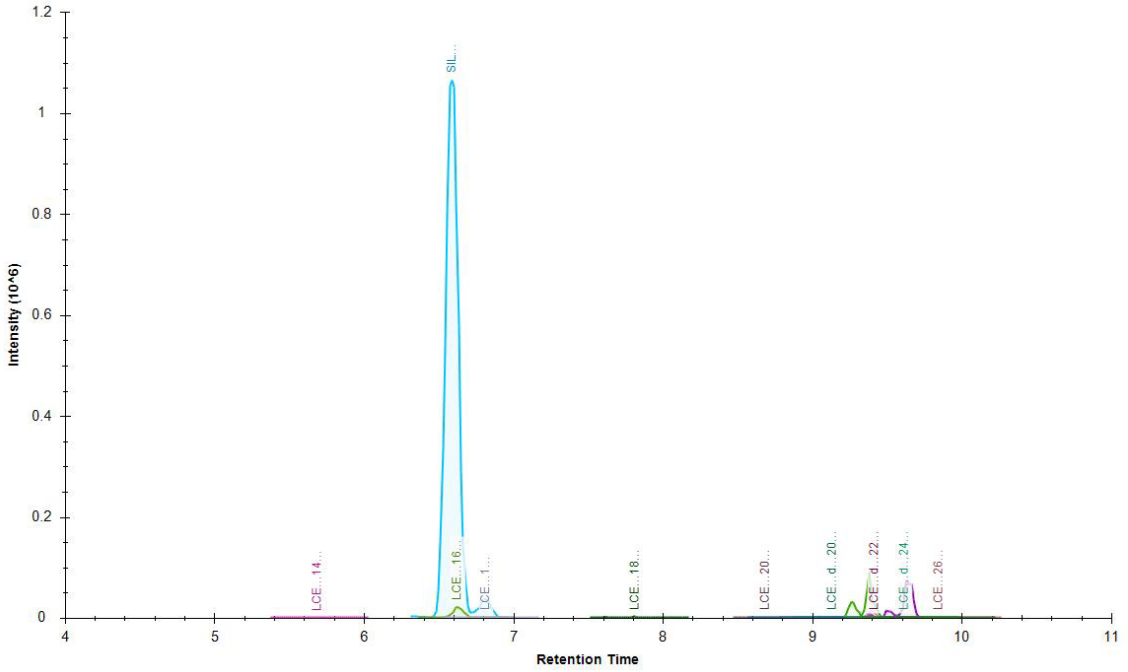
Intensity (10^6)
Retention Time
SIL...
LCE...14...
LCE...16...
LCE...1...
LCE...18...
LCE...20...
LCE...d...20...
LCE...d...22...
LCE...d...24...
LCE...26...

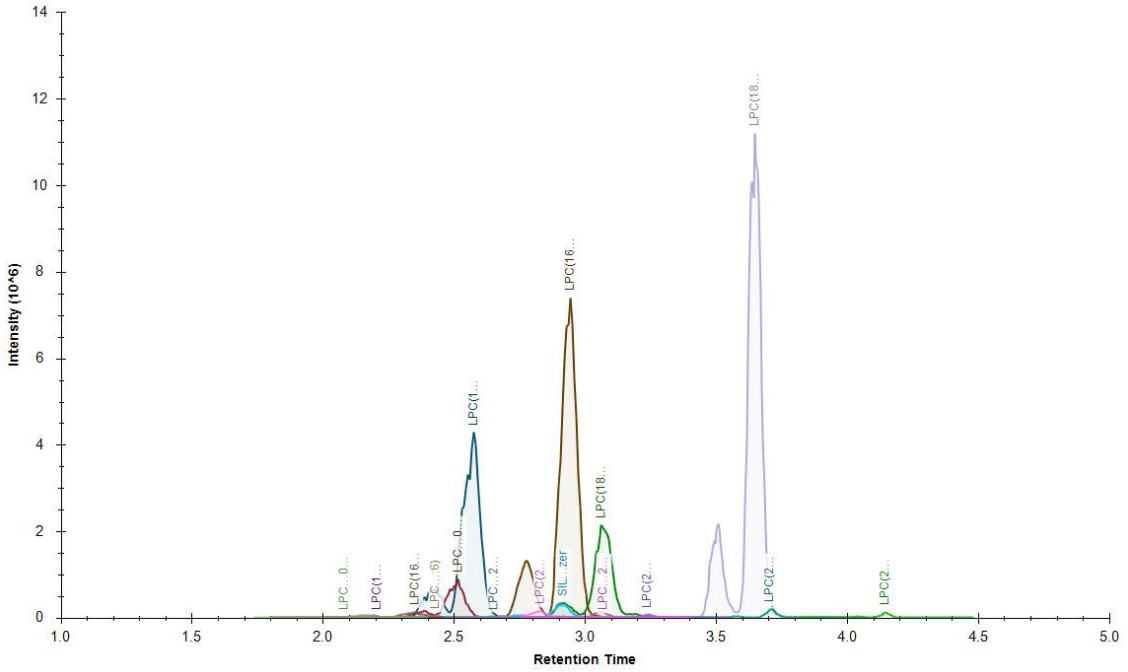
Intensity (10^6)
Retention Time
LPC(18...
LPC(16...
LPC(1...
LPC...0...
LPC...2...
LPC(2...
SIL...2er
LPC...6)

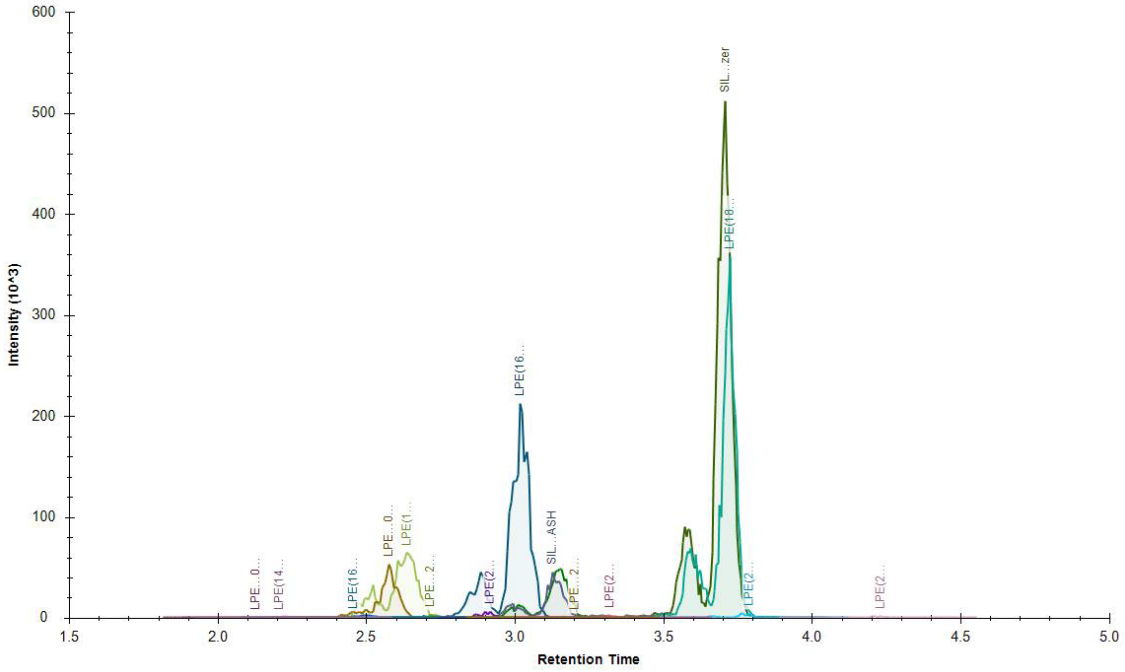
Intensity (10^3)
Retention Time
SIL...zer
LPE(18...
LPE(16...
SIL...ASH

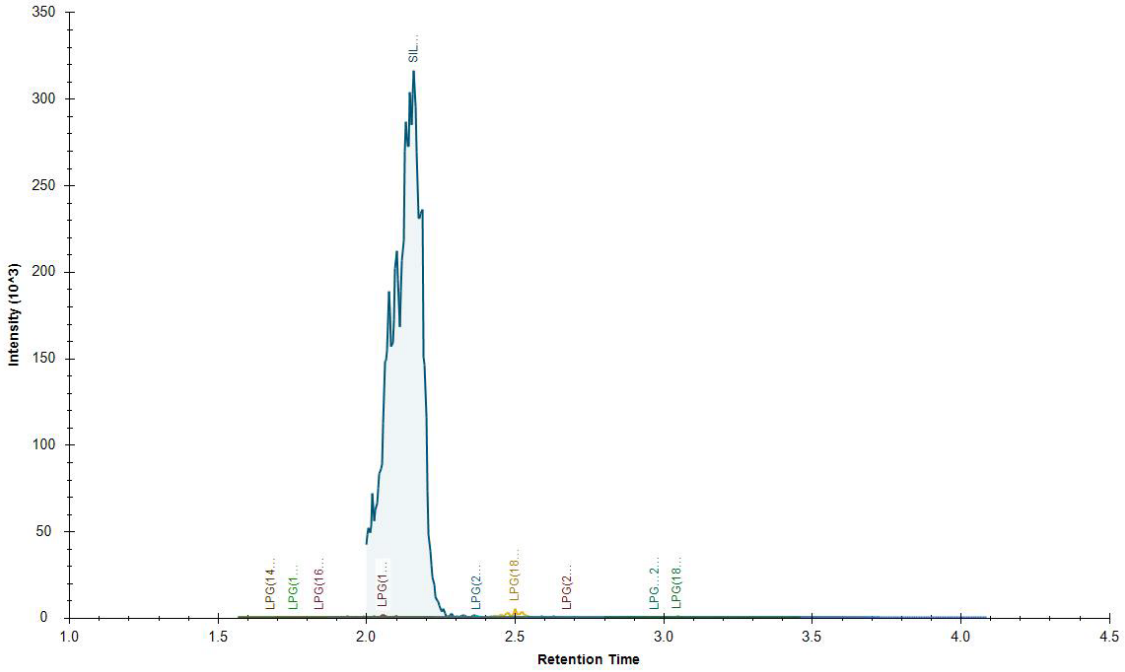
Intensity (10^3)
Retention Time
SIL...

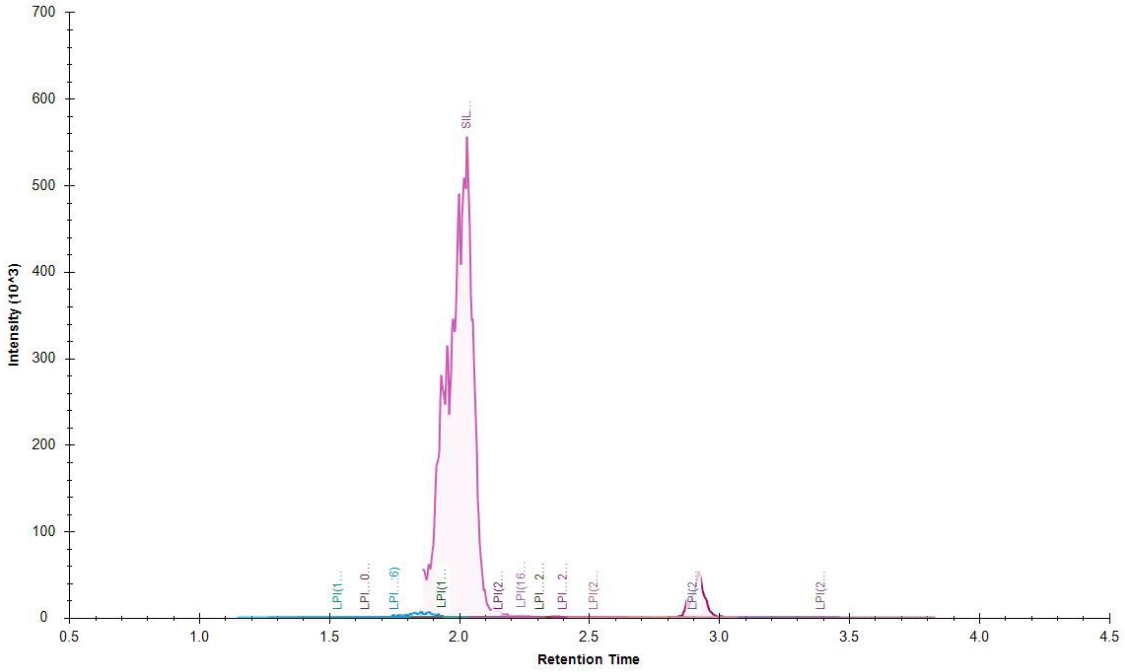
Intensity (10^3)
Retention Time
SIL...
LPI(1...
LPI... 0...
LPI... 6)
LPI(1...
LPI(2...
LPI(16...
LPI... 2...
LPI... 2...
LPI(2...
LPI(2...
LPI(2...

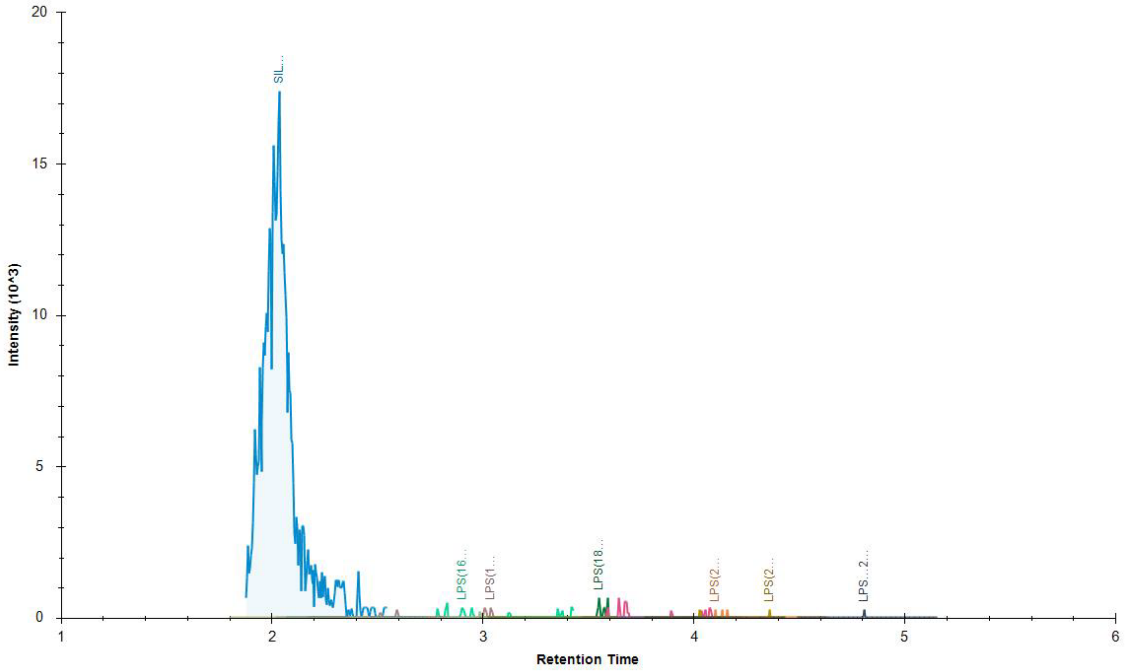
Intensity (10^3)
Retention Time
SIL...
LPS(16...
LPS(1...
LPS(18...
LPS(2...
LPS(2...
LPS... 2...

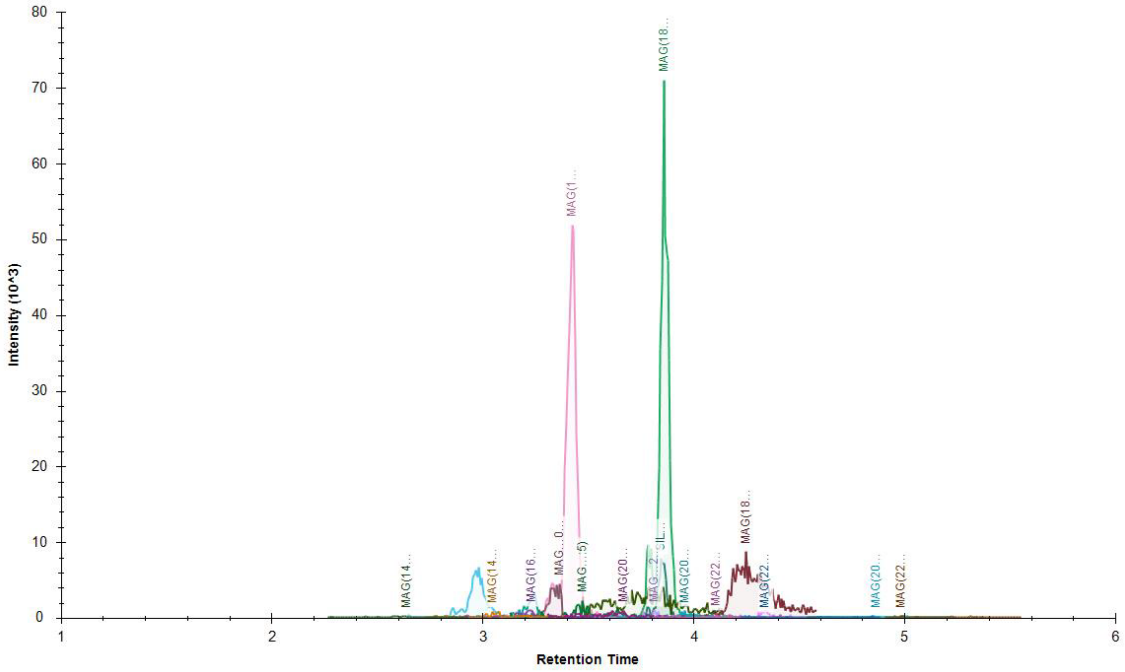
Intensity (10^3)
Retention Time
MAG(14...
MAG(14...
MAG(16...
MAG...0...
MAG(1...
MAG...:5)
MAG(20...
MAG(18...
MAG(20...
MAG(22...
MAG(18...
MAG(22...
MAG(20...
MAG(22...

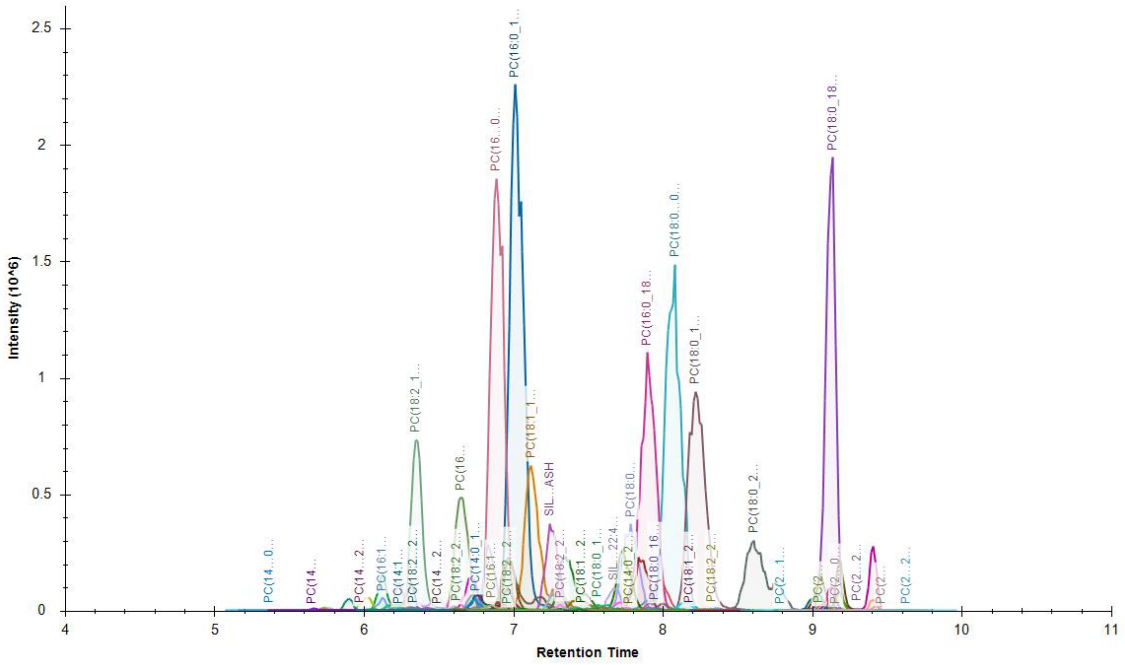
Intensity (10^6)
Retention Time
PC(14...0...
PC(14...
PC(14...2...
PC(16:1...
PC(14:1...
PC(18:2...2...
PC(18:2_1...
PC(14...2...
PC(18:2_2...
PC(16...
PC(14:0_1...
PC(16:1...
PC(18:2...2...
PC(16...0...
PC(16:0_1...
PC(18:1_1...
SIL...ASH
PC(18:2...2...
PC(18:0_1...
SIL...22:4...
PC(18:0...
PC(14:0_2...
PC(18:0_16...
PC(16:0_18...
PC(18:0...0...
PC(18:1_2...
PC(18:0_1...
PC(18:2_2...
PC(18:0_2...
PC(2...1...
PC(18:0_18...
PC(2...0...
PC(2...2...
PC(2...
PC(2...2...

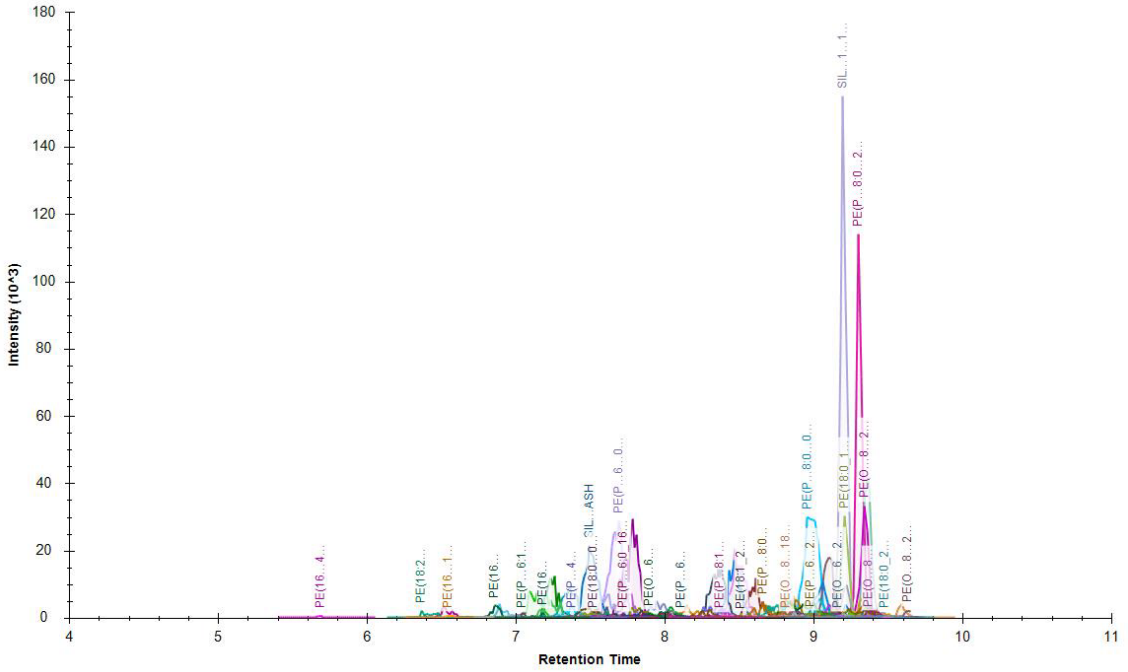
Intensity (10^3)
Retention Time
PE(16...4...
PE(18:2...
PE(16...1...
PE(16...
PE(P...6:1...
PE(16...
PE(P...4...
SIL...ASH
PE(18:0...0...
PE(P...6:0_16...
PE(P...6...0...
PE(O...6...
PE(P...6...
PE(P...8:1...
PE(18:1_2...
PE(P...8:0...
PE(O...8...18...
PE(P...8...2...
PE(P...8:0...0...
PE(O...6...2...
PE(18:0_1...
SIL...1...1...
PE(P...8:0...2...
PE(O...8...2...
PE(18:0_2...
PE(O...8...2...

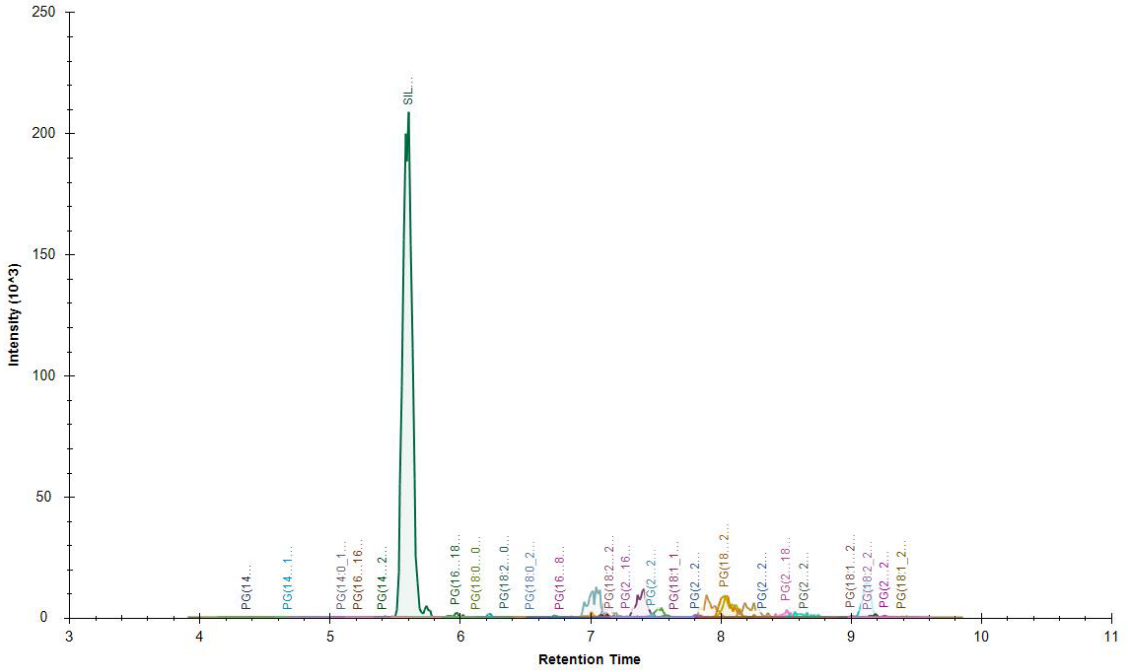
Intensity (10^3)
Retention Time
PG(14...
PG(14...1...
PG(14:0_1...
PG(16...16...
PG(14...2...
SIL...
PG(16...18...
PG(18:0...0...
PG(18:2...0...
PG(18:0_2...
PG(16...8...
PG(18:2...2...
PG(2...16...
PG(2...2...
PG(18:1...1...
PG(2...2...
PG(18...2...
PG(2...2...
PG(2...18...
PG(2...2...
PG(18:1...2...
PG(18:2...2...
PG(2...2...
PG(18:1_2...

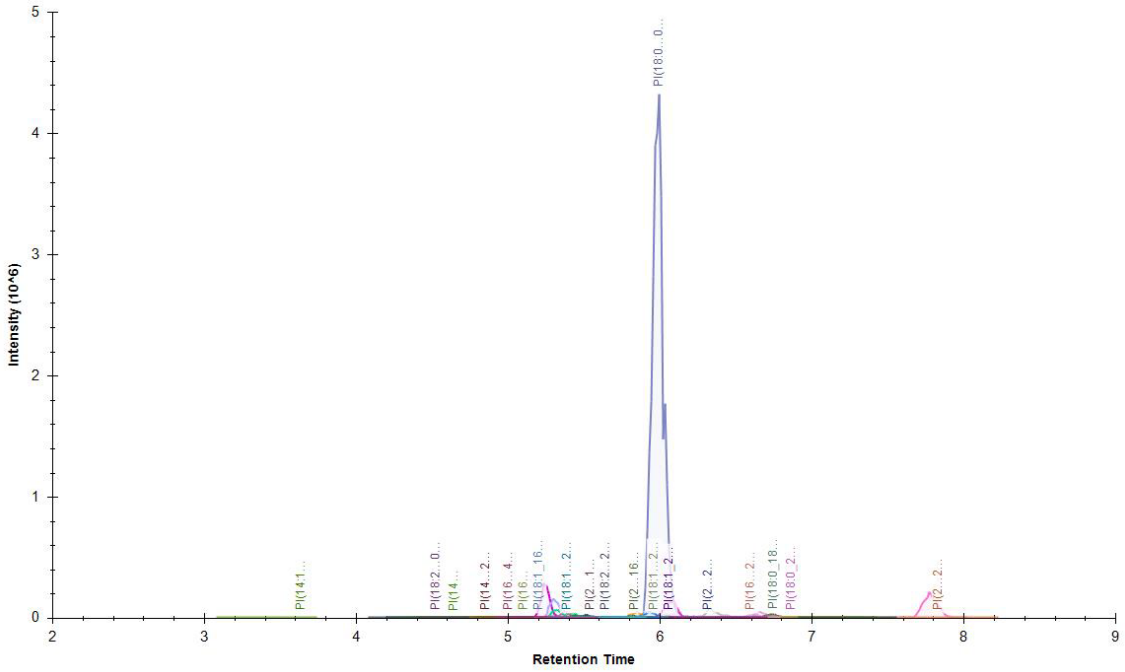
Intensity (10^6)
Retention Time
PI(18:0...0...
PI(14:1...
PI(18:2...0...
PI(14...
PI(14...2...
PI(16...4...
PI(16...
PI(18:1_16...
PI(18:1...2...
PI(2...1...
PI(18:2...2...
PI(2...16...
PI(18:1...2...
PI(18:1...2...
PI(2...2...
PI(16...2...
PI(18:0_18...
PI(18:0_2...
PI(2...2...

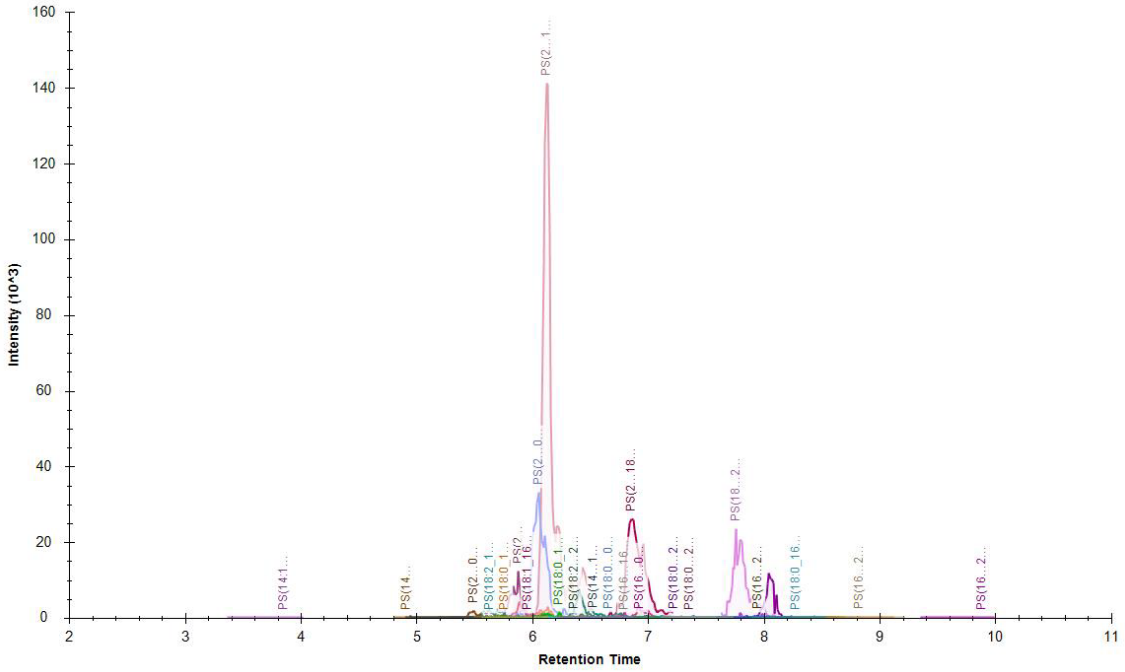
Intensity (10^3)
Retention Time
PS(2...1...
PS(14:1...
PS(14...
PS(2...0...
PS(18:2_1...
PS(18:0_1...
PS(2...
PS(18:1_16...
PS(2...0...
PS(18:0_1...
PS(18:2...2...
PS(14...1...
PS(18:0...0...
PS(16...16...
PS(16...0...
PS(2...18...
PS(18:0...2...
PS(18:0...2...
PS(18...2...
PS(16...2...
PS(18:0_16...
PS(16...2...
PS(16...2...

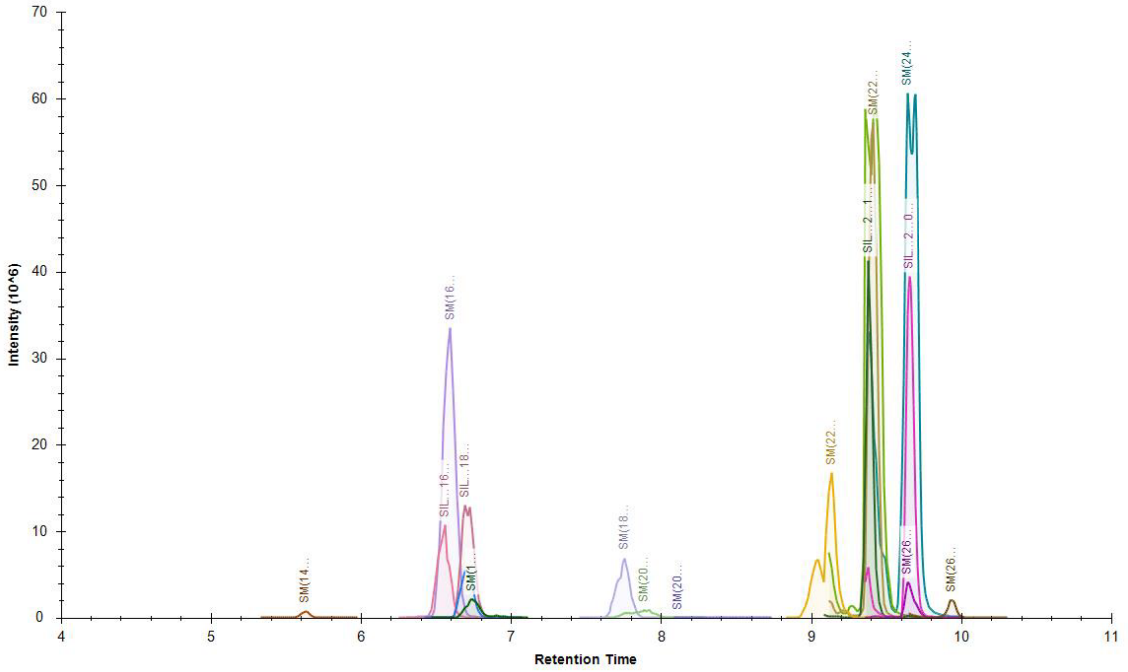
Intensity (10^6)
Retention Time
SM(14...
SM(16...
SIL...16...
SIL...18...
SM(1...
SM(18...
SM(20...
SM(20...
SM(22...
SM(22...
SIL...2...1...
SM(24...
SIL...2...0...
SM(26...
SM(26...

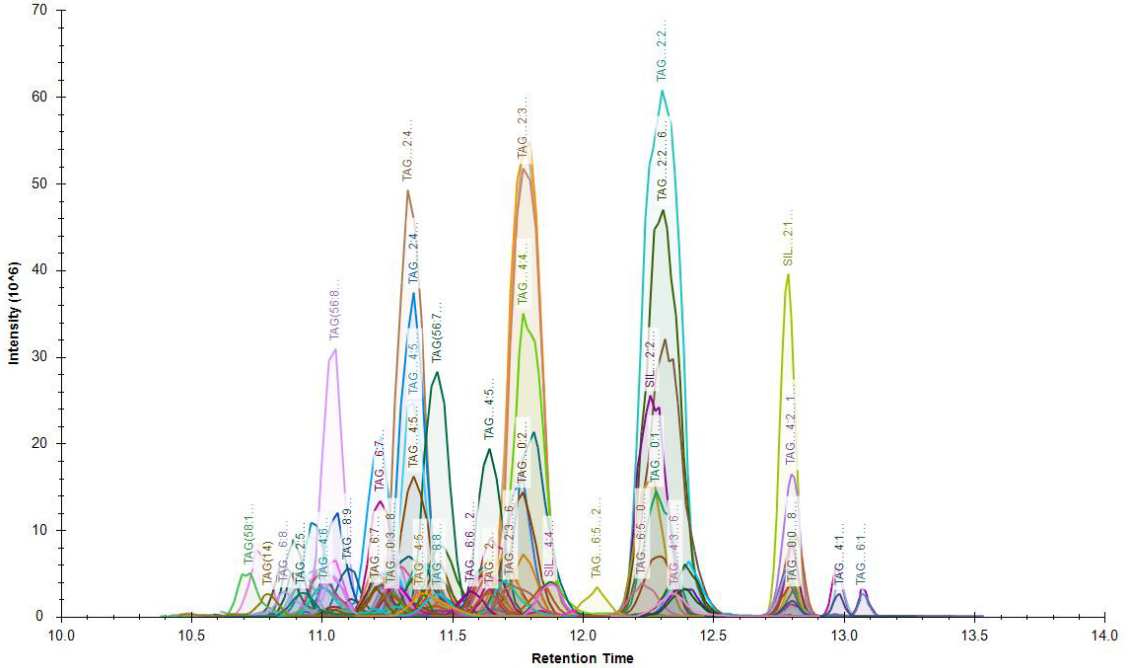
Intensity (10^6)
Retention Time
TAG(681...
TAG(14)
TAG...6:8...
TAG...2:5...
TAG...4:6...
TAG(668...
TAG...8:9...
TAG...6:7...
TAG...6:7...
TAG...0:3...8...
TAG...2:4...
TAG...4:5...
TAG...4:5...
TAG...4:5...
TAG...4:6...
TAG...8:8...
TAG(567...
TAG...6:6...2...
TAG...2...
TAG...4:5...
TAG...2:3...6...
TAG...0:2...
TAG...2:3...
TAG...4:4...
SIL...4:4...
TAG...6:5...2...
TAG...2:2...
TAG...5:5...0...
SIL...2:2...
TAG...0:1...
TAG...4:3...6...
TAG...2:2...
TAG...2:2...6...
SIL...2:1...
TAG...4:2...1...
TAG...0:0...8...
TAG...4:1...
TAG...6:1...

7.3 PCA of chapter 3 cohort

Principal Component Analysis (PCA) with 19 samples (6 from sham controls (red dots), 6 from rats with 1xmTBI (blue dots), and 7 from rats with 2xmTBI (green dots)). The yellow circles represent repeat extractions of a quality control (QC) (n = 5). The QC sample in this study was created from the same sample biofluid type (i.e. serum) but from a different biological source (i.e. sample obtained from outside the study). This was necessary due to the test samples only being available at low volumes, hindering the ability to create a pooled QC sample. In this instance it is recommended that an external pooled QC be processed in an identical manner to those of the experimental samples (138). Clustering of the QC indicated consistent analysis throughout the run. Two samples (overlayed in the PCA) were identified as outliers via Hotelling's T squared test (95% CI). The identification of these sample as outliers is possibly due to sample integrity, extraction error, MS injection error (e.g. a blockage in the injection loop), human error, or Biomek i5 robot error. After review of the raw mass spectrometry data in the data pre-processing stage, the labelled internal standards displayed minimal standard deviation, possibly indicating the error occurred in sample extraction. The outliers were removed from subsequent statistical analysis.

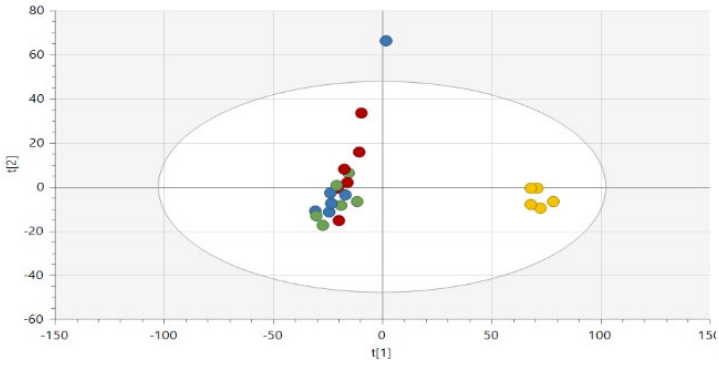

7.4 Kruskal-Wallis test results of lipid species in chapter 3 cohort

A non-parametric Kruskal Wallis Rank Sum Test was performed on all 856 lipid species identified in the data set. A Post hoc Dunn's test was then completed to report inter-class differences. Significance was deemed at less than or equal to 0.05. Eighteen lipid species significantly distinguished between sham control, singular concussion (1xmTBI) and double concussion (2xmTBI).

Lipid Species	p values	Control - 1xmTBI	Control - 2xmTBI	1xmTBI - 2xmTBI
LPE(20:1)	7.59E-03	4.59E-01	8.37E-03	2.45E-03
LPE(22:6)	8.58E-03	7.61E-02	1.03E-01	1.02E-03
PI(16:0_18:2)	1.37E-02	4.49E-01	1.31E-02	3.99E-03
LPE(22:5)	1.65E-02	9.19E-02	1.20E-01	2.09E-03
LPG(18:2)	1.65E-02	1.30E-01	8.43E-02	2.14E-03
PS(14:0_18:2)	1.82E-02	5.69E-03	5.21E-03	4.80E-01
PE(P-18:1_20:4)	2.49E-02	1.66E-01	4.73E-03	3.62E-02
PI(16:0_18:3)	2.89E-02	7.61E-02	1.89E-01	3.99E-03
HCER(d18:0_26:0)	3.23E-02	1.49E-02	6.32E-03	3.87E-01
FFA(20:3)	3.81E-02	5.29E-03	5.71E-02	1.18E-01
PI(18:1_18:2)	3.94E-02	4.29E-01	2.98E-02	9.89E-03
HCER(22:0)	3.99E-02	4.69E-01	2.06E-02	1.35E-02
CE(14:0)	4.13E-02	4.34E-02	5.93E-03	1.98E-01
FFA(18:3)	4.90E-02	5.36E-02	3.22E-01	8.43E-03
PI(20:0_18:2)	4.90E-02	1.59E-01	8.64E-03	6.36E-02

PC(20:0_22:4)	4.93E-02	3.99E-01	3.92E-02	1.13E-02
PE(P-18:0_20:1)	4.93E-02	3.99E-01	3.92E-02	1.13E-02
PI(18:1_18:1)	4.98E-02	2.37E-01	8.09E-02	8.05E-03
LPE(20:4)	5.06E-02	4.49E-01	3.29E-02	1.32E-02
PI(16:0_20:2)	5.29E-02	1.00E-02	2.42E-02	3.18E-01
FFA(20:2)	5.41E-02	1.22E-02	2.42E-01	3.42E-02
LPE(20:0)	5.73E-02	1.31E-02	1.95E-02	4.00E-01
PE(P-16:0_20:4)	5.76E-02	1.47E-01	9.75E-03	7.85E-02
LPE(16:0)	5.79E-02	3.23E-01	5.97E-02	1.11E-02
PI(18:2_18:2)	6.09E-02	3.70E-01	5.09E-02	1.29E-02
CE(22:5)	6.20E-02	7.25E-02	9.18E-03	1.67E-01
CE(22:4)	6.26E-02	9.34E-03	8.43E-02	1.19E-01
CE(22:2)	6.34E-02	4.29E-01	2.55E-02	2.32E-02
PE(P-18:0_20:4)	6.34E-02	4.29E-01	2.55E-02	2.32E-02
FFA(18:1)	6.77E-02	2.60E-02	4.20E-01	2.14E-02
FFA(18:2)	6.91E-02	3.68E-02	4.82E-01	1.67E-02
PG(18:1_18:1)	7.16E-02	1.69E-02	2.67E-01	3.90E-02
DAG(20:0_20:0)	7.29E-02	2.14E-01	1.47E-02	6.25E-02
DCER(24:1)	7.41E-02	3.41E-01	6.53E-02	1.47E-02
LPE(18:1)	7.41E-02	3.41E-01	6.53E-02	1.47E-02
LPE(18:2)	7.41E-02	3.41E-01	6.53E-02	1.47E-02
LPI(18:2)	7.64E-02	1.66E-01	1.35E-02	8.62E-02
TAG(58:6_FA16:0)	7.74E-02	3.89E-01	5.58E-02	1.71E-02
FFA(22:5)	7.92E-02	1.22E-02	7.12E-02	1.69E-01
PC(16:0_18:3)	8.27E-02	2.70E-01	9.53E-02	1.44E-02
LPC(16:0)	8.87E-02	3.14E-01	8.26E-02	1.67E-02
PI(18:2_20:1)	9.18E-02	3.41E-01	2.61E-02	4.35E-02
PC(20:0_22:6)	9.59E-02	3.89E-01	3.13E-02	3.83E-02

PG(20:0_18:2)	9.59E-02	3.89E-01	3.13E-02	3.83E-02
PE(P-18:1_16:0)	9.72E-02	4.09E-01	6.11E-02	2.23E-02
FFA(20:1)	9.74E-02	8.37E-02	3.26E-01	1.74E-02
FFA(24:0)	9.74E-02	8.37E-02	3.26E-01	1.74E-02
FFA(24:1)	9.74E-02	8.37E-02	3.26E-01	1.74E-02
FFA(16:0)	1.03E-01	2.17E-02	2.39E-01	6.15E-02
LPE(18:3)	1.05E-01	2.87E-01	1.03E-01	1.89E-02
PG(20:0_20:4)	1.06E-01	6.25E-02	1.79E-02	2.79E-01
DAG(18:2_22:5)	1.11E-01	2.22E-01	1.44E-01	1.85E-02
PE(P-18:0_20:2)	1.11E-01	2.22E-01	1.44E-01	1.85E-02
PI(16:0_22:6)	1.11E-01	2.22E-01	1.44E-01	1.85E-02
DCER(18:0)	1.11E-01	3.32E-01	8.97E-02	2.18E-02
PC(18:2_18:2)	1.15E-01	1.05E-01	2.98E-01	2.01E-02
TAG(56:6_FA22:4)	1.21E-01	2.61E-01	1.27E-01	2.14E-02
DAG(16:0_22:5)	1.22E-01	4.80E-01	5.71E-02	3.30E-02
PC(18:2_22:5)	1.23E-01	2.93E-02	3.73E-02	4.26E-01
PE(P-16:0_22:5)	1.23E-01	2.93E-02	3.73E-02	4.26E-01
PC(18:0_22:6)	1.25E-01	3.28E-02	3.38E-02	4.70E-01
PC(18:1_18:2)	1.26E-01	1.99E-01	1.74E-01	2.10E-02
LPC(20:1)	1.26E-01	1.20E-01	2.11E-02	1.78E-01
HCER(24:0)	1.32E-01	5.09E-02	4.64E-01	3.62E-02
TAG(53:4_FA20:4)	1.38E-01	3.51E-01	9.72E-02	2.83E-02
PC(18:0_16:1)	1.38E-01	3.51E-01	3.82E-02	6.05E-02
DAG(18:1_20:4)	1.39E-01	2.37E-01	1.55E-01	2.42E-02
TAG(48:4_FA20:4)	1.40E-01	1.79E-01	2.08E-01	2.37E-02
TAG(54:5_FA16:0)	1.40E-01	1.79E-01	2.08E-01	2.37E-02
TAG(56:8_FA20:4)	1.43E-01	6.57E-02	2.68E-02	3.36E-01
PC(18:2_20:4)	1.44E-01	1.15E-01	3.14E-01	2.61E-02

PE(P-16:0_20:3)	1.44E-01	1.15E-01	3.14E-01	2.61E-02
LPI(18:1)	1.48E-01	4.49E-01	7.28E-02	3.69E-02
PE(P-16:0_20:2)	1.49E-01	5.00E-01	6.24E-02	4.19E-02
PI(20:0_18:1)	1.50E-01	4.11E-02	3.51E-01	5.65E-02
TAG(54:6_FA20:4)	1.51E-01	2.78E-01	1.37E-01	2.77E-02
PC(16:0_22:4)	1.51E-01	1.01E-01	3.59E-01	2.94E-02
PE(P-16:0_18:1)	1.51E-01	1.01E-01	3.59E-01	2.94E-02
PE(18:2_20:4)	1.51E-01	1.01E-01	2.61E-02	2.41E-01
PC(18:0_18:1)	1.56E-01	4.83E-02	3.64E-02	4.63E-01
CE(18:1)	1.59E-01	2.76E-02	1.18E-01	1.87E-01
PC(14:0_20:4)	1.60E-01	2.93E-02	8.09E-02	2.68E-01
LPG(18:1)	1.61E-01	3.23E-01	1.20E-01	3.17E-02
LPG(16:0)	1.63E-01	3.32E-01	4.21E-02	7.48E-02
DAG(16:0_18:2)	1.66E-01	1.41E-01	2.86E-01	3.00E-02
TAG(56:5_FA16:0)	1.71E-01	2.53E-01	1.66E-01	3.11E-02
LPC(18:2)	1.76E-01	4.19E-01	9.15E-02	4.12E-02
PE(P-18:1_18:1)	1.76E-01	4.19E-01	9.15E-02	4.12E-02
TAG(58:6_FA20:4)	1.76E-01	4.19E-01	9.15E-02	4.12E-02
LPC(22:4)	1.77E-01	1.25E-01	3.30E-01	3.36E-02
PI(16:0_20:4)	1.77E-01	1.25E-01	3.30E-01	3.36E-02
TAG(56:1_FA16:0)	1.77E-01	1.25E-01	3.30E-01	3.36E-02
PS(20:0_20:3)	1.77E-01	1.25E-01	3.13E-02	2.23E-01
PG(18:0_20:0)	1.79E-01	3.68E-02	6.82E-02	3.45E-01
PI(16:0_18:0)	1.84E-01	1.66E-01	3.38E-02	1.76E-01
DAG(18:2_20:3)	1.85E-01	2.96E-01	1.47E-01	3.55E-02
DAG(18:2_22:4)	1.85E-01	2.96E-01	1.47E-01	3.55E-02
PC(16:0_18:2)	1.85E-01	2.96E-01	1.47E-01	3.55E-02
PE(P-18:0_18:1)	1.85E-01	2.96E-01	1.47E-01	3.55E-02

TAG(56:5_FA20:4)	1.85E-01	2.96E-01	1.47E-01	3.55E-02
TAG(51:1_FA18:0)	1.85E-01	1.10E-01	3.76E-01	3.76E-02
PI(18:0_22:4)	1.87E-01	6.91E-02	3.92E-02	3.96E-01
DAG(14:0_20:4)	1.89E-01	1.72E-01	2.60E-01	3.42E-02
DAG(18:1_20:1)	1.89E-01	1.72E-01	2.60E-01	3.42E-02
TAG(52:4_FA20:0)	1.89E-01	1.72E-01	2.60E-01	3.42E-02
TAG(54:4_FA22:4)	1.89E-01	1.72E-01	2.60E-01	3.42E-02
TAG(56:3_FA16:0)	1.89E-01	1.72E-01	2.60E-01	3.42E-02
TAG(52:1_FA20:1)	1.91E-01	9.61E-02	4.24E-01	4.19E-02
PC(18:0_20:0)	1.91E-01	1.15E-01	3.46E-02	2.57E-01
PE(O-16:0_22:5)	1.94E-01	5.65E-02	4.75E-02	4.83E-01
PE(P-16:0_20:1)	1.97E-01	3.41E-01	1.30E-01	4.04E-02
TAG(58:8_FA22:5)	2.02E-01	2.53E-01	4.32E-02	1.23E-01
PC(14:0_22:6)	2.02E-01	3.68E-02	1.34E-01	2.03E-01
PE(P-16:0_18:3)	2.03E-01	1.53E-01	3.02E-01	3.83E-02
PE(P-18:0_20:3)	2.03E-01	1.53E-01	3.02E-01	3.83E-02
TAG(54:0_FA16:0)	2.03E-01	1.53E-01	3.02E-01	3.83E-02
TAG(54:1_FA18:1)	2.03E-01	1.53E-01	3.02E-01	3.83E-02
TAG(55:2_FA18:2)	2.03E-01	1.53E-01	3.02E-01	3.83E-02
CER(14:0)	2.03E-01	1.53E-01	3.73E-02	2.06E-01
SM(24:0)	2.08E-01	5.09E-02	3.18E-01	8.62E-02
PS(18:0_20:4)	2.13E-01	4.59E-01	7.43E-02	6.57E-02
DAG(18:2_20:4)	2.14E-01	4.90E-01	8.61E-02	5.85E-02
PI(18:1_20:3)	2.14E-01	4.90E-01	8.61E-02	5.85E-02
TAG(58:10_FA18:2)	2.14E-01	4.34E-02	8.61E-02	3.27E-01
PS(20:0_18:1)	2.15E-01	1.36E-01	3.46E-01	4.27E-02
TAG(49:2_FA18:2)	2.15E-01	1.36E-01	3.46E-01	4.27E-02
TAG(56:3_FA18:0)	2.15E-01	1.36E-01	3.46E-01	4.27E-02

TAG(58:2_FA18:1)	2.15E-01	1.36E-01	3.46E-01	4.27E-02
LCER(24:0)	2.19E-01	5.94E-02	3.63E-01	7.85E-02
DAG(18:0_18:2)	2.24E-01	1.20E-01	3.93E-01	4.75E-02
PI(20:0_20:2)	2.24E-01	1.20E-01	3.93E-01	4.75E-02
TAG(51:4_FA18:2)	2.24E-01	1.20E-01	3.93E-01	4.75E-02
TAG(54:1_FA16:0)	2.24E-01	1.20E-01	3.93E-01	4.75E-02
TAG(55:1_FA16:0)	2.24E-01	1.20E-01	3.93E-01	4.75E-02
TAG(55:1_FA18:1)	2.24E-01	1.20E-01	3.93E-01	4.75E-02
TAG(56:2_FA16:0)	2.24E-01	1.20E-01	3.93E-01	4.75E-02
TAG(57:3_FA18:2)	2.24E-01	1.20E-01	3.93E-01	4.75E-02
PE(O-18:0_22:5)	2.24E-01	8.77E-02	4.64E-02	3.74E-01
DAG(18:1_22:5)	2.30E-01	1.85E-01	2.75E-01	4.35E-02
TAG(51:5_FA18:3)	2.30E-01	1.85E-01	2.75E-01	4.35E-02
TAG(52:4_FA16:0)	2.30E-01	1.85E-01	2.75E-01	4.35E-02
TAG(53:0_FA16:0)	2.30E-01	1.85E-01	2.75E-01	4.35E-02
TAG(53:2_FA18:2)	2.30E-01	1.85E-01	2.75E-01	4.35E-02
TAG(54:2_FA18:2)	2.30E-01	1.85E-01	2.75E-01	4.35E-02
TAG(55:3_FA18:2)	2.30E-01	1.85E-01	2.75E-01	4.35E-02
TAG(56:1_FA18:1)	2.30E-01	1.85E-01	2.75E-01	4.35E-02
TAG(56:7_FA22:4)	2.30E-01	1.85E-01	2.75E-01	4.35E-02
TAG(51:4_FA18:3)	2.30E-01	1.05E-01	4.42E-01	5.28E-02
TAG(53:1_FA16:0)	2.30E-01	1.05E-01	4.42E-01	5.28E-02
TAG(56:2_FA18:0)	2.30E-01	1.05E-01	4.42E-01	5.28E-02
TAG(56:5_FA18:0)	2.30E-01	1.05E-01	4.42E-01	5.28E-02
PE(O-16:0_18:0)	2.31E-01	7.98E-02	4.60E-01	6.46E-02
PC(18:2_18:3)	2.33E-01	2.45E-01	2.12E-01	4.42E-02
TAG(54:5_FA20:4)	2.33E-01	2.45E-01	2.12E-01	4.42E-02
TAG(56:4_FA22:4)	2.33E-01	2.45E-01	2.12E-01	4.42E-02

PC(18:0_22:4)	2.35E-01	5.94E-02	6.67E-02	4.53E-01
PE(P-18:0_22:5)	2.35E-01	5.94E-02	6.67E-02	4.53E-01
TAG(56:7_FA20:4)	2.35E-01	5.94E-02	6.67E-02	4.53E-01
LCER(18:1)	2.36E-01	4.58E-02	1.16E-01	2.71E-01
PI(18:0_18:0)	2.36E-01	4.58E-02	1.16E-01	2.71E-01
PG(18:0_18:2)	2.37E-01	3.60E-01	1.39E-01	5.10E-02
FFA(14:0)	2.40E-01	5.65E-02	3.02E-01	1.05E-01
FFA(16:1)	2.40E-01	5.65E-02	3.02E-01	1.05E-01
DAG(16:0_18:3)	2.45E-01	1.66E-01	3.18E-01	4.83E-02
DAG(18:1_22:4)	2.45E-01	1.66E-01	3.18E-01	4.83E-02
TAG(57:2_FA18:1)	2.45E-01	1.66E-01	3.18E-01	4.83E-02
DAG(16:0_20:4)	2.46E-01	4.09E-01	1.23E-01	5.75E-02
DCER(26:1)	2.52E-01	2.87E-01	1.89E-01	5.01E-02
HCER(d18:0_24:0)	2.52E-01	2.87E-01	1.89E-01	5.01E-02
SM(20:0)	2.53E-01	5.36E-02	2.46E-01	1.37E-01
MAG(18:3)	2.55E-01	2.22E-01	2.49E-01	4.92E-02
PC(18:1_20:3)	2.55E-01	2.22E-01	5.21E-02	1.73E-01
MAG(18:0)	2.58E-01	1.47E-01	3.63E-01	5.37E-02
TAG(48:5_FA18:2)	2.58E-01	1.47E-01	3.63E-01	5.37E-02
TAG(52:5_FA16:0)	2.58E-01	1.47E-01	3.63E-01	5.37E-02
TAG(53:1_FA18:1)	2.58E-01	1.47E-01	3.63E-01	5.37E-02
TAG(53:4_FA17:0)	2.58E-01	1.47E-01	3.63E-01	5.37E-02
TAG(54:3_FA20:1)	2.58E-01	1.47E-01	3.63E-01	5.37E-02
LPC(18:3)	2.68E-01	1.30E-01	4.11E-01	5.95E-02
LPC(22:5)	2.68E-01	1.30E-01	4.11E-01	5.95E-02
TAG(51:2_FA18:2)	2.68E-01	1.30E-01	4.11E-01	5.95E-02
TAG(52:5_FA22:5)	2.68E-01	1.30E-01	4.11E-01	5.95E-02
TAG(56:3_FA18:2)	2.68E-01	1.30E-01	4.11E-01	5.95E-02

PE(P-18:0_20:5)	2.69E-01	3.32E-01	1.69E-01	5.65E-02
TAG(56:5_FA22:4)	2.69E-01	3.32E-01	1.69E-01	5.65E-02
TAG(44:2_FA18:2)	2.72E-01	8.77E-02	4.42E-01	7.97E-02
TAG(42:0_FA14:0)	2.72E-01	5.36E-02	1.42E-01	2.54E-01
TAG(53:4_FA18:3)	2.73E-01	1.15E-01	4.60E-01	6.57E-02
DAG(14:0_18:3)	2.74E-01	1.01E-01	4.91E-01	7.25E-02
TAG(50:5_FA18:2)	2.74E-01	1.01E-01	4.91E-01	7.25E-02
TAG(51:2_FA17:0)	2.74E-01	1.01E-01	4.91E-01	7.25E-02
TAG(52:3_FA20:1)	2.74E-01	1.01E-01	4.91E-01	7.25E-02
PS(20:0_20:4)	2.74E-01	6.25E-02	2.86E-01	1.26E-01
TAG(45:0_FA16:0)	2.74E-01	6.25E-02	2.86E-01	1.26E-01
TAG(40:0_FA16:0)	2.74E-01	6.25E-02	9.15E-02	3.90E-01
DAG(18:0_18:3)	2.75E-01	1.99E-01	2.90E-01	5.46E-02
MAG(18:2)	2.75E-01	1.99E-01	2.90E-01	5.46E-02
TAG(52:0_FA20:0)	2.75E-01	1.99E-01	2.90E-01	5.46E-02
TAG(52:3_FA18:3)	2.75E-01	1.99E-01	2.90E-01	5.46E-02
TAG(56:6_FA18:2)	2.75E-01	1.99E-01	2.90E-01	5.46E-02
DAG(18:2_18:3)	2.79E-01	2.61E-01	2.25E-01	5.55E-02
TAG(51:0_FA16:0)	2.79E-01	2.61E-01	2.25E-01	5.55E-02
CE(20:0)	2.79E-01	2.61E-01	6.11E-02	1.59E-01
DCER(22:0)	2.81E-01	2.07E-01	5.71E-02	2.03E-01
FFA(16:2)	2.81E-01	9.19E-02	6.53E-02	4.36E-01
PG(20:0_22:5)	2.81E-01	9.19E-02	6.53E-02	4.36E-01
PI(18:1_20:4)	2.82E-01	3.80E-01	1.50E-01	6.36E-02
PI(18:0_18:3)	2.84E-01	5.94E-02	2.32E-01	1.63E-01
PC(20:0_22:5)	2.84E-01	7.61E-02	7.75E-02	4.76E-01
PE(18:0_22:4)	2.84E-01	7.61E-02	7.75E-02	4.76E-01
PE(P-18:2_20:4)	2.89E-01	4.19E-01	8.79E-02	9.88E-02

PG(18:2_16:1)	2.91E-01	1.47E-01	5.84E-02	2.91E-01
PI(18:0_20:0)	2.91E-01	5.94E-02	1.32E-01	2.91E-01
TAG(44:2_FA16:0)	2.93E-01	1.79E-01	3.34E-01	6.05E-02
TAG(52:2_FA18:2)	2.93E-01	1.79E-01	3.34E-01	6.05E-02
TAG(52:4_FA18:2)	2.93E-01	1.79E-01	3.34E-01	6.05E-02
TAG(52:4_FA18:3)	2.93E-01	1.79E-01	3.34E-01	6.05E-02
TAG(52:5_FA18:3)	2.93E-01	1.79E-01	3.34E-01	6.05E-02
TAG(54:2_FA20:0)	2.93E-01	1.79E-01	3.34E-01	6.05E-02
LPC(20:4)	2.95E-01	4.69E-01	1.01E-01	8.89E-02
TAG(42:0_FA16:0)	2.95E-01	4.69E-01	1.01E-01	8.89E-02
DCER(20:0)	3.01E-01	3.05E-01	7.12E-02	1.45E-01
TAG(54:1_FA18:0)	3.04E-01	2.37E-01	2.64E-01	6.15E-02
TAG(56:4_FA18:2)	3.04E-01	2.37E-01	2.64E-01	6.15E-02
TAG(56:6_FA16:0)	3.04E-01	2.37E-01	2.64E-01	6.15E-02
PC(14:0_18:2)	3.05E-01	8.37E-02	3.76E-01	1.06E-01
TAG(49:1_FA18:1)	3.06E-01	1.59E-01	3.80E-01	6.68E-02
TAG(51:5_FA18:2)	3.06E-01	1.59E-01	3.80E-01	6.68E-02
TAG(53:1_FA17:0)	3.06E-01	1.59E-01	3.80E-01	6.68E-02
TAG(54:3_FA18:3)	3.06E-01	1.59E-01	3.80E-01	6.68E-02
TAG(56:4_FA20:1)	3.06E-01	1.59E-01	3.80E-01	6.68E-02
TAG(58:3_FA18:1)	3.06E-01	1.59E-01	3.80E-01	6.68E-02
MAG(22:5)	3.06E-01	1.92E-01	6.24E-02	2.36E-01
PG(20:0_22:4)	3.06E-01	1.92E-01	6.24E-02	2.36E-01
PI(18:0_18:2)	3.06E-01	1.92E-01	6.24E-02	2.36E-01
PS(20:0_22:5)	3.07E-01	1.36E-01	6.38E-02	3.30E-01
FFA(22:4)	3.08E-01	6.25E-02	1.72E-01	2.38E-01
TAG(40:0_FA14:0)	3.08E-01	6.25E-02	1.72E-01	2.38E-01
HCER(24:1)	3.09E-01	6.91E-02	2.71E-01	1.51E-01

PE(18:1_20:4)	3.10E-01	2.45E-01	6.67E-02	1.87E-01
PI(18:0_20:3)	3.10E-01	2.45E-01	6.67E-02	1.87E-01
DAG(14:0_18:2)	3.15E-01	9.61E-02	4.24E-01	9.74E-02
TAG(49:1_FA17:0)	3.15E-01	6.57E-02	2.18E-01	1.91E-01
DAG(18:1_20:3)	3.16E-01	1.41E-01	4.28E-01	7.36E-02
TAG(48:3_FA18:3)	3.16E-01	1.41E-01	4.28E-01	7.36E-02
TAG(49:1_FA16:0)	3.16E-01	1.41E-01	4.28E-01	7.36E-02
TAG(49:2_FA16:0)	3.16E-01	1.41E-01	4.28E-01	7.36E-02
TAG(52:2_FA18:0)	3.16E-01	1.41E-01	4.28E-01	7.36E-02
TAG(52:6_FA16:0)	3.16E-01	1.41E-01	4.28E-01	7.36E-02
TAG(53:3_FA18:2)	3.16E-01	1.41E-01	4.28E-01	7.36E-02
DAG(16:1_20:4)	3.18E-01	3.51E-01	1.80E-01	7.02E-02
TAG(48:2_FA18:2)	3.20E-01	1.25E-01	4.78E-01	8.10E-02
TAG(51:3_FA18:2)	3.20E-01	1.25E-01	4.78E-01	8.10E-02
TAG(53:3_FA17:0)	3.20E-01	1.25E-01	4.78E-01	8.10E-02
PI(16:0_18:1)	3.20E-01	1.10E-01	4.73E-01	8.89E-02
TAG(49:3_FA16:0)	3.20E-01	1.10E-01	4.73E-01	8.89E-02
TAG(50:1_FA16:1)	3.20E-01	1.10E-01	4.73E-01	8.89E-02
TAG(50:1_FA20:1)	3.20E-01	1.10E-01	4.73E-01	8.89E-02
TAG(51:1_FA17:0)	3.20E-01	1.10E-01	4.73E-01	8.89E-02
TAG(53:2_FA16:0)	3.20E-01	1.10E-01	4.73E-01	8.89E-02
TAG(56:2_FA20:1)	3.20E-01	1.10E-01	4.73E-01	8.89E-02
HCER(26:0)	3.20E-01	1.25E-01	6.97E-02	3.71E-01
TAG(45:0_FA14:0)	3.20E-01	7.25E-02	1.14E-01	3.71E-01
TAG(49:0_FA16:0)	3.27E-01	2.14E-01	3.06E-01	6.79E-02
TAG(52:1_FA16:1)	3.27E-01	2.14E-01	3.06E-01	6.79E-02
TAG(54:4_FA20:4)	3.27E-01	2.14E-01	3.06E-01	6.79E-02
TAG(50:5_FA20:5)	3.30E-01	7.98E-02	3.14E-01	1.39E-01

PC(18:2_20:1)	3.30E-01	1.79E-01	6.82E-02	2.71E-01
TAG(53:6_FA20:4)	3.31E-01	2.78E-01	2.39E-01	6.90E-02
TAG(54:3_FA18:2)	3.31E-01	2.78E-01	2.39E-01	6.90E-02
TAG(56:6_FA18:3)	3.31E-01	2.78E-01	2.39E-01	6.90E-02
TAG(56:4_FA20:4)	3.32E-01	3.99E-01	1.60E-01	7.85E-02
TAG(60:10_FA22:5)	3.32E-01	3.99E-01	9.53E-02	1.19E-01
DAG(14:0_20:0)	3.36E-01	1.05E-01	8.26E-02	4.56E-01
PC(18:0_14:0)	3.40E-01	4.49E-01	1.42E-01	8.76E-02
TAG(58:7_FA20:4)	3.40E-01	4.49E-01	1.09E-01	1.08E-01
TAG(58:9_FA22:5)	3.40E-01	4.49E-01	1.09E-01	1.08E-01
TAG(42:2_FA18:2)	3.43E-01	5.00E-01	1.25E-01	9.74E-02
TAG(52:4_FA20:4)	3.43E-01	5.00E-01	1.25E-01	9.74E-02
HCER(20:1)	3.44E-01	7.25E-02	2.05E-01	2.23E-01
TAG(47:1_FA14:0)	3.45E-01	1.92E-01	3.51E-01	7.48E-02
TAG(52:1_FA20:0)	3.45E-01	1.92E-01	3.51E-01	7.48E-02
TAG(54:6_FA16:0)	3.45E-01	1.92E-01	3.51E-01	7.48E-02
TAG(56:5_FA20:1)	3.45E-01	1.92E-01	3.51E-01	7.48E-02
PS(20:0_22:4)	3.48E-01	9.19E-02	3.59E-01	1.28E-01
TAG(46:3_FA18:2)	3.48E-01	9.19E-02	3.59E-01	1.28E-01
TAG(52:2_FA14:0)	3.48E-01	9.19E-02	3.59E-01	1.28E-01
PE(18:0_22:5)	3.54E-01	3.23E-01	2.15E-01	7.73E-02
PE(P-18:1_18:0)	3.54E-01	3.23E-01	2.15E-01	7.73E-02
TAG(56:6_FA18:0)	3.54E-01	3.23E-01	2.15E-01	7.73E-02
TAG(58:7_FA16:0)	3.54E-01	3.23E-01	2.15E-01	7.73E-02
TAG(54:7_FA18:2)	3.59E-01	2.53E-01	2.79E-01	7.60E-02
TAG(54:8_FA18:2)	3.59E-01	2.53E-01	2.79E-01	7.60E-02
TAG(56:5_FA18:2)	3.59E-01	2.53E-01	2.79E-01	7.60E-02
DCER(26:0)	3.59E-01	1.72E-01	3.98E-01	8.23E-02

TAG(53:1_FA18:0)	3.59E-01	1.72E-01	3.98E-01	8.23E-02
TAG(46:2_FA16:0)	3.61E-01	1.05E-01	4.06E-01	1.18E-01
TAG(46:2_FA18:2)	3.61E-01	1.05E-01	4.06E-01	1.18E-01
TAG(48:2_FA16:0)	3.61E-01	1.05E-01	4.06E-01	1.18E-01
TAG(50:4_FA20:4)	3.61E-01	1.05E-01	4.06E-01	1.18E-01
TAG(54:4_FA20:1)	3.61E-01	1.05E-01	4.06E-01	1.18E-01
LPC(20:5)	3.68E-01	1.53E-01	4.46E-01	9.03E-02
TAG(48:3_FA18:1)	3.68E-01	1.53E-01	4.46E-01	9.03E-02
TAG(50:2_FA18:2)	3.68E-01	1.53E-01	4.46E-01	9.03E-02
TAG(50:3_FA18:3)	3.68E-01	1.53E-01	4.46E-01	9.03E-02
TAG(52:6_FA14:0)	3.68E-01	1.53E-01	4.46E-01	9.03E-02
TAG(52:6_FA18:3)	3.68E-01	1.53E-01	4.46E-01	9.03E-02
TAG(53:4_FA18:2)	3.68E-01	1.53E-01	4.46E-01	9.03E-02
TAG(56:6_FA20:4)	3.68E-01	2.14E-01	7.92E-02	2.52E-01
HCER(14:0)	3.68E-01	1.53E-01	8.09E-02	3.48E-01
TAG(50:1_FA16:0)	3.69E-01	1.20E-01	4.55E-01	1.08E-01
TAG(50:4_FA18:2)	3.69E-01	1.20E-01	4.55E-01	1.08E-01
TAG(50:5_FA16:0)	3.69E-01	1.20E-01	4.55E-01	1.08E-01
TAG(51:2_FA18:1)	3.69E-01	1.20E-01	4.55E-01	1.08E-01
TAG(52:1_FA16:0)	3.69E-01	1.20E-01	4.55E-01	1.08E-01
TAG(52:3_FA14:0)	3.69E-01	1.20E-01	4.55E-01	1.08E-01
TAG(53:2_FA17:0)	3.69E-01	1.20E-01	4.55E-01	1.08E-01
TAG(54:7_FA22:5)	3.69E-01	1.20E-01	4.55E-01	1.08E-01
SM(22:0)	3.70E-01	8.77E-02	2.98E-01	1.65E-01
TAG(46:2_FA18:1)	3.70E-01	8.77E-02	2.98E-01	1.65E-01
TAG(52:2_FA20:1)	3.70E-01	8.77E-02	2.98E-01	1.65E-01
TAG(47:1_FA18:1)	3.72E-01	3.70E-01	1.92E-01	8.62E-02
TAG(58:5_FA18:1)	3.72E-01	3.70E-01	1.92E-01	8.62E-02

TAG(48:4_FA18:2)	3.72E-01	1.36E-01	4.95E-01	9.88E-02
TAG(48:5_FA18:3)	3.72E-01	1.36E-01	4.95E-01	9.88E-02
TAG(50:1_FA18:1)	3.72E-01	1.36E-01	4.95E-01	9.88E-02
TAG(50:2_FA16:0)	3.72E-01	1.36E-01	4.95E-01	9.88E-02
TAG(50:4_FA14:0)	3.72E-01	1.36E-01	4.95E-01	9.88E-02
TAG(51:1_FA16:0)	3.72E-01	1.36E-01	4.95E-01	9.88E-02
TAG(51:3_FA17:0)	3.72E-01	1.36E-01	4.95E-01	9.88E-02
TAG(53:3_FA16:0)	3.72E-01	1.36E-01	4.95E-01	9.88E-02
TAG(54:2_FA20:1)	3.72E-01	1.36E-01	4.95E-01	9.88E-02
HCER(18:0)	3.72E-01	7.98E-02	1.92E-01	2.57E-01
PC(18:0_18:2)	3.75E-01	3.80E-01	1.03E-01	1.43E-01
PE(O-16:0_20:4)	3.75E-01	3.80E-01	1.03E-01	1.43E-01
CER(24:0)	3.78E-01	8.37E-02	2.42E-01	2.08E-01
PC(18:0_20:4)	3.78E-01	8.37E-02	2.42E-01	2.08E-01
PG(18:2_18:2)	3.82E-01	1.41E-01	8.79E-02	3.90E-01
PG(20:0_18:1)	3.82E-01	1.41E-01	8.79E-02	3.90E-01
TAG(52:4_FA22:4)	3.83E-01	2.29E-01	3.22E-01	8.36E-02
TAG(54:3_FA16:0)	3.83E-01	2.29E-01	3.22E-01	8.36E-02
TAG(56:7_FA18:2)	3.83E-01	2.29E-01	3.22E-01	8.36E-02
PE(P-16:0_16:0)	3.83E-01	9.19E-02	1.30E-01	3.93E-01
MAG(20:4)	3.85E-01	4.19E-01	1.72E-01	9.59E-02
PE(P-18:1_22:6)	3.87E-01	2.96E-01	2.53E-01	8.49E-02
LCER(22:0)	3.87E-01	4.29E-01	1.18E-01	1.30E-01
PS(18:0_18:2)	3.87E-01	4.29E-01	1.18E-01	1.30E-01
LPC(20:0)	3.92E-01	4.69E-01	1.52E-01	1.06E-01
LPC(22:6)	3.92E-01	4.69E-01	1.52E-01	1.06E-01
PE(O-16:0_22:4)	3.92E-01	4.69E-01	1.52E-01	1.06E-01
TAG(48:1_FA16:0)	3.92E-01	1.01E-01	3.42E-01	1.53E-01

PI(18:0_20:5)	3.92E-01	1.30E-01	9.53E-02	4.33E-01
LPE(20:2)	3.93E-01	4.80E-01	1.34E-01	1.18E-01
TAG(58:7_FA18:2)	3.93E-01	4.80E-01	1.34E-01	1.18E-01
PE(P-18:1_22:5)	3.94E-01	1.99E-01	8.61E-02	2.88E-01
LCER(d18:0_24:0)	3.97E-01	3.14E-01	9.72E-02	1.85E-01
PC(18:1_20:5)	3.97E-01	3.14E-01	9.72E-02	1.85E-01
TAG(47:0_FA14:0)	3.97E-01	3.14E-01	9.72E-02	1.85E-01
TAG(58:6_FA22:4)	3.97E-01	3.14E-01	9.72E-02	1.85E-01
TAG(58:10_FA22:6)	3.97E-01	1.20E-01	1.03E-01	4.76E-01
FFA(20:5)	3.97E-01	1.10E-01	1.11E-01	4.80E-01
PC(14:0_22:5)	3.97E-01	1.10E-01	1.11E-01	4.80E-01
TAG(47:2_FA18:2)	4.02E-01	2.07E-01	3.67E-01	9.17E-02
TAG(49:3_FA18:3)	4.02E-01	2.07E-01	3.67E-01	9.17E-02
TAG(52:3_FA20:0)	4.02E-01	2.07E-01	3.67E-01	9.17E-02
TAG(54:2_FA16:0)	4.02E-01	2.07E-01	3.67E-01	9.17E-02
TAG(54:5_FA22:5)	4.02E-01	2.07E-01	3.67E-01	9.17E-02
TAG(55:2_FA18:1)	4.02E-01	2.07E-01	3.67E-01	9.17E-02
TAG(55:4_FA18:2)	4.02E-01	2.07E-01	3.67E-01	9.17E-02
TAG(56:7_FA16:0)	4.02E-01	2.07E-01	3.67E-01	9.17E-02
PE(O-16:0_18:1)	4.04E-01	2.53E-01	9.15E-02	2.33E-01
TAG(48:3_FA16:0)	4.09E-01	1.15E-01	3.89E-01	1.41E-01
TAG(49:3_FA18:2)	4.09E-01	1.15E-01	3.89E-01	1.41E-01
TAG(50:3_FA14:0)	4.09E-01	1.15E-01	3.89E-01	1.41E-01
TAG(51:2_FA16:0)	4.09E-01	1.15E-01	3.89E-01	1.41E-01
DAG(16:0_22:6)	4.11E-01	3.41E-01	2.28E-01	9.45E-02
TAG(50:0_FA14:0)	4.11E-01	3.41E-01	2.28E-01	9.45E-02
TAG(51:4_FA20:4)	4.11E-01	3.41E-01	2.28E-01	9.45E-02
TAG(56:7_FA18:3)	4.11E-01	3.41E-01	2.28E-01	9.45E-02

DAG(16:0_20:3)	4.16E-01	1.85E-01	4.15E-01	1.00E-01
FFA(18:0)	4.16E-01	1.85E-01	4.15E-01	1.00E-01
TAG(50:5_FA14:0)	4.16E-01	1.85E-01	4.15E-01	1.00E-01
TAG(51:1_FA18:1)	4.16E-01	1.85E-01	4.15E-01	1.00E-01
TAG(51:3_FA18:3)	4.16E-01	1.85E-01	4.15E-01	1.00E-01
TAG(53:5_FA20:4)	4.16E-01	1.85E-01	4.15E-01	1.00E-01
TAG(54:1_FA20:0)	4.16E-01	1.85E-01	4.15E-01	1.00E-01
TAG(54:2_FA20:2)	4.16E-01	1.85E-01	4.15E-01	1.00E-01
PC(16:0_22:6)	4.16E-01	1.85E-01	9.34E-02	3.27E-01
PC(18:0_22:5)	4.17E-01	2.70E-01	2.94E-01	9.31E-02
PC(18:1_18:3)	4.17E-01	2.70E-01	2.94E-01	9.31E-02
TAG(47:0_FA16:0)	4.17E-01	2.70E-01	2.94E-01	9.31E-02
PE(P-18:1_18:2)	4.19E-01	3.60E-01	1.11E-01	1.69E-01
FFA(14:1)	4.19E-01	9.61E-02	1.69E-01	3.33E-01
HCER(d18:0_20:0)	4.21E-01	1.30E-01	4.37E-01	1.30E-01
PC(14:0_18:3)	4.21E-01	1.30E-01	4.37E-01	1.30E-01
TAG(46:3_FA16:0)	4.21E-01	1.30E-01	4.37E-01	1.30E-01
TAG(48:4_FA16:0)	4.21E-01	1.30E-01	4.37E-01	1.30E-01
TAG(49:1_FA16:1)	4.21E-01	1.30E-01	4.37E-01	1.30E-01
TAG(49:2_FA17:0)	4.21E-01	1.30E-01	4.37E-01	1.30E-01
TAG(50:4_FA16:0)	4.21E-01	1.30E-01	4.37E-01	1.30E-01
TAG(52:4_FA20:2)	4.21E-01	1.30E-01	4.37E-01	1.30E-01
TAG(52:5_FA14:0)	4.21E-01	1.30E-01	4.37E-01	1.30E-01
DAG(18:1_18:2)	4.24E-01	1.66E-01	4.64E-01	1.10E-01
LPC(14:0)	4.24E-01	1.66E-01	4.64E-01	1.10E-01
TAG(50:2_FA18:0)	4.24E-01	1.66E-01	4.64E-01	1.10E-01
TAG(52:6_FA18:2)	4.24E-01	1.66E-01	4.64E-01	1.10E-01
TAG(52:7_FA16:0)	4.24E-01	1.66E-01	4.64E-01	1.10E-01

TAG(54:1_FA20:1)	4.24E-01	1.66E-01	4.64E-01	1.10E-01
TAG(55:5_FA20:4)	4.24E-01	1.66E-01	4.64E-01	1.10E-01
TAG(56:5_FA18:1)	4.24E-01	1.66E-01	4.64E-01	1.10E-01
HCER(d18:0_18:0)	4.26E-01	1.47E-01	4.86E-01	1.19E-01
PC(16:0_20:1)	4.26E-01	1.47E-01	4.86E-01	1.19E-01
TAG(52:1_FA18:0)	4.26E-01	1.47E-01	4.86E-01	1.19E-01
TAG(52:1_FA18:1)	4.26E-01	1.47E-01	4.86E-01	1.19E-01
TAG(53:2_FA18:1)	4.26E-01	1.47E-01	4.86E-01	1.19E-01
LPE(18:0)	4.35E-01	1.72E-01	1.01E-01	3.67E-01
TAG(42:1_FA14:0)	4.36E-01	4.09E-01	1.27E-01	1.55E-01
TAG(58:7_FA22:5)	4.36E-01	4.09E-01	1.27E-01	1.55E-01
DAG(14:0_22:6)	4.36E-01	1.10E-01	3.26E-01	1.80E-01
TAG(46:1_FA14:0)	4.36E-01	1.10E-01	3.26E-01	1.80E-01
TAG(46:2_FA14:0)	4.36E-01	1.10E-01	3.26E-01	1.80E-01
TAG(48:1_FA14:0)	4.36E-01	1.10E-01	3.26E-01	1.80E-01
TAG(48:1_FA18:1)	4.36E-01	1.10E-01	3.26E-01	1.80E-01
PI(18:0_16:1)	4.36E-01	2.96E-01	1.05E-01	2.15E-01
TAG(44:1_FA16:1)	4.37E-01	1.05E-01	1.58E-01	3.74E-01
PE(O-16:0_18:2)	4.42E-01	1.01E-01	2.15E-01	2.77E-01
TAG(48:4_FA16:1)	4.42E-01	1.01E-01	2.15E-01	2.77E-01
TAG(47:1_FA17:0)	4.43E-01	2.45E-01	3.38E-01	1.02E-01
TAG(54:7_FA20:4)	4.43E-01	2.45E-01	3.38E-01	1.02E-01
CE(20:5)	4.45E-01	4.59E-01	1.44E-01	1.41E-01
PG(18:1_20:3)	4.45E-01	4.59E-01	1.44E-01	1.41E-01
TAG(58:6_FA18:1)	4.45E-01	4.59E-01	1.44E-01	1.41E-01
HCER(d18:0_24:1)	4.47E-01	4.90E-01	1.63E-01	1.28E-01
CE(18:0)	4.48E-01	3.14E-01	2.67E-01	1.03E-01
DAG(16:1_20:2)	4.48E-01	3.14E-01	2.67E-01	1.03E-01

TAG(52:2_FA20:0)	4.48E-01	3.14E-01	2.67E-01	1.03E-01
TAG(54:4_FA18:3)	4.48E-01	3.14E-01	2.67E-01	1.03E-01
TAG(54:4_FA20:2)	4.48E-01	3.14E-01	2.67E-01	1.03E-01
TAG(48:1_FA16:1)	4.48E-01	1.05E-01	2.67E-01	2.25E-01
HCER(18:1)	4.50E-01	1.15E-01	1.47E-01	4.16E-01
PC(16:0_20:3)	4.50E-01	1.15E-01	1.47E-01	4.16E-01
LCER(d18:0_22:0)	4.58E-01	1.25E-01	3.72E-01	1.67E-01
TAG(48:2_FA14:0)	4.58E-01	1.25E-01	3.72E-01	1.67E-01
TAG(48:4_FA14:0)	4.58E-01	1.25E-01	3.72E-01	1.67E-01
TAG(50:4_FA18:1)	4.58E-01	1.25E-01	3.72E-01	1.67E-01
TAG(50:5_FA18:1)	4.58E-01	1.25E-01	3.72E-01	1.67E-01
PC(18:0_18:0)	4.58E-01	1.25E-01	1.37E-01	4.59E-01
TAG(44:0_FA18:0)	4.58E-01	1.25E-01	1.37E-01	4.59E-01
HCER(d18:0_26:1)	4.63E-01	2.22E-01	3.85E-01	1.11E-01
TAG(52:2_FA20:2)	4.63E-01	2.22E-01	3.85E-01	1.11E-01
TAG(52:5_FA18:2)	4.63E-01	2.22E-01	3.85E-01	1.11E-01
TAG(56:4_FA18:1)	4.63E-01	2.22E-01	3.85E-01	1.11E-01
PE(18:0_16:0)	4.63E-01	3.41E-01	1.20E-01	1.98E-01
PS(20:0_20:5)	4.63E-01	3.41E-01	1.20E-01	1.98E-01
DCER(16:0)	4.69E-01	1.10E-01	2.02E-01	3.15E-01
PC(18:1_22:4)	4.69E-01	1.10E-01	2.02E-01	3.15E-01
PC(18:1_22:5)	4.69E-01	1.10E-01	2.02E-01	3.15E-01
PE(16:0_20:3)	4.69E-01	1.10E-01	2.02E-01	3.15E-01
TAG(51:0_FA18:0)	4.72E-01	3.60E-01	2.42E-01	1.14E-01
PC(18:1_22:6)	4.73E-01	1.41E-01	4.20E-01	1.55E-01
TAG(46:1_FA16:0)	4.73E-01	1.41E-01	4.20E-01	1.55E-01
TAG(46:3_FA18:3)	4.73E-01	1.41E-01	4.20E-01	1.55E-01
TAG(50:1_FA18:0)	4.73E-01	1.41E-01	4.20E-01	1.55E-01

TAG(50:3_FA18:1)	4.73E-01	1.41E-01	4.20E-01	1.55E-01
TAG(50:3_FA18:2)	4.73E-01	1.41E-01	4.20E-01	1.55E-01
TAG(52:3_FA18:0)	4.73E-01	1.41E-01	4.20E-01	1.55E-01
TAG(52:4_FA18:0)	4.73E-01	1.41E-01	4.20E-01	1.55E-01
TAG(52:4_FA18:1)	4.73E-01	1.41E-01	4.20E-01	1.55E-01
PC(16:0_16:1)	4.73E-01	2.78E-01	1.14E-01	2.49E-01
PC(18:1_20:4)	4.76E-01	1.99E-01	4.33E-01	1.21E-01
TAG(48:0_FA14:0)	4.76E-01	1.99E-01	4.33E-01	1.21E-01
TAG(50:2_FA20:2)	4.76E-01	1.99E-01	4.33E-01	1.21E-01
TAG(51:0_FA17:0)	4.76E-01	1.99E-01	4.33E-01	1.21E-01
TAG(52:3_FA18:2)	4.76E-01	1.99E-01	4.33E-01	1.21E-01
TAG(52:6_FA20:4)	4.76E-01	1.99E-01	4.33E-01	1.21E-01
TAG(54:5_FA18:0)	4.76E-01	1.99E-01	4.33E-01	1.21E-01
TAG(56:8_FA20:5)	4.76E-01	1.99E-01	4.33E-01	1.21E-01
TAG(44:1_FA18:1)	4.80E-01	2.87E-01	3.10E-01	1.13E-01
TAG(49:0_FA18:0)	4.80E-01	2.87E-01	3.10E-01	1.13E-01
TAG(54:6_FA18:1)	4.80E-01	2.87E-01	3.10E-01	1.13E-01
TAG(54:8_FA18:3)	4.80E-01	2.87E-01	3.10E-01	1.13E-01
TAG(49:2_FA18:1)	4.80E-01	1.20E-01	3.10E-01	2.10E-01
PE(O-18:0_18:0)	4.82E-01	1.59E-01	4.69E-01	1.43E-01
TAG(52:5_FA20:3)	4.82E-01	1.59E-01	4.69E-01	1.43E-01
DAG(16:0_18:1)	4.83E-01	1.79E-01	4.82E-01	1.32E-01
TAG(48:4_FA18:1)	4.83E-01	1.79E-01	4.82E-01	1.32E-01
TAG(50:1_FA14:0)	4.83E-01	1.79E-01	4.82E-01	1.32E-01
TAG(50:5_FA18:3)	4.83E-01	1.79E-01	4.82E-01	1.32E-01
TAG(53:4_FA16:0)	4.83E-01	1.79E-01	4.82E-01	1.32E-01
TAG(54:3_FA20:3)	4.83E-01	1.79E-01	4.82E-01	1.32E-01
TAG(58:8_FA18:2)	4.84E-01	3.89E-01	1.37E-01	1.82E-01

PC(20:0_18:1)	4.84E-01	1.15E-01	2.53E-01	2.60E-01
TAG(58:10_FA22:5)	4.91E-01	4.09E-01	2.18E-01	1.26E-01
CER(22:0)	4.98E-01	4.39E-01	1.55E-01	1.67E-01
PE(16:0_18:2)	5.01E-01	4.59E-01	1.96E-01	1.39E-01
HCER(22:1)	5.04E-01	4.90E-01	1.74E-01	1.53E-01
LPI(16:0)	5.04E-01	4.90E-01	1.74E-01	1.53E-01
HCER(26:1)	5.05E-01	1.92E-01	1.25E-01	3.87E-01
PE(18:0_18:0)	5.06E-01	2.61E-01	3.55E-01	1.23E-01
TAG(48:0_FA16:0)	5.06E-01	2.61E-01	3.55E-01	1.23E-01
TAG(49:0_FA17:0)	5.06E-01	2.61E-01	3.55E-01	1.23E-01
TAG(55:5_FA18:1)	5.06E-01	2.61E-01	3.55E-01	1.23E-01
TAG(56:6_FA22:5)	5.06E-01	2.61E-01	3.55E-01	1.23E-01
TAG(54:3_FA16:1)	5.06E-01	1.36E-01	3.55E-01	1.96E-01
DAG(16:0_16:1)	5.06E-01	3.23E-01	1.30E-01	2.30E-01
TAG(58:7_FA22:4)	5.06E-01	3.23E-01	1.30E-01	2.30E-01
PE(P-18:0_18:0)	5.11E-01	3.32E-01	2.82E-01	1.25E-01
TAG(52:0_FA16:0)	5.11E-01	3.32E-01	2.82E-01	1.25E-01
TAG(54:6_FA22:6)	5.11E-01	3.32E-01	2.82E-01	1.25E-01
TAG(51:2_FA16:1)	5.16E-01	1.25E-01	2.39E-01	2.97E-01
TAG(58:9_FA22:6)	5.16E-01	1.25E-01	2.39E-01	2.97E-01
DAG(18:2_20:5)	5.21E-01	1.30E-01	2.94E-01	2.44E-01
FFA(20:4)	5.21E-01	1.30E-01	2.94E-01	2.44E-01
LCER(18:0)	5.21E-01	1.30E-01	2.94E-01	2.44E-01
PC(16:0_16:0)	5.21E-01	1.30E-01	2.94E-01	2.44E-01
PC(16:0_18:0)	5.21E-01	1.30E-01	2.94E-01	2.44E-01
TAG(48:2_FA18:1)	5.21E-01	1.30E-01	2.94E-01	2.44E-01
PC(14:0_20:3)	5.21E-01	1.41E-01	1.66E-01	4.39E-01
PC(18:2_20:2)	5.21E-01	1.41E-01	1.66E-01	4.39E-01

CE(22:6)	5.26E-01	2.37E-01	4.02E-01	1.33E-01
TAG(54:5_FA20:3)	5.26E-01	2.37E-01	4.02E-01	1.33E-01
TAG(56:2_FA20:0)	5.26E-01	2.37E-01	4.02E-01	1.33E-01
TAG(49:2_FA14:0)	5.26E-01	1.53E-01	4.02E-01	1.82E-01
TAG(50:3_FA16:0)	5.26E-01	1.53E-01	4.02E-01	1.82E-01
TAG(50:6_FA20:4)	5.26E-01	1.53E-01	4.02E-01	1.82E-01
TAG(52:4_FA14:0)	5.26E-01	1.53E-01	4.02E-01	1.82E-01
TAG(52:5_FA18:1)	5.26E-01	1.53E-01	4.02E-01	1.82E-01
PE(P-16:0_18:2)	5.26E-01	1.53E-01	1.55E-01	4.83E-01
LCER(16:0)	5.36E-01	3.80E-01	2.56E-01	1.37E-01
LPE(20:3)	5.36E-01	3.80E-01	2.56E-01	1.37E-01
SM(18:1)	5.36E-01	3.80E-01	2.56E-01	1.37E-01
TAG(54:6_FA18:2)	5.36E-01	3.80E-01	2.56E-01	1.37E-01
CE(16:1)	5.36E-01	2.45E-01	1.32E-01	3.24E-01
CER(26:0)	5.39E-01	2.14E-01	4.51E-01	1.45E-01
MAG(18:1)	5.39E-01	2.14E-01	4.51E-01	1.45E-01
PE(18:1_20:1)	5.39E-01	2.14E-01	4.51E-01	1.45E-01
PI(16:0_22:4)	5.39E-01	2.14E-01	4.51E-01	1.45E-01
PS(18:0_20:0)	5.39E-01	2.14E-01	4.51E-01	1.45E-01
TAG(54:4_FA16:0)	5.39E-01	2.14E-01	4.51E-01	1.45E-01
TAG(55:5_FA18:2)	5.39E-01	2.14E-01	4.51E-01	1.45E-01
TAG(56:8_FA22:5)	5.39E-01	2.14E-01	4.51E-01	1.45E-01
DAG(18:0_18:1)	5.39E-01	1.72E-01	4.51E-01	1.69E-01
TAG(52:5_FA20:4)	5.39E-01	1.72E-01	4.51E-01	1.69E-01
TAG(52:6_FA16:1)	5.39E-01	1.72E-01	4.51E-01	1.69E-01
TAG(52:6_FA18:1)	5.39E-01	1.72E-01	4.51E-01	1.69E-01
TAG(54:6_FA22:5)	5.39E-01	1.72E-01	4.51E-01	1.69E-01
TAG(48:1_FA18:0)	5.43E-01	1.92E-01	5.00E-01	1.57E-01

TAG(54:2_FA18:1)	5.43E-01	1.92E-01	5.00E-01	1.57E-01
TAG(56:3_FA18:1)	5.43E-01	1.92E-01	5.00E-01	1.57E-01
PE(P-18:1_20:2)	5.45E-01	3.05E-01	3.26E-01	1.35E-01
TAG(50:0_FA16:0)	5.45E-01	3.05E-01	3.26E-01	1.35E-01
TAG(54:6_FA18:3)	5.45E-01	3.05E-01	3.26E-01	1.35E-01
TAG(54:7_FA18:3)	5.45E-01	3.05E-01	3.26E-01	1.35E-01
PC(18:0_20:5)	5.45E-01	3.05E-01	1.39E-01	2.65E-01
TAG(56:9_FA18:3)	5.50E-01	4.19E-01	1.66E-01	1.96E-01
PE(16:0_22:4)	5.53E-01	4.29E-01	2.32E-01	1.51E-01
PE(18:0_20:3)	5.53E-01	1.47E-01	3.38E-01	2.28E-01
TAG(48:2_FA18:0)	5.53E-01	1.47E-01	3.38E-01	2.28E-01
TAG(48:3_FA14:0)	5.53E-01	1.47E-01	3.38E-01	2.28E-01
PE(18:2_18:2)	5.59E-01	1.41E-01	2.79E-01	2.79E-01
PG(18:1_16:1)	5.59E-01	1.41E-01	2.79E-01	2.79E-01
TAG(48:3_FA18:2)	5.59E-01	1.41E-01	2.79E-01	2.79E-01
TAG(50:2_FA16:1)	5.59E-01	1.41E-01	2.79E-01	2.79E-01
TAG(50:3_FA20:3)	5.59E-01	1.41E-01	2.79E-01	2.79E-01
PC(16:1_18:1)	5.60E-01	4.69E-01	1.86E-01	1.80E-01
PE(P-18:1_20:1)	5.60E-01	4.69E-01	1.86E-01	1.80E-01
TAG(56:10_FA18:2)	5.60E-01	4.69E-01	1.86E-01	1.80E-01
DAG(16:1_18:0)	5.60E-01	2.29E-01	1.42E-01	3.64E-01
PE(O-18:0_16:0)	5.60E-01	2.29E-01	1.42E-01	3.64E-01
PI(18:0_22:5)	5.60E-01	2.29E-01	1.42E-01	3.64E-01
CE(22:0)	5.61E-01	4.80E-01	2.08E-01	1.65E-01
DAG(16:0_20:5)	5.61E-01	4.80E-01	2.08E-01	1.65E-01
LCER(24:1)	5.61E-01	4.80E-01	2.08E-01	1.65E-01
PG(18:1_20:4)	5.66E-01	1.47E-01	2.12E-01	3.77E-01
TAG(44:2_FA18:1)	5.72E-01	2.78E-01	3.72E-01	1.47E-01

TAG(46:3_FA14:0)	5.72E-01	2.78E-01	3.72E-01	1.47E-01
TAG(47:2_FA14:0)	5.72E-01	2.78E-01	3.72E-01	1.47E-01
TAG(54:3_FA18:0)	5.72E-01	2.78E-01	3.72E-01	1.47E-01
TAG(54:5_FA18:2)	5.72E-01	2.78E-01	3.72E-01	1.47E-01
TAG(56:3_FA20:0)	5.72E-01	2.78E-01	3.72E-01	1.47E-01
TAG(56:6_FA18:1)	5.72E-01	2.78E-01	3.72E-01	1.47E-01
TAG(55:7_FA22:6)	5.77E-01	3.51E-01	2.98E-01	1.49E-01
TAG(56:4_FA16:0)	5.77E-01	3.51E-01	2.98E-01	1.49E-01
PC(18:0_20:3)	5.77E-01	3.51E-01	1.58E-01	2.46E-01
PG(18:1_20:2)	5.77E-01	3.51E-01	1.58E-01	2.46E-01
TAG(54:0_FA18:0)	5.77E-01	3.51E-01	1.58E-01	2.46E-01
DAG(18:1_18:1)	5.78E-01	1.66E-01	3.85E-01	2.13E-01
PC(18:1_20:2)	5.78E-01	1.66E-01	3.85E-01	2.13E-01
SM(26:0)	5.78E-01	1.66E-01	3.85E-01	2.13E-01
TAG(48:4_FA18:3)	5.78E-01	1.66E-01	3.85E-01	2.13E-01
TAG(60:11_FA22:6)	5.78E-01	1.66E-01	3.85E-01	2.13E-01
PE(P-16:0_22:4)	5.78E-01	2.14E-01	1.52E-01	4.06E-01
TAG(42:1_FA16:0)	5.80E-01	2.87E-01	1.50E-01	3.03E-01
TAG(45:1_FA16:0)	5.80E-01	2.87E-01	1.50E-01	3.03E-01
PG(18:1_22:6)	5.83E-01	1.59E-01	1.99E-01	4.19E-01
TAG(58:9_FA18:2)	5.83E-01	1.59E-01	1.99E-01	4.19E-01
PC(18:0_20:2)	5.90E-01	1.99E-01	1.63E-01	4.49E-01
TAG(56:8_FA18:2)	5.90E-01	1.99E-01	1.63E-01	4.49E-01
TAG(44:3_FA18:2)	5.91E-01	2.53E-01	4.20E-01	1.59E-01
TAG(54:4_FA18:0)	5.91E-01	2.53E-01	4.20E-01	1.59E-01
TAG(54:5_FA18:3)	5.91E-01	2.53E-01	4.20E-01	1.59E-01
TAG(56:7_FA18:0)	5.91E-01	2.53E-01	4.20E-01	1.59E-01
TAG(56:7_FA22:5)	5.91E-01	2.53E-01	4.20E-01	1.59E-01

TAG(51:3_FA16:1)	5.93E-01	1.53E-01	2.64E-01	3.18E-01
TAG(52:2_FA16:1)	5.93E-01	1.53E-01	2.64E-01	3.18E-01
HCER(16:0)	5.95E-01	1.85E-01	4.33E-01	1.98E-01
TAG(54:4_FA20:3)	5.95E-01	1.85E-01	4.33E-01	1.98E-01
PC(18:2_20:5)	5.97E-01	1.59E-01	3.22E-01	2.63E-01
PE(P-18:0_22:4)	5.97E-01	1.59E-01	3.22E-01	2.63E-01
TAG(50:3_FA16:1)	5.97E-01	1.59E-01	3.22E-01	2.63E-01
TAG(52:7_FA18:1)	5.97E-01	1.59E-01	3.22E-01	2.63E-01
TAG(54:4_FA16:1)	5.97E-01	1.59E-01	3.22E-01	2.63E-01
PG(16:0_18:2)	6.01E-01	3.99E-01	2.71E-01	1.63E-01
TAG(56:8_FA18:3)	6.01E-01	3.99E-01	2.71E-01	1.63E-01
TAG(50:3_FA18:0)	6.02E-01	2.29E-01	4.69E-01	1.71E-01
TAG(52:3_FA16:0)	6.02E-01	2.29E-01	4.69E-01	1.71E-01
TAG(52:3_FA18:1)	6.02E-01	2.29E-01	4.69E-01	1.71E-01
TAG(54:7_FA18:1)	6.02E-01	2.29E-01	4.69E-01	1.71E-01
PI(16:0_20:3)	6.03E-01	2.07E-01	4.82E-01	1.85E-01
PI(16:0_22:5)	6.03E-01	2.07E-01	4.82E-01	1.85E-01
TAG(54:6_FA20:3)	6.03E-01	2.07E-01	4.82E-01	1.85E-01
TAG(48:0_FA18:0)	6.12E-01	3.23E-01	3.42E-01	1.61E-01
LPI(18:0)	6.16E-01	4.49E-01	1.99E-01	2.10E-01
PI(18:0_20:4)	6.16E-01	4.49E-01	1.99E-01	2.10E-01
PC(20:0_20:3)	6.19E-01	3.32E-01	1.69E-01	2.82E-01
TAG(56:9_FA20:4)	6.19E-01	3.32E-01	1.69E-01	2.82E-01
CE(20:3)	6.21E-01	1.66E-01	2.49E-01	3.58E-01
DAG(16:0_16:0)	6.21E-01	1.66E-01	2.49E-01	3.58E-01
FFA(22:6)	6.21E-01	1.66E-01	2.49E-01	3.58E-01
TAG(48:2_FA16:1)	6.21E-01	1.66E-01	2.49E-01	3.58E-01
TAG(48:3_FA16:1)	6.21E-01	1.66E-01	2.49E-01	3.58E-01

TAG(54:7_FA16:1)	6.21E-01	1.66E-01	2.49E-01	3.58E-01
PE(O-18:0_18:2)	6.27E-01	1.79E-01	3.67E-01	2.46E-01
TAG(50:4_FA18:3)	6.27E-01	1.79E-01	3.67E-01	2.46E-01
TAG(50:5_FA20:4)	6.27E-01	1.79E-01	3.67E-01	2.46E-01
PI(18:0_20:2)	6.35E-01	2.53E-01	1.72E-01	3.83E-01
PG(18:1_18:2)	6.36E-01	1.72E-01	3.06E-01	3.00E-01
TAG(52:3_FA20:3)	6.36E-01	1.72E-01	3.06E-01	3.00E-01
TAG(54:6_FA16:1)	6.36E-01	1.72E-01	3.06E-01	3.00E-01
DAG(18:1_20:2)	6.38E-01	2.96E-01	3.89E-01	1.73E-01
TAG(54:5_FA18:1)	6.38E-01	2.96E-01	3.89E-01	1.73E-01
CE(18:2)	6.43E-01	3.70E-01	3.14E-01	1.76E-01
PE(16:0_22:6)	6.43E-01	3.70E-01	3.14E-01	1.76E-01
TAG(54:5_FA20:2)	6.43E-01	3.70E-01	3.14E-01	1.76E-01
PC(18:0_18:3)	6.49E-01	1.99E-01	4.15E-01	2.30E-01
PE(O-18:0_18:1)	6.49E-01	1.99E-01	4.15E-01	2.30E-01
TAG(54:2_FA18:0)	6.49E-01	1.99E-01	4.15E-01	2.30E-01
SM(16:0)	6.49E-01	3.80E-01	1.89E-01	2.63E-01
PC(14:0_14:0)	6.55E-01	3.14E-01	1.80E-01	3.21E-01
TAG(56:7_FA18:1)	6.55E-01	3.14E-01	1.80E-01	3.21E-01
LPC(18:1)	6.56E-01	2.70E-01	4.37E-01	1.87E-01
PI(20:0_16:1)	6.56E-01	2.70E-01	4.37E-01	1.87E-01
TAG(49:1_FA14:0)	6.56E-01	2.70E-01	4.37E-01	1.87E-01
LPC(18:0)	6.57E-01	1.92E-01	2.21E-01	4.43E-01
PC(16:0_20:5)	6.57E-01	1.92E-01	2.21E-01	4.43E-01
PE(16:0_20:1)	6.57E-01	1.92E-01	2.21E-01	4.43E-01
SM(24:1)	6.57E-01	1.92E-01	2.21E-01	4.43E-01
DAG(14:0_18:1)	6.62E-01	2.22E-01	4.64E-01	2.15E-01
TAG(52:5_FA16:1)	6.62E-01	2.22E-01	4.64E-01	2.15E-01

TAG(52:6_FA22:6)	6.62E-01	2.22E-01	4.64E-01	2.15E-01
TAG(56:3_FA20:1)	6.62E-01	2.22E-01	4.64E-01	2.15E-01
TAG(56:4_FA20:3)	6.62E-01	2.22E-01	4.64E-01	2.15E-01
PI(18:1_16:1)	6.64E-01	2.45E-01	4.86E-01	2.01E-01
TAG(52:2_FA16:0)	6.64E-01	2.45E-01	4.86E-01	2.01E-01
TAG(56:9_FA20:5)	6.64E-01	2.45E-01	4.86E-01	2.01E-01
PS(20:0_22:6)	6.66E-01	4.19E-01	2.86E-01	1.91E-01
TAG(46:0_FA14:0)	6.66E-01	4.19E-01	2.86E-01	1.91E-01
PI(20:0_20:4)	6.69E-01	4.29E-01	2.12E-01	2.44E-01
TAG(42:1_FA16:1)	6.69E-01	4.29E-01	2.12E-01	2.44E-01
TAG(58:10_FA20:5)	6.69E-01	4.29E-01	2.12E-01	2.44E-01
CER(16:0)	6.70E-01	1.85E-01	2.90E-01	3.39E-01
DAG(16:1_18:1)	6.70E-01	1.85E-01	2.90E-01	3.39E-01
PI(18:0_22:6)	6.70E-01	1.85E-01	2.90E-01	3.39E-01
TAG(50:2_FA18:1)	6.70E-01	1.85E-01	2.90E-01	3.39E-01
TAG(51:4_FA16:1)	6.70E-01	1.85E-01	2.90E-01	3.39E-01
TAG(52:8_FA16:1)	6.70E-01	1.85E-01	2.90E-01	3.39E-01
TAG(54:5_FA16:1)	6.70E-01	1.85E-01	2.90E-01	3.39E-01
TAG(49:2_FA16:1)	6.72E-01	1.92E-01	3.51E-01	2.82E-01
TAG(50:2_FA14:0)	6.72E-01	1.92E-01	3.51E-01	2.82E-01
TAG(50:5_FA16:1)	6.72E-01	1.92E-01	3.51E-01	2.82E-01
TAG(54:5_FA22:4)	6.72E-01	1.92E-01	3.51E-01	2.82E-01
PE(18:0_18:2)	6.78E-01	3.41E-01	3.59E-01	1.89E-01
TAG(50:0_FA18:0)	6.78E-01	3.41E-01	3.59E-01	1.89E-01
TAG(54:3_FA20:2)	6.78E-01	3.41E-01	3.59E-01	1.89E-01
DAG(14:0_16:1)	6.78E-01	4.69E-01	2.60E-01	2.08E-01
PE(P-18:0_16:0)	6.78E-01	4.69E-01	2.60E-01	2.08E-01
SM(18:0)	6.79E-01	4.80E-01	2.35E-01	2.25E-01

PE(18:0_20:1)	6.86E-01	2.96E-01	1.92E-01	3.61E-01
TAG(47:0_FA17:0)	6.86E-01	2.96E-01	1.92E-01	3.61E-01
TAG(56:5_FA20:2)	6.86E-01	2.96E-01	1.92E-01	3.61E-01
TAG(56:6_FA20:2)	6.92E-01	3.60E-01	2.02E-01	3.00E-01
TAG(58:8_FA20:3)	6.92E-01	3.60E-01	2.02E-01	3.00E-01
DAG(18:0_22:6)	6.97E-01	1.99E-01	2.75E-01	3.80E-01
SM(20:1)	6.97E-01	1.99E-01	2.75E-01	3.80E-01
TAG(50:4_FA16:1)	6.97E-01	1.99E-01	2.75E-01	3.80E-01
PC(18:2_20:3)	7.00E-01	2.14E-01	3.98E-01	2.65E-01
TAG(47:1_FA16:0)	7.04E-01	3.14E-01	4.06E-01	2.03E-01
TAG(54:4_FA18:2)	7.04E-01	3.14E-01	4.06E-01	2.03E-01
TAG(56:5_FA22:5)	7.04E-01	3.14E-01	4.06E-01	2.03E-01
PE(18:0_22:6)	7.09E-01	3.89E-01	3.30E-01	2.06E-01
PE(P-18:1_20:3)	7.09E-01	3.89E-01	3.30E-01	2.06E-01
TAG(46:3_FA18:1)	7.09E-01	3.89E-01	3.30E-01	2.06E-01
TAG(46:4_FA18:2)	7.09E-01	3.89E-01	3.30E-01	2.06E-01
TAG(54:8_FA20:4)	7.09E-01	3.89E-01	3.30E-01	2.06E-01
PE(O-18:0_20:1)	7.09E-01	2.78E-01	2.05E-01	4.03E-01
PE(O-18:0_22:4)	7.09E-01	2.78E-01	2.05E-01	4.03E-01
DAG(16:1_22:6)	7.12E-01	2.07E-01	3.34E-01	3.21E-01
PC(16:1_18:2)	7.12E-01	2.07E-01	3.34E-01	3.21E-01
TAG(56:8_FA16:1)	7.12E-01	2.07E-01	3.34E-01	3.21E-01
TAG(49:3_FA16:1)	7.17E-01	2.37E-01	4.46E-01	2.49E-01
TAG(45:1_FA18:1)	7.18E-01	4.09E-01	2.25E-01	2.79E-01
PE(P-16:1_18:1)	7.24E-01	2.61E-01	4.95E-01	2.33E-01
TAG(52:3_FA20:2)	7.24E-01	2.61E-01	4.95E-01	2.33E-01
PE(18:0_20:4)	7.24E-01	2.61E-01	2.18E-01	4.46E-01
DAG(16:1_16:1)	7.28E-01	2.29E-01	2.46E-01	4.66E-01

TAG(52:3_FA16:1)	7.28E-01	2.29E-01	2.46E-01	4.66E-01
HCER(d18:0_22:0)	7.29E-01	4.39E-01	3.02E-01	2.23E-01
TAG(52:0_FA18:0)	7.29E-01	4.39E-01	3.02E-01	2.23E-01
TAG(56:7_FA22:6)	7.29E-01	4.39E-01	3.02E-01	2.23E-01
PG(16:0_18:1)	7.30E-01	2.45E-01	2.32E-01	4.90E-01
TAG(58:9_FA18:1)	7.30E-01	2.45E-01	2.32E-01	4.90E-01
TAG(56:5_FA20:3)	7.33E-01	4.59E-01	2.49E-01	2.60E-01
TAG(58:6_FA18:0)	7.37E-01	4.90E-01	2.75E-01	2.41E-01
PC(16:0_14:0)	7.43E-01	3.60E-01	3.76E-01	2.20E-01
PC(16:0_20:2)	7.43E-01	3.60E-01	3.76E-01	2.20E-01
TAG(47:1_FA16:1)	7.43E-01	3.60E-01	3.76E-01	2.20E-01
TAG(54:4_FA18:1)	7.43E-01	3.60E-01	3.76E-01	2.20E-01
CE(18:3)	7.45E-01	2.29E-01	3.80E-01	3.03E-01
LCER(d18:0_24:1)	7.45E-01	2.29E-01	3.80E-01	3.03E-01
LPC(20:3)	7.45E-01	2.29E-01	3.80E-01	3.03E-01
PI(16:0_16:0)	7.45E-01	2.29E-01	3.80E-01	3.03E-01
TAG(52:4_FA20:3)	7.45E-01	2.29E-01	3.80E-01	3.03E-01
TAG(52:5_FA20:5)	7.45E-01	2.29E-01	3.80E-01	3.03E-01
TAG(58:8_FA18:1)	7.45E-01	2.29E-01	3.80E-01	3.03E-01
TAG(52:7_FA22:6)	7.45E-01	2.22E-01	3.18E-01	3.61E-01
TAG(58:7_FA18:1)	7.58E-01	3.23E-01	2.28E-01	3.80E-01
CER(24:1)	7.61E-01	3.89E-01	2.39E-01	3.18E-01
PC(18:2_22:6)	7.61E-01	3.89E-01	2.39E-01	3.18E-01
PS(18:0_18:0)	7.61E-01	3.89E-01	2.39E-01	3.18E-01
SM(14:0)	7.61E-01	3.89E-01	2.39E-01	3.18E-01
TAG(58:7_FA22:6)	7.61E-01	3.89E-01	2.39E-01	3.18E-01
DAG(16:1_18:3)	7.67E-01	3.32E-01	4.24E-01	2.36E-01
PC(16:0_18:1)	7.68E-01	2.53E-01	4.28E-01	2.85E-01

TAG(54:5_FA20:5)	7.68E-01	2.53E-01	4.28E-01	2.85E-01
TAG(54:6_FA20:5)	7.68E-01	2.53E-01	4.28E-01	2.85E-01
TAG(55:4_FA18:1)	7.68E-01	2.53E-01	4.28E-01	2.85E-01
TAG(60:10_FA22:6)	7.68E-01	2.53E-01	4.28E-01	2.85E-01
DAG(18:1_20:5)	7.70E-01	2.37E-01	3.02E-01	4.03E-01
TAG(52:4_FA16:1)	7.70E-01	2.37E-01	3.02E-01	4.03E-01
TAG(60:11_FA22:5)	7.70E-01	2.37E-01	3.02E-01	4.03E-01
DCER(22:1)	7.71E-01	4.09E-01	3.46E-01	2.38E-01
CER(18:0)	7.79E-01	3.05E-01	4.73E-01	2.52E-01
TAG(47:2_FA18:1)	7.79E-01	3.05E-01	4.73E-01	2.52E-01
TAG(52:8_FA18:2)	7.79E-01	3.05E-01	4.73E-01	2.52E-01
DAG(14:0_14:0)	7.79E-01	3.05E-01	2.42E-01	4.23E-01
PE(P-18:2_18:2)	7.79E-01	3.05E-01	2.42E-01	4.23E-01
TAG(55:3_FA18:1)	7.80E-01	2.78E-01	4.78E-01	2.68E-01
TAG(56:4_FA18:0)	7.80E-01	2.78E-01	4.78E-01	2.68E-01
TAG(56:6_FA20:3)	7.80E-01	2.78E-01	4.78E-01	2.68E-01
PC(18:1_20:1)	7.83E-01	4.39E-01	2.64E-01	2.97E-01
PE(O-16:0_20:1)	7.83E-01	4.39E-01	2.64E-01	2.97E-01
TAG(46:0_FA18:0)	7.83E-01	4.39E-01	2.64E-01	2.97E-01
PE(18:1_18:2)	7.84E-01	2.45E-01	3.63E-01	3.42E-01
PI(16:0_16:1)	7.84E-01	2.45E-01	3.63E-01	3.42E-01
PI(20:0_20:1)	7.84E-01	2.45E-01	3.63E-01	3.42E-01
CE(20:2)	7.87E-01	2.53E-01	2.86E-01	4.46E-01
PE(P-18:0_18:2)	7.87E-01	2.53E-01	2.86E-01	4.46E-01
TAG(52:7_FA20:5)	7.87E-01	2.53E-01	2.86E-01	4.46E-01
PE(O-18:0_22:6)	7.88E-01	4.59E-01	3.18E-01	2.57E-01
TAG(56:6_FA22:6)	7.88E-01	4.59E-01	3.18E-01	2.57E-01

TAG(56:8_FA16:0)	7.88E-01	4.59E-01	3.18E-01	2.57E-01
TAG(58:8_FA20:4)	7.88E-01	4.59E-01	3.18E-01	2.57E-01
PE(O-18:0_20:4)	7.91E-01	2.87E-01	2.56E-01	4.66E-01
TAG(46:1_FA16:1)	7.91E-01	2.87E-01	2.56E-01	4.66E-01
TAG(46:3_FA16:1)	7.94E-01	2.70E-01	2.71E-01	4.90E-01
PC(16:0_20:4)	7.97E-01	3.70E-01	2.53E-01	3.58E-01
PS(20:0_16:1)	8.04E-01	3.80E-01	3.93E-01	2.54E-01
TAG(44:1_FA14:0)	8.04E-01	3.80E-01	3.93E-01	2.54E-01
TAG(46:1_FA18:1)	8.04E-01	3.80E-01	3.93E-01	2.54E-01
CER(22:1)	8.13E-01	2.70E-01	4.11E-01	3.24E-01
HCER(20:0)	8.13E-01	2.70E-01	4.11E-01	3.24E-01
PC(14:0_18:1)	8.13E-01	2.70E-01	4.11E-01	3.24E-01
TAG(52:2_FA18:1)	8.13E-01	2.70E-01	4.11E-01	3.24E-01
CE(20:4)	8.15E-01	2.61E-01	3.46E-01	3.83E-01
TAG(52:6_FA20:5)	8.15E-01	2.61E-01	3.46E-01	3.83E-01
TAG(54:3_FA18:1)	8.15E-01	2.61E-01	3.46E-01	3.83E-01
TAG(56:3_FA20:2)	8.25E-01	3.51E-01	4.42E-01	2.71E-01
FFA(20:0)	8.25E-01	4.19E-01	2.79E-01	3.36E-01
PC(16:0_22:5)	8.25E-01	4.19E-01	2.79E-01	3.36E-01
TAG(44:2_FA16:1)	8.25E-01	3.51E-01	2.67E-01	4.00E-01
DAG(16:1_20:0)	8.29E-01	2.96E-01	4.60E-01	3.06E-01
TAG(50:4_FA20:3)	8.29E-01	2.96E-01	4.60E-01	3.06E-01
DAG(16:0_18:0)	8.34E-01	3.23E-01	4.91E-01	2.88E-01
PI(16:0_20:5)	8.34E-01	3.23E-01	4.91E-01	2.88E-01
TAG(54:7_FA20:5)	8.34E-01	3.23E-01	4.91E-01	2.88E-01
TAG(54:8_FA22:6)	8.34E-01	3.23E-01	4.91E-01	2.88E-01
TAG(54:7_FA22:6)	8.37E-01	2.78E-01	3.30E-01	4.26E-01
TAG(58:8_FA22:6)	8.37E-01	2.78E-01	3.30E-01	4.26E-01

CER(20:0)	8.40E-01	4.69E-01	3.06E-01	3.15E-01
PE(18:0_20:2)	8.40E-01	4.69E-01	3.06E-01	3.15E-01
DCER(24:0)	8.41E-01	4.80E-01	3.34E-01	2.94E-01
TAG(46:0_FA16:0)	8.41E-01	4.80E-01	3.34E-01	2.94E-01
TAG(56:7_FA20:5)	8.41E-01	4.80E-01	3.34E-01	2.94E-01
LPE(16:1)	8.43E-01	3.32E-01	2.82E-01	4.43E-01
PG(20:0_22:6)	8.49E-01	2.96E-01	3.14E-01	4.70E-01
TAG(56:7_FA16:1)	8.50E-01	2.87E-01	3.93E-01	3.64E-01
TAG(58:10_FA20:4)	8.50E-01	2.87E-01	3.93E-01	3.64E-01
PC(20:0_20:2)	8.51E-01	3.14E-01	2.98E-01	4.86E-01
PS(20:0_18:2)	8.51E-01	3.14E-01	2.98E-01	4.86E-01
TAG(60:12_FA22:6)	8.51E-01	3.14E-01	2.98E-01	4.86E-01
PE(16:0_20:4)	8.59E-01	3.99E-01	4.11E-01	2.91E-01
TAG(46:1_FA18:0)	8.59E-01	3.99E-01	4.11E-01	2.91E-01
DAG(16:1_18:2)	8.72E-01	3.14E-01	4.42E-01	3.45E-01
LPC(16:1)	8.72E-01	3.14E-01	4.42E-01	3.45E-01
PC(20:0_20:4)	8.77E-01	3.70E-01	4.60E-01	3.09E-01
TAG(42:1_FA18:1)	8.77E-01	3.05E-01	3.76E-01	4.06E-01
TAG(46:2_FA16:1)	8.77E-01	3.05E-01	3.76E-01	4.06E-01
TAG(54:8_FA20:5)	8.77E-01	3.05E-01	3.76E-01	4.06E-01
MAG(22:6)	8.81E-01	3.41E-01	4.91E-01	3.27E-01
TAG(44:1_FA16:0)	8.81E-01	3.41E-01	4.91E-01	3.27E-01
TAG(56:9_FA22:6)	8.81E-01	3.41E-01	4.91E-01	3.27E-01
PE(16:0_18:1)	8.81E-01	4.49E-01	3.22E-01	3.55E-01
CER(26:1)	8.84E-01	3.80E-01	3.10E-01	4.19E-01
PC(18:1_18:1)	8.84E-01	3.80E-01	3.10E-01	4.19E-01
PC(18:2_16:1)	8.95E-01	3.23E-01	3.59E-01	4.49E-01

PS(18:0_18:1)	8.95E-01	3.23E-01	3.59E-01	4.49E-01
TAG(56:7_FA20:3)	8.95E-01	3.23E-01	3.59E-01	4.49E-01
PE(18:0_18:1)	8.99E-01	3.60E-01	3.26E-01	4.63E-01
PS(20:0_18:3)	8.99E-01	3.60E-01	3.26E-01	4.63E-01
TAG(58:9_FA20:4)	9.06E-01	3.32E-01	4.24E-01	3.87E-01
LPI(20:4)	9.07E-01	4.19E-01	4.28E-01	3.30E-01
CE(22:1)	9.20E-01	3.60E-01	4.73E-01	3.67E-01
DAG(18:1_22:6)	9.20E-01	3.60E-01	4.73E-01	3.67E-01
DAG(18:2_22:6)	9.21E-01	3.89E-01	4.78E-01	3.48E-01
PE(16:0_16:0)	9.21E-01	3.89E-01	4.78E-01	3.48E-01
LCER(20:0)	9.24E-01	4.69E-01	3.98E-01	3.51E-01
PE(16:0_22:5)	9.24E-01	4.69E-01	3.98E-01	3.51E-01
TAG(58:7_FA18:0)	9.24E-01	4.69E-01	3.98E-01	3.51E-01
TAG(56:8_FA22:6)	9.25E-01	4.80E-01	3.67E-01	3.74E-01
TAG(58:6_FA22:5)	9.25E-01	4.80E-01	3.67E-01	3.74E-01
CE(16:0)	9.29E-01	3.51E-01	4.06E-01	4.29E-01
PE(O-16:0_22:6)	9.29E-01	3.51E-01	4.06E-01	4.29E-01
MAG(16:0)	9.42E-01	3.70E-01	3.89E-01	4.73E-01
PE(P-18:0_22:6)	9.42E-01	3.70E-01	3.89E-01	4.73E-01
PI(18:0_18:1)	9.49E-01	3.80E-01	4.55E-01	4.10E-01
PG(20:0_16:1)	9.53E-01	4.59E-01	3.85E-01	4.16E-01
CER(20:1)	9.56E-01	4.09E-01	4.95E-01	3.90E-01
SM(22:1)	9.58E-01	4.90E-01	4.15E-01	3.93E-01
PE(P-16:0_22:6)	9.70E-01	4.39E-01	4.02E-01	4.59E-01
PE(P-18:1_22:4)	9.70E-01	4.39E-01	4.02E-01	4.59E-01
CE(24:1)	9.75E-01	4.19E-01	4.20E-01	4.97E-01
TAG(44:0_FA14:0)	9.75E-01	4.19E-01	4.20E-01	4.97E-01
TAG(56:6_FA20:5)	9.75E-01	4.19E-01	4.20E-01	4.97E-01

PE(18:1_18:1)	9.76E-01	4.59E-01	4.64E-01	4.13E-01
PE(P-16:0_18:0)	9.76E-01	4.59E-01	4.64E-01	4.13E-01
TAG(44:0_FA16:0)	9.79E-01	4.29E-01	4.86E-01	4.33E-01
TAG(56:4_FA20:2)	9.79E-01	4.29E-01	4.86E-01	4.33E-01
TAG(56:8_FA18:1)	9.79E-01	4.29E-01	4.86E-01	4.33E-01
SM(26:1)	9.81E-01	4.90E-01	4.33E-01	4.36E-01
CE(20:1)	9.92E-01	4.69E-01	4.51E-01	4.80E-01
LPC(20:2)	9.92E-01	4.69E-01	4.51E-01	4.80E-01
PC(18:0_20:1)	9.92E-01	4.69E-01	4.51E-01	4.80E-01
PI(18:2_20:4)	9.92E-01	4.69E-01	4.51E-01	4.80E-01
TAG(44:2_FA14:0)	9.94E-01	4.80E-01	4.82E-01	4.56E-01
TAG(47:2_FA16:1)	1.00E+00	5.00E-01	5.00E-01	5.00E-01

7.5 Chromatograms of data from chapter 4 cohort

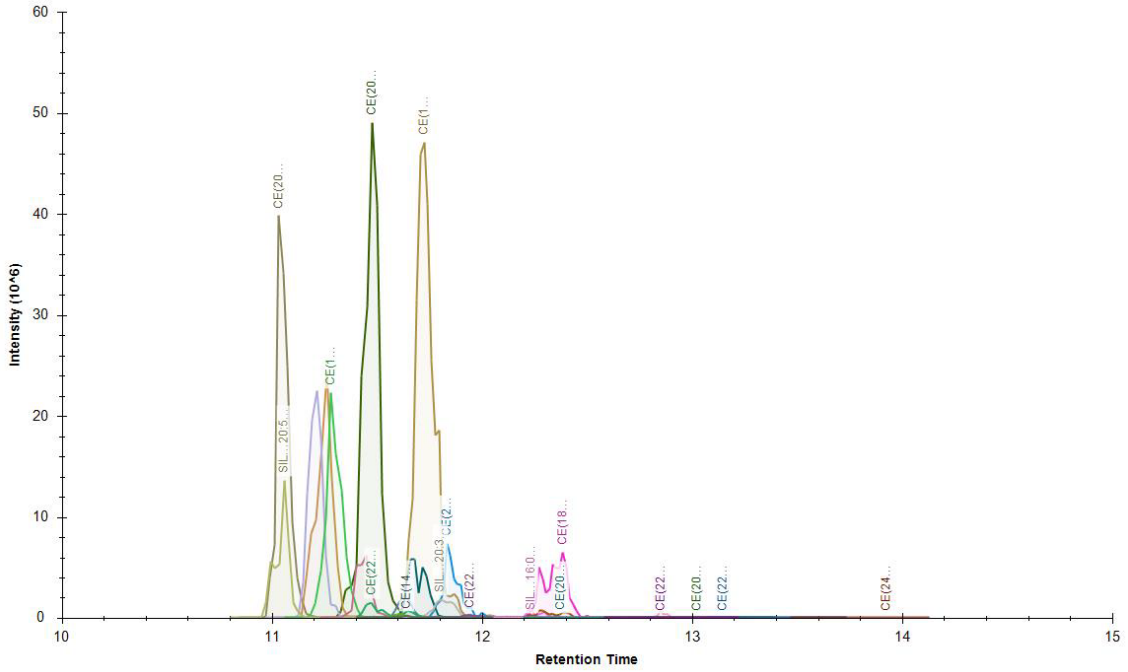
Intensity (10^6)
Retention Time
CE(20...
CE(1...
SIL... 20:5...
CE(22...
CE(14...
SIL... 20:3...
CE(2...
SIL... 16:0...
CE(18...
CE(20...
CE(24...

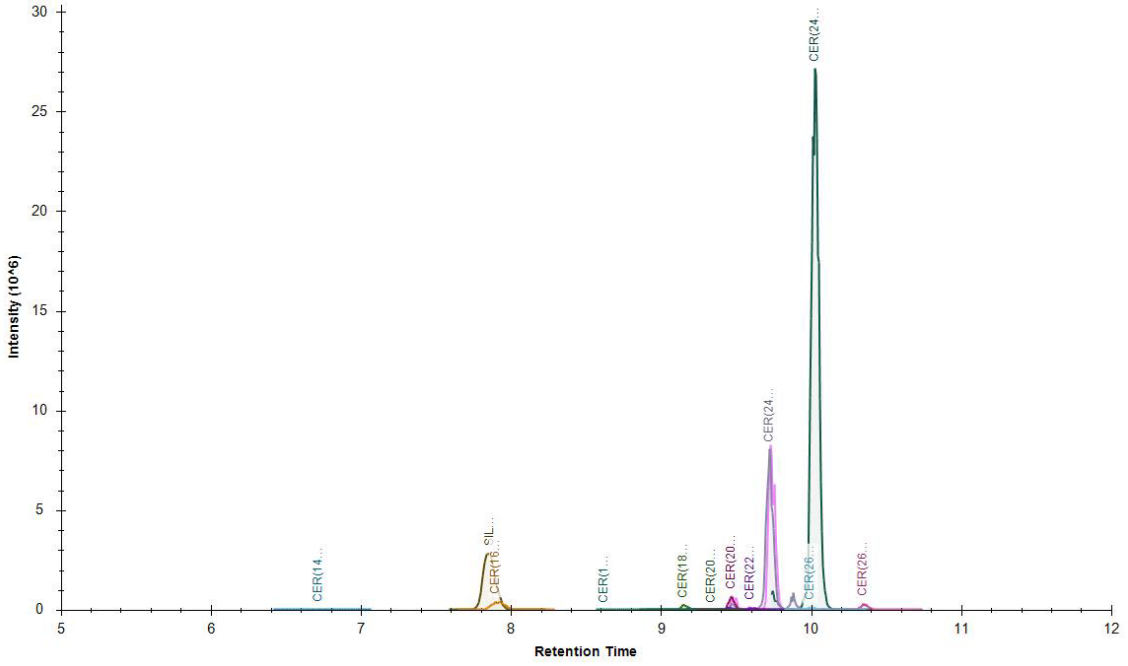
Intensity (10^6)
Retention Time
CER(24...
CER(14...
SIL...
CER(16...
CER(1...
CER(18...
CER(20...
CER(22...
CER(26...

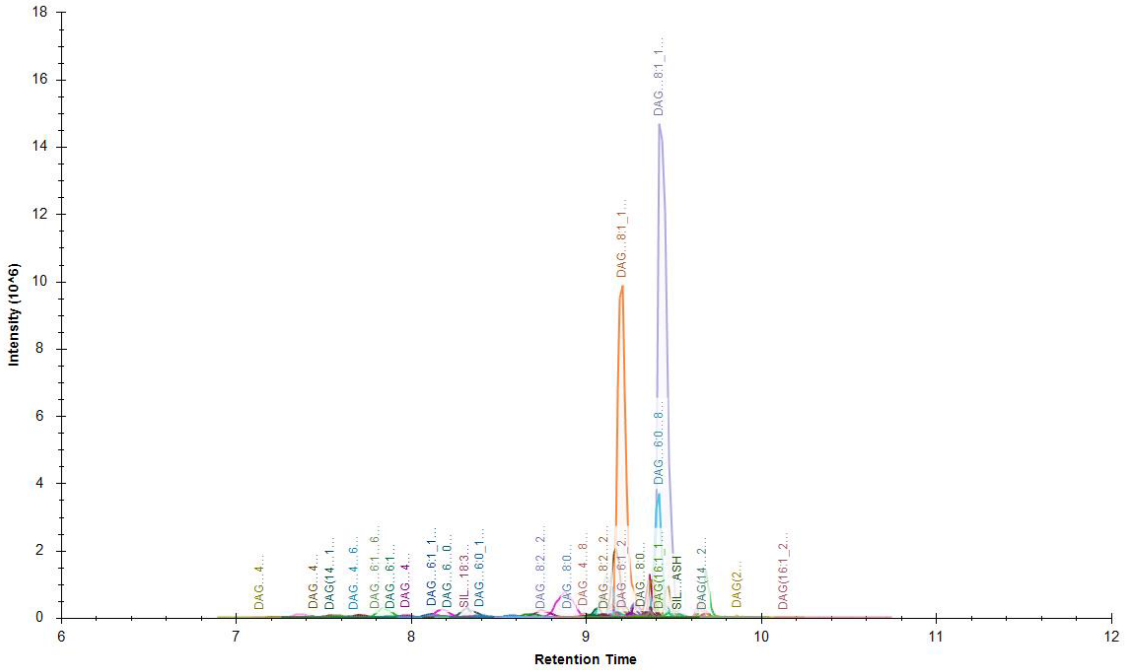
Intensity (10^6)
Retention Time
DAG...4...
DAG...4...
DAG(14...1...
DAG...4...6...
DAG...6:1...6...
DAG...6:1...
DAG...4...
DAG...6:1_1...
DAG...6...0...
SIL...18:3...
DAG...6:0_1...
DAG...8:2...2...
DAG...8:0...
DAG...4...8...
DAG...8:2...2...
DAG...6:1_2...
DAG...8:0...
DAG(16:1_1...
SIL...ASH
DAG(14...2...
DAG(2...
DAG(16:1_2...
DAG...8:1_1...
DAG...6:0...8...

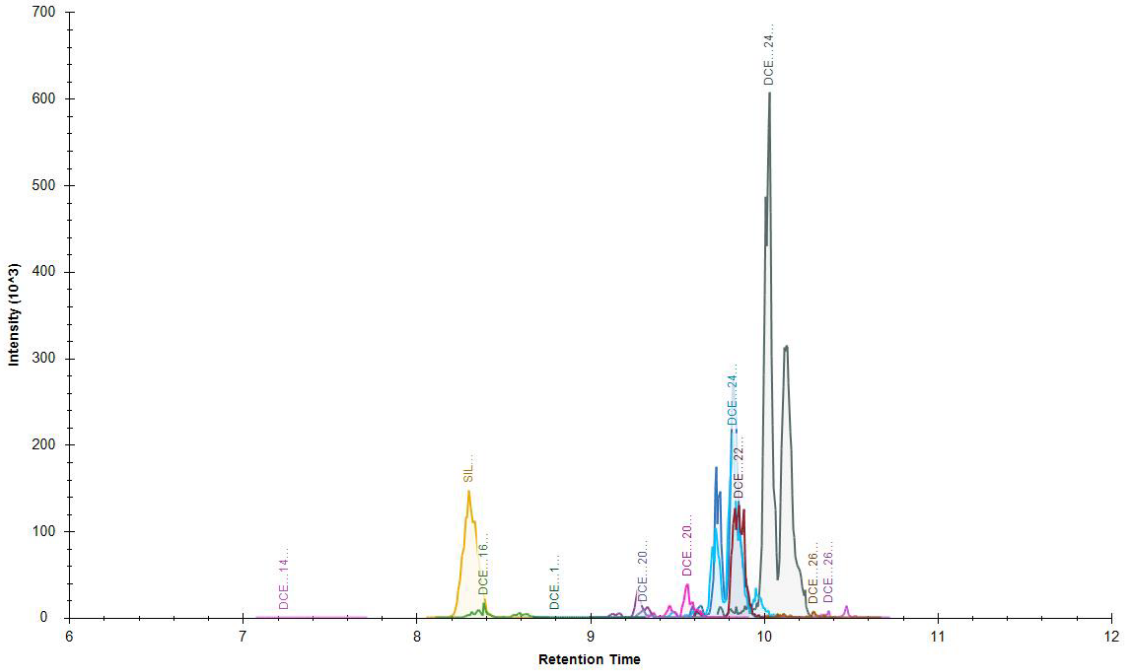
Intensity (10^3)
Retention Time
DCE...14...
SIL...
DCE...16...
DCE...1...
DCE...20...
DCE...20...
DCE...24...
DCE...22...
DCE...24...
DCE...26...
DCE...26...
DCE...24...

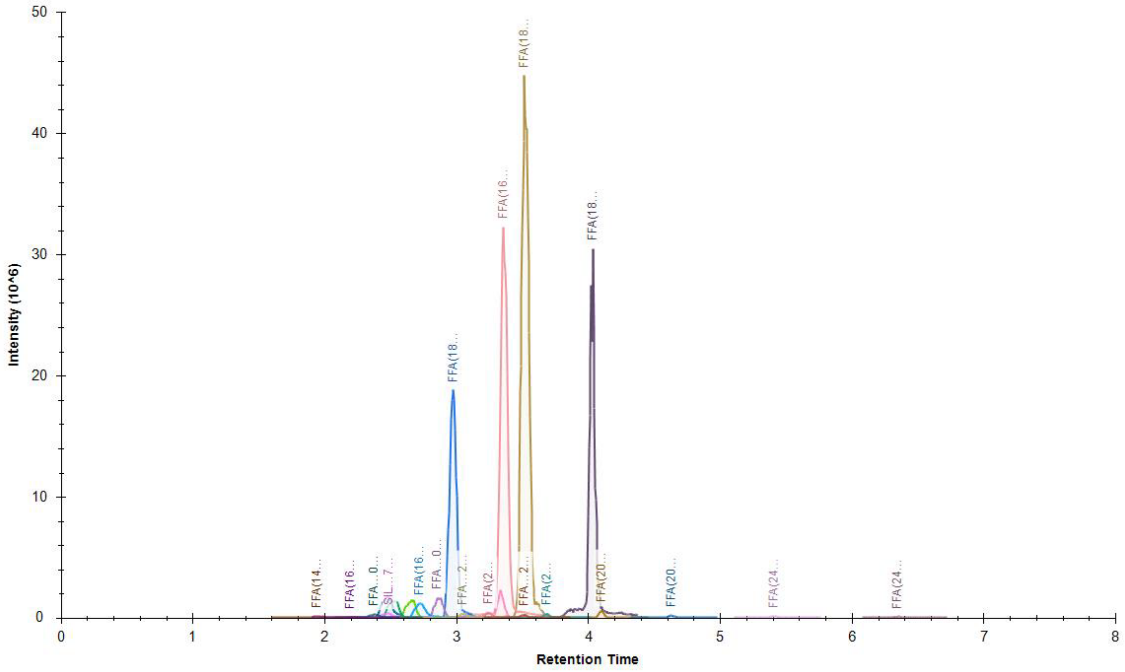
Intensity (10^6)
Retention Time
FFA(14...
FFA(16...
FFA...0...
SIL...7...
FFA(16...
FFA...0...
FFA(18...
FFA...2...
FFA(2...
FFA(16...
FFA(18...
FFA...2...
FFA(2...
FFA(18...
FFA(20...
FFA(20...
FFA(24...
FFA(24...

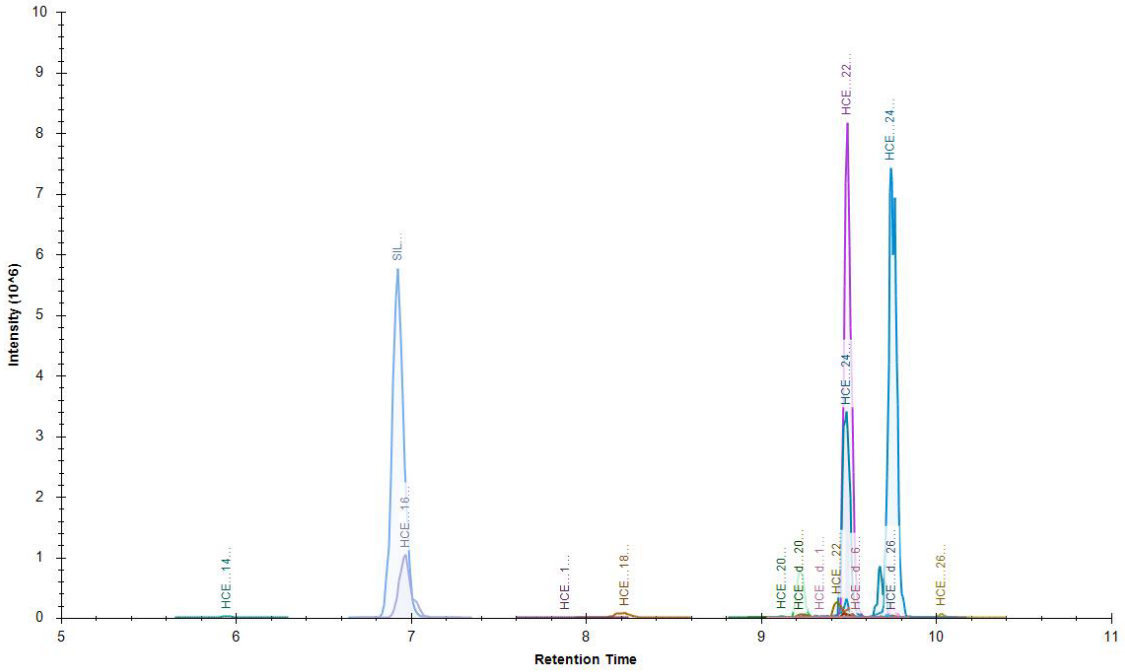
Intensity (10^6)
Retention Time
HCE...14...
SIL...
HCE...16...
HCE...1...
HCE...18...
HCE...20...
HCE...d...20...
HCE...d...1...
HCE...22...
HCE...d...6...
HCE...22...
HCE...24...
HCE...24...
HCE...d...26...
HCE...26...

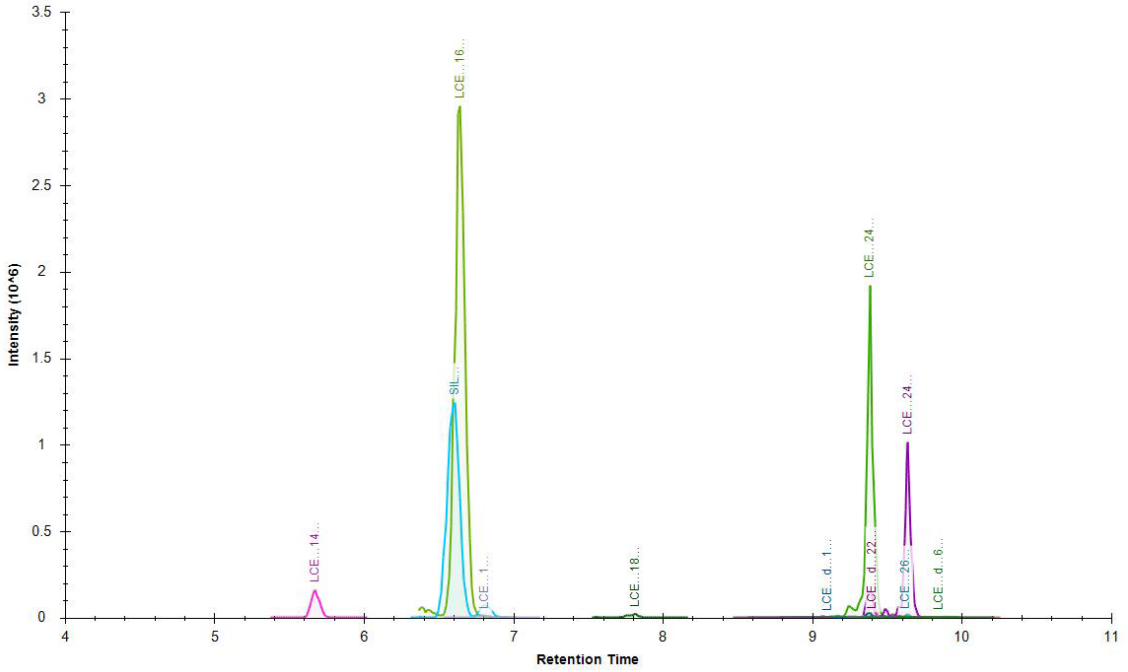
Intensity (10^6)
Retention Time
LCE...16...
SIL...
LCE...24...
LCE...24...
LCE...14...
LCE...1...
LCE...18...
LCE...d...1...
LCE...d...22...
LCE...26...
LCE...d...6...

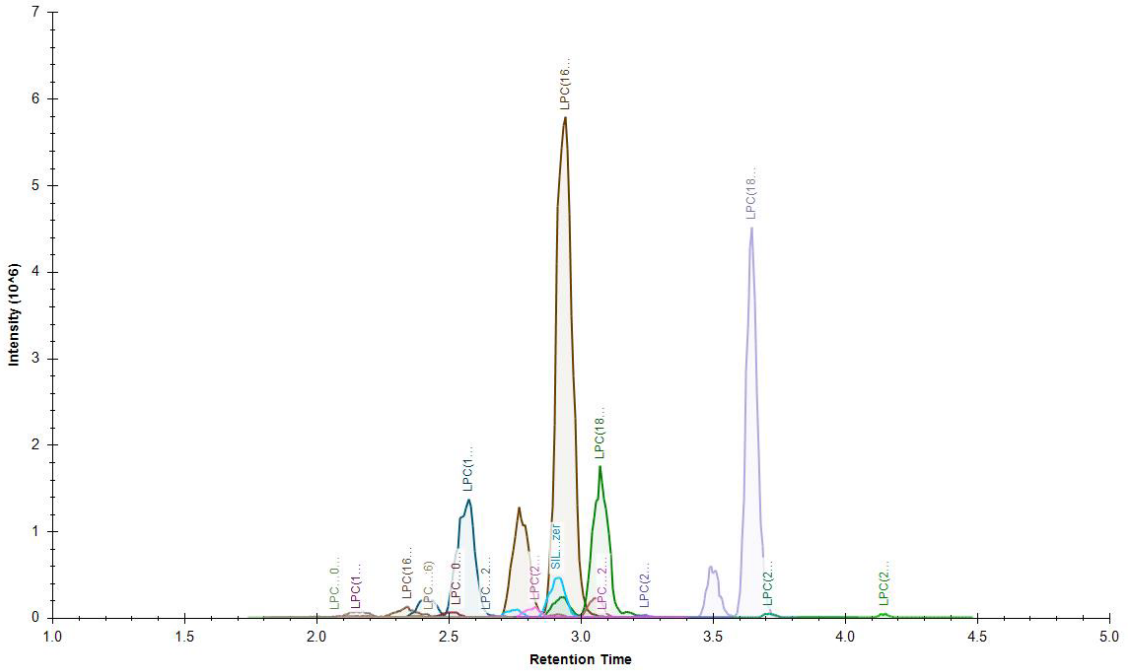
Intensity (10^6)
Retention Time
LPC(16...
LPC(18...
LPC(18...
LPC(1...
SIL...2er
LPC...0...
LPC(1...
LPC(16...
LPC...6)
LPC...2...
LPC(2...
LPC...2...
LPC(2...
LPC(2...
LPC(2...

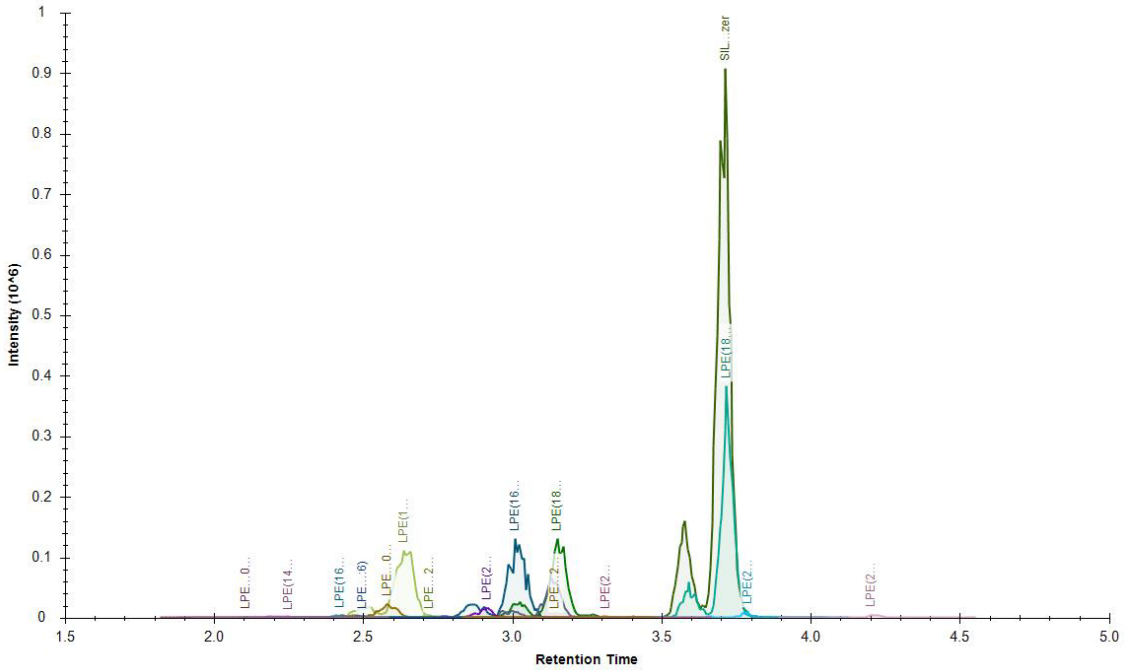
Intensity (10^6)
Retention Time
SIL...zer
LPE(18...
LPE(16...
LPE(18...
LPE(1...
LPE...0...
LPE(14...
LPE(16...
LPE...6)
LPE...0...
LPE...2...
LPE(2...
LPE...2...
LPE(2...
LPE(2...
LPE(2...

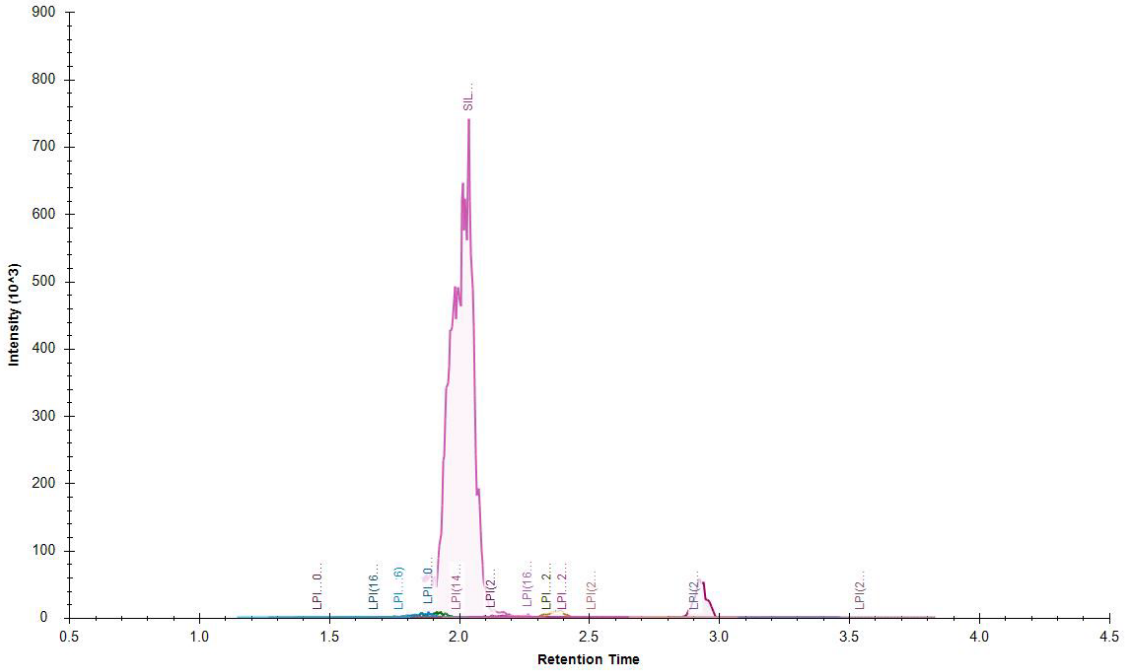
Intensity (10^3)
Retention Time
SIL...
LPI...0...
LPI(16...
LPI...6)
LPI...0...
LPI(14...
LPI(2...
LPI(16...
LPI...2...
LPI...2...
LPI(2...
LPI(2...
LPI(2...

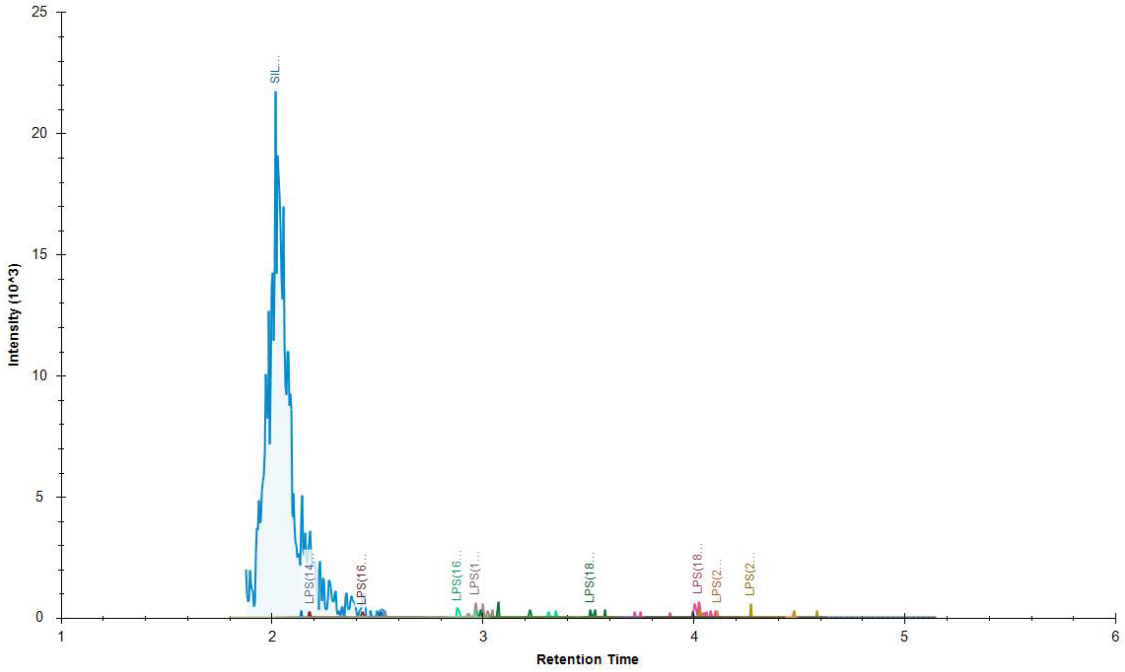
Intensity (10^3)
Retention Time
SIL...
LPS(14...
LPS(16...
LPS(16...
LPS(1...
LPS(18...
LPS(18...
LPS(2...
LPS(2...

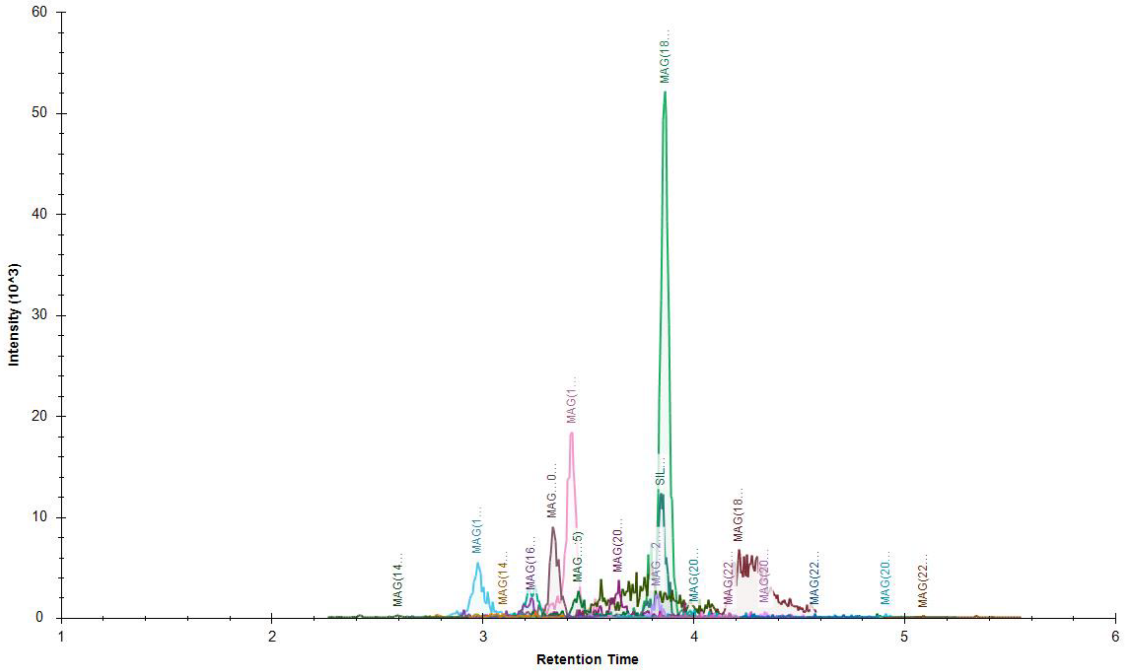
Intensity (10^3)
Retention Time
MAG(18...
MAG(1...
SIL...
MAG(1...
MAG...0...
MAG(14...
MAG(16...
MAG...:5)
MAG(20...
MAG(14...
MAG...2...
MAG(20...
MAG(22...
MAG(18...
MAG(20...
MAG(22...
MAG(20...
MAG(22...

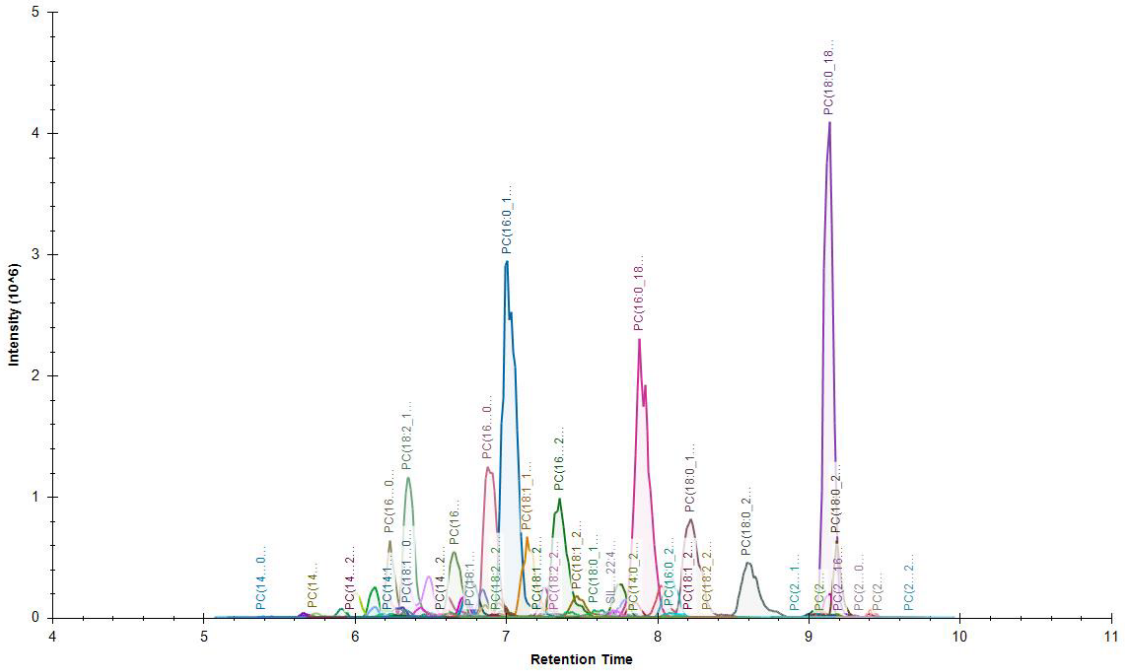
Intensity (10^6)
Retention Time
PC(14...0...
PC(14...
PC(14...2...
PC(14:1...
PC(16...0...
PC(18:1...0...
PC(18:2_1...
PC(14...2...
PC(16...
PC(18:1...
PC(18:2...2...
PC(16...0...
PC(16:0_1...
PC(18:1...2...
PC(18:1_1...
PC(18:2...2...
PC(16...2...
PC(18:1_2...
PC(18:0_1...
SIL...22:4...
PC(14:0_2...
PC(16:0_18...
PC(16:0_2...
PC(18:1_2...
PC(18:2_2...
PC(18:0_1...
PC(18:0_2...
PC(2...1...
PC(2...
PC(2...16...
PC(18:0_18...
PC(18:0_2...
PC(2...0...
PC(2...
PC(2...2...

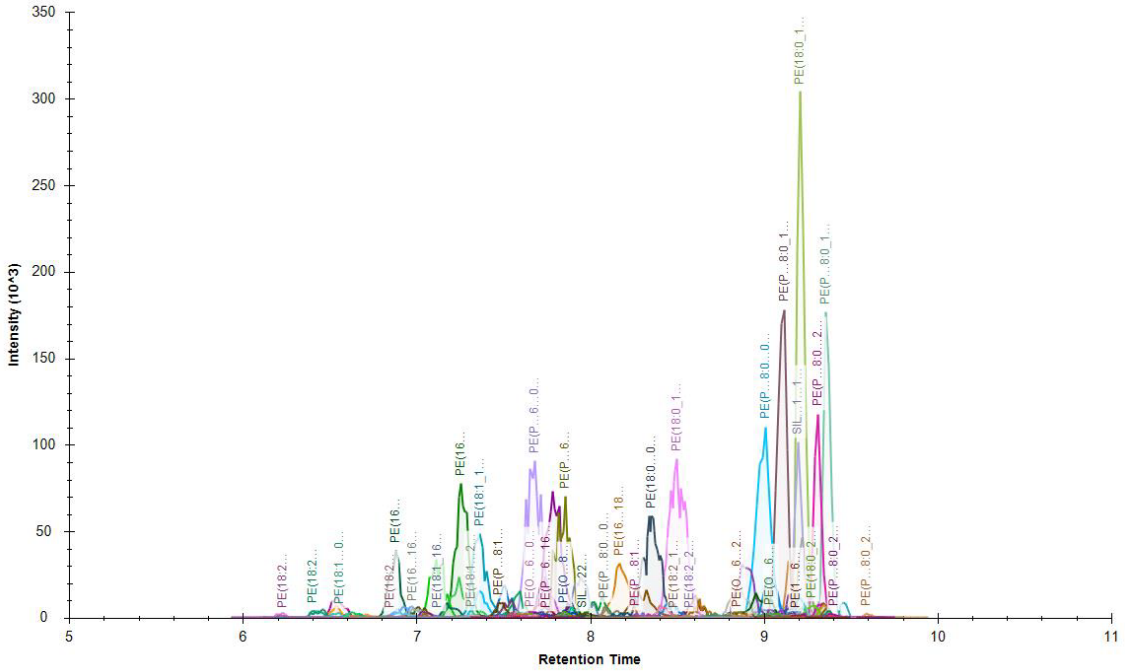
Intensity (10^3)
Retention Time
PE(18:2...
PE(18:2...
PE(18:1...0...
PE(18:2...
PE(16...
PE(16...16...
PE(18:1...16...
PE(16...
PE(18:1_1...
PE(P...8:1...
PE(O...6...0...
PE(P...6...0...
PE(P...6...16...
PE(O...8...
PE(O...22...
PE(P...6...
PE(P...8:0...0...
PE(16...18...
PE(P...8:1...
PE(18:0...0...
PE(18:0_1...
PE(18:2_1...
PE(18:2_2...
PE(O...6...2...
PE(P...8:0...0...
PE(O...6...
PE(18:0_1...
SIL...1...1...
PE(P...8:0...1...
PE(1...6...
PE(P...8:0...2...
PE(18:0_2...
PE(P...8:0...1...
PE(P...8:0...2...
PE(P...8:0_2...

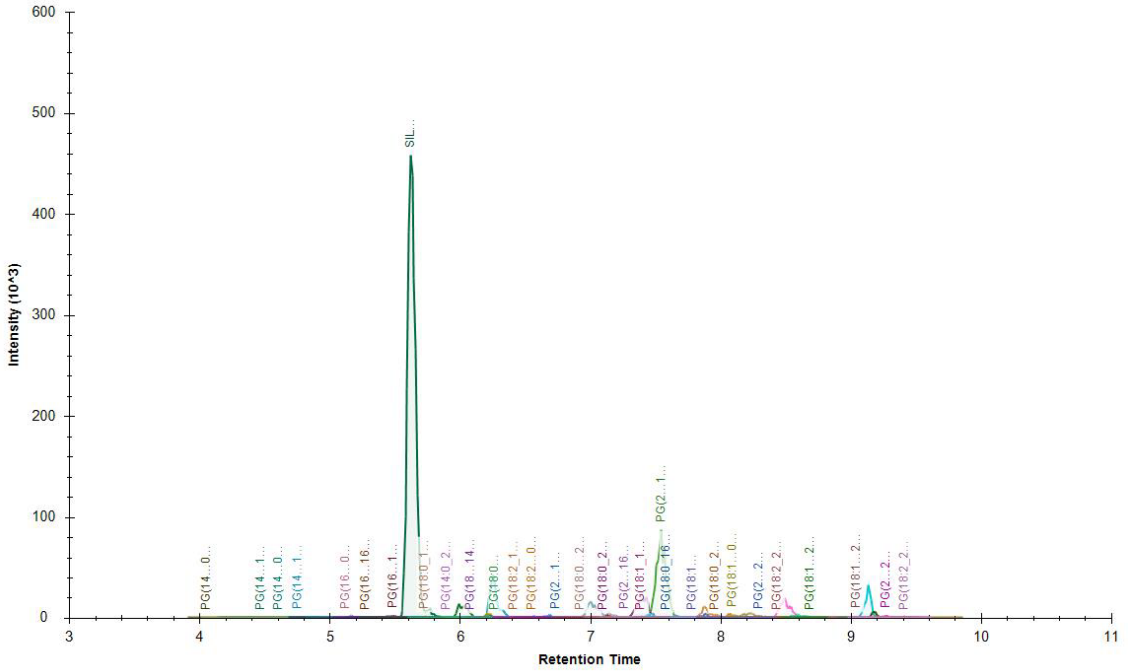
Intensity (10^3)
Retention Time
SIL...

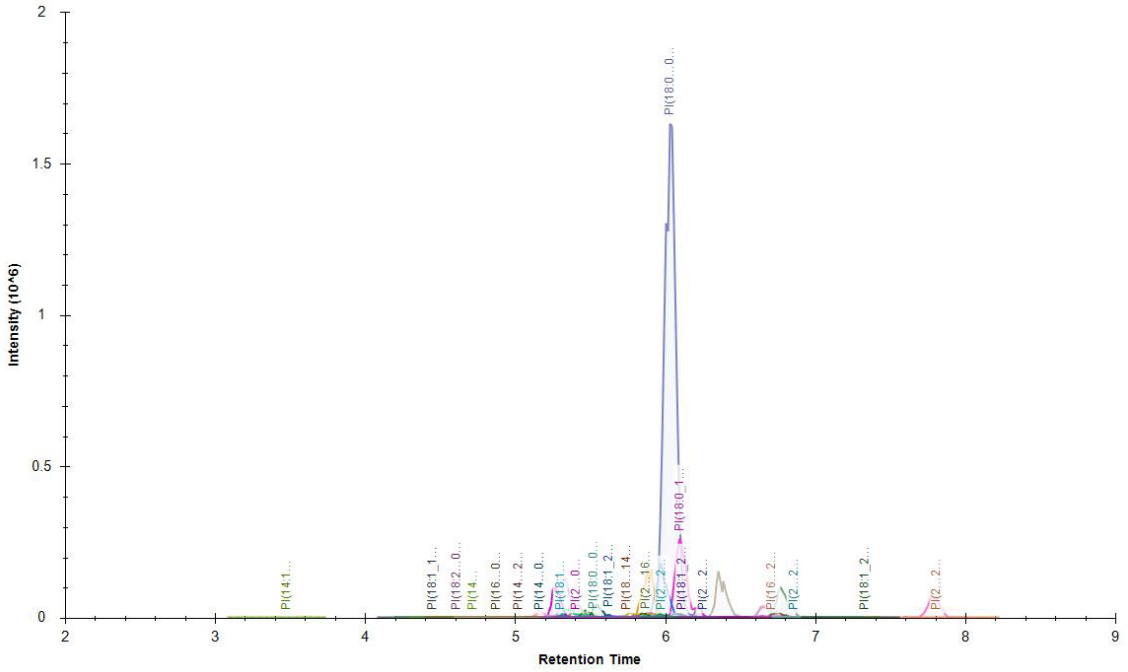
Intensity (10^6)
Retention Time
PI(18:0...0...

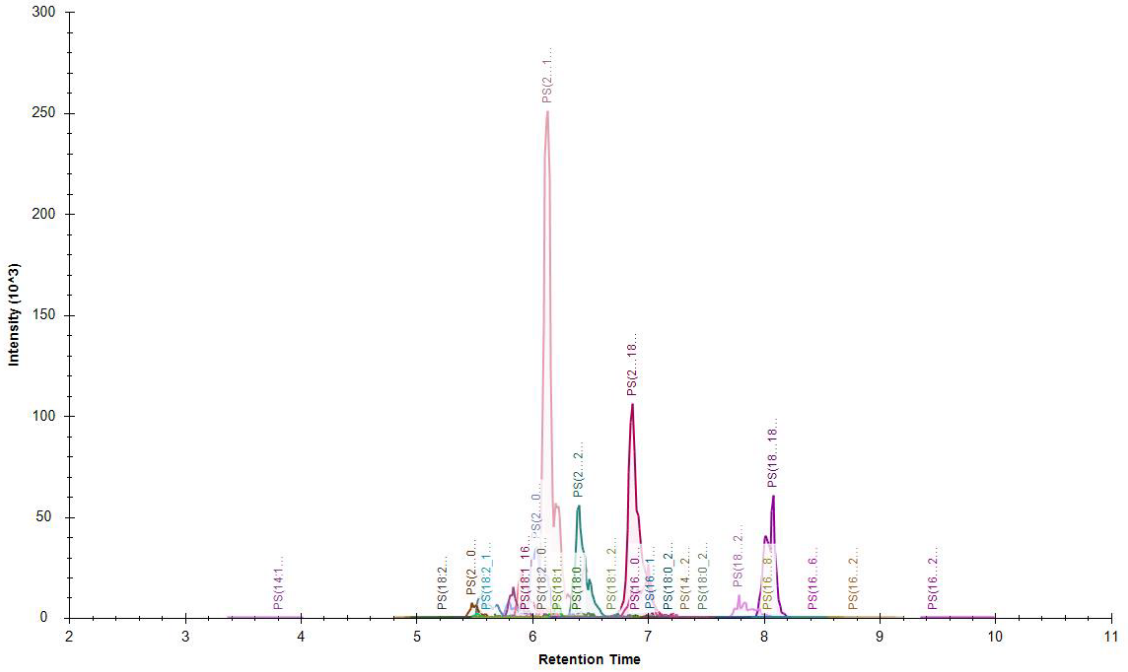
Intensity (10^3)
Retention Time
PS(14:1...
PS(18:2...
PS(2...0...
PS(18:2_1...
PS(18:1_16...
PS(18:2...0...
PS(18:1...
PS(2...1...
PS(2...2...
PS(18:0...
PS(18:1...2...
PS(16...0...
PS(16...1...
PS(18:0_2...
PS(14...2...
PS(18:0_2...
PS(18...2...
PS(2...18...
PS(16...8...
PS(18...18...
PS(16...6...
PS(16...2...
PS(16...2...

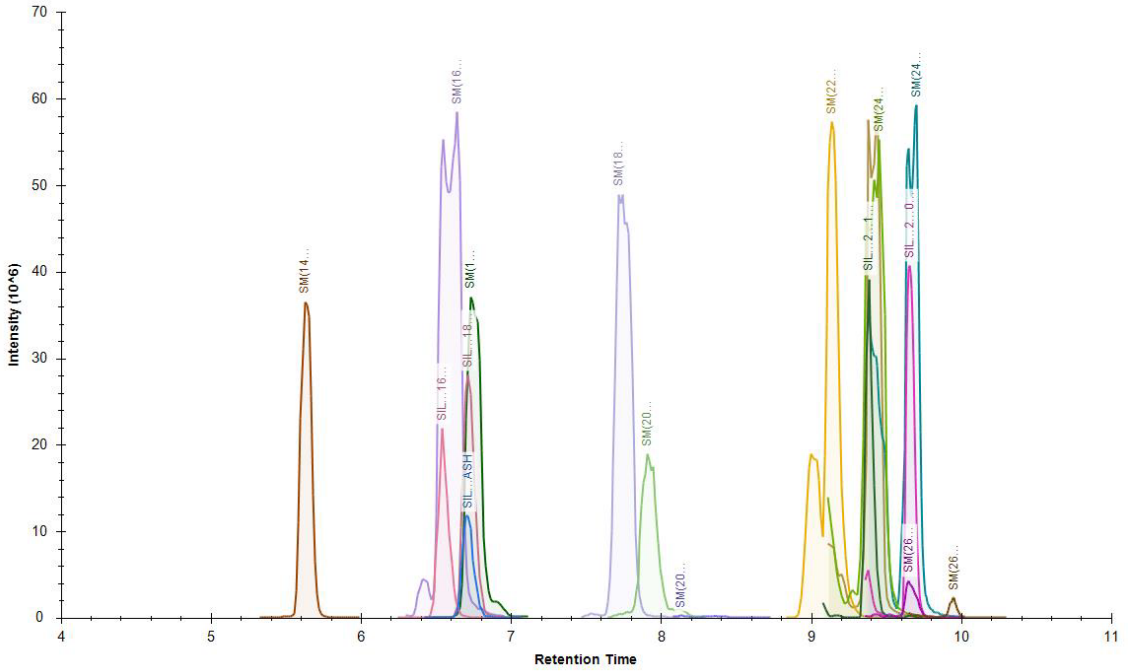
Intensity (10^6)
Retention Time
SM(14...
SIL...16...
SM(16...
SIL...18...
SM(1...
SIL...ASH
SM(18...
SM(20...
SM(20...
SM(22...
SIL...2...1...
SM(24...
SIL...2...0...
SM(24...
SM(26...
SM(26...

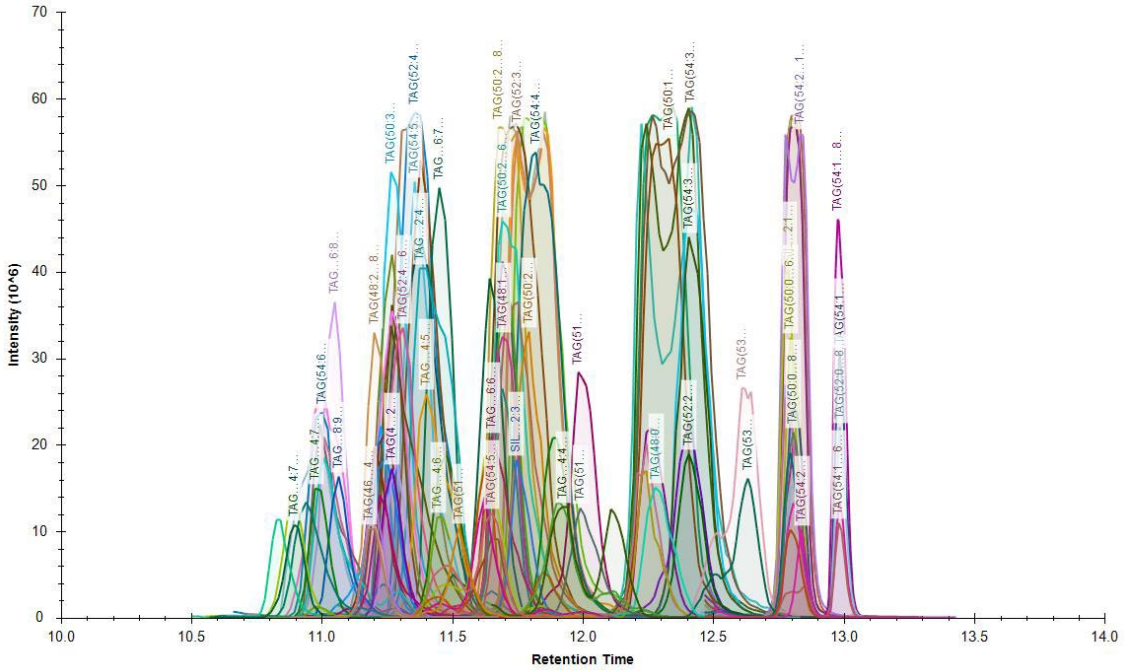

7.6 PCA of chapter 4 cohort

A Unsupervised Principal Component Analysis (PCA) with 96 samples (36 from healthy, age and sex balanced controls, 60 from mTBI patients (patient inception n = 30, patient follow up n = 30). The red circles represent repeat extractions of a quality control (QC) pooled sample (n = 14). Clustering of the QC indicated consistent analysis throughout the run.

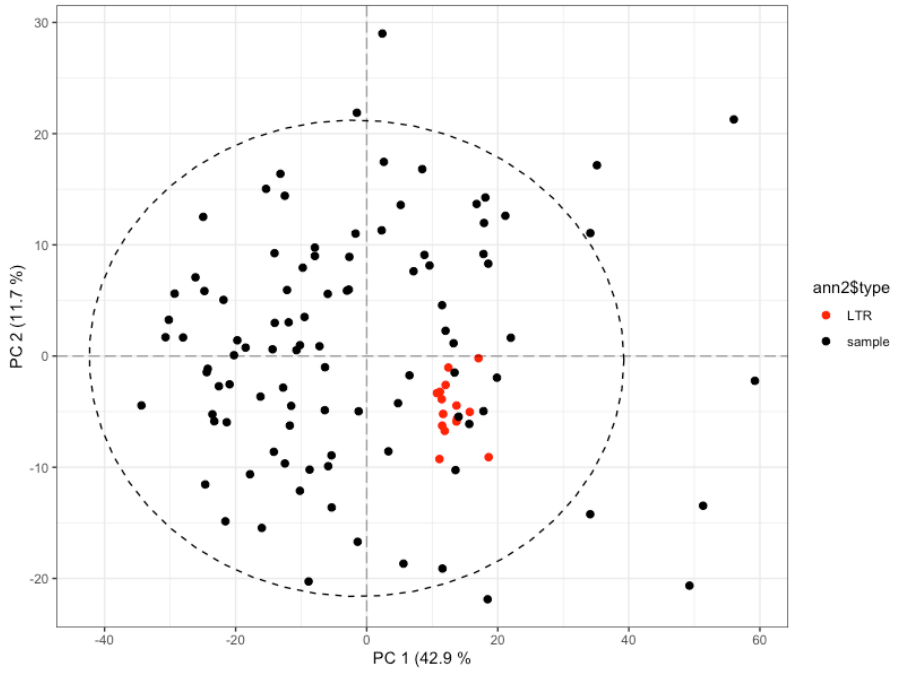

7.7 Visualisations of significant summed lipid class concentrations in the chapter 4 cohort

Three group jitter plot comparisons of the lipid classes that were deemed significant in the Kruskal Wallis test ($p \leq 0.05$) (Table 1). Error bars are shown next to each jitter plot to indicate data variability.

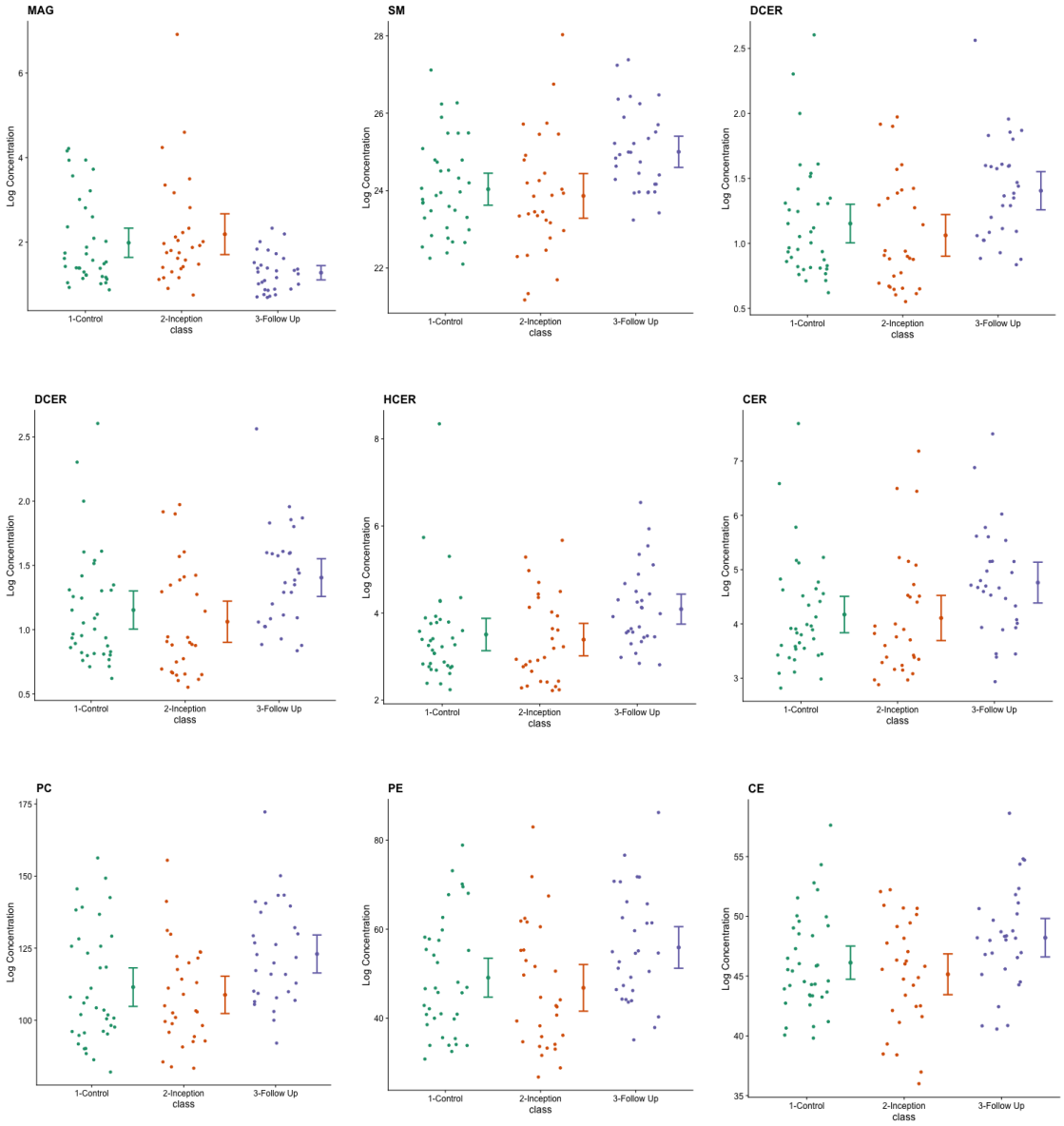

7.8 Visualisations of significant lipid species concentrations in the chapter 4 cohort

Three group jitter plot comparisons of the plasma metabolites that were deemed significant in the Kruskal Wallis test ($p \leq 0.05$) (Table 2). Error bars are shown next to each jitter plot to indicate data variability.

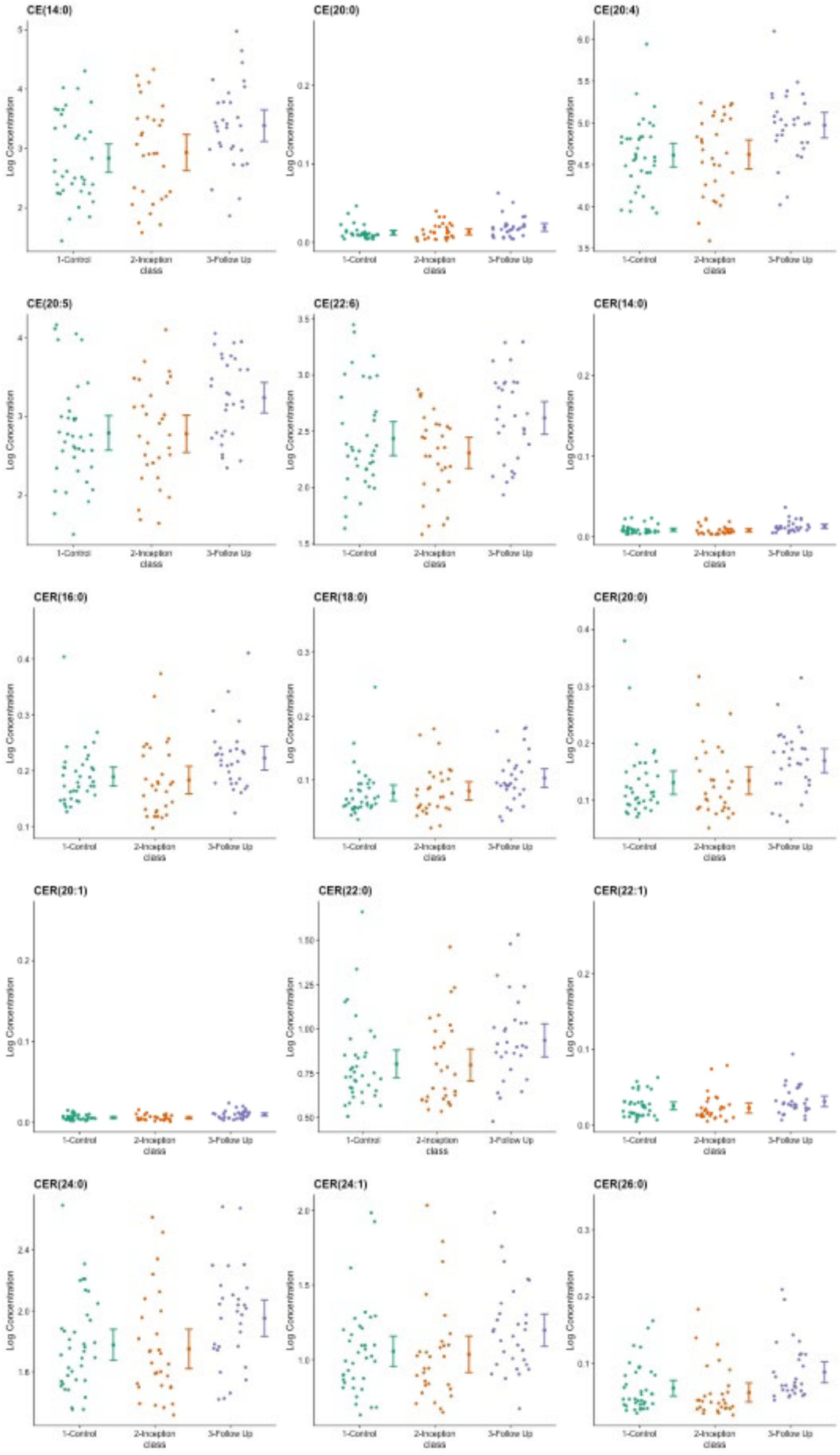
CE(14:0)
CE(20:0)
CE(20:4)
CE(20:5)
CE(22:6)
CER(14:0)
CER(16:0)
CER(18:0)
CER(20:0)
CER(20:1)
CER(22:0)
CER(22:1)
CER(24:0)
CER(24:1)
CER(26:0)
Log Concentration
1-Control
2-Inception
3-Follow Up
class

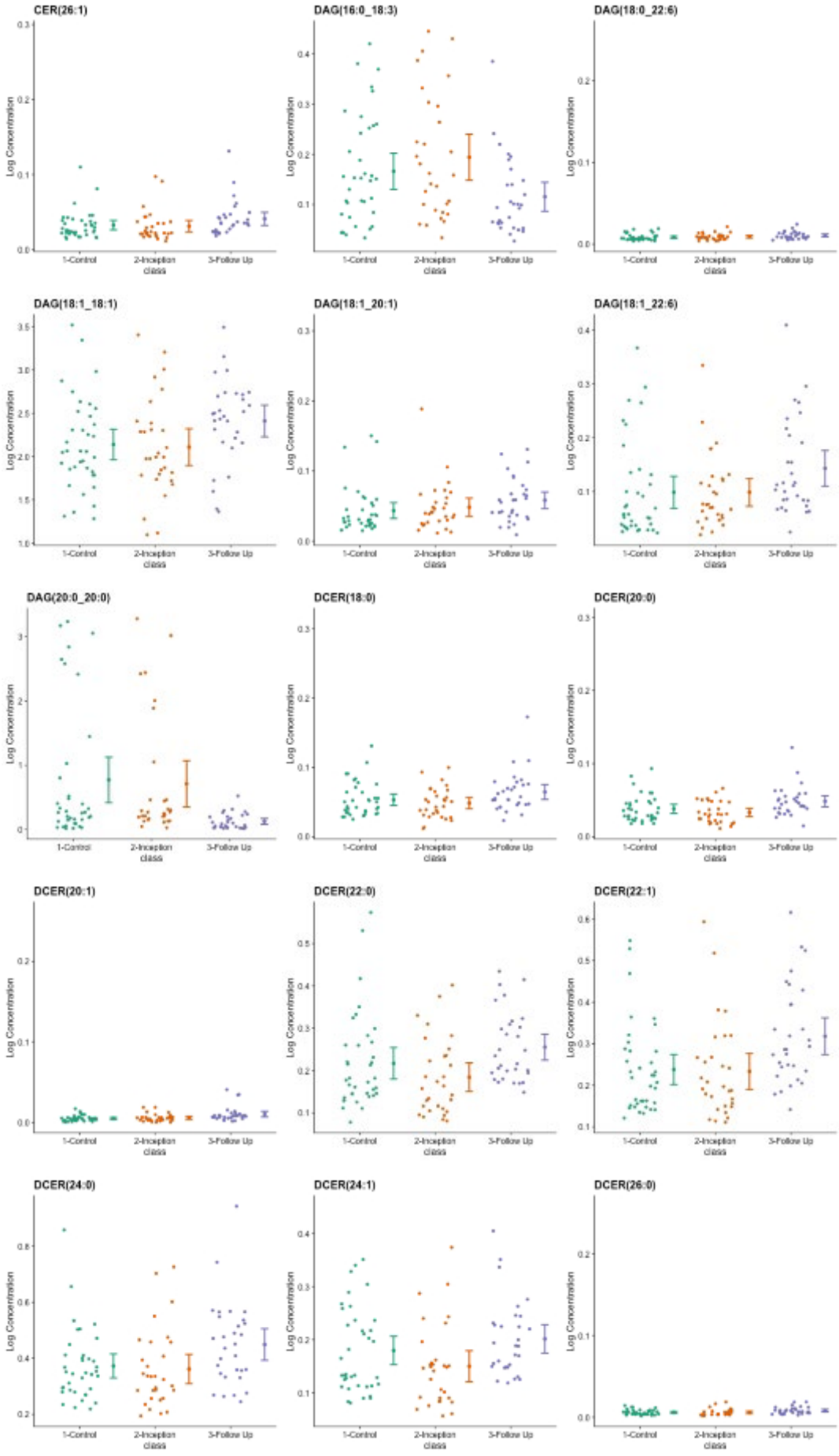
CER(26:1)
DAG(16:0_18:3)
DAG(18:0_22:6)
DAG(18:1_18:1)
DAG(18:1_20:1)
DAG(18:1_22:6)
DAG(20:0_20:0)
DCER(18:0)
DCER(20:0)
DCER(20:1)
DCER(22:0)
DCER(22:1)
DCER(24:0)
DCER(24:1)
DCER(26:0)
Log Concentration
1-Control
2-Inception
3-Follow Up
class

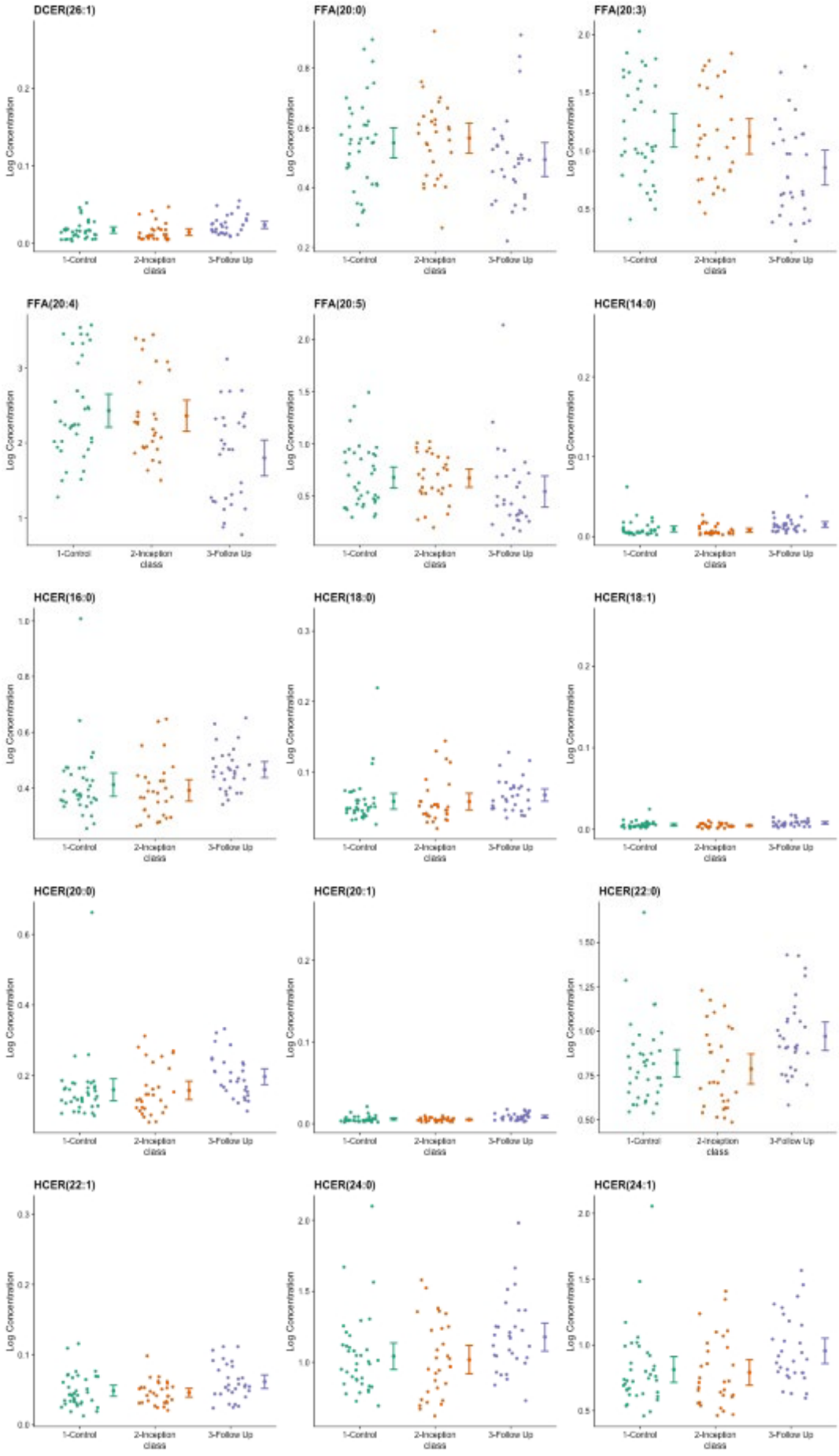
DCER(26:1)
FFA(20:0)
FFA(20:3)
FFA(20:4)
FFA(20:5)
HCER(14:0)
HCER(16:0)
HCER(18:0)
HCER(18:1)
HCER(20:0)
HCER(20:1)
HCER(22:0)
HCER(22:1)
HCER(24:0)
HCER(24:1)
Log Concentration
1-Control
2-Inception
3-Follow Up
class

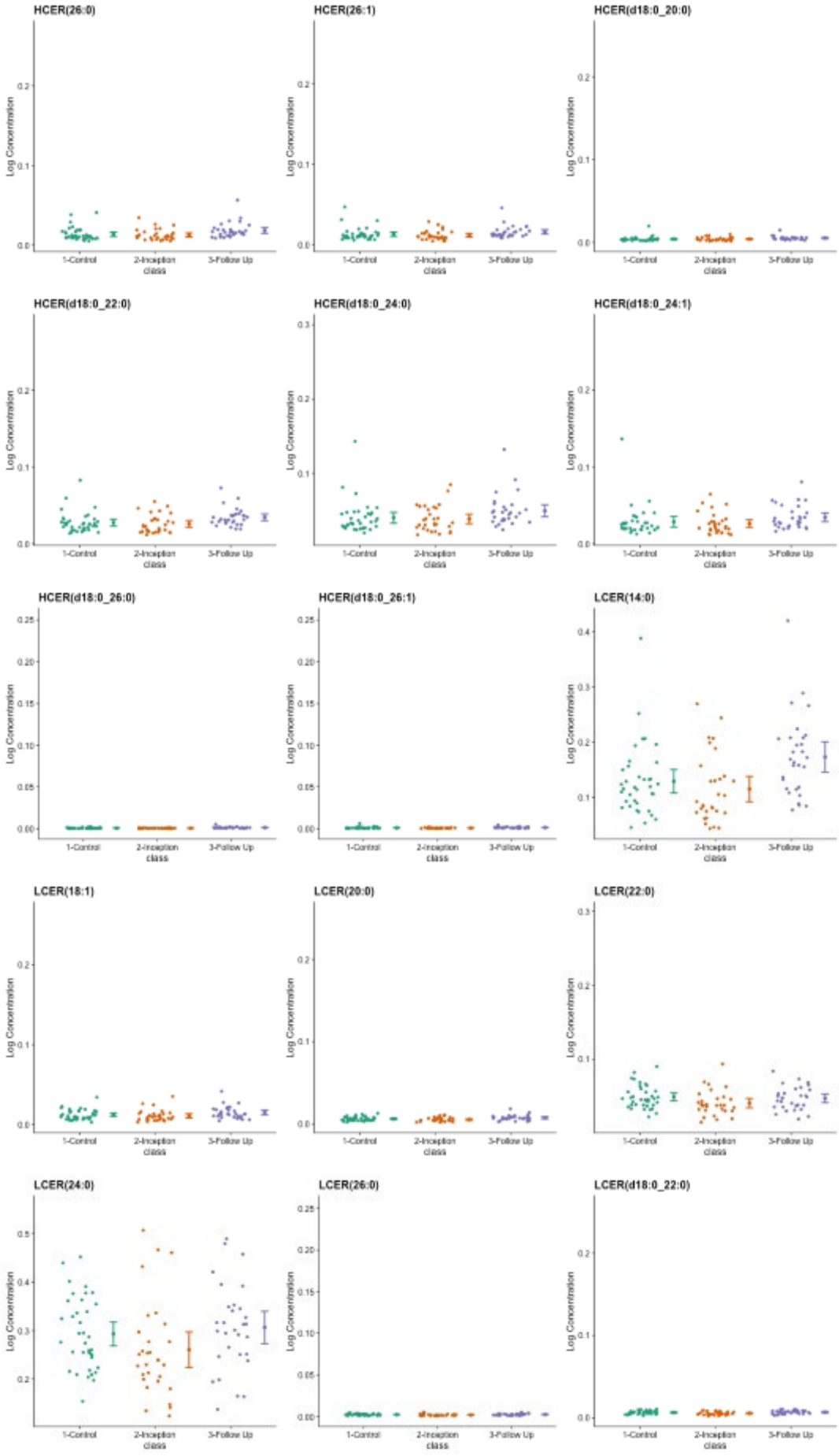
HCER(26:0)
HCER(26:1)
HCER(d18:0_20:0)
HCER(d18:0_22:0)
HCER(d18:0_24:0)
HCER(d18:0_24:1)
HCER(d18:0_26:0)
HCER(d18:0_26:1)
LCER(14:0)
LCER(18:1)
LCER(20:0)
LCER(22:0)
LCER(24:0)
LCER(26:0)
LCER(d18:0_22:0)
Log Concentration
1-Control
2-Inception
3-Follow Up
class

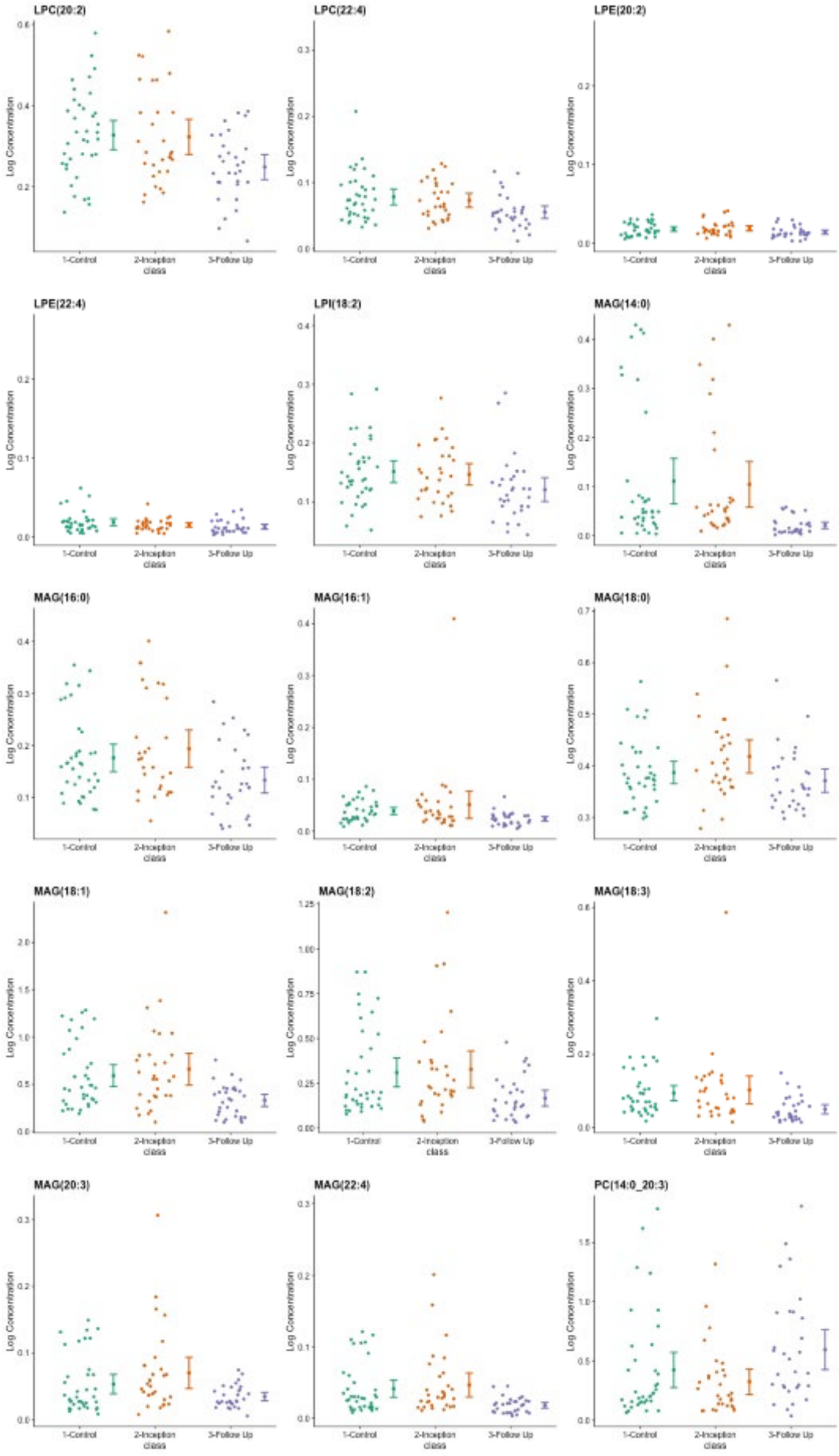
LPC(20:2)
LPC(22:4)
LPE(20:2)
LPE(22:4)
LPI(18:2)
MAG(14:0)
MAG(16:0)
MAG(16:1)
MAG(18:0)
MAG(18:1)
MAG(18:2)
MAG(18:3)
MAG(20:3)
MAG(22:4)
PC(14:0_20:3)
Log Concentration
1-Control
2-Inception
3-Follow Up
class

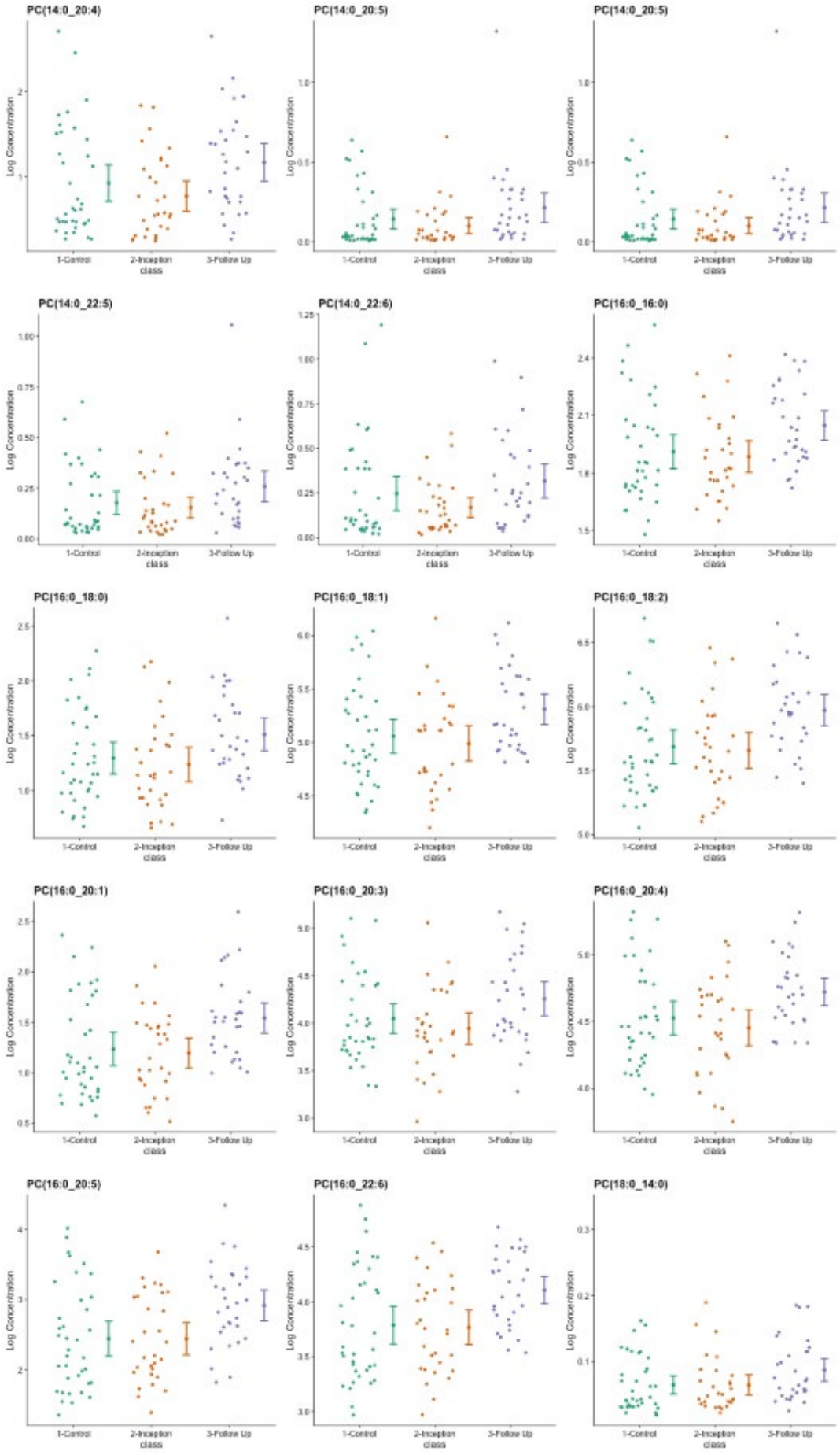
PC(14:0_20:4)
PC(14:0_20:5)
PC(14:0_20:5)
PC(14:0_22:5)
PC(14:0_22:6)
PC(16:0_16:0)
PC(16:0_18:0)
PC(16:0_18:1)
PC(16:0_18:2)
PC(16:0_20:1)
PC(16:0_20:3)
PC(16:0_20:4)
PC(16:0_20:5)
PC(16:0_22:6)
PC(18:0_14:0)
Log Concentration
1-Control
2-Inception
3-Follow Up
class

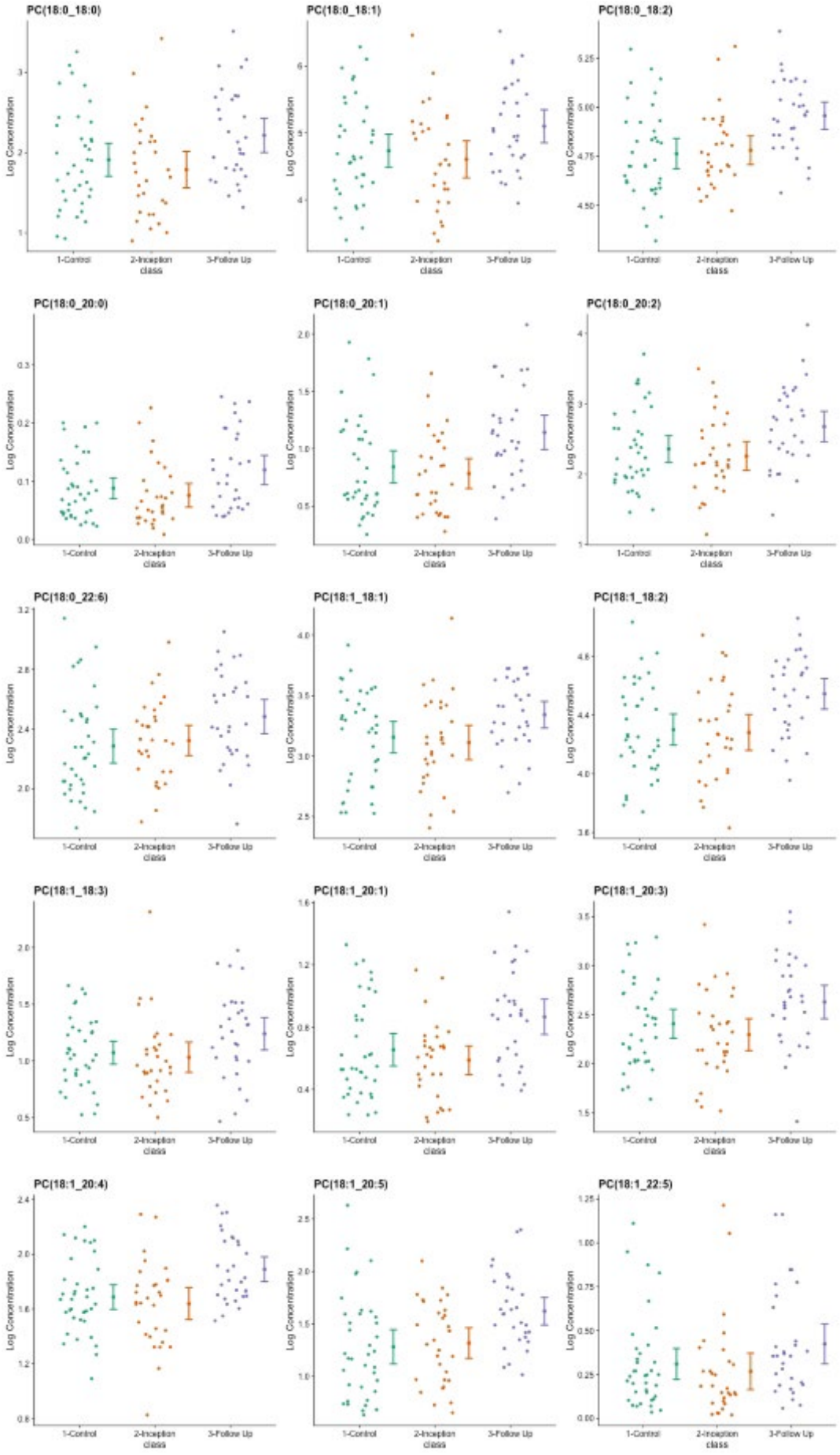
PC(18:0_18:0)
PC(18:0_18:1)
PC(18:0_18:2)
PC(18:0_20:0)
PC(18:0_20:1)
PC(18:0_20:2)
PC(18:0_22:6)
PC(18:1_18:1)
PC(18:1_18:2)
PC(18:1_18:3)
PC(18:1_20:1)
PC(18:1_20:3)
PC(18:1_20:4)
PC(18:1_20:5)
PC(18:1_22:5)
Log Concentration
1-Control
2-Inception
3-Follow Up
class

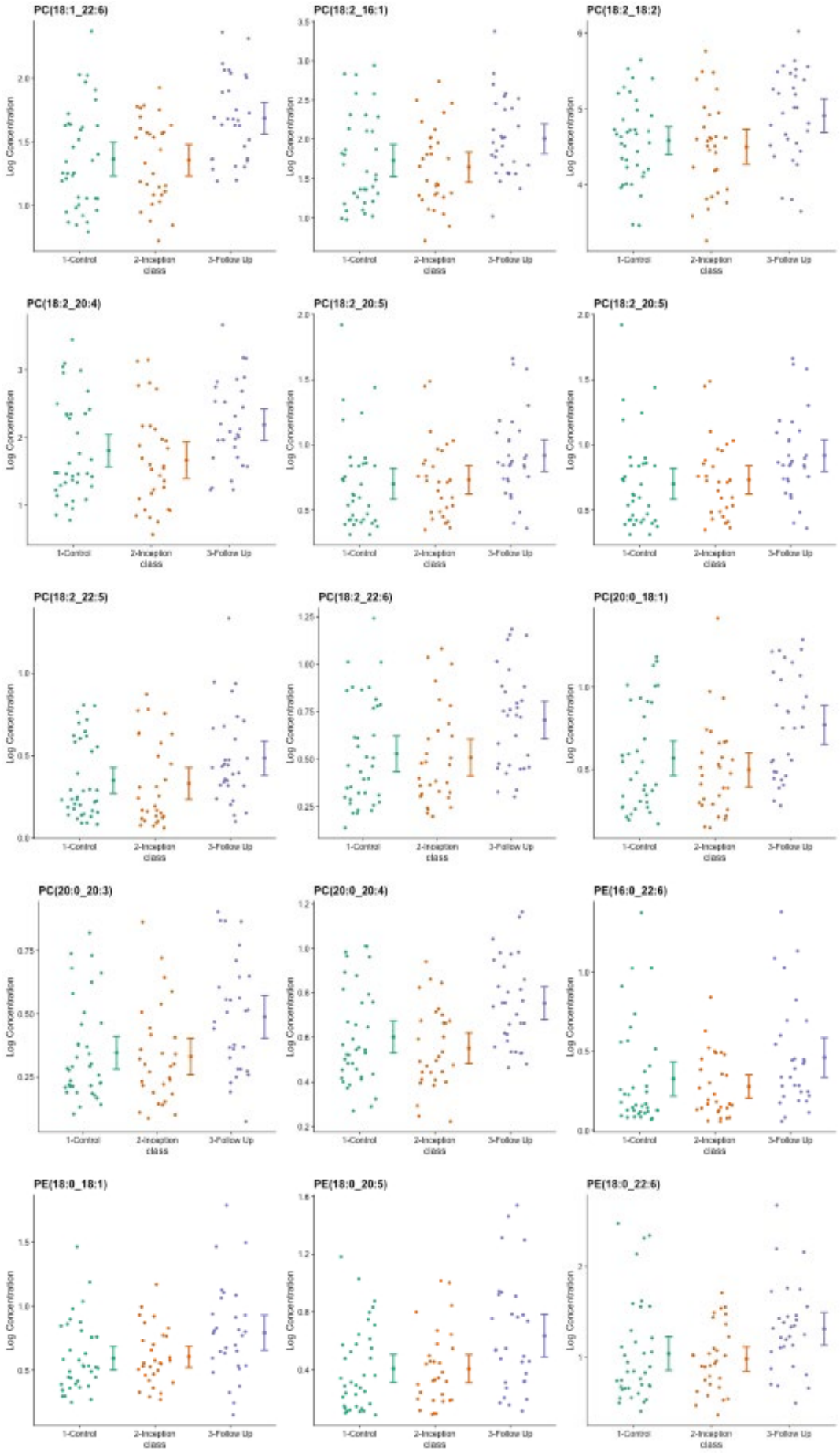
PC(18:1_22:6)
PC(18:2_16:1)
PC(18:2_18:2)
PC(18:2_20:4)
PC(18:2_20:5)
PC(18:2_20:5)
PC(18:2_22:5)
PC(18:2_22:6)
PC(20:0_18:1)
PC(20:0_20:3)
PC(20:0_20:4)
PE(16:0_22:6)
PE(18:0_18:1)
PE(18:0_20:5)
PE(18:0_22:6)
Log Concentration
1-Control
2-Inception
3-Follow Up
class

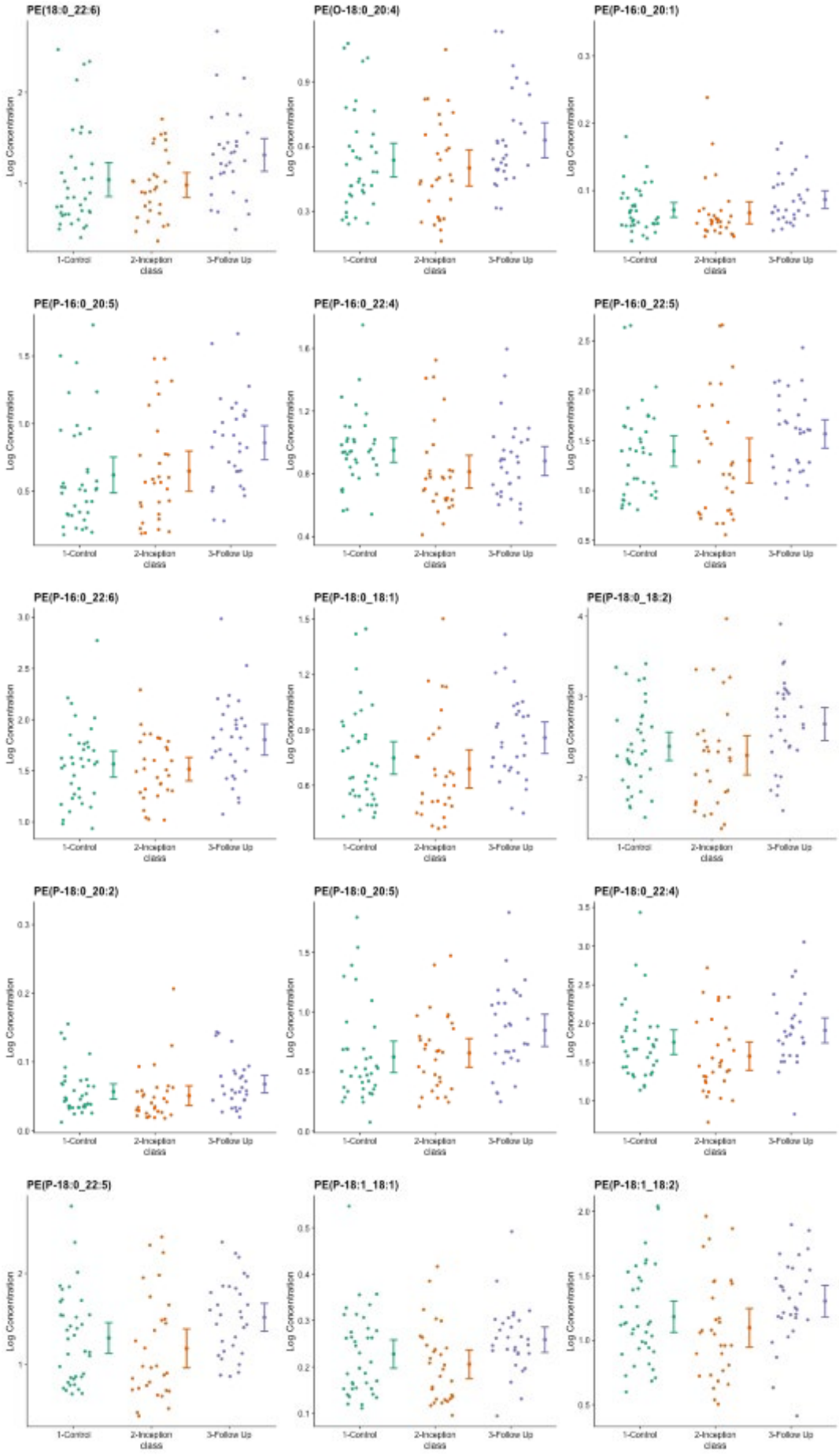
PE(18:0_22:6)
PE(O-18:0_20:4)
PE(P-16:0_20:1)
PE(P-16:0_20:5)
PE(P-16:0_22:4)
PE(P-16:0_22:5)
PE(P-16:0_22:6)
PE(P-18:0_18:1)
PE(P-18:0_18:2)
PE(P-18:0_20:2)
PE(P-18:0_20:5)
PE(P-18:0_22:4)
PE(P-18:0_22:5)
PE(P-18:1_18:1)
PE(P-18:1_18:2)
Log Concentration
1-Control
2-Inception
3-Follow Up
class

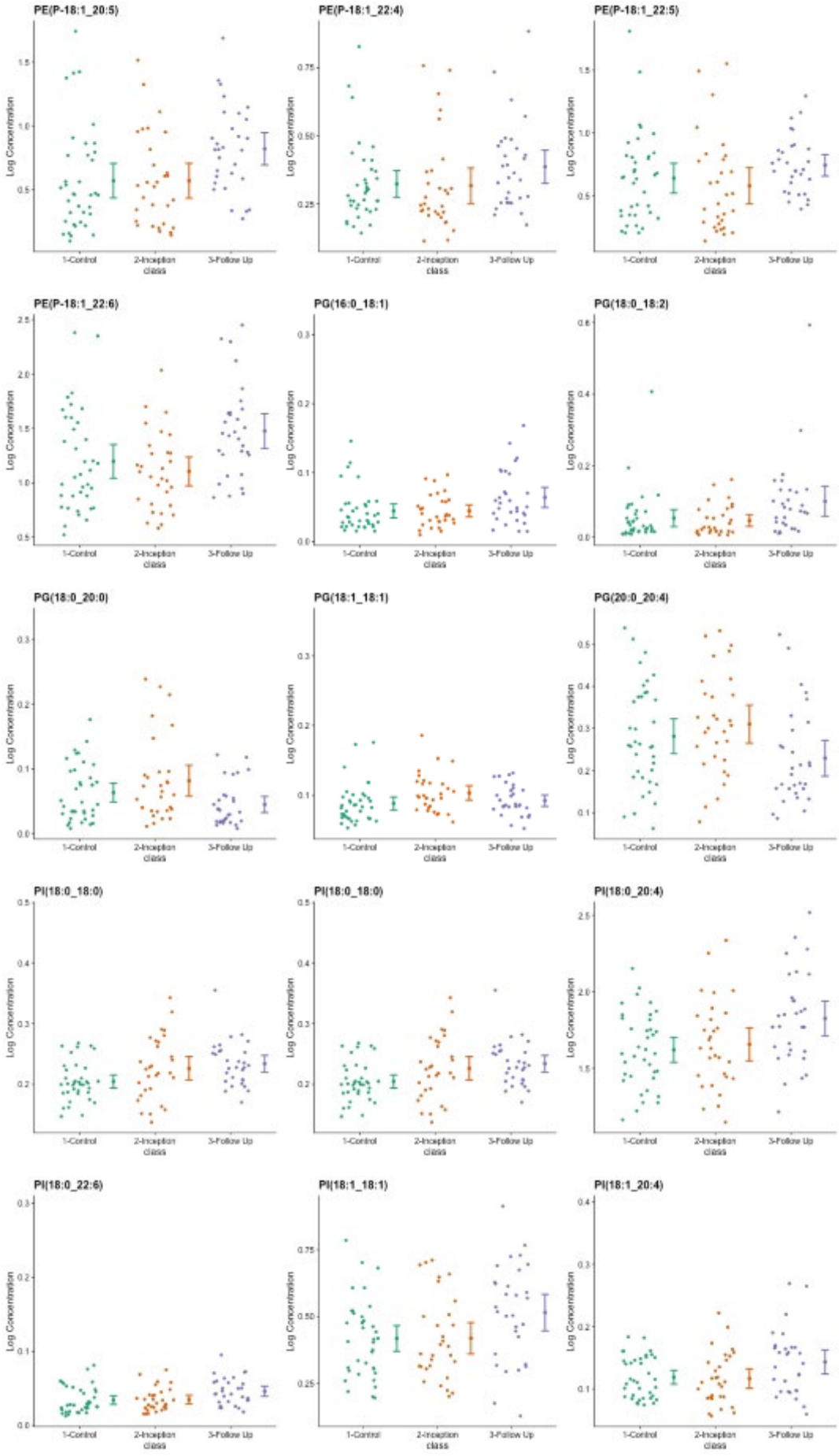
PE(P-18:1_20:5)
PE(P-18:1_22:4)
PE(P-18:1_22:5)
PE(P-18:1_22:6)
PG(16:0_18:1)
PG(18:0_18:2)
PG(18:0_20:0)
PG(18:1_18:1)
PG(20:0_20:4)
PI(18:0_18:0)
PI(18:0_18:0)
PI(18:0_20:4)
PI(18:0_22:6)
PI(18:1_18:1)
PI(18:1_20:4)
Log Concentration
1-Control
2-Inception
3-Follow Up
class

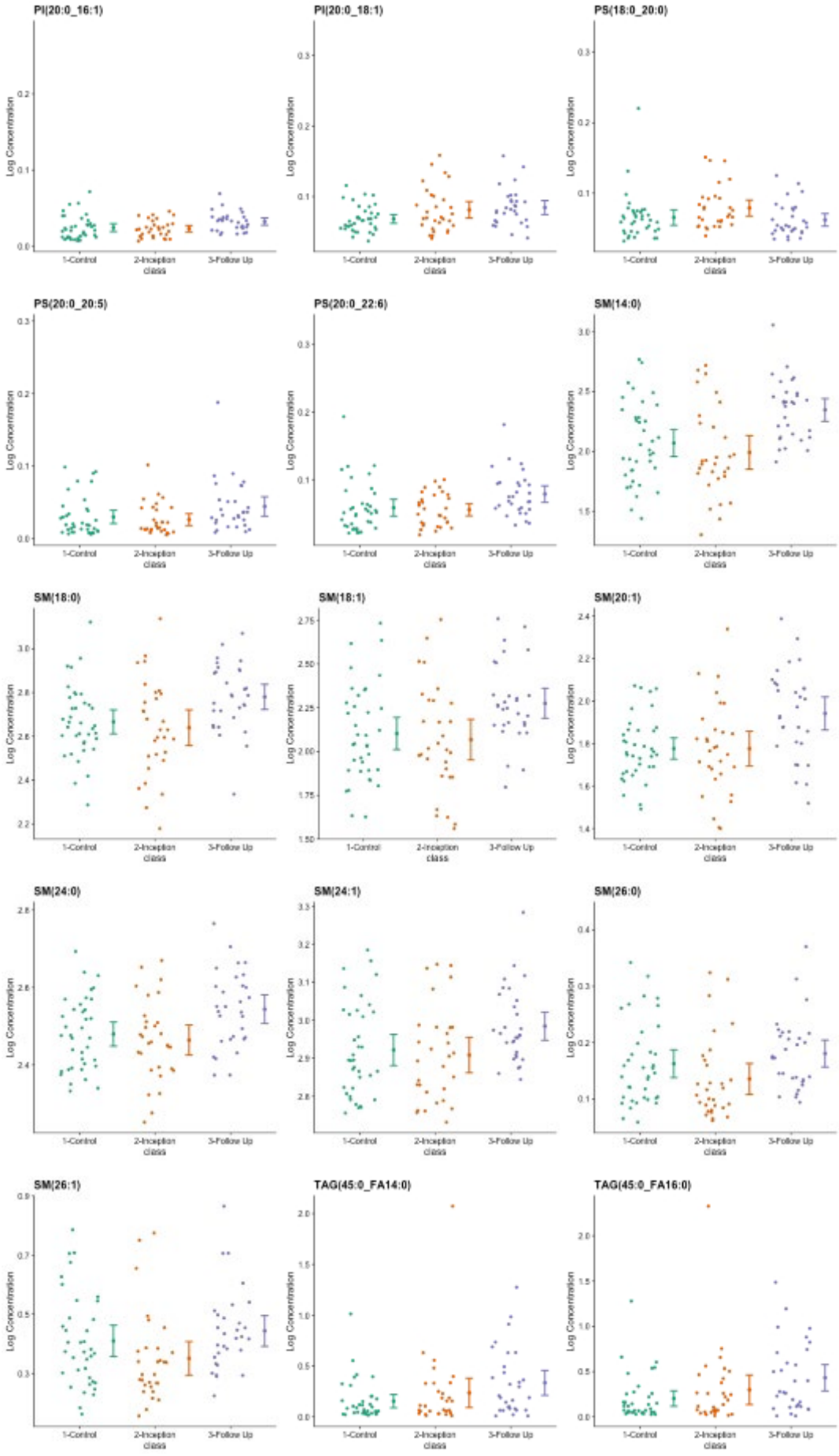
PI(20:0_16:1)
PI(20:0_18:1)
PS(18:0_20:0)
PS(20:0_20:5)
PS(20:0_22:6)
SM(14:0)
SM(18:0)
SM(18:1)
SM(20:1)
SM(24:0)
SM(24:1)
SM(26:0)
SM(26:1)
TAG(45:0_FA14:0)
TAG(45:0_FA16:0)
Log Concentration
1-Control
2-Inception
3-Follow Up
class

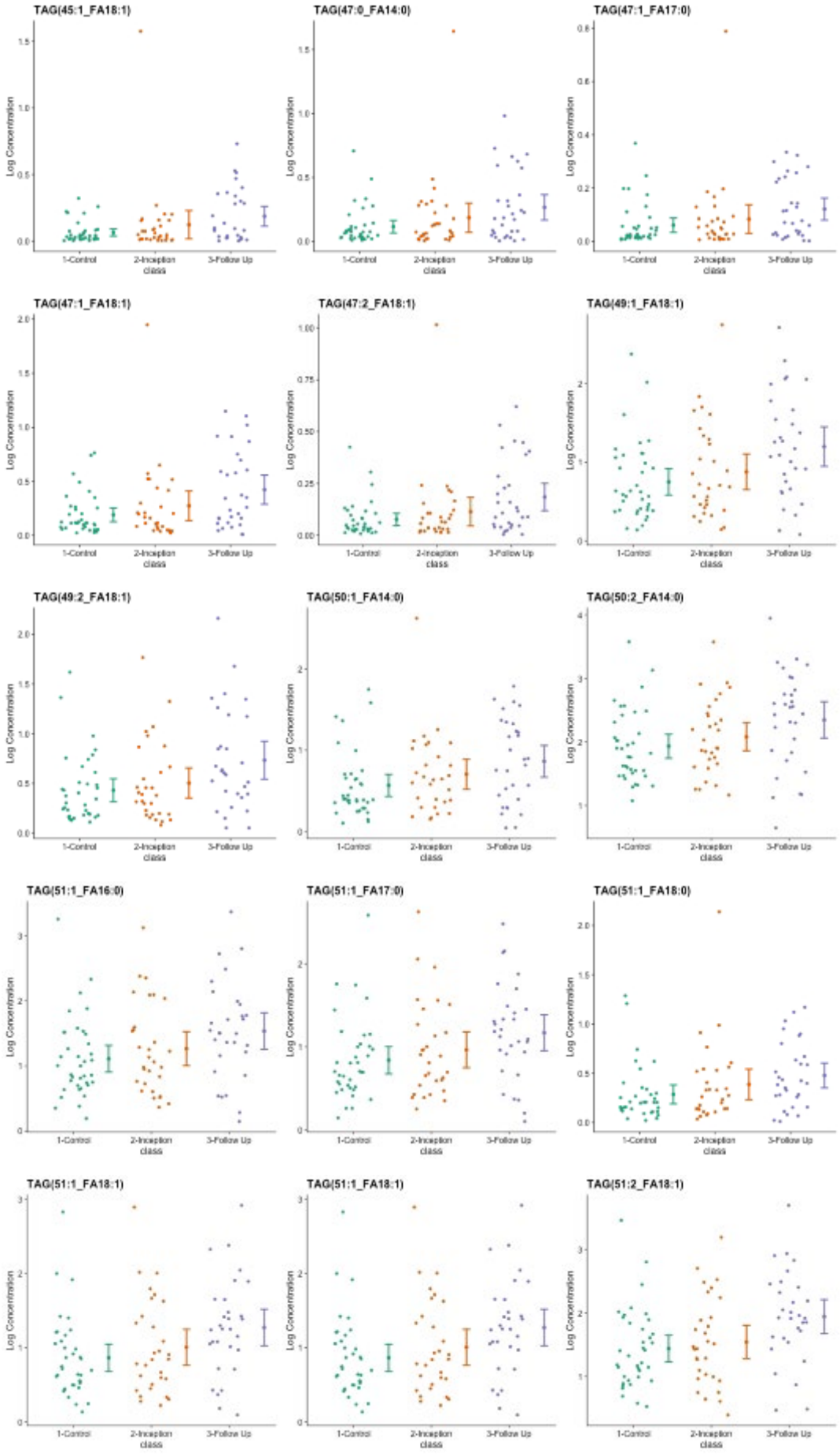
TAG(45:1_FA18:1)
TAG(47:0_FA14:0)
TAG(47:1_FA17:0)
TAG(47:1_FA18:1)
TAG(47:2_FA18:1)
TAG(49:1_FA18:1)
TAG(49:2_FA18:1)
TAG(50:1_FA14:0)
TAG(50:2_FA14:0)
TAG(51:1_FA16:0)
TAG(51:1_FA17:0)
TAG(51:1_FA18:0)
TAG(51:1_FA18:1)
TAG(51:1_FA18:1)
TAG(51:2_FA18:1)
Log Concentration
1-Control
2-Inception
3-Follow Up
class

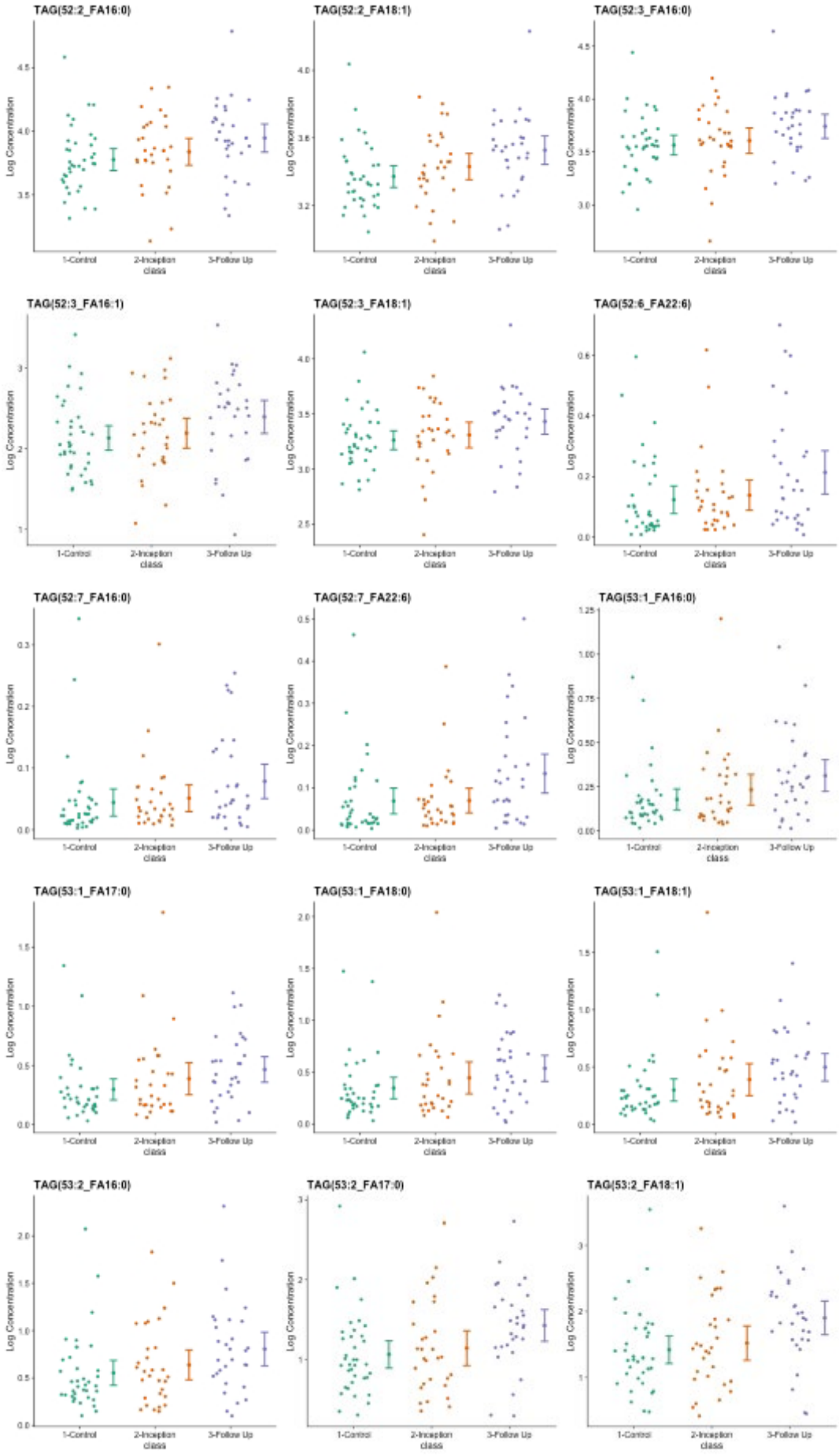
TAG(52:2_FA16:0)
TAG(52:2_FA18:1)
TAG(52:3_FA16:0)
TAG(52:3_FA16:1)
TAG(52:3_FA18:1)
TAG(52:6_FA22:6)
TAG(52:7_FA16:0)
TAG(52:7_FA22:6)
TAG(53:1_FA16:0)
TAG(53:1_FA17:0)
TAG(53:1_FA18:0)
TAG(53:1_FA18:1)
TAG(53:2_FA16:0)
TAG(53:2_FA17:0)
TAG(53:2_FA18:1)
Log Concentration
1-Control
2-Inception
3-Follow Up
class

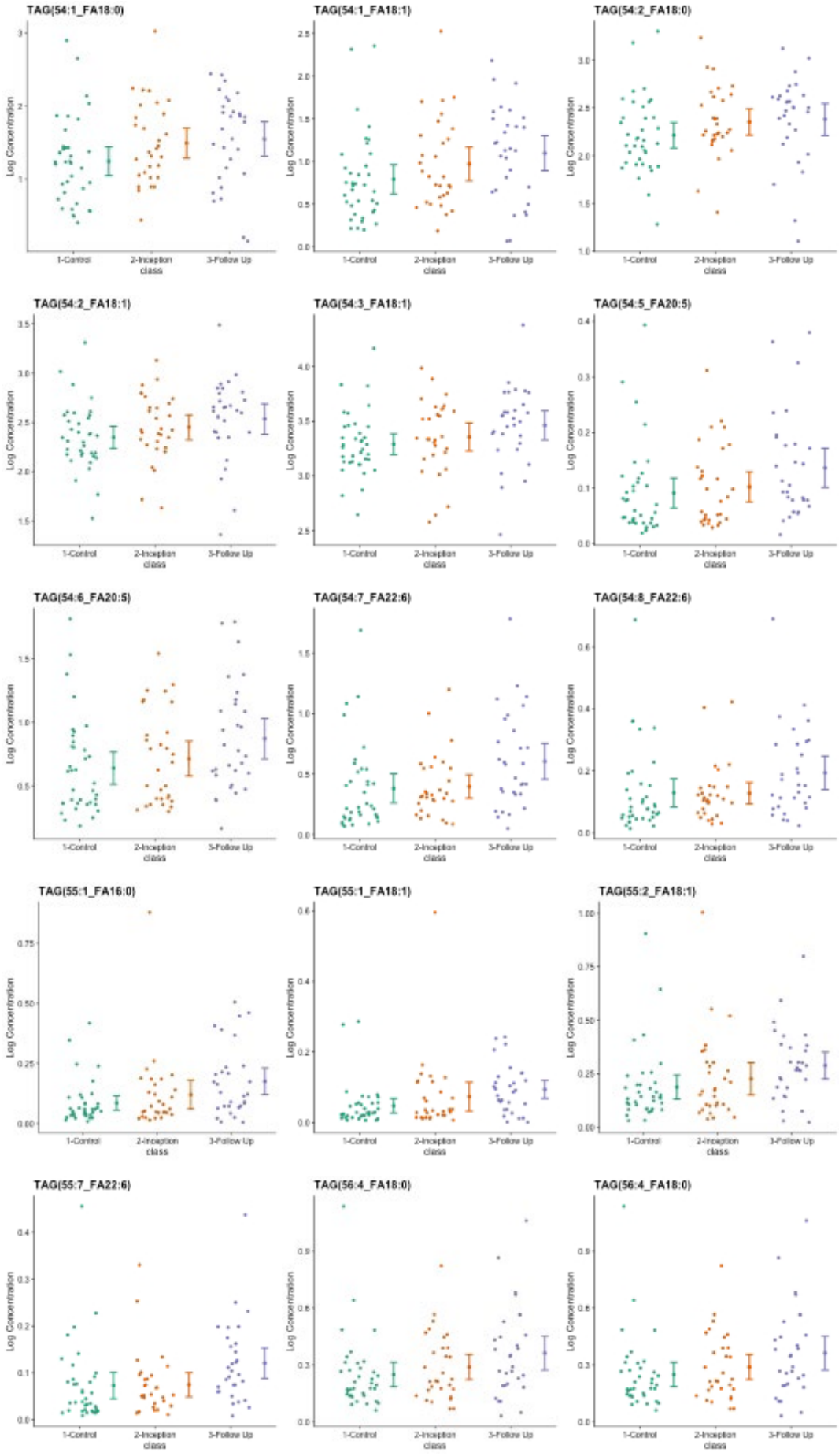
TAG(54:1_FA18:0)
TAG(54:1_FA18:1)
TAG(54:2_FA18:0)
TAG(54:2_FA18:1)
TAG(54:3_FA18:1)
TAG(54:5_FA20:5)
TAG(54:6_FA20:5)
TAG(54:7_FA22:6)
TAG(54:8_FA22:6)
TAG(55:1_FA16:0)
TAG(55:1_FA18:1)
TAG(55:2_FA18:1)
TAG(55:7_FA22:6)
TAG(56:4_FA18:0)
TAG(56:4_FA18:0)
Log Concentration
1-Control
2-Inception
3-Follow Up
class

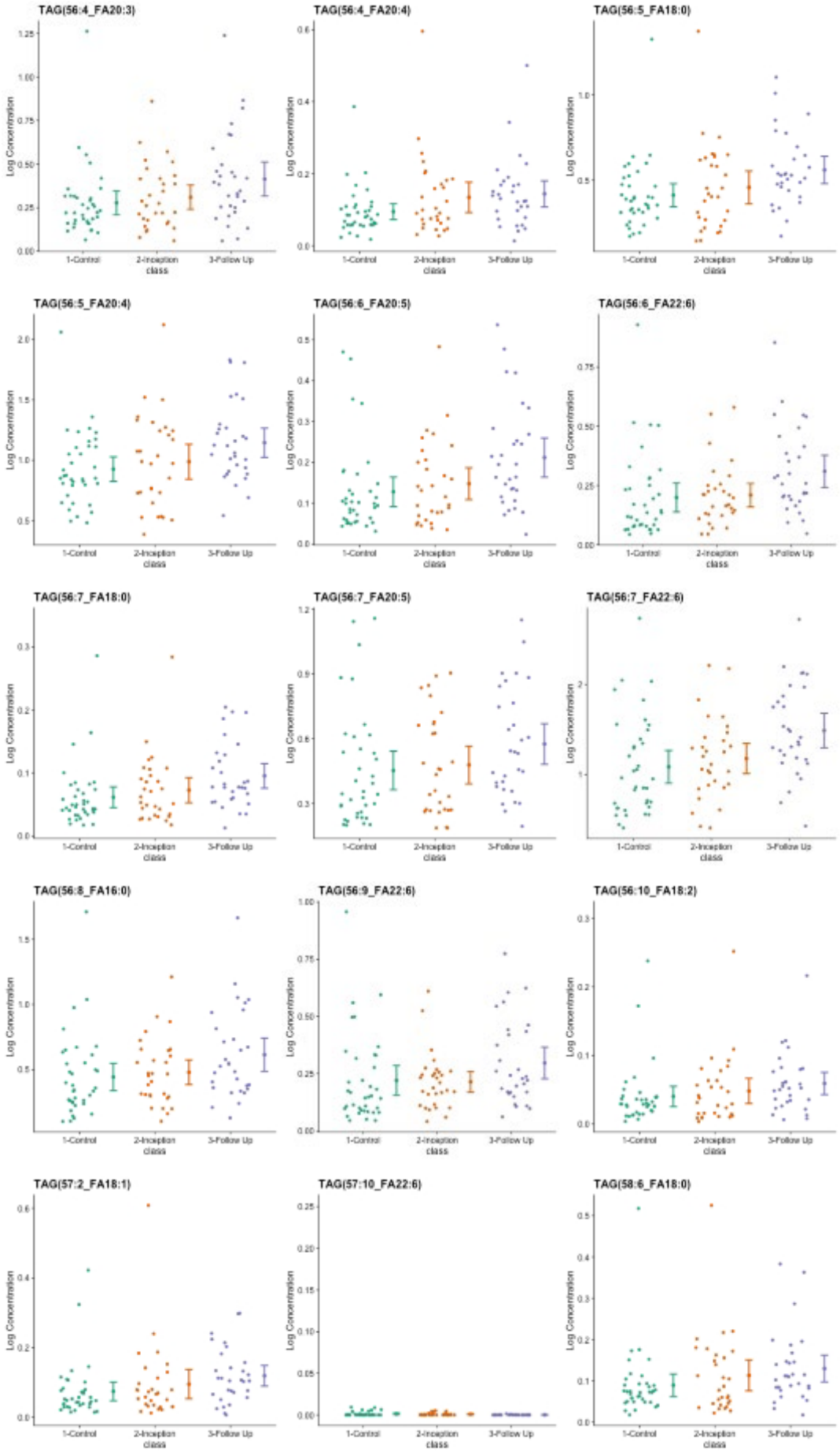
TAG(56:4_FA20:3)
TAG(56:4_FA20:4)
TAG(56:5_FA18:0)
TAG(56:5_FA20:4)
TAG(56:6_FA20:5)
TAG(56:6_FA22:6)
TAG(56:7_FA18:0)
TAG(56:7_FA20:5)
TAG(56:7_FA22:6)
TAG(56:8_FA16:0)
TAG(56:9_FA22:6)
TAG(56:10_FA18:2)
TAG(57:2_FA18:1)
TAG(57:10_FA22:6)
TAG(58:6_FA18:0)
Log Concentration
1-Control
2-Inception
3-Follow Up
class

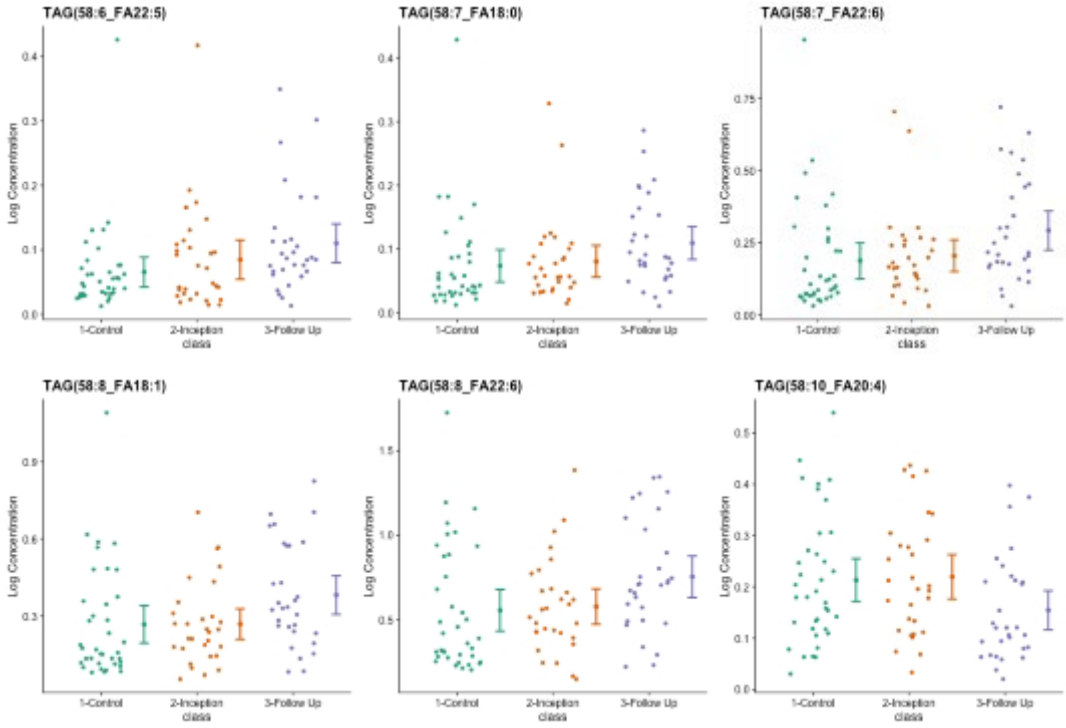
TAG(58:6_FA22:5)
TAG(58:7_FA18:0)
TAG(58:7_FA22:6)
TAG(58:8_FA18:1)
TAG(58:8_FA22:6)
TAG(58:10_FA20:4)
Log Concentration
1-Control
2-Inception
3-Follow Up
class

7.9 Kruskal-Wallis test results of lipid species in chapter 4 cohort

A non-parametric Kruskal Wallis Rank Sum Test was performed on all 856 lipid species identified in the data set. A Post hoc Dunn's test was then completed to report inter-class differences. Significance was deemed at less than or equal to 0.05. The 226 lipid species listed below were deemed significant

Lipid Species	*p* value	Control-Inception	Control-Follow Up	Inception-Follow Up
MAG(14:0)	6.25E-06	3.40E-01	1.47E-05	6.31E-06
HCER(d18:0/26:0)	2.14E-05	1.67E-01	1.46E-04	6.31E-06
HCER(14:0)	8.53E-05	2.89E-01	1.66E-04	3.99E-05
DAG(20:0/20:0)	8.85E-05	2.91E-01	1.69E-04	4.15E-05
CER(26:0)	1.20E-04	1.14E-01	9.59E-04	2.06E-05
SM(14:0)	1.57E-04	1.96E-01	5.17E-04	4.15E-05
MAG(18:3)	1.98E-04	4.62E-01	9.41E-05	2.67E-04
MAG(22:4)	3.89E-04	2.60E-01	6.67E-04	1.24E-04
PC(18:0/18:2)	4.10E-04	4.00E-01	1.37E-04	6.41E-04
HCER(16:0)	4.27E-04	2.78E-01	6.44E-04	1.45E-04
CER(14:0)	4.50E-04	2.30E-01	9.16E-04	1.22E-04
PC(18:1/22:6)	5.40E-04	4.91E-01	2.52E-04	5.03E-04
MAG(18:1)	5.42E-04	3.15E-01	6.31E-04	2.10E-04
PC(20:0/20:4)	7.63E-04	2.07E-01	1.63E-03	1.73E-04
HCER(18:1)	7.84E-04	1.44E-01	2.81E-03	1.33E-04
LCER(14:0)	7.91E-04	1.46E-01	2.78E-03	1.35E-04
DCER(20:1)	8.60E-04	3.28E-01	2.04E-04	1.64E-03
HCER(20:1)	8.69E-04	4.80E-01	4.27E-04	6.41E-04
CE(20:4)	1.08E-03	2.54E-01	1.94E-04	3.00E-03
PC(16:0/18:2)	1.14E-03	4.27E-01	6.76E-04	6.31E-04
HCER(d18:0/26:1)	1.20E-03	1.40E-01	4.04E-03	1.92E-04
PC(18:0/20:1)	1.28E-03	3.24E-01	1.21E-03	4.49E-04
SM(20:1)	1.30E-03	4.72E-01	4.99E-04	1.09E-03
HCER(d18:0/20:0)	1.37E-03	2.04E-01	2.06E-04	5.04E-03
FFA(20:4)	1.38E-03	3.69E-01	3.61E-04	1.87E-03
CER(20:1)	1.40E-03	3.06E-01	1.42E-03	4.49E-04
HCER(d18:0/22:0)	1.60E-03	3.26E-01	1.44E-03	5.46E-04
MAG(16:1)	1.63E-03	4.98E-01	6.74E-04	1.16E-03
PC(18:1/18:2)	1.66E-03	4.34E-01	8.97E-04	8.79E-04
DCER(22:1)	1.79E-03	3.81E-01	1.21E-03	7.51E-04
PC(18:1/20:4)	1.82E-03	3.66E-01	1.31E-03	7.17E-04
DCER(26:1)	1.95E-03	1.46E-01	5.48E-03	3.11E-04
HCER(22:0)	2.22E-03	3.45E-01	1.71E-03	7.76E-04
PC(18:1/20:1)	2.41E-03	3.03E-01	2.25E-03	7.05E-04
HCER(26:0)	2.43E-03	3.57E-01	1.75E-03	8.79E-04

TAG(56:7/FA18:0)	2.48E-03	1.18E-01	2.90E-04	1.59E-02
DCER(20:0)	2.49E-03	1.81E-01	4.95E-03	4.49E-04
PC(16:0/20:1)	2.49E-03	4.29E-01	1.30E-03	1.20E-03
PC(18:1/20:5)	2.65E-03	2.80E-01	4.89E-04	4.91E-03
TAG(56:6/FA20:5)	2.65E-03	1.45E-01	3.32E-04	1.27E-02
PC(20:0/18:1)	2.74E-03	2.21E-01	4.02E-03	5.73E-04
DCER(22:0)	2.85E-03	1.08E-01	1.07E-02	3.80E-04
HCER(20:0)	2.90E-03	4.89E-01	1.07E-03	1.90E-03
TAG(55:7/FA22:6)	2.95E-03	2.66E-01	5.18E-04	5.75E-03
PE(P-18:1/22:6)	3.20E-03	2.31E-01	4.27E-03	6.83E-04
CER(20:0)	3.33E-03	4.19E-01	9.47E-04	2.88E-03
PE(P-18:1/20:5)	3.36E-03	3.90E-01	8.65E-04	3.31E-03
PC(16:0/22:6)	3.38E-03	4.63E-01	1.47E-03	1.77E-03
HCER(26:1)	3.59E-03	2.16E-01	5.14E-03	7.17E-04
TAG(52:2/FA18:1)	3.65E-03	6.33E-02	4.04E-04	4.15E-02
SM(18:0)	3.76E-03	3.69E-01	2.37E-03	1.33E-03
TAG(56:6/FA22:6)	3.81E-03	1.53E-01	4.86E-04	1.52E-02
TAG(53:2/FA18:1)	3.97E-03	2.36E-01	6.30E-04	8.54E-03
PS(20:0/22:6)	4.05E-03	3.97E-01	1.05E-03	3.70E-03
TAG(56:7/FA22:6)	4.23E-03	1.60E-01	5.48E-04	1.54E-02
CE(20:5)	4.39E-03	4.65E-01	1.42E-03	2.92E-03
PC(20:0/20:3)	4.54E-03	4.17E-01	2.27E-03	1.87E-03
TAG(55:1/FA18:1)	4.54E-03	9.54E-02	5.20E-04	3.03E-02
MAG(18:2)	4.68E-03	2.95E-01	4.04E-03	1.22E-03
PC(18:2/20:5)	4.72E-03	2.15E-01	7.04E-04	1.10E-02
CER(16:0)	4.91E-03	2.79E-01	4.57E-03	1.20E-03
TAG(58:7/FA22:6)	5.40E-03	8.54E-02	6.18E-04	3.83E-02
PI(18:0/18:0)	5.77E-03	1.43E-02	1.03E-03	1.98E-01
TAG(51:2/FA18:1)	5.88E-03	2.56E-01	9.72E-04	1.00E-02
SM(26:0)	6.08E-03	2.87E-02	7.42E-02	7.28E-04
PE(P-18:0/22:4)	6.11E-03	6.46E-02	3.34E-02	7.17E-04
TAG(53:2/FA17:0)	6.21E-03	3.02E-01	1.16E-03	8.12E-03
PC(16:0/20:5)	6.38E-03	4.47E-01	1.87E-03	4.23E-03
PE(P-16:0/20:1)	6.60E-03	1.02E-01	2.13E-02	8.52E-04
DAG(18:1/22:6)	6.74E-03	2.12E-01	9.89E-04	1.45E-02
PG(18:0/18:2)	6.80E-03	4.23E-01	3.14E-03	2.68E-03
TAG(58:6/FA22:5)	6.97E-03	1.21E-01	8.43E-04	3.03E-02
PE(P-16:0/20:5)	7.05E-03	3.23E-01	1.39E-03	8.02E-03
TAG(56:5/FA18:0)	7.31E-03	1.78E-01	9.87E-04	1.95E-02
PE(18:0/22:6)	7.37E-03	4.39E-01	2.07E-03	4.91E-03
TAG(54:7/FA22:6)	7.86E-03	1.78E-01	1.06E-03	2.04E-02
PC(16:0/16:0)	7.87E-03	4.21E-01	3.59E-03	3.00E-03
TAG(55:2/FA18:1)	7.98E-03	1.83E-01	1.09E-03	1.99E-02
TAG(55:1/FA16:0)	8.05E-03	1.55E-01	1.04E-03	2.48E-02
PC(18:2/22:6)	8.34E-03	4.42E-01	3.48E-03	3.40E-03
PE(P-16:0/22:6)	8.63E-03	3.52E-01	5.15E-03	2.53E-03
HCER(24:1)	8.66E-03	3.83E-01	4.53E-03	2.84E-03
SM(18:1)	8.84E-03	3.78E-01	4.70E-03	2.84E-03
PI(18:0/22:6)	8.88E-03	3.57E-01	1.91E-03	8.12E-03
PC(18:2/20:4)	8.92E-03	2.29E-01	9.80E-03	1.71E-03
PE(P-18:0/22:5)	9.06E-03	1.51E-01	1.70E-02	1.35E-03

LPC(20:2)	9.10E-03	3.16E-01	1.74E-03	1.00E-02
PC(16:0/18:1)	9.23E-03	3.27E-01	6.08E-03	2.46E-03
PI(20:0/16:1)	9.27E-03	4.84E-01	3.28E-03	4.35E-03
TAG(57:10/FA22:6)	9.30E-03	1.33E-01	2.02E-02	1.31E-03
TAG(52:7/FA22:6)	9.40E-03	1.98E-01	1.33E-03	2.02E-02
SM(26:1)	9.55E-03	2.83E-02	1.01E-01	1.23E-03
PC(14:0/20:5)	9.84E-03	2.90E-01	7.66E-03	2.29E-03
LPC(22:4)	9.85E-03	3.66E-01	2.16E-03	8.43E-03
SM(24:0)	1.00E-02	3.19E-01	6.78E-03	2.57E-03
TAG(58:7/FA18:0)	1.04E-02	1.33E-01	1.31E-03	3.54E-02
CER(18:0)	1.07E-02	3.31E-01	2.11E-03	1.05E-02
HCER(d18:0/24:0)	1.07E-02	4.90E-01	3.42E-03	5.38E-03
FFA(20:3)	1.09E-02	3.50E-01	2.27E-03	9.78E-03
PC(16:0/20:4)	1.09E-02	3.47E-01	6.38E-03	3.04E-03
LCER(20:0)	1.12E-02	7.78E-02	4.24E-02	1.39E-03
TAG(58:8/FA18:1)	1.12E-02	2.49E-01	1.79E-03	1.67E-02
TAG(49:1/FA18:1)	1.13E-02	2.08E-01	1.64E-03	2.15E-02
PE(P-16:0/22:4)	1.17E-02	1.44E-03	8.01E-02	6.68E-02
PE(P-18:0/18:1)	1.18E-02	1.50E-01	2.09E-02	1.74E-03
PC(18:1/20:3)	1.25E-02	1.89E-01	1.65E-02	2.07E-03
TAG(54:2/FA18:1)	1.26E-02	4.76E-02	1.69E-03	1.15E-01
HCER(d18:0/24:1)	1.33E-02	2.90E-01	9.78E-03	3.00E-03
TAG(57:2/FA18:1)	1.33E-02	1.59E-01	1.76E-03	3.40E-02
TAG(58:8/FA22:6)	1.36E-02	2.16E-01	2.00E-03	2.33E-02
DCER(26:0)	1.37E-02	2.46E-01	1.25E-02	2.68E-03
TAG(53:1/FA18:1)	1.41E-02	1.47E-01	1.83E-03	3.87E-02
DCER(24:0)	1.43E-02	2.69E-01	1.16E-02	3.00E-03
PC(18:0/20:0)	1.50E-02	1.60E-01	2.32E-02	2.26E-03
PE(P-18:0/20:5)	1.54E-02	2.31E-01	2.34E-03	2.33E-02
TAG(45:0/FA16:0)	1.55E-02	1.94E-01	2.18E-03	2.94E-02
PI(18:0/20:4)	1.56E-02	3.44E-01	3.13E-03	1.32E-02
TAG(47:2/FA18:1)	1.56E-02	2.20E-01	2.33E-03	2.51E-02
FFA(20:5)	1.57E-02	3.50E-01	8.61E-03	4.23E-03
DCER(24:1)	1.58E-02	7.00E-02	6.04E-02	1.98E-03
CE(14:0)	1.59E-02	3.22E-01	3.00E-03	1.48E-02
PC(18:0/20:2)	1.59E-02	3.08E-01	1.05E-02	3.75E-03
CER(26:1)	1.65E-02	2.01E-01	1.90E-02	2.80E-03
PC(14:0/20:3)	1.65E-02	3.02E-01	1.11E-02	3.80E-03
TAG(52:2/FA16:0)	1.66E-02	9.99E-02	2.10E-03	6.62E-02
PC(14:0/20:4)	1.67E-02	1.84E-01	2.14E-02	2.68E-03
TAG(49:2/FA18:1)	1.71E-02	2.48E-01	2.70E-03	2.28E-02
CER(22:0)	1.74E-02	3.95E-01	7.88E-03	5.38E-03
TAG(47:1/FA18:1)	1.76E-02	2.52E-01	2.81E-03	2.28E-02
PE(P-18:0/18:2)	1.78E-02	1.91E-01	2.15E-02	2.92E-03
CER(24:1)	1.79E-02	2.97E-01	1.21E-02	4.01E-03
TAG(51:1/FA18:1)	1.81E-02	1.96E-01	2.58E-03	3.23E-02
TAG(53:1/FA16:0)	1.82E-02	1.27E-01	2.34E-03	5.42E-02
DAG(16:0/18:3)	1.85E-02	1.72E-01	2.52E-02	2.88E-03
SM(24:1)	1.86E-02	3.42E-01	1.03E-02	4.78E-03
CER(24:0)	1.87E-02	2.74E-01	1.41E-02	3.90E-03

PC(18:0/18:0)	1.90E-02	2.05E-01	2.08E-02	3.22E-03
PG(20:0/20:4)	1.92E-02	1.65E-01	2.73E-02	2.92E-03
TAG(52:3/FA18:1)	1.92E-02	1.07E-01	2.46E-03	6.80E-02
PS(18:0/20:0)	1.93E-02	1.08E-02	3.39E-01	4.91E-03
PE(16:0/22:6)	1.97E-02	4.77E-01	5.67E-03	9.31E-03
LCER(26:0)	1.98E-02	1.26E-02	3.07E-01	4.53E-03
PE(18:0/18:1)	2.01E-02	3.01E-01	3.58E-03	1.95E-02
PS(20:0/20:5)	2.05E-02	4.51E-01	7.42E-03	7.43E-03
PC(16:0/18:0)	2.09E-02	3.16E-01	1.27E-02	4.91E-03
TAG(53:1/FA17:0)	2.09E-02	1.20E-01	2.71E-03	6.33E-02
TAG(56:5/FA20:4)	2.11E-02	2.05E-01	3.06E-03	3.40E-02
PC(18:2/22:5)	2.13E-02	2.85E-01	1.49E-02	4.53E-03
TAG(56:4/FA20:3)	2.24E-02	1.68E-01	3.06E-03	4.53E-02
LPI(18:2)	2.25E-02	3.61E-01	4.64E-03	1.63E-02
PC(18:0/14:0)	2.32E-02	4.37E-01	5.86E-03	1.23E-02
DAG(18:1/18:1)	2.33E-02	4.06E-01	9.75E-03	7.15E-03
PC(18:2/18:2)	2.35E-02	2.71E-01	1.73E-02	4.78E-03
PG(18:1/18:1)	2.35E-02	3.08E-03	1.05E-01	7.89E-02
TAG(54:8/FA22:6)	2.36E-02	1.67E-01	3.24E-03	4.75E-02
HCER(24:0)	2.37E-02	4.43E-01	8.68E-03	8.22E-03
PE(P-18:1/18:1)	2.37E-02	1.12E-01	4.98E-02	3.22E-03
PE(P-18:1/22:5)	2.38E-02	1.63E-01	3.27E-02	3.60E-03
PC(18:2/16:1)	2.41E-02	3.68E-01	1.16E-02	6.54E-03
PE(18:0/20:5)	2.42E-02	4.40E-01	6.15E-03	1.26E-02
PC(14:0/22:5)	2.43E-02	3.75E-01	1.13E-02	6.71E-03
PC(18:1/22:5)	2.52E-02	1.67E-01	3.32E-02	3.85E-03
PC(18:0/22:6)	2.55E-02	2.40E-01	3.97E-03	3.19E-02
TAG(45:0/FA14:0)	2.55E-02	2.14E-01	3.78E-03	3.68E-02
CE(22:6)	2.56E-02	1.77E-01	3.14E-02	4.01E-03
TAG(54:5/FA20:5)	2.56E-02	1.77E-01	3.58E-03	4.66E-02
MAG(16:0)	2.58E-02	2.88E-01	1.72E-02	5.45E-03
PC(18:0/18:1)	2.58E-02	2.55E-01	2.02E-02	4.97E-03
LCER(18:1)	2.66E-02	1.01E-01	6.04E-02	3.60E-03
PG(16:0/18:1)	2.74E-02	2.87E-01	4.70E-03	2.65E-02
TAG(53:1/FA18:0)	2.75E-02	1.38E-01	3.70E-03	6.51E-02
TAG(54:3/FA18:1)	2.76E-02	8.31E-02	3.77E-03	1.10E-01
HCER(18:0)	2.80E-02	3.99E-01	1.17E-02	8.22E-03
PC(18:1/18:1)	2.84E-02	2.25E-01	2.56E-02	5.00E-03
TAG(51:1/FA17:0)	2.86E-02	2.20E-01	4.30E-03	3.87E-02
MAG(20:3)	2.87E-02	3.97E-02	1.57E-01	4.29E-03
TAG(53:2/FA16:0)	2.92E-02	1.81E-01	4.13E-03	4.98E-02
TAG(52:6/FA22:6)	2.93E-02	1.16E-01	3.94E-03	8.23E-02
PE(P-16:0/22:5)	2.94E-02	1.45E-01	4.43E-02	4.29E-03
TAG(51:1/FA18:0)	3.11E-02	1.62E-01	4.31E-03	5.94E-02
PE(P-18:0/20:2)	3.16E-02	8.86E-02	7.89E-02	4.29E-03
PC(18:1/18:3)	3.28E-02	1.93E-01	3.47E-02	5.31E-03
PE(P-18:1/18:2)	3.30E-02	1.72E-01	3.97E-02	5.10E-03
TAG(45:1/FA18:1)	3.33E-02	2.62E-01	5.44E-03	3.47E-02
PI(18:1/18:1)	3.34E-02	4.91E-01	9.62E-03	1.37E-02
TAG(47:1/FA17:0)	3.38E-02	1.90E-01	4.87E-03	5.22E-02
TAG(56:8/FA16:0)	3.38E-02	1.69E-01	4.76E-03	6.00E-02

DAG(18:1/20:1)	3.40E-02	1.32E-01	4.66E-03	7.89E-02
LCER(d18:0/22:0)	3.40E-02	3.44E-02	1.99E-01	5.60E-03
TAG(52:3/FA16:0)	3.40E-02	1.19E-01	4.66E-03	8.80E-02
TAG(51:1/FA16:0)	3.45E-02	1.97E-01	5.04E-03	5.08E-02
MAG(18:0)	3.46E-02	5.87E-02	1.25E-01	4.91E-03
TAG(54:2/FA18:0)	3.50E-02	3.75E-02	6.59E-03	2.53E-01
TAG(54:6/FA20:5)	3.50E-02	1.63E-01	4.91E-03	6.39E-02
TAG(50:2/FA14:0)	3.52E-02	1.60E-01	4.92E-03	6.56E-02
DCER(18:0)	3.56E-02	3.14E-01	2.01E-02	7.92E-03
TAG(56:4/FA20:4)	3.56E-02	5.62E-02	5.67E-03	1.84E-01
TAG(58:10/FA20:4)	3.58E-02	3.52E-01	1.74E-02	8.86E-03
PC(14:0/22:6)	3.59E-02	3.20E-01	1.97E-02	8.12E-03
PI(20:0/18:1)	3.59E-02	6.15E-02	5.54E-03	1.71E-01
PC(16:0/20:3)	3.60E-02	3.07E-01	2.09E-02	7.82E-03
CE(20:0)	3.64E-02	3.69E-01	7.50E-03	2.30E-02
TAG(52:7/FA16:0)	3.72E-02	1.22E-01	5.15E-03	9.10E-02
PG(18:0/20:0)	3.76E-02	1.58E-01	4.86E-02	5.67E-03
TAG(54:1/FA18:0)	3.76E-02	3.62E-02	7.40E-03	2.71E-01
TAG(58:6/FA18:0)	3.83E-02	1.67E-01	5.43E-03	6.62E-02
PE(P-18:1/22:4)	3.91E-02	2.01E-01	3.80E-02	6.46E-03
LPE(22:4)	3.94E-02	2.04E-01	5.86E-03	5.37E-02
TAG(54:1/FA18:1)	3.98E-02	7.05E-02	6.06E-03	1.62E-01
TAG(56:10/FA18:2)	4.06E-02	2.07E-01	6.07E-03	5.37E-02
TAG(56:9/FA22:6)	4.15E-02	1.51E-01	5.86E-03	7.82E-02
TAG(52:3/FA16:1)	4.21E-02	2.36E-01	6.60E-03	4.70E-02
CER(22:1)	4.24E-02	1.18E-01	7.34E-02	6.05E-03
HCER(22:1)	4.25E-02	3.91E-01	1.75E-02	1.16E-02
LCER(24:0)	4.25E-02	2.48E-02	3.00E-01	8.97E-03
FFA(20:0)	4.43E-02	2.50E-01	3.23E-02	8.22E-03
TAG(47:0/FA14:0)	4.49E-02	1.92E-01	6.62E-03	6.33E-02
TAG(56:4/FA18:0)	4.52E-02	1.14E-01	6.46E-03	1.11E-01
TAG(50:1/FA14:0)	4.57E-02	1.13E-01	6.54E-03	1.13E-01
PE(O-18:0/20:4)	4.58E-02	3.29E-01	2.35E-02	1.04E-02
LPE(20:2)	4.78E-02	3.32E-01	2.41E-02	1.09E-02
DAG(18:0/22:6)	4.82E-02	1.38E-01	6.90E-03	9.56E-02
PI(18:1/20:4)	4.85E-02	4.16E-01	1.80E-02	1.40E-02
LCER(22:0)	4.93E-02	9.48E-03	3.41E-01	3.26E-02
TAG(56:7/FA20:5)	5.00E-02	2.23E-01	7.73E-03	5.73E-02